INVESTIGATION OF THE BINDING SPECIFICITY OF IGF-1R USING MONOCLONAL ANTIBODIES

By

Mehrnaz Keyhanfar, Pharm.D.

A thesis submitted to the University of Adelaide, South Australia
in fulfilment of the requirements for the degree of
Doctor of Philosophy

THE UNIVERSITY
OF ADELAIDE
AUSTRALIA

School of Molecular and Biomedical Science
The University of Adelaide
Adelaide, South Australia, 5005

September 2005

Abstract

The insulin-like growth factor type one receptor (IGF-1R) plays a critical role in cancer. The receptor is over expressed in many tumours and mediates growth, motility, and survival from apoptosis. Several studies have shown that the inhibition of IGF-1R's expression or its function blocks tumour growth or metastasis, and also enhances sensitivity to cytotoxic drugs and irradiation. To date, IGF-1R is widely considered as a very promising target for cancer treatment.

Among different techniques for targeting IGF-1R, blocking the receptor with specific monoclonal antibodies (MAbs) is an attractive way to inhibit the receptor signalling. In addition, antibodies specific for the IGF-1R are potential diagnostic reagents as the IGF-1R is overexpressed in several cancers. A similar approach has been successfully utilized in the treatment of breast cancer using Herceptin, which is a humanised MAb against human epidermal growth factor receptor-2.

In this thesis, two high affinity murine MAbs against IGF-1R namely 7C2 and 9E11 were isolated and cloned. To obtain these MAbs, s-IGF-1R (the soluble extracellular part of the IGF-1R, amino acids 1-906) was used as an immunogen. These MAbs were IgG1κ isotype and did not cross react with either insulin receptor isoform IR-A or IR-B. MAbs 7C2 and 9E11 successfully detected IGF-1R in a number of immunoassays such as in enzyme linked immunosorbent assays (ELISAs), flow cytometry and immunohistochemistry. The MAbs also immunoprecipitated IGF-1R from lysates of cells overexpressing recombinant IGF-1R. Both MAbs 7C2 and 9E11 showed high affinity to the s-IGF-1R. The binding affinities of the MAbs 7C2 and 9E11 to s-IGF-1R were 0.5±1.6 nM and 2.1±0.4 nM, respectively. The sequences of the variable regions of these MAbs' heavy and light chains were also described in this study. Comparison of the CDR sequences of the MAbs with those of other MAbs against the IGF-1R showed that MAbs 7C2 and 9E11 each had a unique sequence.

During this research it was found that MAbs 7C2 and 9E11 blocked the binding of IGF-I to the IGF-1R, but did not show an inhibitory effect on the binding of IGF-II to this receptor. Moreover, epitope mapping of MAbs 7C2 and 9E11 revealed that they both bound to the cysteine-rich domain of the receptor. These findings support a previous study, which demonstrated that the cysteine-rich domain of IGF-1R is critical for specific binding of IGF-I but not IGF-II to the receptor.

In this thesis, further epitope mapping studies on MAbs 7C2 and 9E11 using alanine mutants of the IGF-1R in the cysteine-rich domain are reported. The results showed that amino acids F241, F251 and F266 were involved in binding to both MAbs 7C2 and 9E11. On the other hand, another study showed that amino acids F241 and F251 were crucial for IGF-I binding to the receptor. Therefore, binding to these two amino acids by MAbs 7C2 and 9E11 is most likely responsible for the selective blocking of IGF-I but not IGF-II to the receptor.

Competition experiments performed during this research revealed that the chimeric IGF analogues IGF-ICII (IGF-I with IGF-II C domain) and IGF-IICI (IGF-II with IGF-I C domain) behaved like IGF-II and IGF-I, respectively in their ability to inhibit the binding of MAbs 7C2 and 9E11 to s-IGF-1R. These findings imply that out of all four domains of IGF-I, it is the C domain, which binds to residues in IGF-1R that form the epitope for MAbs 7C2 and 9E11. Because in the C domain of IGF-I, amino acids R36 and R37 and also Y31 have been shown to be important for binding to IGF-1R, it could be proposed that the binding of the IGF-I C domain to the IGF-1R cysteine-rich domain is through binding amino acids R36, R37 and Y31 of IGF-I to residues F241 and F251, or to the nearby residues, which are sterically affected by the presence of the MAbs binding to the receptor.

In this research, *in vitro* studies, using MAbs as anti-cancer reagents revealed that both MAbs 7C2 and 9E11 inhibited the proliferation of colon cancer cell (HT-29) induced by IGF-I and IGF-II. However, the neutralizing effect for IGF-II was less potent than for IGF-I. Since the MAbs did not inhibit binding of IGF-II to the receptor, their effect on IGF-II induced cell proliferation could be claimed to be due to an indirect effect. This is consistent

with the *in vitro* result for the receptor down-regulation experiment, which showed that 24 h incubation of breast cancer cells (MCF-7) with MAbs 7C2 and 9E11, significantly reduced the IGF-1R expression. In this study it was also shown that MAbs 7C2 and 9E11 inhibited MCF-7 cells migration induced by IGF-I. This could indicate a potential anti-metastatic property of MAbs 7C2 and 9E11.

Taken together, the *in vitro* effects of MAbs 7C2 and 9E11 reported in this thesis revealed that they had inhibiting effects on cancer cell proliferation and migration and they also induced IGF-1R down-regulation. Therefore, they could be potentially valuable prospects for cancer treatment if humanised.

Finally, MAbs 7C2 and 9E11 could be used as diagnostic reagents to detect IGF-1R in cells or tissue samples in a range of immunoassays as mentioned earlier. Due to the IGF-1R overexpression in several cancer tumours, MAbs 7C2 and 9E11 could be utilized for malignant tumour recognition. Furthermore, as another application, these MAbs could also be used to identify tumours overexpressing the IGF-1R, allowing tailored anti-cancer treatment including an IGF-1R blocking agent.

Statement of Originality

This thesis contains no material that has been accepted for the award of any other degree or diploma in any University. To the best of my knowledge and belief it contains no material that has previously been published by any other person except where due reference is made. The author consents to this thesis being made available for photocopy or loan.

Mehrnaz Keyhanfar

Acknowledgments

I am sincerely grateful to my supervisors Professor John Wallace, Dr. Grant Booker and Dr. Briony Forbes, whose encouragement, guidance and endless support have allowed me to complete these studies.

Throughout my PhD, I collaborated with Professor Jonathan Whittaker (Case Western Reserve University, USA) who kindly provided me the alanine mutants of the IGF-1R for epitope mapping studies. Thanks to Dr. Raymond Rodgers, Dr. Claire Roberts, Ms. Helen Irving-Rodgers and Ms. Stephanie Morris (Obstetrics and Gynaecology, Medical school, The University of Adelaide) who helped me in immunohistochemistry assays. Thank you also to Professor Axel Ullrich (Max-Planck-Institute of Biochemistry, Germany) who generously sent me the chimeric IR/IGF-1R expressing cells. I would like express my gratefulness to Dr. Leah Cosgrove (CSIRO, Division of Health Science and Nutrition, Adelaide, Australia) who gave me many worthwhile advises during this work. She also kindly provided some laboratory materials that I used in my experiments. I am indebted Mr. John Mackrill for his extensive assistance with the hybridoma production procedure. Thanks also to Dr. Steven Polyak for his help in molecular biology manners and Ms. Carlie Delaine for her extensive technical assistance.

A warm thanks to all my friends in the laboratory who were the most amazing, cheerful and understanding people imaginable; Adam Denley, Kathy Surinya, Kerrie McNeil, Sarawut (Yui) Jitrapakdee, Teerakul (Gap) Arpornsuwan, Lisa Bailey, Nicole Pendini, Zhihe (Wau) Kuang, Thirajit (O) Boonsaen, Lisa Clark and Clair Alvino.

Thanks to Dr. Jack da Silva who provided me a quite spot in his laboratory for writing up my thesis. Thank you also to Ravinder Anand Ivell, Chareeporn (Koi) Akekawatchai, Yinghong Liu for their companionship and practical tips.

There are many people in the School of Molecular and Biomedical Science who have helped me in my journey including all people in CSU, Brian Denton, Martin Lennon, Chris

Cursaro, Serge Volgin, Lynda Gregory-Badger, Sharon Kolze, Janis Soltys, Pam Lovison and Garry Penney.

I also would like to thank everyone in the discipline of biochemistry. The technical assistance and friendship they offered me have been invaluable. Thank you also to people in the university's IT help desk who aided me several times to overcome the computer problems. Thanks for the help that Dr. Keith Thompson (Institute of Immunology, Rikshospitalet University Hospital, Norway) and Dr. Pat Wallace (GroPep Limited, Adelaide, Australia) provided me during this research.

Throughout my PhD, I have been supported by an Iranian postgraduate scholarship from Ministry of Science, Research and Technology. I have also been recipient of financial support for travel and conference attendance from the School of Molecular and Biomedical Science, the committee of the 2nd International GH-IGF Symposium and from the Cancer Council, South Australia.

I dedicate this thesis to my wonderful family. I am forever indebted to my parents, Moones and Hossein, my two brothers and their families who have provided me with more love and support than I could imagine. I would like to express my gratitude to my mother-in-law who took care of the bureaucracy related to my scholarship in Iran. Thanks also to my grandparents for their encouragement and continuous words of wisdom. Finally, I would not be here today if it was not my husband's, Hooman, enormous patience, support and endless love. I have also benefited from his great knowledge with the computer related issues

Table of Content

List of Figures

List of Tables

List of Publications

Patent

Adelaide Research and Innovation Pty Ltd (Applicant). "Antibodies to insulin-like growth factor I receptor" Provisional patent number: 2004901994, 16 April, 2004.

Journals

M. Keyhanfar, B.E. Forbes, G.W. Booker and J.C. Wallace (2005) "Production and characterisation of monoclonal antibodies against insulin-like growth factor type 1 receptor (IGF-1R)" (*manuscript in preparation*).

M. Keyhanfar, B.E. Forbes, G.W. Booker, J. Whittaker and J.C. Wallace "Using monoclonal anibodies to investigate the binding specificity of IGF-1R" (*manuscript in preparation*).

Conference Proceedings

M. Keyhanfar, A. Denley, G.W. Booker, J. Whittaker, B.E. Forbes and J.C. Wallace "Orienting the insulin-like growth factors (IGF) in the IGF receptor" In Proceedings of 6th Australian Peptide Conference, Hamilton Island, Great Barrier Reef, Australia, 9-14 October, 2005 (*accepted for oral presentation - presenter: J.C. Wallace*).

M. Keyhanfar, B.E. Forbes, G.W. Booker, J. Whittaker and J.C. Wallace "Epitope mapping of monoclonal antibodies (MAbs) against insulin-like growth factor type one receptor (IGF-1R) and detection of specific binding sites for IGF-I on the receptor" In Proceedings of ComBio 2005, Adelaide Convention Centre, Adelaide, Australia, 25-29 September, 2005 (*poster presentation*).

M. Keyhanfar, B.E. Forbes, G.W. Booker and J.C. Wallace "Developing monoclonal antibodies against insulin-like growth factor type 1 receptor (IGF-1R) as a diagnostic and potential anticancer reagents" In Proceedings of ComBio 2004, Intercontinental Burswood Resort, Perth, Australia, 26-30 September, 2004 (*poster presentation*).

M. Keyhanfar, B.E. Forbes, G.W. Booker and J.C. Wallace "Characterization of monoclonal antibodies against the insulin-like growth factor type one receptor and their effects on IGF-I and IGF-II binding" In Proceedings of Annual Scientific Meeting the Australian Society for Medical Research South Australian Division, Entertainment Centre, Adelaide, Australia, 4 June, 2004 (*oral presentation*).

M. Keyhanfar, B. Forbes, G. Booker and J. Wallace " Development and characterization of two high affinity monoclonal antibodies against IGF-1R" In Proceedings of Second International GH-IGF Symposium, Cairns Convention Centre, Queensland, Australia, 18-22 April, 2004 (*oral presentation*).

M. Keyhanfar, B. Forbes, G. Booker and J. Wallace "Development of monoclonal antibodies against IGF-1R" In Proceedings of the Australian Society for Medical Research 42nd National Scientific Conference, Glenelg, Adelaide, South Australia, 23-25 November, 2003 (*poster presentation*).

M. Keyhanfar, G. Booker, J. Wallace and B. Forbes "Monoclonal Antibodies as Antitumour and Diagnostic Reagents" In Proceedings of Annual Scientific Meeting the Australian Society for Medical Research South Australian Division, Enterprise House, South Australia, 30 May, 2003 (*oral presentation*).

List of Abbreviations

AA	amino acid
ABTS	2,2′ azinobis 3-ethylbenzthiazoline-6 sulfonic acid
ALS	acid labile subunit
Amp	ampicillin
APS	ammonium persulphate
ATP	adenosine triphosphate
BCA	bicinchoninic acid
BLAST	basic local alignment search tool
BME	beta-mercaptoethanol
bp	base pair
BSA	bovine serum albumin
C-	carboxyl-
Cα	central carbon atom
cDNA	complementary deoxyribonucleic acid
CDR	complementarity determining regions
DEPC	diethyl pyrocarbonate
DMEM	Dulbecco's modified eagles medium
DMSO	dimethyl sulfoxide
DNA	deoxynucleotide triphosphate
dNTPs	deoxynucleotide triphosphates
DTT	dithiothreitol
E.coli	*Escherichia coli*
ECL	enhanced chemiluminescence
ECM	extracellular matrix
EDTA	ethylene diamine tetra-acetic acid
EGF	epidermal growth factor
EGTA	ethylene glycol-O,O'-bis-[2-amino-ethyl]-N,N,N',N',-tetraacetic acid
ELISA	enzyme linked immunosorbent assay
Eu	europium
Eu-7C2	europium labelled 7C2 (Fab)
Eu-9E11	europium labelled 9E11 (Fab)
Eu-IGF-I	europium labelled IGF-I
Eu-IGF-II	europium labelled IGF-II
FBS	fetal bovine serum
FCS	fetal calf serum
FITC	fluorescein isothiocyanate
FR	framework
G418	geneticin
GH	growth hormone
Grb2	growth factor receptor binding protein 2
GS	glutamine synthetase

h	hour
HBS	hepes buffered saline
HEPES	4-(2-hydroxyethyl)-1-piperazine-ethanesulphonic acid
HER2	human epidermal growth factor receptor-2
HRP	horseradish peroxidase
IC_{50}	concentration of inhibitor which reduces binding or activating by 50%
IGFBP	insulin-like growth factor binding protein
IGF-I or -II	insulin-like growth factor I or II
IL-2 or -8	interlukin 2 or 8
INS	insulin
IP	immunoprecipitation
IR	insulin receptor
IR-A	insulin receptor isoform A
IR-B	insulin receptor isoform B
IRS-1	insulin receptor substrate 1
JNK	c-Jun amino-terminal kinase
JNK	jun amino-terminal kinase
kb	kilobase pair
KDa	kilo dalton
LB	luria broth
Lb	loading buffer
m	metre
M	molar
µ	micron
mA	milliampere
MAb	monoclonal antibody
MAPK	mitogen-activated protein kinase
Min	minute, minutes
MOPS	3-morpholinopropanesulfonic acid
MSX	methionine sulfoximine
mTOR	mammalian target of rapamycin
MW	molecular weight
MWCO	molecular weight cut-off
n	nano
N-	amino-
NMR	nuclear magnetic resonance
$OD_{x\ nm}$	optical density at x nm wavelength
ORF	open reading frame
PBS	phosphate buffered saline
PBS-T	phosphate buffered saline and 0.1% (v/v) Tween-20
PCR	polymerase chain reaction
PEG	polyethylene glycol
PI3K	phosphoinositide 3-kinase

PKB	protein kinase B
PMSF	phenylmethylsulfonylfluoride
RNA	ribonucleic acid
RNase	ribonuclease
rpm	revolutions per minute
RT	room temperature
RU	resonance units
SDS	sodium dodecyl sulphate
SDS-PAGE	sodium dodecyl sulphate polyacrylamide gel electrophoresis
sec	Second
SEM	standard error of the mean
SH2	src homology 2
Shc	src homology/ collagen proteins
s-IGF-1R	recombinant soluble extracellular part of the IGF-1R
Sos	son of sevenless protein
TAE	tris acetate EDTA
TBS	tris buffered saline
TBS-T	tris buffered saline and 0.05% (v/v) Tween-20
TEMED	N,N.N,N'N'-tetramethylethylene-diamine
Tris	2-amino-2-hydroxymethylpropane-1,3-diol
Tween-20	polyoxyethylene-sorbitan monolaurate
U	units (active)
UV	ultra violet
V_K	variable region of the kappa light chain
V_H	variable region of the light chain
V_L	variable region of the heavy chain
Wb	western blot
WT	wild type

Chapter 1

Literature Review

1. Literature Review

1.1. Introduction

The insulin like growth factor (IGF) system plays important roles in normal prenatal and postnatal development and growth in the mammalian body. It has been conserved evolutionarily from yeast to human (Barbieri *et al.,* 2003). The IGF system is a family of ligands, receptors and binding proteins that are involved in a range of growth and differentiation processes as well as in pathological circumstances. The biological effects of IGF-I and IGF-II are regulated by various soluble binding proteins (IGFBP) and mediated through transmembrane receptors, which include the insulin receptor (IR), the insulin like growth factor type one receptor (IGF-1R) and IGF-II/mannose-6-phosphate (M-6-P) receptor (IGF-2R) (Werner and LeRoith, 1996). The IGF-1R and IR exhibit high structural and sequence similarity but they bind the IGF ligands with different affinities. Binding of the ligands IGF-I, IGF-II or the structurally related insulin to the α subunits of the IGF-1R induces conformational changes in the receptor leading to autophosphorylation of three tyrosine residues in the kinase domains of the β subunits (Kato *et al.,* 1993; Kato *et al.,* 1994). Today it is widely established that most of the biological effects of the IGFs on differentiation and growth are mediated through the ligand-dependent activation of the IGF-1R.

Clinical and *in vitro* studies reveal that the IGF-1R and its ligands have a critical role in cancer. Activation of the IGF-1R increases the proliferation and metastasis of cancer cells (Pollak *et al.,* 2004). IGFs also protect cells against death by a range of cytotoxic drugs (Sell *et al.,* 1995; Dunn *et al.,* 1997). Sell *et al.* (Sell *et al.,* 1993; Sell *et al.,* 1994) demonstrated that R^- cells (mouse 3T3-like cells with a targeted removal of the IGF-1R gene) could not be transformed by a number of cellular and viral oncogenes. In conclusion, these observations suggest the potential use of IGF-1R antagonists in cancer therapy. A variety of therapeutic methods to inhibit this receptor have been identified so far (reviewed in (Bahr and Groner, 2004; Pollak *et al.*, 2004)).

Among different methods for targeting the IGF-1R, blocking the receptor with specific monoclonal antibodies (MAb) is an attractive way to inhibit the receptor signalling. A similar approach has been successfully used in the treatment of breast cancer using Herceptin, which is a humanised MAb against human epidermal growth factor receptor-2 (HER2) (Baselga, 2001). It has been shown that IGF-1R overexpression mediates resistance to inhibitors of EGF receptor and HER2 receptors (Lu *et al.,* 2001; Chakravarti *et al.,* 2002). Some mouse, single chain and humanised antibodies have been developed directed against the IGF-1R (Kull *et al.,* 1983; Soos *et al.,* 1992; Benini *et al.,* 2001; Burtrum *et al.,* 2003; Jackson-Booth *et al.,* 2003). It has been shown that αIR-3, which is a mouse MAb directed against the IGF-1R inhibits cancer cell growth in a variety of human tumour cell types *in vitro* as well as *in vivo* (Arteaga and Osborne, 1989a; Arteaga *et al.*, 1989; Furlanetto *et al.*, 1993; Kalebic *et al.*, 1994; Scotlandi *et al.*, 1998; Benini *et al.*, 2001). In addition, Benini *et al.* (Benini *et al.,* 2001) showed that the combination of αIR-3 with chemotherapeutics increased the anti-tumour activity of drugs in Ewing's sarcoma cells. MAbs also can be used to study the detailed structure of the complex between ligands and IGF-1R and detect the important binding sites for different ligands. In addition, these MAbs can be applied as diagnostic tools to detect the expression of IGF-1R in tumours before using them as therapeutics.

The following literature review provides an overview of the members of the IGF family; the role of different parts of this system in cancer; targeting IGF-1R for cancer therapy; overview of immunoglobulin (Ig) and MAb structure and function; MAbs as therapeutics for cancer therapy; The antigen-antibody interaction and epitope mapping of MAbs.

1.2. Introduction to the IGF System

The IGF system is a complex family consisting of three ligands (IGF-I, IGF-II and insulin), six high affinity IGF binding proteins (IGFBPs-1 to -6), three receptors: type 1 IGF receptor (IGF-1R), type 2 IGF receptor (IGF-2R) and the insulin receptor (IR), as well as some other

molecules and enzymes that operate to influence the activities of the IGF system as shown in Figure 1.1. The IR is expressed in two isoforms (IR-A and IR-B), which are different by 12 amino acids at the C-terminus of the receptor α-subunit due to the alternative splicing of exon 11 (Moller *et al.,* 1989). The ligands bind to the IGF-1R or IR isoforms and activate the intrinsic kinase activities. Activation of these receptors generates signalling cascades that lead to regulation of a range of biological responses. Functional hybrid receptors between the IGF-1R and either IR-A or IR-B can also be formed. Formation of the hybrids between IR-A and IR-B is also theoretically possible however it has not yet been shown experimentally. IGF-2R structure and function are distinct from IGF-1R, and the IGF-2R is known as a tumour suppressor by mediating the degradation of IGF-II. The IGFBPs regulate the IGFs in a number of different ways including prolonging the lifetime of the IGFs in the circulating system, transporting the IGFs to their target cells and modulating the interaction of IGFs with their receptors. Also, the IGF binding protein proteases (BP protease) act as modulators of the system.

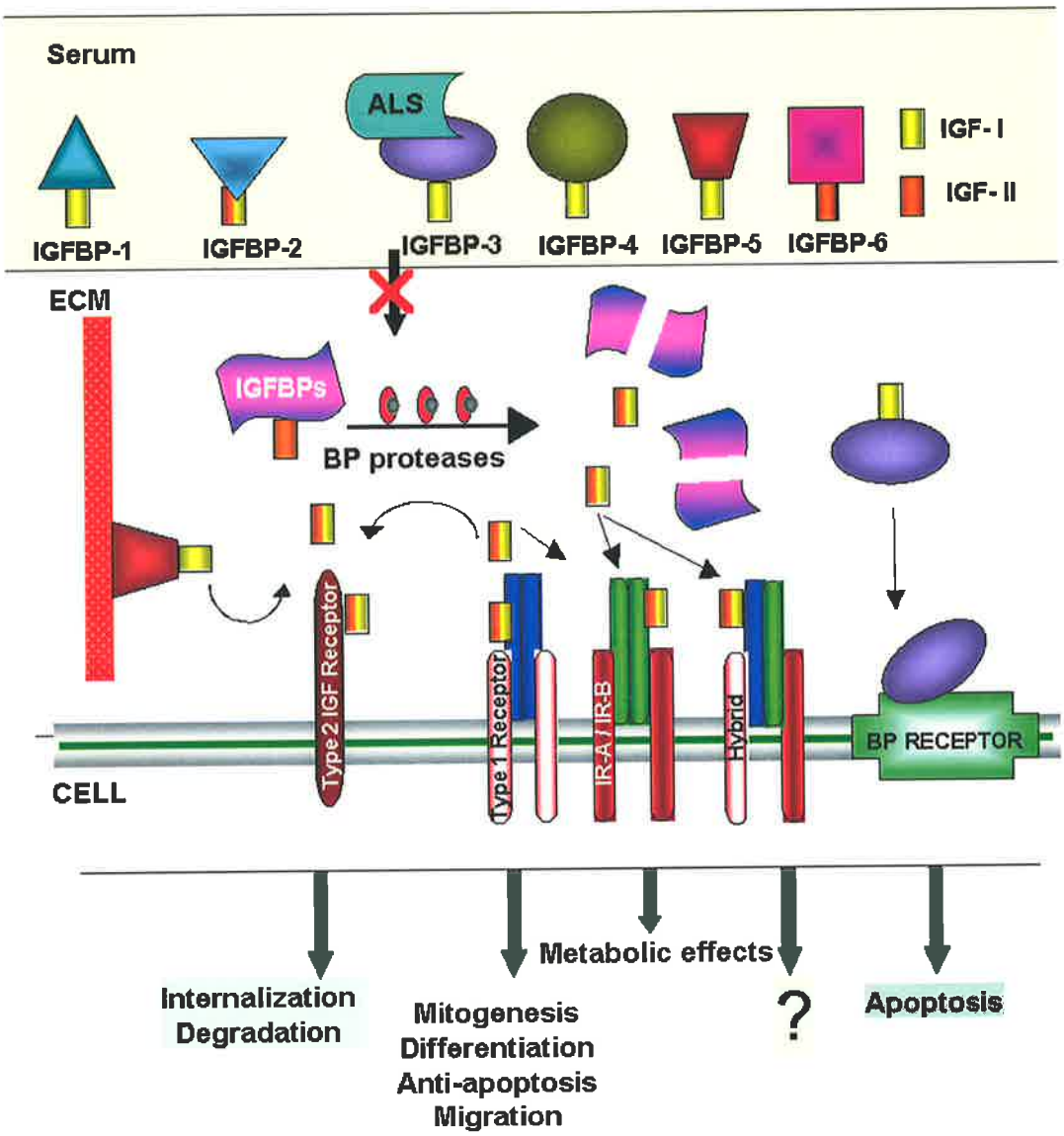

Figure 1.1 Schematic of the insulin/IGF system.

This figure shows most components of the insulin/IGF system and their interactions. Although all six binding proteins bind IGF-I and IGF-II in the circulation, IGFBP-3 is the most abundant binding protein and binds the majority of circulating IGF-I and IGF-II in a 150 kDa complex with acid-labile subunit (ALS). This ternary complex protects the IGFs from proteases in circulation and also prevents the IGFs traversing the vascular membrane into the extracellular space (Jones and Clemmons, 1995). Association of IGFBPs with the extracellular matrix (ECM) decreases their affinity for the IGFs and then allows the binding of the IGFs to an insulin/IGF family receptor. Binding of an IGF to either of the insulin receptor isoforms or IGF-1R causes a number of biological responses (Adams *et al.*, 2000; Denley *et al.*, 2003). So far, the exact role of the hybrid receptors is not well understood in cell biology. The IGF-2R acts to internalise and degrade IGF-II but has no signalling capabilities (Scott and Firth, 2004). An IGFBP-3 receptor has been postulated, however its existence is yet to be confirmed (Firth and Baxter, 2002). Figure is adapted from (Denley *et al.*, 2005a).

1.3. IGF Ligands

IGFs are related to insulin at both the primary and tertiary levels of structure. These molecules have been widely conserved throughout vertebrate evolution as shown by the sequence of

IGF-I from the Atlantic Hagfish (Upton *et al.,* 1997) and lamprey (Moriyama *et al.,* 2000) (Figure 1.2).

IGF-I and IGF-II were first isolated from human serum nearly 30 years ago (Rinderknecht and Humbel, 1976). Although the main source of circulating IGFs is the liver, they are also produced in most tissues (O'Dell and Day, 1998). For example, the mRNA of IGF-I has been found in most human tissues in both the developing foetus and adult (Han *et al.*, 1988; Daughaday and Rotwein, 1989).

The physiological stimuli that regulate IGF-I production are not fully understood. However, growth hormone (GH) levels and nutrition show strong influences on IGF-I levels (Thissen *et al.,* 1994). In mice, pituitary secreted GH increases production of IGF-I by the liver (Mathews *et al.,* 1986). Although IGF-I can also be produced in tissues such as heart, uterus, spleen, lung and testes, the production in these tissues is mostly independent from GH (Mathews *et al.,* 1986; Lupu *et al.,* 2001).

The regulation of IGF-II production is not well understood in humans but is not regulated by GH. IGF-II can be found in many tissues and its level is generally higher than IGF-I (Han *et al.,* 1988). Recently some regulators for IGF-II expression have been reported. In skeletal myogenesis, nutrients and mammalian target of rapamycin (mTOR) regulate IGF-II expression at the cellular level (Erbay *et al.,* 2003). In addition, IGF-II expression is up-regulated during soleus regeneration following cardiotoxin injection in mice with targeted ablation of FGF6 (fibroblast growth factor 6) (Armand *et al.,* 2004).

Mice heterozygous for a targeted disruption of IGF-II exhibit a growth deficiency, achieving only 60% of their litter mates' body weight. These growth-deficient animals were otherwise normal and fertile. The effect of the disruption was exerted during the embryonic period (DeChiara *et al.,* 1990). In addition, homozygous mice with targeted disruption of IGF-I gene show a similar growth deficiency at 60%. However, these mice continue to show growth retardation postnatally and their average bodyweight is 30% of wild type mice (Liu *et al.,* 1993).

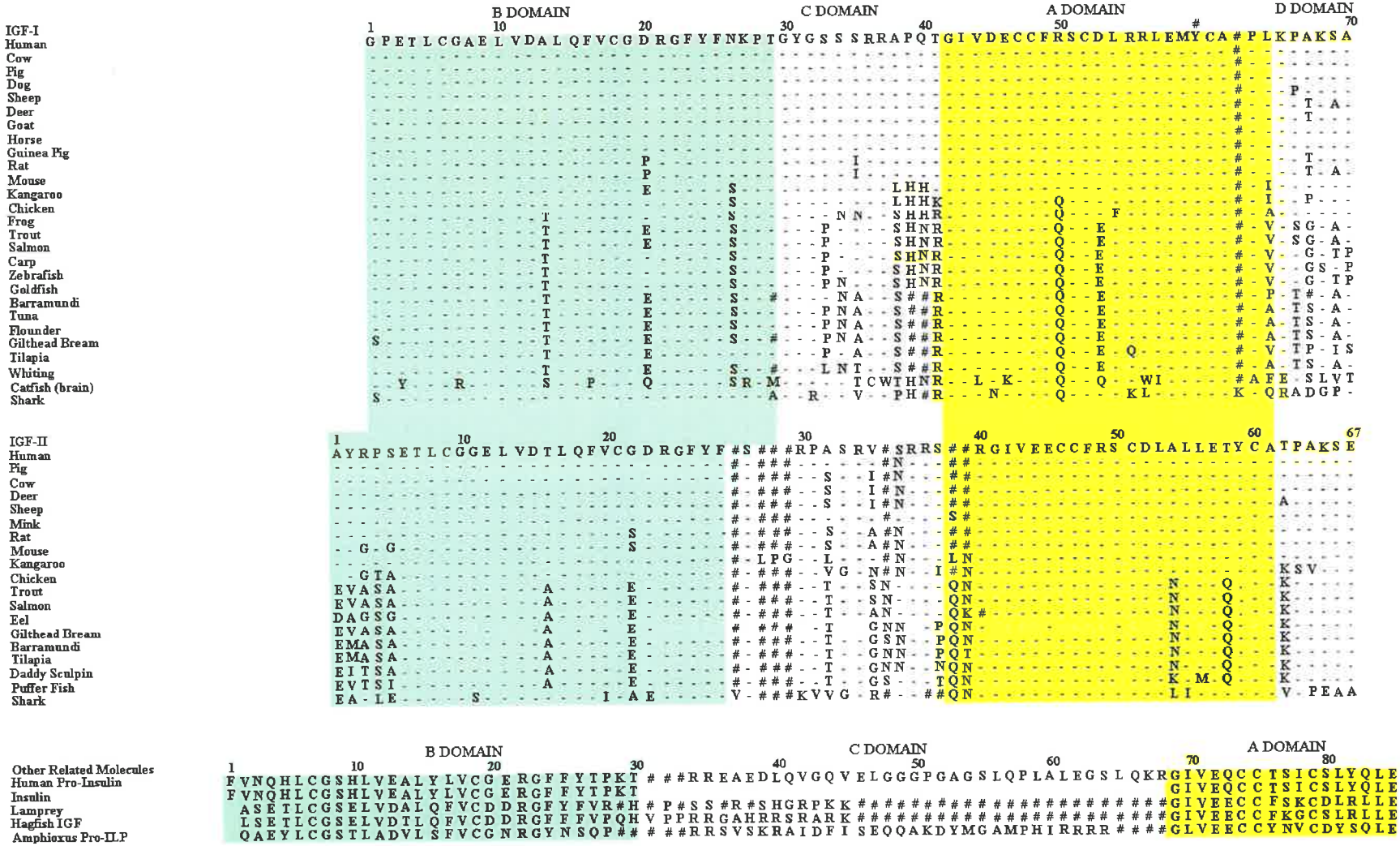

Figure 1.2 Comparative sequence data of the insulin-like growth factors.
Known amino acid sequences of different IGF-I and IGF-II species. Dashed lines represent identical sequences compared to human counterparts and # was used to frame shift peptides for maximal alignment between sequences. Complete amino acid sequences are given for IGF related molecules. Figure is adapted from a leaflet produced by GroPep Ltd., Thebarton, SA, Australia.

IGF-I and IGF-II have a high degree of sequence identity (70%) to each other and to proinsulin (50%) (Rotwein, 1991; Werner and LeRoith, 1996). In addition, IGFs and insulin share a common three-dimensional (3D) structure (Sato *et al.,* 1993; Terasawa *et al.,* 1994; Torres *et al.,* 1995). IGF-I and IGF-II are 70 and 67 amino acid single-chain polypeptide hormones with the molecular weight of 7649 and 7471 Daltons respectively (Daughaday and Rotwein, 1989; Humbel, 1990; Thissen *et al.*, 1994). The structure of IGFs is composed of four domains named B, C, A and D from the N-terminus. For IGF-I, amino acid residues Gly1 to Thr29, Gly30 to Thr41, Gly42 to Cys62 and Ala63 to Ala70 and for IGF-II, Ala1 to Phe28, Ser29 to Arg40, Gly41 to Ala61 and Thr62 to Glu67 of IGF-II, correspond to domains B, C, A and D respectively (Rotwein, 1991). In IGF-I and IGF-II the C domain is a highly mobile region linking the B and A chains. In proinsulin the C peptide is analogous to the C domain of IGF-I and IGF-II but it is normally removed by enzymatic processing in insulin (Foulstone *et al.,* 2005). Both IGF-I and IGF-II contain a D domain at the C-terminus and it has no equivalent in insulin. The prepropeptide forms of the IGFs are made of an N-terminal signal sequence and one of the two alternative forms of C-terminal E domain that arise from alternative splicing of the mRNA (Daughaday and Rotwein, 1989). Both the N- and C-terminal extensions are post-translationally cleaved (de Pagter-Holthuizen *et al.,* 1986).

The first attempts for modelling the molecular structure of IGFs were based on the crystal structure of insulin (Blundell *et al.,* 1978; Blundell *et al.,* 1983). Since then, the three-dimensional structure of IGF-I has been identified by both Nuclear magnetic resonance (NMR) (Figure 1.3) (Cooke *et al.,* 1991; Sato *et al.,* 1993; Schaffer *et al.,* 2003) and X-ray crystallography methods (Vajdos *et al.,* 2001; Zeslawski *et al.,* 2001; Brzozowski *et al.,* 2002). The structure of IGF-II has only been studied by NMR (Terasawa *et al.,* 1994; Torres *et al.,* 1995).

It can be seen from structural studies that human IGFs and insulin consist of a small hydrophobic core which is composed of three major alpha helices and stabilised by three disulphide bonds (Hober *et al.,* 1992; Milner *et al.,* 1995). The first helix is in the B domain

and includes amino acids Gly7-Cys18 for IGF-I and Glu 12-Cys 21 for IGF-II. The second and third helices are both located in the A domain. Helix 2 is comprised of residues Ile43-Cys47 for IGF-I and Glu44-Arg49 for IGF-II. Helix 3 incorporates Leu54-Leu57 (Brzozowski *et al.*, 2002) for IGF-I and Leu53-Tyr59 for IGF-II (Torres *et al.*, 1995). Three disulphide bonds hold the folded three-dimensional structure of the IGFs together. The location of three disulphide bonds are Cys6-Cys48, Cys18-Cys61 and Cys47-Cys52 for IGF-I and Cys9-Cys47, Cys21-Cys60 and Cys46-Cys51 for IGF-II.

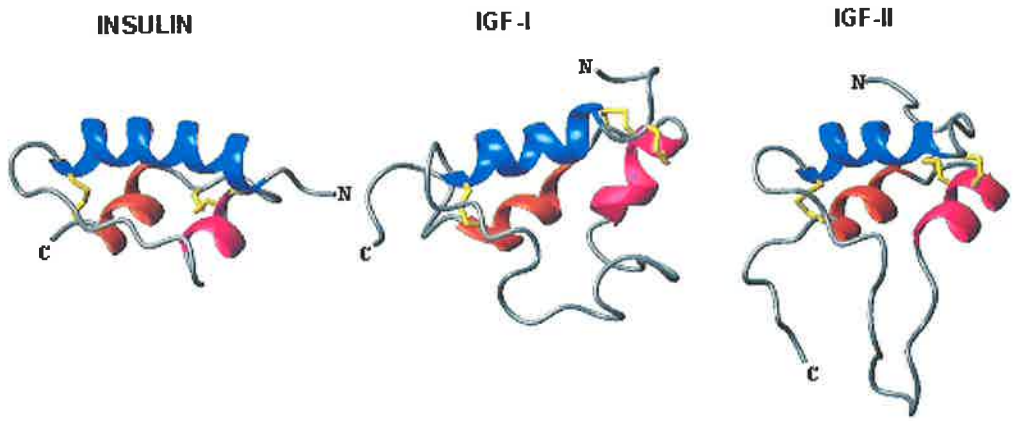

Figure 1.3 Comparison of the 3D structures of insulin, IGF-I and IGF-II.

The structure of insulin (Bentley *et al.*, 1976), IGF-I (Sato *et al.*, 1992; Sato *et al.*, 1993) and IGF-II (Torres *et al.*, 1995) are aligned along the B domain helix shown in blue. The N- and C-termini are symbolised as N and C respectively. The first and second A domain helix are shown in pink and red respectively. The three disulphide bonds are coloured in gold. Figure is adapted from (Denley *et al.*, 2005a).

The two crystal structure studies on IGF-I in the presence of detergents have shown the C-region of the IGF-I extends away from the hydrophobic core of the IGF-I and both revealed a type-II β turn comprised of residues Gly30-Ser33 of the C domain, displaying Tyr 31 at the tip of the region (Vajdos *et al.*, 2001; Brzozowski *et al.*, 2002). In addition, in the secondary structure of IGF-I there are two other small β turns. A type II′ β turn and a type VIII β turn which are located at residues 18-21 and 24-27 of IGF-I respectively. The type II′ β redirects the B-helix into an extended region while the type VIII β turn makes the C-domain extend away from the core of the molecule (Vajdos *et al.*, 2001).

1.3.1. IGF Ligand Binding Characterisation

Although there are considerable structural similarities between IGF-I and IGF-II, they do show different functional and hence physiological properties in the mammalian body. IGF-I and IGF-II have different affinities for the receptors and IGFBPs of the IGF system. As outlined in Table 1-1, IGF-I and IGF-II have different affinities for each of the six IGFBPs (Magee *et al.*, 1999; Nakae *et al.*, 2001). In addition, IGF-I binds to IGF-1R with a higher affinity than IGF-II (Hodgson *et al.*, 1996; Denley *et al.*, 2004) and binds to the IGF-2R with much less affinity than IGF-II as shown in Table 1-1 (Tong *et al.*, 1988). Table 1-1 shows the relative affinities of IGF-I and IGF-II for the IGFBPs (1-6) and the IGF system receptors; IGF-1R, IGF-2R, IR-A, IR-B and hybrid receptors.

Receptor	IGF-I (IC_{50} nM)	IGF-II (IC_{50} nM)	Insulin (IC_{50} nM)
IGF-1R (Pandini *et al.*, 2002)	0.2	0.6	> 100*
IR-A (Pandini *et al.*, 2002)	120*	0.9	0.2
IR-B (Pandini *et al.*, 2002)	366*	11	0.3
Hybrid-A (Pandini *et al.*, 2002)	0.3	0.6	3.7
Hybrid-B (Pandini *et al.*, 2002)	2.5	15	> 100*

Receptor/IGFBP-	IGF-I (K_D nM)	IGF-II (K_D nM)	Insulin (K_D nM)
IGF-2R (Tong *et al.*, 1988)	4×10^{-4}	0.2	N.B.
IGFBP-1 (Bach *et al.*, 1993)	125 (12.1)[a]	77 (5.3)[a]	N.B.
IGFBP-2 (Bach *et al.*, 1993)	19.6	5.9	N.B.
IGFBP-3 (Bach *et al.*, 1993)	3.3	1.3	N.B.
IGFBP-4 (Bach *et al.*, 1993)	17.2	9.1	N.B.
IGFBP-5 (Bach *et al.*, 1993)	45.4	6.25	N.B.
IGFBP-6 (Bach *et al.*, 1993)	1.75	0.25	N.B.

Table 1-1 Binding affinities of IGF-I and IGF-II for different IGFBPs, IR-A, IR-B, IGF-1R and IR/IGF-1R hybrids.

*=(Denley *et al.*, 2004) N.B.= no binding
[a]=affinities propably representing phosphorylated (high affinity) and dephosphorylated (low affinity) IGFBP-1.

1.4. IGFBP Structure and Function

To date, six IGFBPs have been isolated and sequenced from biological fluids and shown to bind IGFs with high affinity. In addition, several low affinity IGFBPs have been reported (Hwa *et al.*, 1999). The length of these six IGFBPs is between 216 to 289 amino acids

(Rosenzweig, 2004). Based on the IGFBPs structure, each IGFBP consists of three distinct domains of approximately equal size. The N- and C-terminal are highly conserved, and together contain 16–18 spatially conserved cysteine residues, which form the several intra-domain disulphide bonds, 5 or 6 in N-domain and 3 in C-domain (Forbes *et al.*, 1998; Hwa *et al.*, 1999). The middle or linker domain is the least conserved region across the six IGFBPs (Hwa *et al.*, 1999). In spite of clues from structural homology among the six IGFBPs, the actual identification of the IGF binding domain is yet to be completely defined. Accumulating evidence implies that sequences and residues important for IGF binding may vary across the IGFBP family (Rosenzweig, 2004). Based on study of mutations, truncations, and modifications of residues and regions of the N- and C-terminal, both domains are involved as participants in IGF binding (Rosenzweig, 2004). The high affinity IGFBPs are widely known as modulators of IGFs activity (reviewed in (Jones and Clemmons, 1995; Firth and Baxter, 2002)). These binding proteins increase the half-life of IGFs and can inhibit IGFs binding to their receptors.

The regulating effects and action of IGFBPs in circulation have been addressed in several reviews (Baxter, 1995; Jones and Clemmons, 1995; Murphy, 1998). Briefly, IGFBP-3, which is the most abundant circulating IGFBP, has the major IGF transport function in plasma. More than 75% of serum IGF-I and IGF-II are transported in heterotrimeric complexes that contain a liver-derived acid-labile subunit (ALS). IGFBP-5 can form similar ternary complexes to a lesser degree (Daughaday and Rotwein, 1989; Rosen and Pollak, 1999). In addition, all six IGFBPs are found in the circulation in the free form or in binary complexes with IGFs. These free or binary complexed IGFBPs exit the circulation rapidly while ternary complexes are essentially limited to the vascular compartment (Guler *et al.*, 1989; Young *et al.*, 1992; Lewitt *et al.*, 1994).

In addition to the IGFBPs' roles in IGF transport, these six binding proteins regulate cell activity in different ways (reviewed in (Firth and Baxter, 2002)). The IGFBPs, by sequestering the IGFs away from the IGF-1R, can inhibit mitogenesis, differentiation,

survival, and other IGF stimulated effects. IGFBP proteolysis can revoke this inhibition or generate IGFBP fragments with different bioactivity. Alternatively, IGFBP interaction with cell or matrix components may concentrate IGFs near their receptor, increasing IGF activity. IGF receptor-independent IGFBP activities are also increasingly recognized. IGFBP-1 interacts with alpha (5) beta (1) integrin, affecting cell adhesion and migration. IGFBP-2, -3, -5, and -6 contain heparin-binding domains and can bind glycosaminoglycans. IGFBP-3 and -5 have C-terminal basic motifs incorporating heparin-binding and extra basic residues, which interact with the cell surface and matrix, the nuclear transporter importin-beta, and also other proteins. Serine/threonine kinase receptors are anticipated for IGFBP-3 and -5, however their signaling functions are less understood. Other cell surface IGFBP-interacting proteins are uncharacterised as functional receptors. However, IGFBP-3 binds and regulates the retinoid X receptor-alpha, interacts with TGFbeta signaling through Smad proteins, and affects other signaling pathways. These interactions can modulate cell cycle and apoptosis. Since IGFBPs regulate cell functions by diverse mechanisms, manipulation of IGFBP-regulated pathways is considered to provide therapeutic opportunities in cancer and other diseases (Firth and Baxter, 2002).

1.5. The Structure and Function of the Receptors

In the IGF system, three main receptors have been described with different affinities for IGF-I and IGF-II: the IGF 1R, the IR and the M6-P/IGF2R (Czech, 1989). The first two receptors belong to the transmembrane tyrosine kinase receptors family (Hubbard and Till, 2000).

The first evidence for distinction of IGF-1R from IR was reported in 1974 (Megyesi *et al.,* 1974). The structure of the IGF-1R and IR are very similar but IGF-2R exhibits a different structure. The IGF-1R and the IR are tyrosine kinase receptors and exhibit 41% to 84% amino acid sequence identity depending on the domain (Ullrich and Schlessinger, 1990; Adams *et al.*, 2000). They are both tetrameric transmembrane receptors made of two α and two β subunits. The α subunits are entirely extracellular while the β subunits are membrane

spanning and the subunits arrange a β-α-α-β configuration (Czech, 1982). The α subunits contain the majority of ligand binding sites (Schaefer *et al.,* 1990; Brandt *et al.,* 2001) and the β subunits contain the tyrosine kinase domain (Kasuga *et al.,* 1982).

The IGF-1R and IR can also form hybrid heterodimer receptors that are comprised of one half of each receptor (Soos *et al.,* 1990).The hybrid receptors exhibit high affinity for the IGF-I and low affinity for insulin (Soos *et al.,* 1993). The hybrid receptors containing the IR-A (IGF-1R/IR-A) bind to IGF-I and IGF-II with high affinity and they bind to insulin with about 20 fold lower affinity than IR-A (Table 1-1) (Pandini *et al.,* 2002). However, the hybrid receptors containing the IR-B (IGF-1R/IR-B) bind with high affinity to IGF-I and with low affinity to IGF-II and trivially to insulin (Pandini *et al.,* 2002). In addition, IGF-1R/IR-A exhibits higher affinity for IGFs compared to IGF-1R/IR-B (Pandini *et al.,* 2002).

IGF-2R is a transmembrane and monomeric receptor that binds to mannose 6-phosphate residues on lysosomal enzymes (reviewed in (Nielsen, 1992; Jones and Clemmons, 1995)). This receptor is a multifunctional protein. It binds to both IGF-II and to M6-P-bearing lysosomal enzymes and mediates the rapid internalisation and degradation of IGF-II. Hence, this receptor might be involved in the IGF-II clearance from the circulation (Nielsen, 1992; Pavelic *et al.*, 2003). Mutant mice lacking IGF-2R/M6P usually die perinatally and hardly ever survive to adulthood while they were completely rescued when they carry a second mutation eliminating either IGF-II or IGF1R (Ludwig *et al.,* 1996). The IGF-2R mutants also exhibited increased serum and tissue levels of IGF-II and had overgrowth (Ludwig *et al.,* 1996).

1.5.1. IR Function and Structure

Many mutagenesis studies have shown the IR is essential for normal postnatal growth and fuel homeostasis. Although mice homozygous for a targeted disruption of the IR are born with a slight reduction in birth weight (10%), they die from diabetic ketoacidosis several days after birth (Louvi *et al.,* 1997). Therefore, these results suggest that the IR is not crucial for

embryonic growth but it is very important for postnatal normal metabolic actions. The expression of IR isoforms varies in different tissues. In normal human physiology the IR-A is expressed predominantly in fetal tissues including liver, fibroblast, kidney and muscle (Frasca *et al.,* 1999). The IR-B has been shown to be expressed mostly in adipose tissue and the liver (Seino and Bell, 1989; Mosthaf *et al.*, 1990). These suggest that the IR-A could be considered as the fetal form, while IR-B exists in differentiated and adult tissues (Denley *et al.,* 2003). Alternative splicing of the IR exon 11 is regulated both developmentally and in a tissue-specific manner (Moller *et al.*, 1989; Seino and Bell, 1989; Mosthaf *et al.*, 1990; Frasca *et al.*, 1999). For instance, in some cell lines and tissues which are responsive to insulin, the expression of IR-B is induced by insulin and high glucose concentration (Denley *et al.,* 2003).

The biochemical and biophysical properties of the IR isoforms have been investigated as possible causes for various diseases particularly in cancer and type 2 diabetes (Belfiore *et al.,* 1999; Sesti *et al.,* 2001). Interestingly in myotonic dystrophy, increased prevalence of the lower kinase activity of IR-A was considered as the cause of insulin resistance (Savkur *et al.,* 2001; Savkur *et al.,* 2004). The role of the IR isoforms in cancer will be discussed more in Section 1.6.4.

As mentioned earlier, the structure of the IR is very similar to IGF-1R (reviewed in (Adams *et al.*, 2000; Siddle *et al.*, 2001; De Meyts and Whittaker, 2002)). The early studies on the primary structure of the IR revealed two different sequences for the receptor which were differed by 12 amino acids (Figure 1.4) (Ebina *et al.*, 1985; Ullrich *et al.*, 1985). Further characterisation of the receptor showed that the alternative splicing of exon 11, which is a 36 base-pair exon, resulted in the 12 amino acid difference between the two isoforms (Seino and Bell, 1989). These 12 amino acids (residues 717-728) can be found at the extreme C-terminus of the α subunits of the IR-B isoform. The IR-A isoform does not contain these 12 residues and shows different ligand binding properties (Seino and Bell, 1989; Denley *et al.*, 2004). Binding affinities of IGF-I and IGF-II for different IGFBPs, IR-A, IR-B, IGF-1R and IR/IGF-1R hybrid receptors is summarized in (Table 1-1) (Mosthaf *et al.*, 1990; McClain, 1991;

Yamaguchi *et al.*, 1991; Yamaguchi *et al.*, 1993; Kotzke *et al.*, 1995; Frasca *et al.*, 1999). Interestingly, variability has been observed for absolute affinities in different binding studies. For example, the affinity of IR-B for IGF-I, IGF-II and insulin is reported as less than these for IR-A (Pandini *et al.*, 2002) (Table 1-1). However, in another study using a different assay, it has been shown that the affinity of IR-B for insulin is slightly higher than that for IR-A (Denley *et al.*, 2004). Though, in both studies the difference between the affinities of IR-A and IR-B to insulin is very small and about 2-fold.

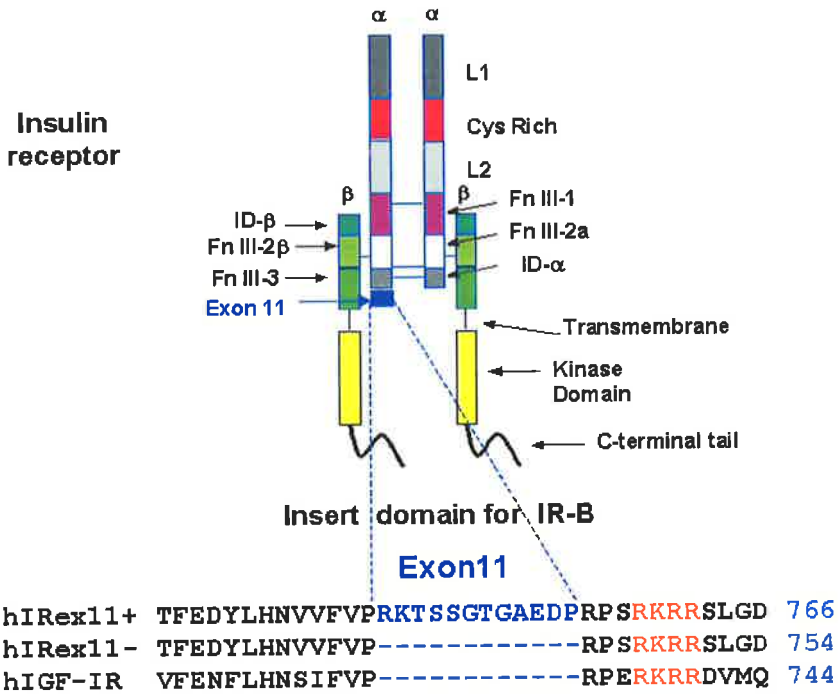

Figure 1.4 The mature insulin receptor.

Domain structure of the IR is shown: L1 and L2; large domains 1 and 2 (Leucine-rich repeats); Cysteine-Rich, cysteine rich domain; FnIII-1, FnIII-2, FnIII-3, fibronectin type III domains; ID, Insert domain; Exon 11, Exon 11 encoded peptide; Transmembrane, Transmembrane domain, kinase domain, Tyrosine-kinase domain; and C-terminal tail. Exploded is the amino acid sequence of Exon 11 (coloured blue) and its flanking residues. Shown for comparison are the sequences of the human IR Exon 11+, human IR Exon 11- and human IGF-1R. Orange residues indicate the furin cleavage site, which upon cleavage of the proreceptor liberates discrete α and β subunits. Figure is adapted from (Denley *et al.*, 2003).

1.5.2. IGF-1R Function and Structure

Most of the cellular effects of the IGFs are mediated by the IGF-1R and this receptor plays crucial roles in mammalian growth and development. Mutant mice null for the IGF-1R gene exhibit growth deficiencies and die after birth (Baker *et al.*, 1993; Liu *et al.*, 1993). IGF-1R

mutations, partial deletions or hemizygosity at the IGF-1R locus in humans either reduce the number of cell surface receptors or sensitivity to IGF-I and lead to prenatal growth retardation that continues to adulthood (Roback *et al.,* 1991; Tamura *et al.,* 1993; Peoples *et al.,* 1995; Siebler *et al.,* 1995; Abuzzahab *et al.,* 2003; Okubo *et al.,* 2003). The IGF-1R is also important in proliferation and differentiation, apoptosis and cellular transformation (reviewed in (Adams *et al.,* 2000)). The involvement of the IGF-1R in cancer is widely known and will be discussed in Section 1.6.5.

The size of the human *IGF-1R* gene is greater than 100 kb and has 21 exons, 10 in the α-chain and 11 in the β chain (Abbott *et al.,* 1992).

Several studies have implied that heterogeneity exists in the β subunit of IGF-1R. Two alternatively spliced human IGF-1R messenger RNA (mRNA) transcript have been reported which differ by three nucleotides (CAG) starting at position 2829. This results in the replacement of Thr-Gly to Arg in the extracellular portion of IGF-1R beta subunit. The isoform with no CAG displays reduced internalisation and increased signalling properties compared with the other isoform (CAG +) (Yee *et al.,* 1989; Condorelli *et al.,* 1994).

The human IGF-1R complementary DNA (cDNA) was cloned and sequenced about 20 years ago (Ullrich *et al.,* 1986). It contains 4989 nucleotides, which codes for a 1367 amino acid precursor. The preproreceptor includes a signal peptide (residues –30 to – 1) and also an Arg-Lys-Arg-Arg furin protease cleavage site at residues 708-711, which on cleavage yields one α chain and one β chain encompassing residues 1-707 and 712-1337 respectively (Adams *et al.,* 2000).

Figure 1.5 shows the structure of the mature IGF-1R. The extracellular part of the receptor contains the α subunits of the receptor and 194 residues of the β subunits (Ullrich *et al.,* 1986). The cytoplasmic domain of the IGF-1R contains the tyrosine kinase domain (Ullrich *et al.,* 1986).

Several studies to determine the steps involved in the expression, folding and assembly of the mature human IR homodimer have been conducted and provides a good

model for the biosynthesis of IGF-1R (reviewed in (Adams *et al.*, 2000)). The IGF-1R is glycosylated via 16 potential N-linked glycosylation sites (Ebina *et al.*, 1985; Ullrich *et al.*, 1985; Ullrich *et al.*, 1986). Residue numbers of the potential N-linked glycosylation sites in human IGF-1R are as follows: 21, 72, 105, 214, 284, 387, 408, 504, 577, 592, 610, 717, 726, 734, 870, 883 (Elleman *et al.*, 2000).

Comparative sequence analyses have shown that many eukaryotic extracellular proteins are comprised of several different or sometimes repeated structural units (Adams *et al.*, 2000). In each monomer of the IGF-1R, 11 different regions have been recognized. The N-terminal part of the receptor ectodomain contains L1, cysteine-rich and L2 domains. The cysteine-rich domain is placed between the L1 and L2 domains (Bajaj *et al.*, 1987; Ward *et al.*, 1995; Garrett *et al.*, 1998) (Figure 1.5). The C-terminal part of the IGF-1R ectodomain is comprised of three domains, which are fibronectin type III (FnIII) with the second one containing an insert domain of 120-130 amino acids (O'Bryan *et al.*, 1991; Marino-Buslje *et al.*, 1998; Mulhern *et al.*, 1998). The intracellular part of each monomer contains the tyrosine kinase catalytic domain (residues 973-1229) flanked by a juxtamembrane region (residues 930-972) and C-tail region comprised of 108 residues (1230-1337), which contain the phosphotyrosine binding sites for signalling molecules (Adams *et al.*, 2000).

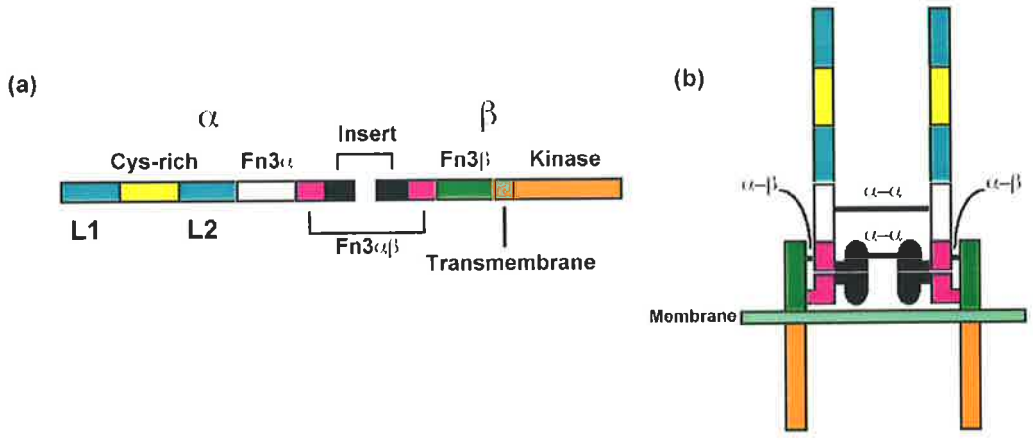

Figure 1.5 The α and β chains form an αβ heterodimer, of which two then associate to form the intact $(\alpha\beta)_2$ receptor.

(a) The domain structure of the insulin-receptor family αβ subunit. (b) Schematic of the intact receptor, showing the interchain α-α and α–β disulphide linkages. Figure is adapted from (Mulhern *et al.*, 1998).

The 3D structure of the first 3 domains of the IGF-1R (L1-cysteine-rich-L2) has been solved as shown in Figure 1.6. This 3D crystal structure shows the size of this molecule is approximately 40 × 48 × 105 Å. The cysteine-rich domain occupies two-thirds of the length of the molecule and is in contact with L1 region but appears to have very little contact with the L2 region (Garrett *et al.,* 1998). The different orientations of L1 and L2 relative to the cysteine-rich domain are possibly due to an artefact of crystal packing. In the native structure, the L2 domain position could be more parallel to L1 (De Meyts and Whittaker, 2002). This crystal structure has a 24 Å diameter space in the centre of the molecule and of adequate size to accommodate the ligands IGF-1 or IGF-II. This space is surrounded on three sides by the regions of IGF-1R which are important in ligand binding derived from studies of receptor chimeras, chemical cross-linking and natural or site-specific mutants (Garrett *et al.,* 1998). However, the structures of the intact IGF-1R or IR have not been solved yet (Garrett *et al.,* 1998). It should be noted that this L1-cystein-rich-L2 fragment does not bind the ligand (De Meyts and Whittaker, 2002) but after the addition of α-subunit carboxy-terminal peptide (residues 704-719), does bind with low affinity (Kristensen *et al.*, 1998; Molina *et al.*, 2000).

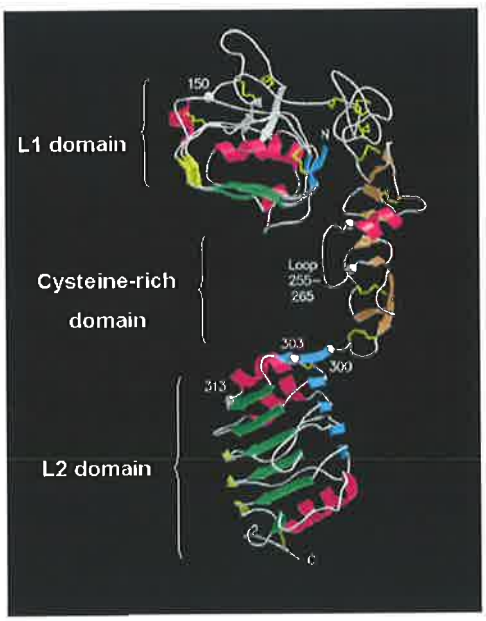

Figure 1.6 Crystal structure of the first three domains of the IGF-1R (residues 1-459).

The L1 domain is at the top, viewed from the N-terminal end. The space at the centre is of adequate size to accommodate IGF-I. Helices are indicated by curled ribbon and β-strands by broad arrows for the IGF-1R. Figure is adapted from (Garrett *et al.,* 1998).

Both L1 and L2 domains of the IGF-1R (residues 1-150 and 300-460) are approximately 24 × 32 × 37 Å. Each of them is formed from a single-stranded right-handed β-helix, capped on the ends by short helices and disulphide bonds (Garrett *et al.,* 1998). The base consists of a flat six-stranded β-sheet five residues long (green in Figure 1.6) and the sides comprised from β-sheets three residues long (blue and yellow in Figure 1.6) and each has an irregular top (Garrett *et al.,* 1998). A remarkable difference between the L1 and L2 domains at their C-terminal ends has been reported. The indole ring of Trp176 from the cysteine-rich region, is inserted into a pocket in the hydrophobic core of L1 shaped by residues Ile98, Gly99, Leu100 and Leu103 from the fourth turn and Val125, Trp127 and Ile130 from the fifth turn of L1, which are the last two turns of the β-helix (Garrett *et al.,* 1998; Adams *et al.,* 2000). The sequence motif of residues that form the Trp pocket in L1, does not arise in L2 of the IR/IGF-1R family (Garrett *et al.*, 1998).

The cysteine-rich region is made of modules with disulphide bond connectivities which are similar to parts of the tumour-necrosis-factor (TNF) receptor (Banner *et al.,* 1993) and laminin repeats (Garrett *et al.,* 1998; Stetefeld *et al.,* 2000). The first module sits at the end of L1 domain and the rest of the modules (seven) form a curved rod running diagonally across L1 and reaching to L2 (Garrett *et al.,* 1998) (Figure 1.6).

The FnIII domain is one of the most common structural modules in many membrane-anchored receptors. The 3D structures for several FnIII domains have been reported (Dickinson *et al.,* 1994; Adams *et al.,* 2000). These domains are comparatively small, made of about 100 residues and consist of a seven-stranded β-sandwich in a three-on-four (EBA:GFCC') topology. The major function of a FnIII domain is to mediate protein-protein interactions such as ligand binding and to act as a spacer to properly position functionally important regions of extracellular proteins (Adams *et al.,* 2000).

The 3D structure of the tyrosine-kinase domain of the human IR, which is closely related to IGF-1R, has been solved for both the inactive state (unphosphorylated) (Hubbard *et*

al., 1994) and the active state (tris-phosphorylated in combination with and ATP analogue and a peptide substrate) (Hubbard, 1997). Also the crystal structures of the activated (Favelyukis *et al.,* 2001; Pautsch *et al.,* 2001) and unactivated (Munshi *et al.,* 2002; Munshi *et al.,* 2003) forms of IGF-1R kinase have been solved. The studies on activated form of the kinase domain have shown a 2.1 Å crystal structure of the IGF-1R tyrosine kinase phosphorylated at two tyrosine residues in the activation loop (IGF-1RK2P) and bound to an ATP analog. The ligand is not in a conformation compatible with phosphoryl transfer and the activation loop is partially disarranged. Compared to the insulin receptor kinase, IGF-1RK2P is trapped in a half-closed conformation. Conformational changes upon kinase activation are triggered by the degree of phosphorylation and are critically dependent on the conformation of the proximal end of the kinase activation loop (Pautsch *et al.,* 2001). The studies on unactivated kinase domain have shown it is composed of two lobes linked by a hinge region. The kinase's N-terminal lobe is a twisted beta-sheet flanked by a single helix, and the C-terminal lobe includes four short beta-strands and eight alpha-helices. The ATP binding pocket and the catalytic centre are at the interface of the two lobes. Although this tyrosine domain is generally similar to other receptor tyrosine kinases, the following notable conformational modifications were observed: this kinase with its two lobes rotated further toward each other and adopts a more closed structure, the conformation of the proximal end of the activation loop (residues 1121-1129) is not the same and the orientation of the nucleotide-binding loop is changed (Munshi *et al.,* 2002). Together, these alterations lead to a different ATP-binding pocket that might impact on design of inhibitor of the kinase domain. Two unactivated kinase domain molecules are seen in the asymmetric unit. They are associated as a dimer with their ATP binding clefts facing each other. The ordered N-terminus of one monomer approaches the active site of the other, implying that the juxtamembrane region of one molecule could come into close proximity to the active site of the other (Munshi *et al.,* 2002).

1.5.2.1. The IGF-1R and IR Ectodomain Structure

The major aspect that segregates the IGF-1R and other members of IR family from most other receptor families is that they are on the cell surface as disulphide-linked dimers and require domain re-arrangements rather than receptor oligomerization for cell signaling. To date, it is not known how the IGF-1R various domains are organized in the dimeric native receptor. Suggestions came from electron microscopy (EM) of single-molecule images of the IGF-1R ectodomain and more specifically the IR ectodomain and its complexes with three different well-characterised MAb derived Fab fragments (Tulloch *et al.*, 1999; Adams *et al.*, 2000). To obtain information about the molecular envelope and the arrangement of the IR domain, single-molecule images of the receptor ectodomain and its complexes with three different Fabs (originated from MAbs to IR) have been analysed by EM. The images exhibited that the IGF-1R and IR ectodomains resemble a U-shaped prism of approximate dimension 90 × 80 × 120 Å (Figure 1.7) (Tulloch *et al.*, 1999). These images revealed clearly the dimeric structure of IGF-1R and IR ectodomains (Adams *et al.*, 2000). The width of the cleft (assumed membrane-distal) between the two side arms is about 30 Å, which is sufficient to accommodate ligands (Tulloch *et al.*, 1999; Adams *et al.*, 2000).

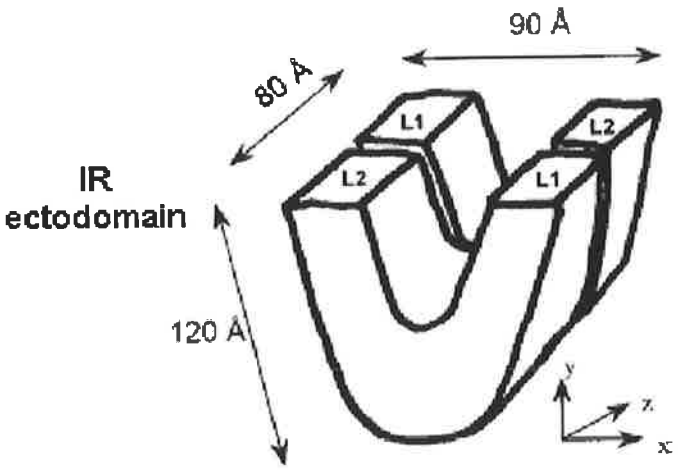

Figure 1.7 Schematic illustrating the proposed model of the IR ectodomain based on EM imaging. Figure is adapted from (Tulloch *et al.*, 1999).

The MAbs 83-7, 83-14 and 18-44 recognize the cysteine-region (residues 191-297), the first fibronectin type III domain (residues 469-592) and the insert domain (residues 765-770) of the IR respectively (Table 1-2). The Fab 83-7 binds half way up one end of each side arm in a diametrically opposite manner, indicating a two-fold axis of symmetry normal to the membrane surface (Tulloch *et al.,* 1999). Studies on the location of the sequence differences between human and mouse IRs and the EM images indicates residues 210 in the third cysteine-rich module and 236 in the fourth cysteine-rich module are part of the 83-7 epitope. They are located at one corner of the fragment in line with the centre of the L1 domain. This implies that the L1/cysteine-rich/L2 fragment spans the cleft between the parallel bars rather than lying within each parallel bar. Fabs 83-14 and 18-44 (see Table 1-2) bound close to base of the prism at opposite corners (Tulloch *et al.*, 1999). The single molecule images, together with the data from the 3D structure of the L1/cysteine-rich/L2 domains of the IGF-1R (Garrett *et al.,* 1998) indicate that the ectodomain dimer is organized into two layers with the L1/cysteine-rich/L2 domains occupying the upper (membrane-distal) region of the U-shaped prism while the fibronectin type III domains and the insert domains (and the disulphide bonds involved in dimer formation) are mainly located in the membrane-proximal region (Tulloch *et al.,* 1999; Adams *et al.,* 2000).

MAbs	Epitope	Effect on insulin binding
83-7	191-297 (CR)	No effect (Taylor *et al.,* 1987)
83-14	469-593 (Fn3α)	Inhibits (Taylor *et al.,* 1987)
18-44	765-770 (ID)	Inhibits (Taylor *et al.,* 1987)

Table 1-2 The epitopes of some of the anti-IR MAbs on the IR and their effect on insulin binding to the IGF-1R.

In other studies, T-, X- or Y-shaped structures have been identified with recombinant ectodomain (Schaefer *et al.,* 1992), detergent-solubilized whole receptors or vesicle-reconstituted whole receptors (reviewed in (Adams *et al.*, 2000)), which are substantially different from the U-shaped structure (Tulloch *et al.,* 1999). In addition, Luo *et*

al. (1999) and Ottensmeyer *et al.* (2000) suggested from their studies with electron cryomicroscopy and 3D reconstruction that the insulin-IR complexes adopted an approximately spherical structure with 150 Å diameter. They used existing structures of the L1-cysteine-rich-L2 domain of the IGF-1R (Garrett *et al.,* 1998) and the IR tyrosine kinase domain and fibronectin type III domains (Fn_{0-2}) to model the entire IR envelope obtained from the EM images. However, the details of these models should be regarded with doubt (De Meyts and Whittaker, 2002). For example, it is not obvious how the domains were docked in the protein envelope. Moreover, in these studies, the structures of unglycosylated recombinant mouse (Luo *et al.,* 1999) and human FnIII domains (Ottensmeyer *et al.,* 2000) of less than 100 residues were used, while the first two IR FnIII domains are substantially larger and glycosylated and there is no known structure of the large insert (De Meyts and Whittaker, 2002). In these studies also it is assumed that the native structure of L1-cysteine-rich-L2 is that obtained in the crystal structure of the IGF-1R whereas, this construct does not bind the ligand. The model is also inconsistent with the U-shaped prism for IR or IGF-1R ectodomain (Tulloch *et al.,* 1999). In addition, the predictions obtained from the model about the binding site for receptor-ligand binding (Luo *et al.,* 1999) ignore the role of the crucial amino acids, such as A19, for insulin binding (De Meyts and Whittaker, 2002).

1.5.2.2. IGF-1R Signaling

Activation of the IGF-1R upon ligand binding results in activation of a range of intracellular signalling pathways (reviewed in (Gray *et al.*, 2003; O'Connor, 2003)). As mentioned earlier, IGF-1R and IR are structurally very similar and they both initiate overlapping signalling pathways. Many reviews have discussed whether IGF-1R and IR signalling pathways are the same or distinct (Benito *et al.*, 1996; Dupont and LeRoith, 2001; Nakae *et al.*, 2001; Siddle *et al.*, 2001; Kim and Accili, 2002). Here the pathways and molecular events of the major mechanisms for IGF-1R signalling will be discussed. However, they are also applicable to IR signalling.

Binding of ligands to the IGF-1R allows transphosphorylation of the receptor. Phosphorylation of tyrosine residues in the β subunit provides docking sites for proteins such as IRS-1 (insulin receptor substrate 1) and Shc (Src homology/ collagen). These adaptor proteins are phosphorylated by the IGF-1R kinase and these phosphorylation sites then provide binding sites for SH2 domains of signalling molecules such as Grb2 (Growth factor receptor binding protein 2). The guanine nucleotide exchange factor Sos is constitutively connected to Grb2 and it promotes the exchange of Ras-bound GDP to GTP thereby activating Ras. The progression of protein-protein interactions then comprise the mitogen-activated protein kinase (MAPK) pathway (Chang and Karin, 2001).

Once IRS-1 is phosphorylated, p85, which is the regulatory subunit of PI3K (phosphoinositide 3-kinase), can bind by its two SH2 domains. The p85 binds to the catalytic subunit of PI3K, of which p110 is one isoform, which consequently induces phosphorylation of phosphatidylinositol lipids such as phosphatidyl inositol (4,5) bisphosphate (PI (4,5) P2) and phosphatidyl inositol (4) phosphate (PI (4) P1). The P13K pathway is essential for protection from apoptosis, stimulation of protein synthesis through mTOR and its down stream targets and also the regulation of the cell cycle (Cantrell, 2001). JNK is a stress-activated kinase and the JNK pathway regulates transcription through phosphorylation of Jun proteins and it is also involved in apoptosis (Chang and Karin, 2001). The role of JNK in the IGF-1R signalling is not yet clear. JNK stimulates some cellular responses and also shows feedback regulatory effects for others (O'Connor, 2003). A summary of the signalling pathways for IGF-1R is shown in Figure 1.8.

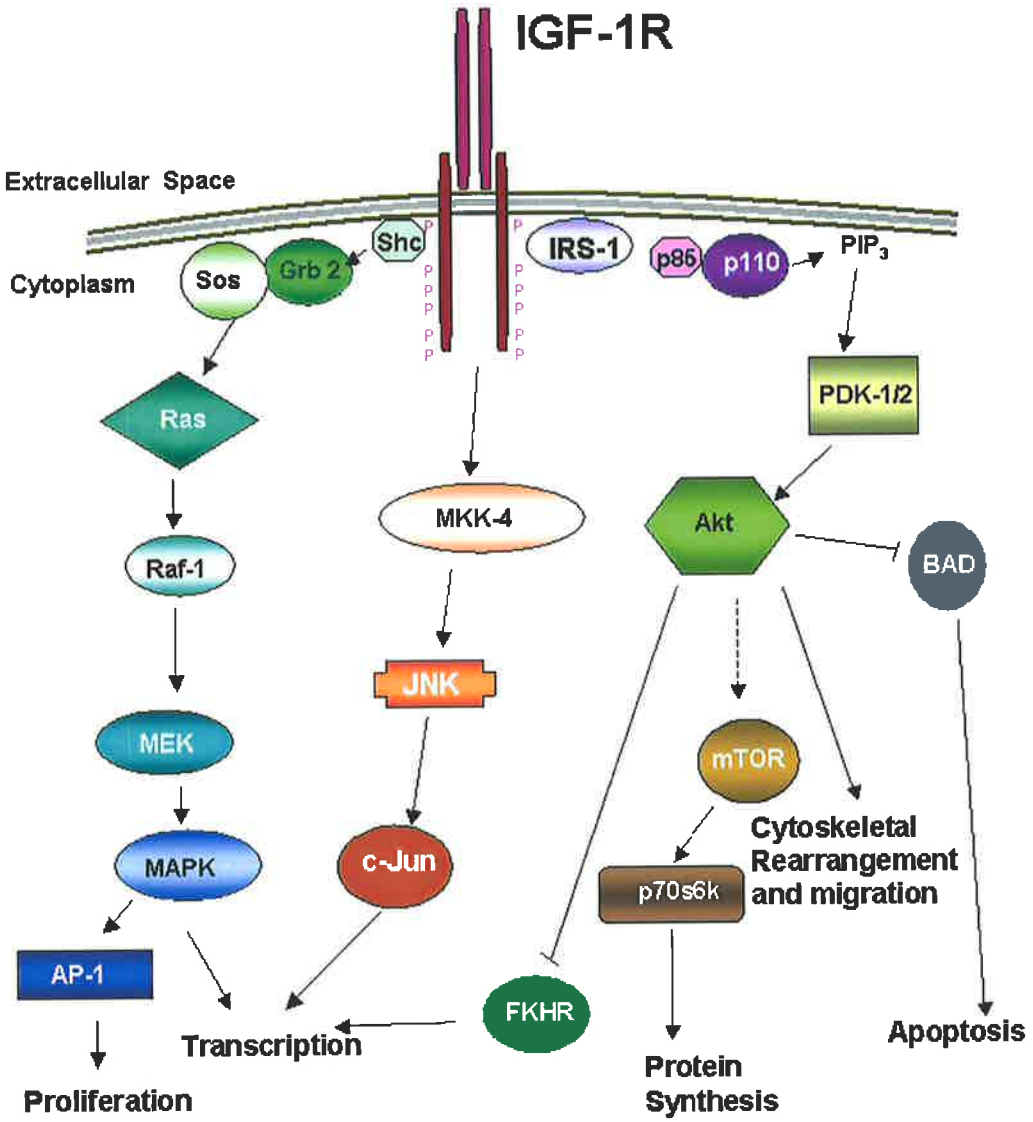

Figure 1.8 Signalling pathways activated by the IGF-1R (or IR).

Recruitment of IRS-1 and Shc to an activated IGF-1R/IR provides a mechanism for the activation of the MAPK and PI3K pathways. A sequence of molecular interactions results in either a change in transcription, cell proliferation, protein synthesis, protection from apoptosis or cytoskeleton rearrangement and promotion of migration. Figure is adapted from (Denley, 2004).

1.5.2.3. IGF-1R Residues Involved in IGF Binding

Chimeric IR/IGF-1R and alanine mutants of the IGF-1R have been used to determine the binding sites of the IGF-1R for binding to different ligands such as IGF-I and IGF-II. However, very little is understood about the exact location and nature of the ligand binding sites.

To determine the specificity for insulin and IGF-I binding different regions of the IGF-1R and IR have been used to generate chimeras of the two receptors and tested for ligand binding (Figure 1.9) (reviewed in (Adams *et al.*, 2000)). Data for human IGF-1R/IR chimeras

revealed the importance of the cysteine-rich region of the IGF-1R in IGF-I binding (Gustafson and Rutter, 1990). Studies with ectodomain chimeras provided similar results to those obtained with whole-receptor chimeras and showed that the IR based chimera containing IGF-1R residues 1-284 is similar to the IGF-1R ectodomain and exhibited high affinity for IGF-I but poor binding for insulin (Andersen *et al.,* 1990). However, the chimeras with smaller IGF-1R fragments, either 1-180 or 1-162, lack the appropriate specificity determinants for both ligands and revealed poor binding of both ligands (Kjeldsen *et al.,* 1991). The results obtained from other studies on IR/IGF-1R chimeras of both full-length receptor and ectodomain showed the cysteine-rich region of the IGF-1R play an important role to control specific binding to IGF-I and not to insulin (Gustafson and Rutter, 1990; Hoyne *et al.*, 2000b). It has been shown that the chimeric receptor in which residues 260 to 277 of IR were replaced with residues 253 to 266 of the IGF-1R increased the capacity of IGF-I to competitively displace labelled insulin compared to the parent IR (Hoyne *et al.,* 2000b). Moreover, it has been shown that the 52 amino acids in the cysteine-rich region between His-223 and Met-274 on the IGF-1R are crucial for IGF-I binding to the receptor. These studies also revealed that the residues 131-315 in the IGF-1R cysteine-rich domain plus flanking regions from L1 and L2 are the major binding sites for IGF-I (Schumacher *et al.,* 1991; Schumacher *et al.,* 1993).

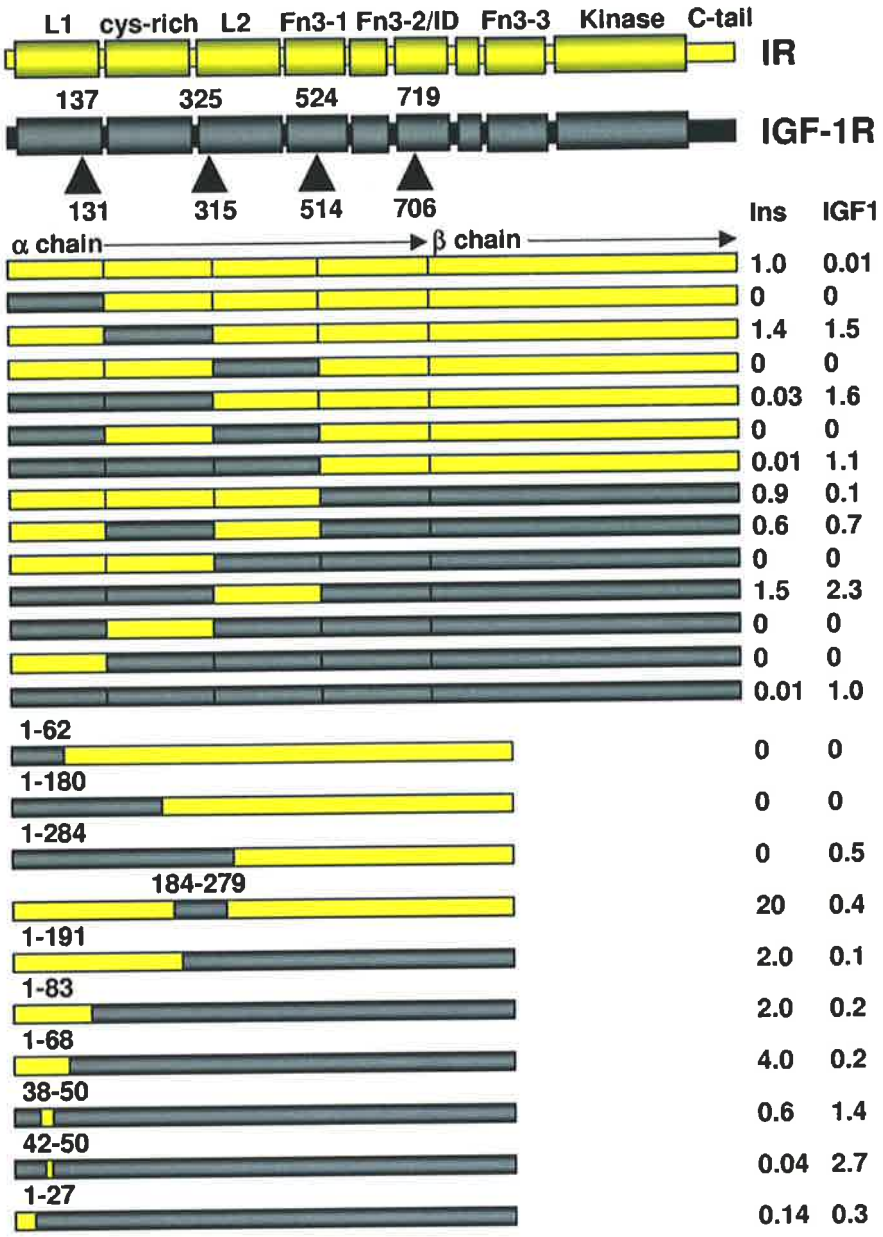

Figure 1.9 Schematic summary of the chimeras of the IR/IGF-1R.

The domain organisation of the receptors is shown at the top. The approximate locations of the fragment boundaries exchanged in the whole receptor chimeras are shown, as are the α-β cleavage sites for IR (yellow) and IGF-1R (grey). Solid and open boxes show the fragment composition of each chimera. The residues substituted in the ectodomain IR-based or IGF-1R-based chimeras are indicated above each construct. The relative binding affinities of the parent receptors and the various chimeras are shown opposite each construct on the right hand side. Figure is reproduced from (Adams *et al.*, 2000). The arrows indicate the situation of the related amino acids in IR or IGF-1R.

More specific examinations of binding have been conducted using single-site mutants. Alanine scanning mutagenesis has been carried out on the L1 domain, cysteine-rich domain and C-terminal end of the α- chain of IGF-1R. In the second and third β-sheet of the L1 domain 29 residues were mutated to alanine (Mynarcik *et al.*, 1997; Whittaker *et al.*, 2001). The mutants Tyr54 and Thr93 were not secreted in detectable quantities. Among the 27

secreted mutants in the L1 domain, the mutation of Asp8, Asn11, Tyr28, His30, Leu33, Leu56, Phe58, Arg59, and Trp79 to Ala resulted in 2- to 10- fold reduction in affinity for IGF-I while mutation of Phe90 to alanine caused a 23-fold decrease in affinity for IGF-I (Figure 1.10 A) (Whittaker *et al.*, 2001).

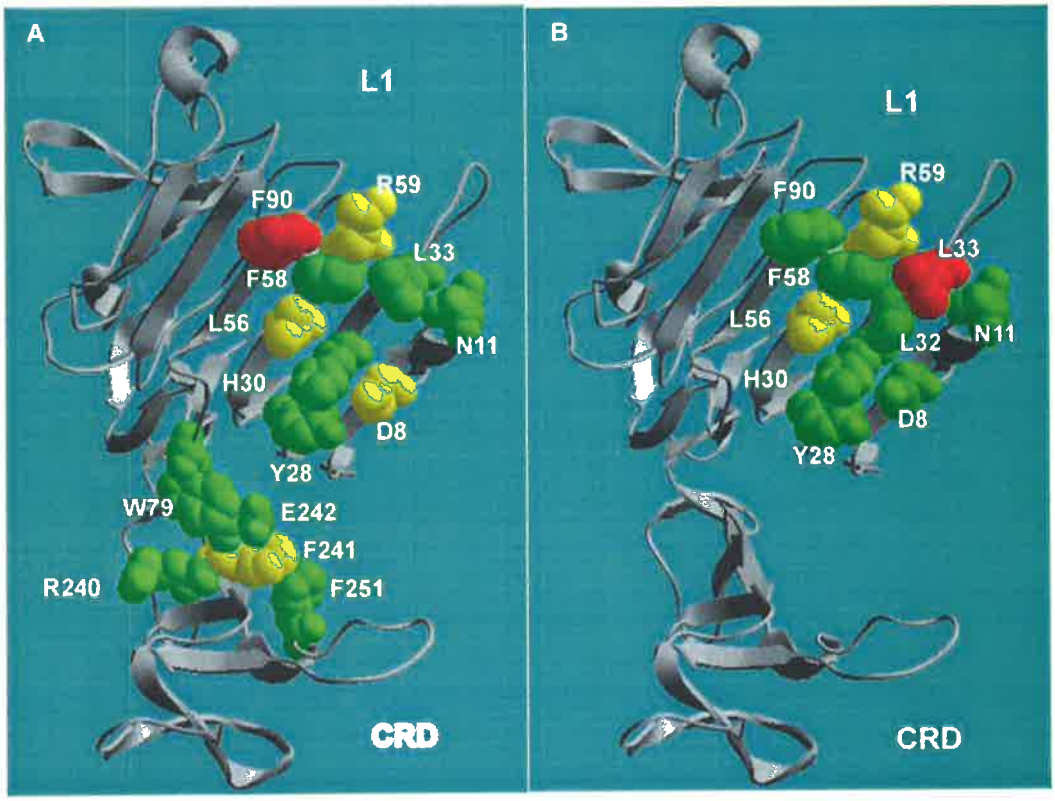

Figure 1.10 Comparison of the structures of the functional epitopes of the L1 and cysteine-rich domains for IGF-I (A) and IGF-II (B) binding.

The Cα backbone of the L1 and CRDs (cysteine-rich domain) is represented as a ribbon. The amino acids forming the functional epitopes for IGF-I (A) and IGF-II (B) are shown in space-filling illustration. Alanine mutations of amino acids colored green produced a 2- to 5-fold decrease in affinity, those colored yellow produced a 5- to 10-fold decrease and those colored red produced a larger than 10-fold decrease. Amino acids are indicated by the single letter code. Figures are adapted from (Sorensen *et al.*, 2004).

Twenty five alanine mutants of residues in the cysteine-rich region of IGF-1R were made to test predictions that these residues formed part of the IGF binding site, based on the IGF-1R fragment 3D structure (Garrett *et al.*, 1998; Whittaker *et al.*, 2001). The alanine mutants are between amino acids 240 and 284 of the cysteine-rich domain and the binding experiments revealed that only four of them, which are located at the N-terminus of the region, exhibited a significant (2-6 fold) decrease in affinity for IGF-I (Whittaker *et al.*,

2001). Three of these amino acids, Arg240, Phe241 and Glu242, are in cysteine-rich module 5, while Phe251 is placed at the start of module 6 (Figure 1.10 A) (Garrett *et al.,* 1998).

An eleven residue sequence in the C-terminus of the α chain of IGF-1R, was studied by alanine mutation (Whittaker *et al.,* 2001). The results of this analysis revealed that the amino acids 692-702 in this region are critical for IGF-I binding to the receptor and provide the majority of the free energy of the interaction between the IGF-I and the IGF-1R (Whittaker *et al.,* 2001). In this region, mutation of Phe695, Ser699 and Val702 did not have any effect on IGF-I binding affinity. Mutation of Phe701 produced a receptor, with no detectable IGF-I binding activity, while mutation of Phe692, Glu693, Asn694, Leu696, His697, Asn698 and Ile700 to alanine caused a 10-29 fold decrease in affinity for IGF-I binding (Whittaker *et al.,* 2001).

Recently, mapping of the IGF-II binding sites on the IGF-1R has been performed using secreted recombinant IGF-1R with alanine mutants in the L1 and cysteine-rich domains and amino acids 692-702 (Sorensen *et al.,* 2004). This study revealed that among the alanine mutations in the L1 domain of IGF-1R, mutation of Asp8, Asn11, Tyr28, His30, Leu32, Leu33, Leu56, Phe58, Arg59 and Phe90 resulted significant decrease in the affinity for IGF-II. However, only the mutations of Leu33, Leu56 and Arg59 caused 5-fold or more increase in K_d (Sorensen *et al.,* 2004). Interestingly, none of the alanine mutations in the cysteine-rich domain produced any significant effect in affinity of the receptor for IGF-II (Figure 1.10 B) (Sorensen *et al.,* 2004). In the C-terminus of the α subunit, alanine mutations of Phe692, Glu693, Asn694, Phe695, His697, Asn698 and Ile700 caused 4–27 fold increase in Kd and the alanine mutant of Phe701 did not bind to IGF-II (Sorensen *et al.,* 2004). Comparison of the binding epitopes for IGF-I and IGF-II in the L1, cysteine-rich and C-terminal α subunit domains of IGF-1R shows that the epitopes are very similar but there are certain residues that selectively participate in binding IGF-I or IGF-II (Sorensen *et al.,* 2004). In the L1 domain, Trp79 contributing in affinity for IGF-I but was not involved in IGF-II binding. Alanine mutation of L32, which compromised IGF-II binding, had no

influence on IGF-I binding to the IGF-1R (Figure 1.10) (Sorensen *et al.,* 2004). The most interesting differences were seen in the cysteine-rich domain. The residues Arg240, Phe241, Glu242 and Phe251 form a small patch on the cysteine-rich domain together with Trp79 in the L1 domain for binding to IGF-I (Whittaker *et al.,* 2001). None of these residues was significantly involved in binding to IGF-II.

Comparison of the L1 residues involved in functional epitopes in the context of the topology of this domain of IGF-1R revealed interesting differences between the IGF-I and IGF-II binding sites (Sorensen *et al.,* 2004). The mutation of amino acids in the first (Asp8 and Asn11) and fourth turns (Phe90) of this domain β helix showed more impact on IGF-I than IGF-II binding, whereas mutants of the amino acids in the second (Tyr28, His30, Leu32 and Leu33) and third turns (Leu56, Phe58 and Arg59) were more disruptive to IGF-II binding than to IGF-I (Sorensen *et al.,* 2004).

There are also differences on the effects of alanine mutants in the C-terminus of the α subunit for binding to the ligands. Mutation of Phe695 to alanine caused a 15-fold decrease in affinity for IGF-II but had no significant effect on IGF-I binding and the mutation of Phe692, Glu693, Asn694 and His697 showed more effects on reducing IGF-II affinity than IGF-I (Sorensen *et al.,* 2004). In contrast, the mutations of Leu696, Asn698 and Ile700 decreased the IGF-I affinity more than IGF-II (Sorensen *et al.,* 2004). The mutation of Phe701 showed disruptive effects on binding both IGF-I and IGF-II (Sorensen *et al.,* 2004).

1.5.2.4. IGF Ligand Residues Involved in IGF-1R Binding

As described before, the structure of the first three domains of the IGF-1R and also the structure of IGF-I and IGF-II have been solved. However, a structural complex of IGF-I or IGF-II with any fractions of the IGF-1R is not available so far. Therefore, other techniques have been employed to probe the residues on IGF-I and IGF-II that interact with the receptor. The results of these experiments will be discussed below to determine the important IGF

residues for binding to the IGF-1R by considering each domain of IGF. These results have been summarized in Figure 1.11.

B domain

In the B domain of the IGF-I, replacement of Tyr24 by Ser or Leu caused a 16- to 32-fold decrease in IGF-1R binding affinity respectively (Cascieri *et al.,* 1988; Bayne *et al.,* 1990) and replacement of Phe23 by glycine resulted in a 48-fold lower affinity for IGF-1R (Hodgson *et al.,* 1996). In contrast to these results, not all residues in the B domain are important for IGF-1R binding. It has been revealed that replacing the first 16 residues of IGF-I with the first 17 residues of insulin, which includes 10 sequence differences, caused only a two-fold reduction in IGF-1R binding (Bayne *et al.,* 1988). However, the mutation of Ala8 to Leu caused a 6-fold decrease in IGF-1R binding (Shooter *et al.,* 1996). In addition, in IGF-I, mutation of Val11 to Thr, but not Ile caused a 3-fold reduction in IGF-1R binding affinity (Hodgson *et al.,* 1995). Surface plasmon resonance analysis (BIAcore) showed that mutation to alanine of selected residues within the B domain α-helix of IGF-I caused reduction in affinity for IGF-1R between 2- to 4-fold for Val11, Asp12, Gln15 and 37-fold for Phe16 (Jansson *et al.,* 1997). The reduction of binding affinity for these mutants is not only because of the removal of specific interactions through amino acid replacement, but also more likely due to changing the local structure (Jansson *et al.,* 1997). Another study showed the IGF-I mutation of Arg21 to alanine resulted in a 3-fold decrease in IGF-1R binding as determined by surface plasmon resonance studies (Jansson *et al.,* 1998).

Although some studies have been conducted on the IGF-II B domain, it has not been studied as widely as the IGF-I B domain. Substitution of Phe26 with Ser and Tyr27 with Leu caused 5 and 132 fold decrease in binding affinity to the human placental IGF-1R respectively relative to recombinant human IGF-II (Sakano *et al.,* 1991). Another point mutation study also showed the critical role of the Tyr27 for binding to the IGF-1R (Roth *et al.,* 1991). Deletion mutants of the N-terminus of IGF-II showed that Thr7 and Leu8 are important for

IGF-1R binding (Hashimoto *et al.,* 1995). In addition, a variant of human IGF-II with a replacement of Ser29 with Arg-Leu-Pro-Gly resulted in a 2- to 3-fold reduction in IGF-1R binding (Hampton *et al.,* 1989).

C domain

The IGF-I C domain is also important in IGF-1R binding. Linking the IGF-I C domain to the C-terminus of the insulin B chain caused a 67-fold enhancement in IGF-1R binding affinity compared to native human insulin (Cara *et al.,* 1990). Replacement of Arg36 and Arg37 with alanine showed a 15-fold decrease (Zhang *et al.,* 1994) or a 5-fold reduction in IGF-1R affinity (Jansson *et al.,* 1998). The other important amino acid in C domain of IGF-I for binding to the IGF-1R is Tyr31 and its mutation to alanine resulted in a 6-fold reduction in the IGF-1R binding affinity (Bayne *et al.,* 1990). The crystal structure studies on the IGF-I in the presence of detergent implied that the Tyr31 lies at the tip of the C-region and its location places it in an ideal location to interact with a receptor molecule (Vajdos *et al.,* 2001). Substitution of the whole C domain with a tetra-glycine bridge ([1-27, Gly4, 38-70] IGF-I), made to maintain the tertiary structure, caused a 30-fold reduction in the affinity for the IGF-1R (Bayne *et al.,* 1989). Deletion of residues 29-41 of the IGF-I C-region resulted in no detectable affinity for the IGF-1R (Gill *et al.,* 1996) and also non-native reorientation of the A domain helices, accounting for the failure in IGF-1R binding affinity (De Wolf *et al.,* 1996).

A domain

The role of the IGF-I A domain has also been studied. Replacement of residues 42-56 in IGF-I with the first 15 residues of the insulin A chain which contains 8 amino acid differences, and also substitution of Phe49, Arg50 and Ser51 to corresponding regions in the A chain of insulin did not show any effect on binding to IGF-1R (Cascieri *et al.,* 1989). In addition, mutation of Arg55 and Arg56 to tyrosine and glutamine respectively resulted in no reduction for IGF-1R binding (Cascieri *et al.,* 1989). However, another study has shown the

mutation of Arg56 to alanine lead to a 2-fold decrease in IGF-1R (Jansson *et al.,* 1998). It has been revealed that the residues at the end of the second α-helix are important in maintaining the high affinity binding of IGF-I for IGF-1R. Mutation of Met59 to phenylalanine caused a 5-fold decrease in IGF-1R binding affinity (Shooter *et al.,* 1996) and also mutation of Tyr60 to leucine resulted in a 20-fold reduction in affinity for the IGF-1R (Bayne *et al.,* 1990). In addition, mutation of Val44 to methionine caused a 90-fold decrease in affinity to IGF-1R (Denley *et al.*, 2005b).

Some studies have also been conducted on the IGF-II A domain. The mutation of Val43 in IGF-II to leucine causes a 16-fold reduction in IGF-1R affinity (Sakano *et al.,* 1991) however the mutation of Ala54 and Leu55 of IGF-II to the corresponding residues in IGF-I, which are Arg55 and Arg56, showed no effect on binding affinity to the IGF-1R (Forbes *et al.,* 2001).

D domain

Separate groups have studied the role of the IGF-I D domain in binding to the IGF-1R and different results have been observed. In one study, removal of the D domain showed a very small effect on IGF-1R binding (Bayne *et al.,* 1989). However, another study showed the substitution of Lys65 and Lys68 with alanine reduced the affinity to IGF-1R by 10-fold (Zhang *et al.,* 1994). In contrast to IGF-I, deletion of the D domain in IGF-II caused a 5-fold reduction in binding affinity (Roth *et al.,* 1991).

In another study, chimeras of IGF-I and IGF-II were made where their C and D domains were exchanged either alone or together. This study showed that residues in the C and D domains of IGF-I and IGF-II contribute to IGF-1R binding specificity and play a role in binding to IGF-1R and its activation (Denley *et al.,* 2004). The IC_{50} values and relative binding affinities of these chimeras compared with IGF-I are listed in Table 1-3.

Ligand	IC_{50} (nM)	IC_{50} Relative to IGF-I (%)
Insulin	>100	<1
IGF-I	0.8 ± 0.2	100
IGF-IDII	0.7 ± 0.2	114
IGF-ICII	3.2 ± 1.4	25
IGF-ICIIDII	7.4 ± 2.6	11
IGF-II	4.4 ± 1.1	18
IGF-IIDI	1.7 ± 0.5	47
IGF-IICI	1.5 ± 0.5	53
IGF-IICIDI	1.1 ± 0.3	73

Table 1-3 IC_{50} values derived from competition binding studies comparing insulin, IGF-I and IGF-II and chimeras binding to the IGF-1R.

Values are the means and ± SEM from three separate experiments. Relative binding affinities compared to IGF-I are also shown. The table is adapted from (Denley *et al.*, 2004).

As a summary, certain residues in the B and A domains of IGF-I and its secondary structure are involved in IGF-1R binding. However, the C domain and certain residues in the D domain are also essential for high affinity binding of IGF-I to the IGF-1R. For IGF-II, the important residues for binding to the IGF-1R have not been widely studied. The IGF-I and IGF-II residues involved in IGF-1R binding are summarized in Figure 1.11.

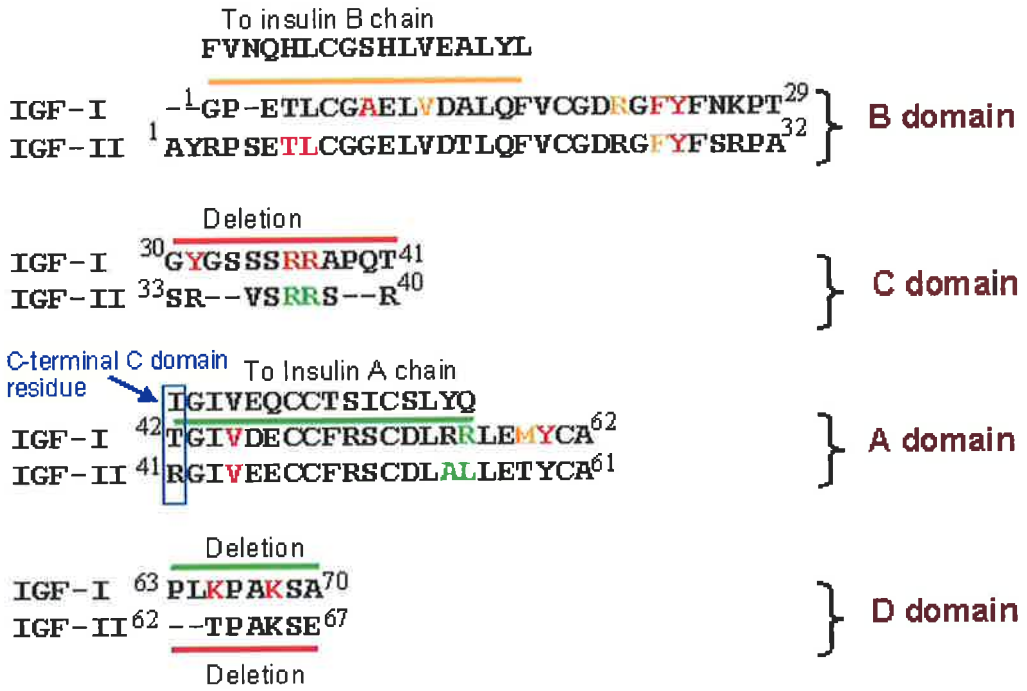

Figure 1.11 Summary of the effect of mutation of different residues of IGF-I and IGF-II on their binding to the IGF-1R.

Sequence alignment of the B, C, A and D domains of IGF-I and IGF-II highlighting in different colours residues that when mutated affect IGF-1R binding. ■ ≤ 2-fold decrease, 2-fold ≤ ■ ≤ 6-fold decrease and ■ ≥ 6-fold decrease.

1.6. The IGF System and Cancer

It is widely known that the IGF system plays a crucial role in cancer (Pollak *et al.,* 2004). The involvement of different parts of this system will be discussed in details below.

1.6.1. IGF Ligands and Cancer

Much evidence shows IGFs are potent mitogenic proteins and that they have a crucial role in abnormalities such as cancer. The overexpression of IGFs and their effects on tumourigenesis and neoplastic growth have been reviewed in (Khandwala *et al.,* 2000; Pollak *et al.,* 2004). There is some evidence for a relationship between increased circulating levels of IGFs and an increased risk of cancer, although the level of IGFs is noticeably variable among normal people (Pollak *et al.,* 2004). It has been revealed that within the normal range for IGF-I concentration, the risk of common cancers is increased in individuals with higher circulating levels of IGF-I (Pollak *et al.,* 2004).

In an epidemiological study it has been reported that the risk of colorectal cancer might be positively related to IGF-I/IGFBP-3 level even within the normal population (Ma *et al.,* 1999). Another study has revealed that in patients with primary breast cancer, circulating IGF-I levels were increased compared to controls (Peyrat *et al.,* 1993). A study in 1998 by Hankinson *et al.* demonstrated a positive correlation between plasma concentration of IGF-I and risk of breast cancer among premenopausal women (Hankinson *et al.,* 1998). A prospective study of breast cancer risk and serum concentration of IGF-I, IGF-II and IGF-binding protein-3 (Allen *et al.,* 2005) revealed that premenopausal women with comparatively high circulating concentration of IGF-I and low IGFBP-3 were at a bigger risk of developing breast cancer, but serum IGF-II concentration was not related with risk in pre- or postmenopausal women. In postmenopausal women, the IGF-I and IGFBP-3 were not associated with risk (Allen *et al.,* 2005). In prostate cancer it has been reported that increases in IGF-I and intact IGFBP-3 levels were positively related with the presence of prostatic carcinoma (Khosravi *et al.,* 2001). However, a case-control study has reported that the

circulating level of free IGF-I, total IGF-I and IGFBP-3 did not predict the future risk to develop prostate cancer (Janssen *et al.*, 2004).

Several studies have demonstrated the effect of IGFs on the growth of different cancer cell lines. It has been shown that IGFs have mitogenic effects on central nervous system neoplasms. The [^{3}H] thymidine incorporation (DNA synthesis) was increased by IGF-I in primary meningioma cultures (Kurihara *et al.*, 1989). Moreover, the effect of IGFs on gastrointestinal carcinomas has been reported in a number of studies. A study on eight human colon cancer cell lines has revealed that the growth of five lines (HT-29, LS411N, LS513, SW480, WiDr) was stimulated by both IGF-I and IGF-II (Lahm *et al.*, 1992). The mitogenic effects of exogenous [Thr59] IGF-I and IGF-II on human gastric cancer cell line (LIM-1839) has also been shown (Thompson *et al.*, 1990).

In the human hepatoma cell line (PLC) both IGF-I and IGF-II dose dependently increased the [^{3}H] thymidine incorporation (Scharf *et al.*, 1998). IGF-I also showed mitogenic effect on an established cell line (TC-cells) derived from human papillary thyroid cancer cell line (Onoda *et al.*, 1992). In addition, the IGFs play a mitogenic role in lung cancer. In 2 of 7 human small cell lung cancer (SCLC) cell lines, IGF-I increased [^{3}H] thymidine incorporation (Jaques *et al.*, 1988). Moreover, in a separate study, IGF-I increased the cell number by 52% in the human lung cancer cell line, CALU-6 (Minuto *et al.*, 1988) and both IGF-I and IGF-II elevated cell growth by approximately 250% in several SCLC cell lines (Nakanishi *et al.*, 1988).

The involvement of IGFs in breast cancer has also been reported in a number of studies. In four different breast cancer cell lines (MCF-7, T47D, MDA-MB-231 and HBL-100) DNA synthesis was stimulated by IGF-I as measured by [^{3}H] thymidine incorporation (Furlanetto and DiCarlo, 1984). In addition, both IGF-I and IGF-II stimulated cell growth in MCF-7 and T47-D cells (Karey and Sirbasku, 1988).

The IGFs also play a mitogenic role in the female and male reproductive neoplasms. Exogenous IGF-I in the ovarian cancer cell line OVCAR-3 increased cell growth (Yee *et al.*,

1991). Both IGF-I and IGF-II enhanced cell proliferation in two human endometrial adenocarcinoma cell lines, HEC1-A and KLE (Pearl *et al.,* 1993). In prostate cancer cell lines, LNCaP, PC-3 and DU-145, IGF-I stimulated cell growth (Pietrzkowski *et al.,* 1993). In the human testicular cancer cell line Tera-2 cell proliferation and [^{3}H] thymidine incorporation were increased by both IGF-I and IGF-II (Biddle *et al.,* 1988).

The mitogenic effect of IGFs on bone neoplasms has also been reported. IGF-I stimulated proliferation of human osteosarcoma cell lines MG-63 (Pollak *et al.,* 1990), while exogenous IGF-I and IGF-II showed mitogenic effects on the human osteosarcoma cell line U-2 OS (Raile *et al.,* 1994).

In addition, the IGFs play a role in haematological malignancies. In a Burkitt-type ALL- cell line (X308) and Hodgkin's disease-derived cell line (L 428 KSA), IGF-I increased [^{3}H] thymidine incorporation dose dependently (Vetter *et al.,* 1986). The growth of freshly obtained marrow cells from 4 of 5 patients with childhood acute lymphoblastic leukemia and 4 of 4 with acute myeloblastic leukemia was stimulated with IGF-I (Estrov *et al.,* 1991).

1.6.2. IGFBPs and Cancer

Several studies have demonstrated the significant association between IGFBPs and cancer. The role of the IGFBPs in some cancer cell lines such as colorectal (Durai *et al.,* 2005) and prostate cells (Kambhampati *et al.,* 2005; Kehinde *et al.,* 2005) has been revealed. In epidemiological studies, IGFBP-3 has been shown as a negative risk factor for breast, prostate and colorectal cancers, with low serum IGFBP-3 and high IGF-I levels presenting the highest statistical risk (LeRoith and Roberts, 2003). In addition, in two separate studies in men and women it has been shown that the risk of colorectal cancer was negatively correlated with IGFBP-3 levels (Ma *et al.,* 1999; Giovannucci *et al.,* 2000). In cell culture models IGFBP-3 inhibits neoplastic cell growth, which is consistent with the anti-cancer role of this protein (Hong *et al.,* 2002; Lee *et al.,* 2002).

Furthermore, other IGFBPs also are negative risk factors for cancer due to their IGF antagonist effects, yet recent microarray-based gene profiling studies have showed increased IGFBP-2 expression in glioblastoma multiforme (Fuller *et al.,* 1999), glioblastoma (Wang *et al.,* 2003a), brain tumours (Sallinen *et al.,* 2000), synovial sarcoma (Allander *et al.,* 2002) and prostate cancer (Bubendorf *et al.,* 1999; Moore *et al.,* 2003). IGFBP-2 also has been involved in other studies with enhanced tumourigenicity (Hoeflich *et al.,* 2001). Adding to this complication is the observation that IGFBP-2 inhibited the growth of normal prostate epithelial cells while enhancing the growth of prostate cancer cells (Moore *et al.,* 2003). It hence remains difficult to generalize about a unified role for IGFBPs in cancer, underlining the need for careful further investigation (Rosenzweig, 2004).

1.6.3. The IGF-2R and Cancer

The IGF-2R mediates IGF-II degradation and internalisation (Kornfeld, 1992). The M6P/IGF-2R gene encoding the IGF-2R is frequently inactivated in cancers with loss of IGF-II binding leading to an increase in the level of circulating IGF-II (Byrd *et al.,* 1999; Devi *et al.,* 1999). Numerous studies have revealed that the IGF-2R is a tumour suppressor. For example, loss of heterozygosity has been reported in a range of human cancers such as adrenocortical (Leboulleux *et al.,* 2001) and hepatocarcinoma (Kishimoto *et al.,* 2001) tumours and aggressive early breast cancer (Chappell *et al.,* 1997; Rey *et al.,* 2000). Moreover, a transfected colorectal cancer cell line (SW48) overexpressing the IGF-2R showed enhanced death and decreased growth compared with untransfected cells (Souza *et al.,* 1999). It has been demonstrated that down-regulation of the IGF-2R promoted the growth of transformed murine L cells (D9) by increasing IGF-II level, which binds to and activates IGF-1R and insulin receptor to enhance intracellular growth signals (Osipo *et al.,* 2001). Hence, down-regulation of IGF-2R increases the level of IGF-II, leading to induced growth by increasing the intracellular growth signals.

1.6.4. The Roles of IR Isoforms and Hybrid Receptors in Cancer

Differential expression of the IR isoforms in cancer cells compared to their normal counterparts has been shown in several studies. IR-A is the predominant isoform in many cancer cell lines such as breast, lung, colon (Frasca *et al.,* 1999; Sciacca *et al.,* 1999), ovaries (Kalli *et al.,* 2002), smooth and striated muscle (Sciacca *et al.,* 2002) and thyroid (Vella *et al.,* 2002). An increase in IR-A expression has also been reported in several tumours such as colon and breast (Frasca *et al.,* 1999). In addition, the down-regulation of IR-B in hepatoblastomas has been reported (von Horn *et al.,* 2001). IGF-II is overexpressed by many cancer cells such as colorectal cancer (Renehan *et al.,* 2000), breast cancer (Quinn *et al.,* 1996) and sporadic adrenocortical (Gicquel *et al.,* 1994) tumours, all cancers which also express the IR-A as the predominant isoform of the IR (Denley *et al.,* 2004). As thyroid cancer progresses to a more malignant dedifferentiated phenotype, the expression of the IR-A and IGF-II increases (Vella *et al.,* 2002). The IR-A expressing cancer cells migrate and are protected from apoptosis by exposure to IGF-II but not when exposed to equal levels of IGF-I (Sciacca *et al.,* 2002). Moreover, IGF-II is as potent as insulin in stimulating ovarian cancer cell proliferation, suggesting the presence of IR-A (Kalli *et al.,* 2002). These observations suggest that the interaction of IGF-II with IR-A might be important in both fetal growth and cancer (Denley *et al.,* 2003). Furthermore, in certain tumours IGF-II and IR-A might form an autocrine/paracrine growth stimulatory loop, which may increase cancer progression (Denley *et al.,* 2003).

Several studies have shown that expression of hybrid receptors has been elevated in cancer. The level of hybrid receptors expression is increased in breast (Pandini *et al.,* 1999) and thyroid (Belfiore *et al.,* 1999) cancer. In addition, during the differentiation of colon carcinoma cells (HT29-D4) the hybrid IGF-1R/IR is up-regulated and IGF-1R is down-regulated (Garrouste *et al.,* 1997). As mentioned in Section 1.5, hybrid receptors show different binding affinities and signaling properties. The activation of hybrids results in responses similar to those seen upon activation of the IGF-1R. It has shown that, cell

proliferation and migration in response to both insulin and IGFs were more effectively stimulated in Hybrid IGF-1R/IR-A expressing cells than in Hybrid IGF-1R/IR-B expressing cells. Hence, the relative abundance of IR isoforms therefore affects IGF system activation through hybrid receptors with important consequences for tissue-specific responses to both insulin and IGFs (Pandini *et al.*, 2002).

1.6.5. The Role of IGF-1R in Cancer

It is well established that IGF-1R plays essential roles in proliferation, transformation, motility and metastasis of certain cancer cells. Clinical and *in vitro* studies have revealed that the activation of the IGF-1R increases the proliferation and metastasis of cancer cells (reviewed in (Pollak *et al.*, 1990)). Experiments *in vitro* and *in vivo* have shown that IGF-1R overexpression promotes ligand-dependent growth in serum-free media, formation of ligand-dependent aggregates in tissue culture dishes, colony formation in soft agar and tumour formation in nude mice (Kaleko *et al.*, 1990; Pietrzkowski *et al.*, 1992).

For the potential transforming effects of many oncogenes such as SV40 T antigen (Sell *et al.*, 1993), the epidermal growth factor receptor (EGFR) (Coppola *et al.*, 1994) and Ha-Ras (Sell *et al.*, 1994), the existence of IGF-1R is essential. However, for some oncogenes such as *v-src* and the highly oncogenic GTPase-deficient mutant of Galpha13, the presence of IGF-1R is not critical (Liu *et al.*, 1997; Valentinis *et al.*, 1997)

IGF-1R over-expression or increased IGF-1R kinase activity is associated with a broad range of human cancers (Rubin and Baserga, 1995; Resnik *et al.*, 1998) such as breast cancer tumour tissue (Cullen *et al.*, 1990; Webster *et al.*, 1996) and both primary and immortalized cervical cancer cell lines (Steller *et al.*, 1996). Also, there is a significant up-regulation of the IGF-1R in primary prostate cancer cells compared to benign prostatic epithelium (Hellawell *et al.*, 2002). Immunohistochemical analysis has revealed a correlation between the strong staining of IGF-1R and both higher grade and higher-stage tumours in human colorectal cancer (Hakam *et al.*, 1999).

The IGF-1R is also involved in protection of the tumour cells from cytotoxic effects of chemotherapeutic agents (Gooch *et al.,* 1999). In addition, overexpression of the IGF-1R has been shown to influence cellular radioresistance and local breast cancer reappearance after radiation therapy and lumpectomy (Turner *et al.,* 1997).

It has been shown that cross talk between the IGF-1R and members of distinct receptor families plays an essential role in modulating intracellular signalling. Recently, a number of studies have emphasized the interaction(s) between the IGF-1R and the EGFR, another transmembrane tyrosine kinase that is involved in cancer (Adams *et al.,* 2004). In addition, it has been suggested that the activation of IGF-1R signaling may cause resistance to the anti-HER2 antibody trastuzumab (Herceptin) in some breast cancer types (Lu *et al.,* 2001).

Taken together, inhibition of the IGF-1R is now a well established and promising anti-cancer strategy (Bahr and Groner, 2004; Pollak *et al.*, 2004). For this reason, a variety of techniques have been investigated so far and they will be discussed below.

1.7. Different Strategies for Targeting IGF-1R as an Anti-cancer Therapy

For inhibition the IGF-1R effects in cancer, most recent studies have been designed to block either the expression or the function of the IGF-1R. The following strategies to inhibit different aspects of IGF-1R biology have been examined as methods for challenging cancer:

1- *suppressing the expression of the IGF-1R* by using antisense RNA, antisense expressing vectors (Resnicoff *et al.,* 1995b; Burfeind *et al.,* 1996; Lee *et al.,* 1996; Pass *et al.,* 1996; Nakamura *et al.,* 2000; Macaulay *et al.,* 2001), a triple helix strategy (Rininsland *et al.,* 1997) or small interfering RNAs (Bohula *et al.,* 2003b)

2- *decreasing kinase activity* using tyrosine kinase inhibitors (Blum *et al.,* 2000; Blum *et al.,* 2003; Garcia-Echeverria *et al.,* 2004; Mitsiades *et al.,* 2004; Warshamana-Greene *et al.,* 2005)

3- *disrupting ligand binding* or *down-regulating the level of the IGF-1R* using antibodies directed against the receptor (Arteaga *et al.,* 1989; Zia *et al.,* ; Burtrum *et al.,* 2003; Sachdev *et al.,* 2003; Ye *et al.,* 2003; Lu *et al.,* 2004)

4- *inhibition of the downstream signals of the IGF-1R* using dominant-negative receptors, in the form of IGF-1R truncated within the β-subunit, resulting in the formation of inactive heterodimers of mutant and wild type receptors unable to transduce downstream signals (Prager *et al.,* 1994). Other dominant negatives lack the transmembrane region and so are secreted from the cell to compete for ligand binding with wild type receptors (D'Ambrosio *et al.,* 1996).

Each method has shown inhibitory effects on cancer cell growth at least *in vitro* while most of them reduced *in vivo* tumour growth in mouse models. Among these strategies, antibodies directed against the receptor, particularly α-IR3, have been shown to be effective in inhibiting cancer cell proliferation *in vitro* and tumourigenesis *in vivo* for a range of human tumour cell types (Arteaga *et al.*, 1989; Arteaga and Osborne, 1989b; Furlanetto *et al.*, 1993; Kalebic *et al.*, 1994; Scotlandi *et al.*, 1998; Li *et al.*, 2000). These studies have established that targeting IGF-1R by a specific antibody is a valuable strategy to inhibit the receptor signaling. The antibodies and their use will be discussed in detail in the following sections.

1.8. Antibodies

1.8.1. Antibodies Structure

Antibodies also known as immunoglobulins (Ig) are large glycoproteins. In the immune systems of vertebrates, antibodies provide excellent specificity for detecting foreign antigens and launching the defensive response. There are some sites on foreign substances called antigenic determinants, which can be recognised by the immune system. B-cells carrying specific receptors recognize and bind antigens. This binding stimulates the B-cells to multiply, differentiate and finally synthesize and secrete antibodies into the bloodstream.

The general structure of Ig is made of two identical light chains and two identical heavy chains, which are linked together by disulphide bonds. There are two different classes of light chains, λ and κ with no known functional differences between them. In addition, Ig are divided into five different functional classes or isotypes, IgG (γ), IgA (α), IgM (μ), IgD (δ) and IgE (ε), based on the components of their heavy chain. The IgG class of antibody is the major type of immunoglobulin in normal serum. In addition, IgG is the most useful tool of the immunochemist due to its stability and specificity. This class of antibody will be described below in more detail. The mouse IgG exists in four subclasses known as IgG1, IgG2a, IgG2b and IgG3, depending on the heavy chain (γ) subclass (Harlow and Lane, 1999).

The IgG molecules are Y shape and have three protein regions Figure 1.12. Two of them are identical and form the 'arms' and each 'arm' contains a binding site for binding to an antigen. The third region is the base or tail of the Y shape molecule. This tail plays a role in certain aspects of immune response such as interaction with macrophages or the activation of complement. The IgG structure contains four polypeptide chains, two heavy (H) chains (approximately 55 kDa each) and two light (L) chains (approximately 25 kDa each) (Figure 1.12). The N-terminal region of one heavy chain associates with one light chain to make an antigen-binding domain and the C-terminal region of two heavy chains fold together to form the Fc (fragment crystallisable) domain which is constant (Harlow and Lane, 1999; Kolar and Capra, 2003). The two Fv (fragment variable) regions include the antigen recognition sites. They contain amino acid sequences, which are hypervariable between different antibodies and are called complementarity determining regions (CDR) (Figure 1.13). Each Fv region includes six CDRs and they interact with the target antigen (Branden and Tooze, 1991; Harlow and Lane, 1999; Kolar and Capra, 2003). The enzyme papain splits the IgG molecule into two Fab fragments and one Fc fragment (Branden and Tooze, 1991).

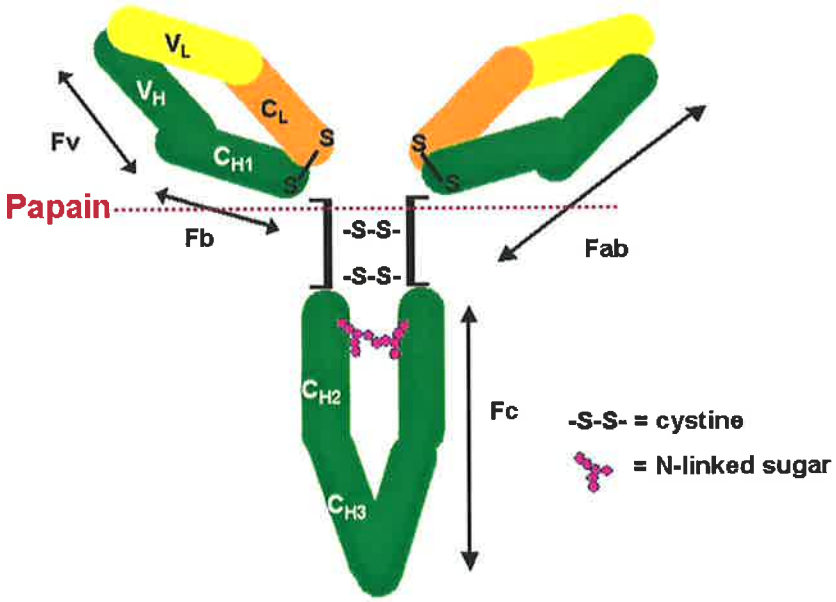

Figure 1.12 Schematic representation of the structure of an IgG molecule.

The ovals represent the various domains in the heavy (green) and light chain (yellow and orange) of the antibody molecule, which is made up of two heavy chains (H) and two light chains (L). Single interchain disulphide bonds link light and heavy chains and heavy chains are linked together by two interchain disulphide bounds. Fc represents fragment crystallizable, Fab represents fragment antigen binding and Fv represents the variable part of Fab. Figure is designed based on (Kolar and Capra, 2003) and (Branden and Tooze, 1999).

Comparison of the amino acid sequences from many different immunoglobulin IgG molecules reveals the most important aspect of the antibody molecule. It shows that the N-terminal domains have constant sequences for each class. Thus a light chain is built up from one N-terminal variable domain (V_L) and one C-terminal constant domain (C_L). A heavy chain is made from one N-terminal variable domain (V_H) followed by three constant domains (C_{H1}, C_{H2}, and C_{H3}) (Figure 1.12) (Branden and Tooze, 1991).

The variable domains are not uniformly variable through their lengths. As mentioned earlier, there are three small regions within the variable domains, which show much more variability than the rest of the chain and they are called hypervariable regions or complementarity determining regions, CDR1, 2 and 3 (Figure 1.13). They are different in both size and in sequence between different immunoglobulins. These regions determine the specificity of the antigen-antibody interactions. The remaining parts of the variable domains have similar amino acid sequences (except a fourth hypervariable region of unknown function in the heavy chain). In fact, all variable domains show significant overall sequence homology and therefore evolutionary relationships among each other. Furthermore, the different

constant domains C_L, C_{H1}, C_{H2} and C_{H3} show significant (30-40%) sequence identity to each other and the constant domains from immunoglobulin chains of different classes. This strongly suggests that the genes, which code for current constant domains arose by successive gene duplication of an ancestral antibody gene. Although there is no significant sequence homology between constant and variable domains, there are noticeable structural similarities (Branden and Tooze, 1991).

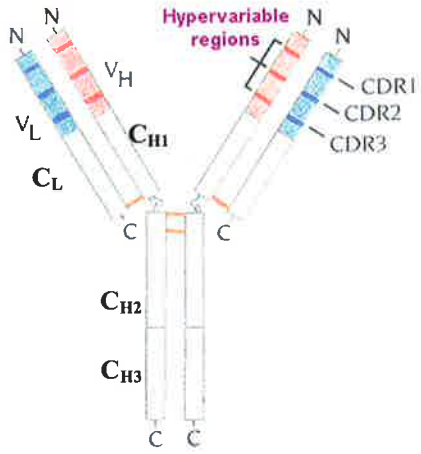

Figure 1.13 The hypervariable regions or complementarity determining regions (CDRs) in both light and heavy chains of an IgG molecule.

Figure is adapted from (Branden and Tooze, 1991).

The genetic information for the diversity of antibody molecules in the mammalian body is contained in many small segments of DNA (about 1,000 for human). The elucidation of the mechanisms for the generation of this antibody diversity is one of the excellent achievements of modern biology. The gene segments, which encode the variable and constant regions of antibodies, are clustered in three gene pools, one for the class G heavy chain and one for each of the two light-chain isotypes (κ and λ), on separate chromosomes. The variable domain is encoded by three types of segments, V, D, and J (Figure 1.14). In the heavy-chain gene pool, V codes for the first 90 residues, D for the hypervariable region CDR3, and J for the remaining residues of the variable domain. For mouse the gene-segment pool for an H chain contains about 1,000 V segments, 12 D segment, 4 J segments and an ordered cluster of C segments each encoding a different class of H chains. The DNA for the variable domains of

a new B cell is put together by random joining of one of each of these segments into a single continuous exon. The process is called combinatorial joining and there are thousands of different ways it can arise. Furthermore, the joining of these segments is not precise and this creates more diversity, which is called junctional diversity, where D recombines with V and J. In addition, extra nucleotides can be added during the joining procedure, giving still further diversity. The D segment encodes CD3, which is thus a focus of particular diversity in the heavy chain. The newly created V-D-J exon becomes joined to one of the eight C segments that encode the constant region domains of the heavy chain as separate exons. Usually, a variable region is expressed in an IgM molecule first and afterwards, further genetic rearrangements will delete the mu (μ) exons encoding the IgM constant region and the variable region will be joined to a second set of constant-region exons, most commonly those encoding IgG. The genetic mechanisms underlying light-chain diversity are similar except that there are no D segments and hence the diversity of CDR3 depends mostly on junctional diversity generated through V-J joining (Figure 1.14) (Branden and Tooze, 1991).

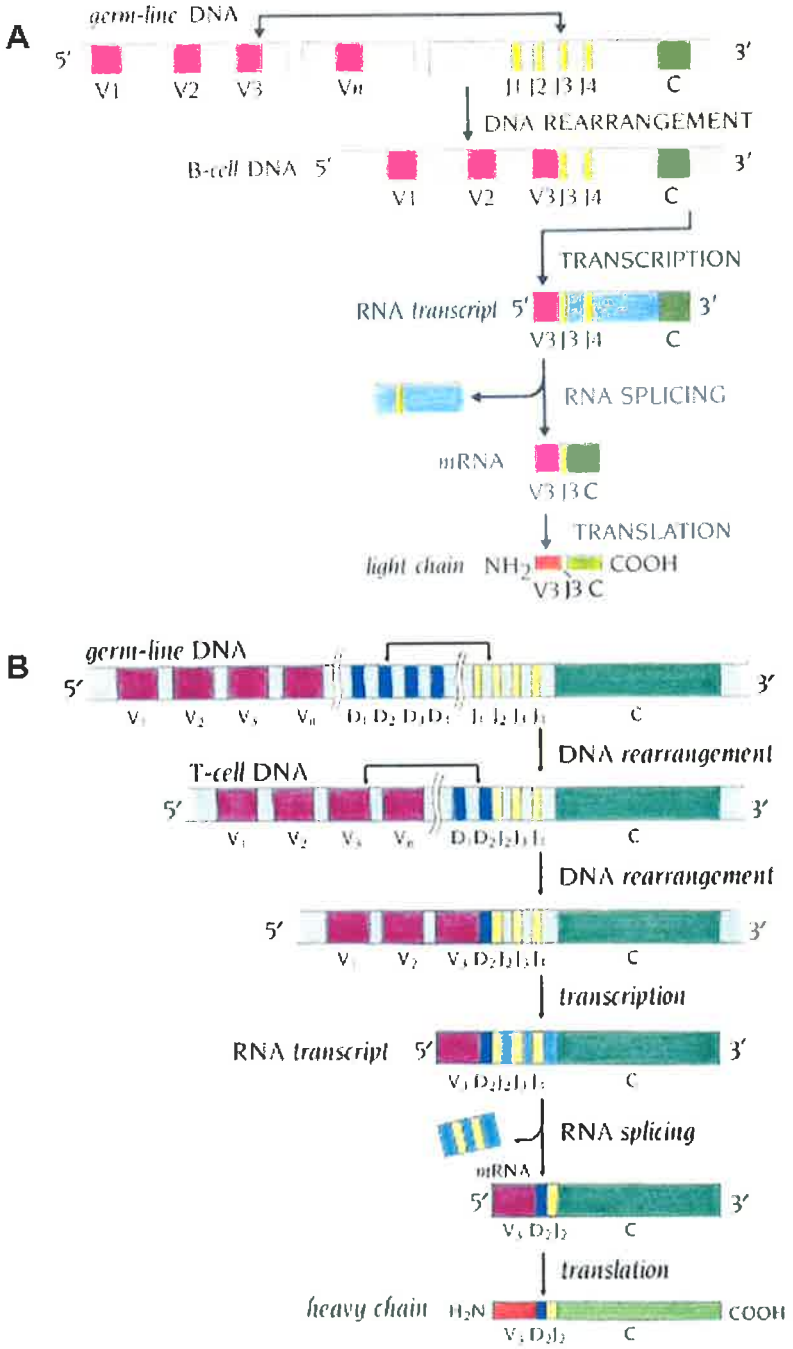

Figure 1.14 Combinatorial joining of gene segments to form the variable domains of immunoglobulins.

A) The V-J joining process involved in making a κ light chain in the mouse. Figure is adapted from (Branden and Tooze, 1991).
B) The V-D-J joining process involved in making a heavy chain in the mouse. Figure is adapted from (Branden and Tooze, 1999).

1.8.2. Antibodies Application

Antibodies are widely used in immunoassays. There are two general types of the antibodies, which can be used in these assays, and they are polyclonal and monoclonal antibodies (MAb).

Polyclonal antibodies are antibodies that are derived from different cell lines. Monoclonal antibodies are derived from a single cell line.

Polyclonal antibody production results from the immune reaction of an animal to an injected antigen. The antiserum can be absorbed to eliminate antibodies that react with unrelated material and its IgG fraction can be purified. Even then, a pure preparation of IgG made from antiserum contains a mixture of several hundred different antibodies (Diamandis and Christopoulos, 1996).

In MAb production, the short-lived B lymphocytes from the spleen are individually immortalized by fusion with an immortal myeloma cell line to make a range of clones of B lymphocytes (hybridomas), each secreting its own antibody. Then the most appropriate clones are selected and expanded in tissue culture (Diamandis and Christopoulos, 1996).

1.8.3. Monoclonal Antibodies

In 1975, the introduction of the first version of a method to make MAbs by Köhler and Milstein, allowed the production of large amounts of murine monoclonal IgG antibodies from continuous culture of fused cells which are called hybridoma cells (Kohler and Milstein, 1975). The MAbs have specific and easily studied properties of antigen recognition (Harlow and Lane, 1999). There are many uses for the MAbs in immunochemical techniques such as staining, immunoprecipitations, immunoblots and immunoaffinity purification. They also can be used in the clinic as therapeutic and diagnostic reagents. For these reasons, this source of identical antibodies enabled the production of recombinant Fv fragments, Fab fragments, single chain Fv (scFv) molecules, diabodies, triabodies, tetrabodies, chimeric antibodies, humanised antibodies and bioactive paratope-derived peptides (PDP) through recombinant engineering techniques (Laune *et al.*, 1997; Monnet *et al.*, 1999; Hudson and Souriau, 2003; Gonzales *et al.*, 2005).

1.8.4. Epitope Mapping

The immune system has an extraordinary specificity and it can distinguish between two proteins, which differ by only one amino acid, or even between two identical molecules presenting a different three-dimensional conformation (Saint-Remy, 1997). An epitope is a specific region on an antigen molecule that is involved in recognition by an antibody and a paratope is the area of an antibody in contact with an epitope (Jerne, 1960; Harlow and Lane, 1999). Epitope mapping is a methodology to study the specificity of antibodies or to distinguish between different antibodies (Harlow and Lane, 1999). It can also be used to determine the properties of proteins in the cell membrane such as the sites of protein modification, origin of protein fragments, or orientation of proteins (Harlow and Lane, 1999).

Although epitope mapping can be applied to both MAbs and polyclonal antisera, it is easier to determine the epitope for the MAbs. Polyclonal antisera could be considered as a mixture of MAbs. Since polyclonal antibodies react with a great number of epitopes of the antigen, it would be difficult to identify a difference between two antigens that may differ by just one epitope using these antibodies. By definition, MAbs have the ability to distinguish single epitopes and are therefore extremely useful for making comparisons between two almost identical molecules (Saint-Remy, 1997).

There are two classes of epitopes that can be functionally distinguished, which are linear epitopes (continuous) and conformational (discontinuous) epitopes. Linear epitopes can be mapped to a small linear peptide sequence of 5-20 amino acids. These form highly structured multiple interactions between the antibody binding site, while multiple amino acid side chains and backbone may also make contacts within a contiguous peptide sequence (Harlow and Lane, 1999). For conformational epitopes, the folding of proteins in larger domains forms the epitopes. These epitopes show interactions with residues that are close together in the folded protein but are widely separated in the linear sequence (Harlow and Lane, 1999). As expected, linear epitopes that are formed by contiguous or nearly contiguous amino acids are stable through denaturation whereas the conformational epitopes formed by

noncontiguous amino acids are lost when the protein unfolds (Harlow and Lane, 1999). The antibodies, which recognize denaturation-resistant epitopes, work well in immunoblotting. The epitope of these antibodies can be mapped easily and precisely to small peptide segments (Harlow and Lane, 1999). For conformational epitopes, accurate epitope mapping is much more difficult (Harlow and Lane, 1999).

1.8.4.1. Methods Used to Localize Epitopes in Proteins

Structural and functional approaches to the study of protein antigenicity provide two different perceptions of the nature of protein epitopes. The structural approach focuses on the purely spatial arrangements of atoms found in the antigen-antibody complex and reveals that approximately 15 amino acids could be involved in each epitope. The functional approach takes the form of cross-reactive binding measurements and leads to the view that a smaller number of residues are involved in each epitope. Furthermore, different types of epitopes are identified using different probes (Van Regenmortel, 1989).

The different approaches that have been used for mapping protein epitopes are summarized in Table 1-4 (Atassi, 1984; Benjamin *et al.*, 1984). Only method 1 (Table 1-4) is based on a structural analysis and in contrast, all other methods correspond to a functional analysis taking the form of binding measurements. It has been shown that the structuralist perspective inherent in X-ray crystallography (Table 1-4) leads to the view that an epitope is composed of approximately 15 residues that are in contact with the paratope (Amit *et al.*, 1986; Sheriff *et al.*, 1987; Colman, 1988). Residues in the interface that essentially contribute to the binding energy can be identified in binding measurements. It has been demonstrated that methods 2-5 (Table 1-4) analysing cross-reactivity instead of residue burial, which lead to the conclusion that fewer residues (between 1 and 5) are essential to antibody binding. Hence, the epitope defined in a functional way involves fewer residues than the epitope defined in structural terms (Van Regenmortel, 1989).

Method	Type of epitope identified	Criterion for allocating residues to epitope	Average number of residues recognised in epitope
1. X-ray crystallography of antigen-Fab complexes	Discontinuous epitope reacting with homologous antibody	Van der Waal's contact in epitope-paratope interface	15
2. Study of cross-reactive binding of peptide fragments with anti-protein antibodies	Continuous epitope cross-reacting with heterologous antibody	Residual binding of linear fragment above threshold of assay	3-8
3. Study of cross-reactive binding of protein with anti-peptide antibodies	Continuous epitope cross-reacting with heterologous antibody	Induction of cross-reactive antibodies	3-8
4. Determination of critical residues in peptide by systematic substitution with other amino acids	Continuous, cross-reacting epitope containing crucial residues interspersed with unimportant residues	Abrogation of cross-reactivity by substitution of crucial and functionally important residues	3-5
5. Study of cross-reactivity between homologous proteins or point mutants	Discontinuous epitope	Abrogation of cross-reactivity by replacement of crucial residue	1-3

Table 1-4 Methods which are utilised to localise epitopes in proteins.

Table is adapted from (Van Regenmortel, 1989).

1.8.5. Clinical Applications of Monoclonal Antibodies

MAbs are used in the clinic in many different ways. They are widely used *in vitro* for several diagnostic tests by different methods such as RIA (radioimmunoassay), ELISA (enzyme linked immunosorbent assay) and IH (immunohistochemistry) to detect small amounts of substances such as drugs, toxins, and hormones in biological fluids. The application of MAbs as therapeutic and diagnostic reagents particularly in cancer is well established (Hudson and Souriau, 2001; Hudson and Souriau, 2003). Regulatory approval has been achieved in USA and elsewhere for the use of several MAbs as therapies for cancer, Crohn's disease, transplant

rejection, rheumatoid arthritis and antiviral prophylaxis (Brekke and Sandlie, 2003). As more molecules obtain approval and more molecular targets are found, the use of the MAbs is expected to grow rapidly (Hudson, 1999; Hudson and Souriau, 2003).

In cancer therapy, the MAbs are used as either unconjugated (Baselga *et al.,* 1996) or toxin-coupled (Frankel *et al.,* ; Kreitman *et al.,* 2001) or radio-labelled (Carrasquillo *et al.*, 1984; Horak *et al.*, 1997; Brechbiel and Waldmann, 1999) monoclonal antibodies.

More recently the success of targeting the function of receptors in the EGFR family with trastuzumab (Herceptin), which is a humanised anti-HER2 receptor MAb has been demonstrated as a breast cancer therapy (Esteva, 2004). The HER2 is a tyrosine kinase receptor of the ErbB family and it is overexpressed in 25–30% of human breast cancers (Molina *et al.,* 2001). Herceptin provides a model for the development of further MAbs targeting receptors such as IGF-1R to suppress cancer (Pollak *et al.,* 2004).

1.9. Monoclonal Antibodies Directed Against the IGF-1R

So far, several MAbs have been developed directed against the IGF-1R. These MAbs can be employed to study the structure of the IGF-1R and the interaction of the receptor with ligands. They have different epitopes on the IGF-1R and different characteristics. The first mouse MAb directed against the α subunit of the human IGF-1R named αIR-3 was developed more than 20 years ago (Kull *et al.,* 1983). This antibody blocks the binding of ^{125}I-IGF-I to the α subunit of the IGF-1R on human placental membrane but had little effect on the binding of ^{125}I-IGF-II to the same receptor (Casella *et al.,* 1986). In another study it has also shown that αIR-3 inhibited the binding of IGF-I but not IGF-II to the solubilized expressed receptor (Steele-Perkins and Roth, 1990). Surprisingly, this antibody inhibited the ability of both IGF-I and IGF-II to stimulate thymidine synthesis in cells expressing the IGF-1R indicating that this antibody does not inhibit the IGF-II binding but inhibits the subsequent ability of the receptor to be activated (Steele-Perkins and Roth, 1990) . This antibody inhibited the growth of several cancer cell types *in vitro* and to some extent *in vivo*. It inhibits the growth of MCF-7 cells (an

estrogen dependent human breast carcinoma cell line) in culture (Rohlik *et al.,* 1987). Studies on Ewing's sarcoma (ES) tumour showed that *in vitro* simultaneous or sequential treatment with αIR-3 significantly increased the anti-tumour effects of doxorubicin and vincristine (two drugs with a leader action on ES) (Rohlik *et al.*, 1987; Arteaga and Osborne, 1989a; Arteaga *et al.*, 1989; Furlanetto *et al.*, 1993; Kalebic *et al.*, 1994; Scotlandi *et al.*, 1998; Benini *et al.*, 2001). The αIR-3 antibody also inhibited the mitogenic effect of exogenous IGF-I in MCF-7 and MDA-231 breast cancer cell lines *in vitro* and also inhibited the estrogen-independent MDA-231 cells growing *in vivo* in nude mice. However, the MCF-7 cells' growth is not blocked *in vivo* (Arteaga *et al.,* 1989). In melanoma cell lines WM 373 and WM 852, the αIR-3 suppressed the cell replication which was stimulated with IGF-I (Furlanetto *et al.,* 1993). This MAb also inhibited the progression of human rhabdomyosarcoma (RMS) tumour growth in both tumour-bearing animals and formation of newly established tumours (Kalebic *et al.,* 1994). The αIR-3 antibody also caused a complete regression of tumours in almost one-half of the animals tested, after subcutaneous inoculation with TC-71 ES cells (Scotlandi *et al.,* 1998).

It has been shown that the epitope for the MAb αIR-3 is located between His-223 and Met-274 on the IGF-1R using chimeric insulin/IGF-1 receptors (Table 1-5) (Gustafson and Rutter, 1990).

Several other mouse MAbs have also been derived and tested against the IGF-1R. Soos *et al.* obtained 20 mouse MAbs directed against the human IGF-1R, which bind to different parts of the receptor and also show different effects on binding IGF-I to the IGF-1R (Soos *et al.,* 1992). In Table 1-5 several of these MAbs are listed and their effect on IGF-I binding is shown. The epitopes of these MAbs, have been studied by examining the binding with chimeric constructs in which portions of the insulin receptor were substituted by the corresponding IGF-1R sequences or *vice versa* (Kjeldsen *et al.,* 1991; Soos *et al.,* 1992). The results of epitope mapping for several MAbs are also shown in Table 1-5 compared to αIR-3.

MAbs	Epitope	Effect on IGF-I binding
αIR-3 (murine)	223-274 (CR)	Inhibits (Gustafson and Rutter, 1990)
4-52 (murine)	62-184 (L1-CR)	Enhances (Soos *et al.*, 1992)
16-13 (murine)	62-184 (L1-CR)	Enhances (Soos *et al.*, 1992)
17-69 (murine)	514-586 (Fn3α)	Inhibits (Soos *et al.*, 1992)
24-31 (murine)	283-440 (CR-L2)	No effects (Soos *et al.*, 1992)
24-55 (murine)	440-586 (L2-Fn3α)	Inhibits (Soos *et al.*, 1992)
24-60 (murine)	184-283 (CR)	Inhibits (Soos *et al.*, 1992)
25-57 (murine)	440-586 (L2-Fn3α)	Inhibits (Soos *et al.*, 1992)
26-3 (murine)	283-440 (CR-L2)	Enhances (Soos *et al.*, 1992)

Table 1-5 The epitopes of some of the anti-IGF-1R MAbs on the IGF-1R and their effect on IGF-I binding to the IGF-1R.

Other mouse MAbs directed against the IGF-1R are MAb MAB391 (Hailey *et al.*, 2002), MAbs 1H7 and 2C8 (Li *et al.*, 1993), MAb 4G11 (Jackson-Booth *et al.*, 2003) and MAb EM164 (Maloney *et al.*, 2003) for ImmunoGen and Sanofi-Aventis. The MAB 391 inhibits the IGF-I dependent autophosphorylation of the receptor and also causes down-regulation of the IGF-1R in MCF-7 human mammary carcinoma, HT29 colorectal and Du145 prostate cancer cells (Hailey *et al.*, 2002). MAbs 1H7 and 2C8 both bind to the α-subunit of the IGF-1R as shown by immunoblotting. MAb 1H7 has an inhibiting effect on the binding of IGF-I and IGF-II to the IGF-1R but MAb 2C8 shows no effect on the binding of either ligand to the receptor. In NIH 3T3 cells expressing human IGF-1R, MAb 1H7 also inhibits basal IGF-I or IGF-II stimulated DNA synthesis while 2C8 stimulates basal DNA synthesis but provides no synergism in the presence of IGF-I or IGF-II (Li *et al.*, 1993). Two soluble forms of 1H7 based anti-IGF-1R antibodies have been generated (Li *et al.*, 1993). ScFv is a monovalent antibody and scFv-Fc is a divalent antibody that contains the human IgG1 Fc domain. They showed the extracellular addition of αIGF-1R scFv-Fc or 1H7 to NIH3T3 cells overexpressing IGF-1R significantly inhibited the cell growth *in vitro*. Furthermore the recombinant scFv-Fc antibody blocked MCF-7 tumour cell growth in athymic mice (*in vivo*) alone or in combination with doxorubicin (Anti-neoplastic Agent). Also, This recombinant single chain antibody in combination with Tamoxifen (anti-estrogen drug) inhibits T61 tumour cell growth *in vivo* (Ye *et al.*, 2003). The MAb 4G11 inhibits the

binding of ^{125}I-IGF-I to the fibroblast receptor and also potently down-regulates the IGF-1R in MCF-7 cells, a panel of colon cancer cells and MG-63 (osteosarcoma) cells (Jackson-Booth *et al.,* 2003). The MAb EM164 also inhibits binding of IGF-I and blocks its effects on cells (Maloney *et al.,* 2003). Furthermore, this antibody inhibits IGF-I and IGF-II and serum-stimulated proliferation and survival of a variety of human cancer cell lines, including lung, breast, colon, ovarian, cervical, prostate, pancreatic, melanoma, neuroblastoma, rhabdomyosarcoma and osteosarcoma cancer lines *in vitro*. This antibody also inhibits establishment of BxPC-3 human pancreatic tumour xenografts in SCID mice *in vivo* (Maloney *et al.,* 2003).

Murine MAbs are not ideal for human therapeutics because they have immunogenic properties. In a study to overcome this problem the murine MAb 1H7 has been converted into a single chain humanised scFv-Fc consisting of the anti-IGF-1R MAb scFv and human IgG1 Fc domain (Li *et al.,* 2000). *In vivo* treatment of mice bearing MCF-7 xenograft tumours with this scFv-Fc, caused almost complete down-regulation of the IGF-1R (Sachdev *et al.,* 2003). Furthermore, co-treatment of the estrogen receptor positive T61 human breast cancer xenograft in athymic mice with tamoxifen and the scFv-Fc antibody was more effective in inhibition of tumour growth than scFv-Fc or tamoxifen treatment alone (Ye *et al.,* 2003).

A fully human antibody (A12) has been generated for ImClone through screening of a Fab phage display library (Burtrum *et al.,* 2003). This antibody blocks IGF-I and IGF-II binding and thereby subsequent IGF-1R activation. A12 antibody also induced IGF-1R internalization and degradation (Burtrum *et al.,* 2003). In xenograft tumour models *in vivo*, treatment with the A12 antibody significantly inhibits the growth of breast, renal and pancreatic tumours and, moreover, a significant increase in apoptotic tumour cells was detected.

Another humanised MAb (h7C10) from an original murine MAb has been recently made for Pierre Fabre and Merck by the CDR grafting technology (Goetsch *et al.,* 2005). This antibody inhibits the cell proliferation of MCF-7 breast cancer cells induced by IGF-I and

IGF-II *in vitro*. Both h7C10 and its murine parental form 7C10, significantly suppress the *in vivo* tumour growth of either human breast cancer cells (MCF-7) or non small cell lung cancer cells (A549) in nude mice (Goetsch *et al.*, 2005). It is widely known that both IGF-1R and EGFR have a major role in a variety of human cancers, thereby suggesting that a combined therapy targeting both receptors could be advantageous in treating such tumours (Chakravarti *et al.*, 2002). Co-treatment of mice with this anti-IGF-1R antibody and either a chemotherapeutic agent (vinorelbine) or an anti-epidermal growth factor receptor (EGFR) antibody 255, resulted in almost complete inhibition of A549 tumour growth. Moreover, the combination of the anti-IGF-1R antibody with an anti-EGFR antibody had a greater effect than the combination of the anti-IGF-1R antibody with Vinorelbine (a chemotherapeutic agent) to prolong the life span of mice in an orthotopic *in vivo* model of A549 (Goetsch *et al.*, 2005).

A fully humanised IgG2 antibody CP-751,871, raised for Pfizer against human IGF-1R has been generated using XenoMouse technology (Cohen *et al.*, 2005). This antibody blocked binding of IGF-I to its receptor (IC_{50} 1.8 nmol/L), IGF-I induced receptor autophosphorylation (IC_{50} 0.42 nmol/L) and caused the down-regulation of IGF-1R *in vitro* and in tumour xenografts. The degree of IGF-1R down-regulation *in vivo* was proportional to CP-751, 871 concentrations in the serum of tumour-bearing mice. CP-751, 871 displays significant anti-tumour activity either as a single agent or combined with Adriamycin, 5-fluorouracil, or tamoxifen in multiple tumour models (Cohen *et al.*, 2005). Interestingly CP-751,871 also lead to down-regulation of IGF-1R on peripheral blood cells (Cohen *et al.*, 2005).

A new approach using a single biopharmaceutical for targeted combination therapy was investigated by generating bispecific antibodies. A fully human recombinant bispecific antibody, BsAb-IGF-IR-EGFR, was generated to combine two previously identified neutralizing antibodies targeting IGF-1R (A12 scFv) and EGFR (11F8 scFv) in a single antibody (Lu *et al.*, 2004). This bispecific antibody bound to both the receptors and blocked

IGF and EGF binding to their relevant receptors, and caused inhibition of downstream signaling and cellular proliferation. Moreover, the anti-tumour efficacy of a similar bispecific antibody *in vivo*, now referred to as a Di-diabody, has been recently reported (Lu *et al.,* 2005).

Another fully humanized neutralizing antibody to the IGF-1R is 19D12 (reviewed in (Hofmann and Garcia-Echeverria, 2005)). This antibody inhibits IGF-1R autophosphorylation, as well as downstream signaling, and causes a down-regulation of IGF-1R expression *in vitro* and *in vivo*. In addition to blocking the *in vitro* proliferation of several cancer cell lines, this antibody showed efficacious in a variety of xenograft models including ovarian (A2780) and non-small cell ling (H322), breast (MCF-7) and colon (HT-29) cancer.

In addition to the MAbs directed against the human IGF-1R that have been published in journals and discussed before, there is patent literature describing further MAbs for the IGF-1R. These will be discussed below.

Fully human MAbs directed against the human IGF-1R have generated for Schering-Plough corporation by immunising HuMAb mice of the Hco7 genotype with recombinant sIGF-1R (an antigenic IGF-1R polypeptide, amino acids 30-902), and IGF-1R transfected HEK293 cells (Wang *et al.,* 2003b). This group showed that the antibodies 1H3, 15H12 and 19D12 competed with IGF-I for binding to IGF-1R. These MAbs also inhibited the IGF-1R autophosphorylation with an IC_{50} of 0.1 nM. In addition, it has been shown that these anti-IGF-1R antibodies could inhibit anchorage-independent growth of MCF-7 (human breast cancer cell line), HT-29 (human colorectal cancer cell) and DU145 (human prostatic cancer cell) malignant cell lines tested.

MAbs 18 and 22 also produced directed against the IGF-1R by immunising Hco7 transgenic mice with NIH 3T3 cells, transfected with an expression vector for IGF-1R and with soluble extracellular domain of IGF-1R (Graus *et al.,* 2005). MAb 18 inhibited IGF-I and IGF-II binding to tumour cells expressing IGF-1R (HT-29 and NCI H322M). In a similar experiment both the MAbs competed for binding to IGF-1R with the MAb α-IR3 which is known to bind to residues 223-274 (Gustafson and Rutter, 1990). The number and also the

size of colonies were reduced in presence of MAb 18. In addition, a dose dependent growth inhibition of NCI H322M (lung cancer) tumour cells expressing IGF-1R in 3D culture under treatment with MAb 18 was observed. It was also observed that MAb 18 blocked the IGF-I induced phosphorylation of both IGF-1R and Akt/PKB. This MAb also induced down-regulation of IGF-1R and did not interfere with binding of insulin ligand to the IR. Treatment of the induced tumours in nude mice once with different concentrations of the MA18 showed a concentration-dependent decrease of IGF-1R levels with an EC50 at 0.6 mg/kg. MAb 18 also inhibited the growth of H322M tumours induced in nude mice, *in vivo* alone or in combination with gemcitabine (a known antimetabolic compound). Moreover, this antibody inhibited the growth of 3T3 tumours induced in nude mice.

Another series of specific antibodies directed against the receptor has been generated for Pharmacia Corporation using an scFv phagemid library, which is an expanded version of the 1.38×10^{10} library (Vaughan *et al.,* 1996) to select antibodies specific for the human IGF-1R (Morton *et al.,* 2004). Some of these antibodies inhibited [^{125}I]-labelled IGF-I binding and some of them inhibited [^{125}I]-labelled IGF-II at 4°C on NIH3T3-fibroblasts expressing the human IGF-1R. Among them, the antibodies 11A1, 11A3, 11A5, 11A7, 11A11, 12A1, 12A2 and 12A3 inhibited IGF-II binding with an $IC_{50} < 10$ nM while the antibodies 7A2, 7A4, 7A6, 8A1 and 9A2 inhibited IGF-II binding with an $IC_{50} < 0.8$ nM. For the antibody 11A4 the IC_{50} value for inhibiting IGF-I or IGF-II binding was > 50 nM and > 75 nM respectively. The antibodies 7A2, 7A4, 8A1, 9A2, 11A1 and 11A4 inhibited the IGF-I dependent proliferation of IGF-1-transfected NIH-3T3 cells with an $IC_{50} < 10$ nM. Some of the antibodies (7A2, 7A4, 7A6, 8A1, 9A2, 11A1 and 11A4) blocked IGF-I mediated IGF-1R tyrosine phosphorylation with an $IC_{50} < 10$ nM. In addition, a time-dependent loss of total IGF-1R was observed when A549 tumour cells (non small cell lung cancer human line) were treated with 8A1, 9A2 and 11A4. Moreover, 11A4, 8A1 and 9A2 decreased the level of cell surface IGF-1R on NIH-3T3 fibroblasts transfected with the human IGF-1R (Morton *et al.,* 2004). Epitope mapping studies showed 8A1 and 7A4 share a common epitope that overlaps the MAbs 24-31, 24-60 and

24-57 (Soos *et al.,* 1992; Morton *et al.,* 2004). Both 8A1 and 11A4 significantly inhibited the 3T3/IGF-1R-S tumour growth and IGF-1R expression (Morton *et al.,* 2004).

1.10. Aims and Experimental Strategy

IGF-I and IGF-II bind to the transmembrane IGF-1R and activate the receptor. To date, the involvement of the IGF system and particularly IGF-1R in cancer aspects such as cellular mitogenesis, angiogenesis, tumour cell survival and tumourigenesis is widely known (Pollak *et al.,* 2004). In addition, the IGF-1R is overexpressed in certain cancers.

Recently, the IGF-1R has become of great interest as a possible target for cancer treatment. The inhibition of the IGF-1R activation using different methods is the focus of the studies that were mentioned above.

One of the strategies to inhibit the IGF-1R activation is developing MAbs against the receptor, which inhibits the binding of the ligands or down-regulate the receptor. Some other MAbs has been generated against the IGF-1R, and different levels of characterisation have been performed on them. These MAbs and their properties were discussed in the literature review.

The major goal of this thesis was to generate MAbs against the IGF-1R, which hopefully have better inhibitory effects than other antibodies on IGF-1R activation, induced by ligands. In addition, these MAbs could be used in different immunoassay techniques to detect the IGF-1R overexpression as diagnostic tools. Furthermore, epitope mapping of these MAbs could provide information to investigate the mechanism of binding the IGF-1R to the MAbs and ligands. In brief, production of these MAbs allowed investigation into the following:

- General characterisation of the MAbs to determine their ability to utilise in different immunoassays for IGF-1R detection.

- Sequencing the variable regions of the MAbs to determine the amino acids involved in binding to the receptor and comparing to the sequence of other MAbs against the receptor.
- Investigation of the biological effect of the MAbs on cancer cell proliferation, metastasis, and the IGF-1R down-regulation *in vitro*.
- Determination of the binding affinity of the MAbs to the receptor and their effect to inhibit the IGF-I and IGF-II binding to the IGF-1R.
- Investigation of the effect of chimeric ligands, such as exchanging C domains between IGF-I and IGF-II (IGF-ICII and IGF-IICI) on binding the MAbs to IGF-1R.
- Epitope mapping of the MAbs
- Investigation of the role of different residues of the IGF-1R in binding to ligand or MAbs.

Despite the structural similarity of IGF-I and IGF-II, they exhibit different binding affinities to almost all proteins with which they both interact including IGF-1R. Using MAbs and fine epitope mapping of them can be useful to investigate the IGFs binding sites and their mechanism of binding to the IGF-1R.

Chapter 2

Materials and General Methods

2. Materials and General Methods

2.1. Materials

The materials that were used and their main supplier/manufacturer are listed below.

2.1.1. General Materials

Name	Address to Access
AC96 NeuroProbe A Series 96 well chamber	NeuroProbe, Gaithersburg, USA
BioTrace™ nitrocellulose membrane	Pall Gelman Laboratory, Ann Arbor, MI, USA
Cellu.Sep®T2 cellulose tubular membrane (MWCO 6000-8000)	Membrane Filtration Products Inc., Seguin, TX, USA
Centricon YM-10 centrifugal filter devices	Millipore Corporation, Bedford, MA, USA
Cryotube ™ vials	Nunc, Roskilde, Denmark
Fibra-cel® disc cell carriers	New Brunswick Scientific Co, Edison, NJ, USA
Filter 1μm (GMF 150)	Whatman International Ltd. Middlesex, UK
Greiner Lumitrac 600 96-well plates (white)	Omega Scientific, Tarzana, USA
Minisart syringe top 0.2 or 0.45 μM filter	Sartorius, Goettingen, Germany
Nuclon Delta white microwells S1 (96-well)	Nunc, Roskilde, Denmark
Nunc MaxiSorp™ flat-bottom 96 well plate	Nunc, Roskilde, Denmark
PD-10 column	Pharmacia Biotech, Uppsala, Sweden
Polycarbonate filters with pore size 12 μm	NeuroProbe, Gaithersburg, USA
Protein A-Sepharose chromatography column (1 ml Hitrap affinity column)	Pharmacia Biotech, Uppsala, Sweden
PVDF membrane (Hybond P)	Amersham Life Sciences Ltd, Buckinghamshire, UK
Sensor chip CM5	Biacore, Uppsala, Sweden
Spinner flasks	New Brunswick Scientific Co, Edison, NJ, USA
Tissue culture vessels, various	Falcon, NJ, USA
X-ray film (Curix ortho HT-G 100 NIF Ecopac)	Agfa, Belgium

2.1.2. Chemicals Reagents

All chemicals and reagents were of analytical grade, or of the highest purity available. The majority of common laboratory chemicals were obtained from either SIGMA-ALDRICH Inc. (St.Louis, MO, USA) or BDH Chemicals Ltd. (Vic, Australia). Specialized reagents and their suppliers are listed below.

Name	Address to Access
2,2′ azinobis 3-ethylbenzthiazoline-6 sulfonic acid (ABTS). Each tablet contains 5mg ABTS	Roche, Mannheim, Germany
2-Log DNA Ladder (0.1-10.0 kb)	New England Biolabs, MA, USA
Acrylamide solution (40%)	Bio-Rad Laboratories Inc., Hercules, CA, USA
Affi-Gel® 10 Gel	Bio-Rad Laboratories Inc., Hercules, CA, USA
Agarose powder	Sigma, St.Louis, MO, USA
Ammonium persulphate (APS)	BDH Chemicals, Vic, Australia
Ampicillin	Sigma, St.Louis, MO, USA
Azaserine	Sigma, St Louis, MO, USA
Beta-mercaptoethanol (BME)	Sigma, St Louis, MO, USA
Bicinchoninic acid (BCA) protein assay reagent	Pierce, Rockford, IL, USA
Big Dye Sequencing reagent, Version 3	Applied Biosystems, CA, USA
Bis solution (2%)	Bio-Rad Laboratories Inc., Hercules, CA, USA
BovoStar Bovine serum albumin (BSA) #	Bovogen, Melbourne, Australia
Bradford protein assay reagent	Bio-Rad Laboratories Inc., Hercules, CA, USA
Bromophenol Blue	Sigma, St.Louis, MO, USA
Calcein	Molecular Probes, Oregon, USA
Casein	Sigma, St.Louis, MO, USA
Chloroform	BDH Chemicals, Vic, Australia
Citric acid	Ajax chemicals LTD, Sydney, Australia
Collagen type 1	Cohesion, Palo Alto, USA
Coomassie Brilliant Blue R™ stain	Sigma, St Louis, MO, USA
DELFIA® enhancement solution	PerkinElmer, Turku, Finland
Dialyzed fetal bovine serum (dFBS)	Gibco-BRL, Grand Island, NY, USA
Diethyl pyrocarbonate (DEPC)	Sigma, St.Louis, MO, USA
Diethylenetriaminepentaacetic acid dianhydride (DTPA)	Sigma, St.Louis, MO, USA
Dimethyl sulfoxide (DMSO)	Sigma, St Louis, MO, USA
Di-sodium hydrogen orthophosphate	BDH Chemicals, Vic, Australia
DMEM (Dulbecco's Modified Eagle Medium)	Gibco-BRL, Grand Island, NY, USA
DNTPs	Promega, NSW, Australia
Donkey serum (normal)	Sigma, St.Louis, MO, USA
DPX mounting medium	BDH laboratory supplies, Dorset, England
DTT (0.1M)	Invitrogen, Melbourne, Australia
EcoRI Buffer	New England Biolabs, MA, USA
EcoRI Restriction enzyme	New England Biolabs, MA, USA
EDTA	Boehringer Mannheim GmbH, Mannheim, Germany
EGTA	Sigma, St.Louis, MO, USA
Ethanol	BDH Chemicals, Vic, Australia
Ethanolamine-HCl (1 M, pH 8.5)	Biacore, Uppsala, Sweden
Ethidium Bromide	Sigma, St.Louis, MO, USA
Europium labelled IGF-I (Eu-IGF-I)	Mr. Peter Hoyne, CSIRO Health Science and

Tested and found not to interfere with the assays.

	Nutrition, Parkville, Australia
Europium labelled IGF-II (Eu-IGF-II)	Mr. Peter Hoyne, CSIRO Health Science and Nutrition, Parkville, Australia
F-12 Nutrient Mixture (HAM)	Gibco-BRL, Grand Island, NY, USA
Fetal calf serum (FCS)	Gibco-BRL, Grand Island, NY, USA
First-Strand Buffer (5′)	Invitrogen, Melbourne, Australia
Fluorescent mounting medium	Dako, Botany, NSW, Australia
Full range Rainbow™ recombinant protein molecular weight marker (MW range 10,000-250,000)	Amersham Biosciences UK Ltd, Buckinghamshire, UK
Geneticin (G418)	Gibco-BRL, Grand Island, NY, USA
Gentamicin	Gibco-BRL, Grand Island, NY, USA
Glacial Acetic Acid	BDH Chemicals, Vic, Australia
Glutamine synthetase (GS) supplement (50×)	JRH Biosciences Inc., Kansas, USA
Glutamine-free Glasgow's Modified Eagle's Medium (GMEM-S)	JRH Biosciences Inc., Kansas, USA
Glycogen	GeneWorks Pty Ltd, SA, Australia
Goat serum (normal)	IMVS, Veterinary Services, SA, Australia
HAT (Hypoxanthine, Aminopterin, Thymidine) selection medium	Gibco-BRL, Grand Island, NY
Hematoxylin	Sigma, St.Louis, MO, USA
Hydrogen peroxidase	Sigma, St Louis, MO, USA
Hypoxanthine	Sigma, St Louis, MO, USA
IGF-I, receptor grade	GroPep Ltd, Adelaide, SA, Australia
IGF-ICII (IGF-I with IGF-II C domain chimera)	Dr. A. Denley, The University of Adelaide, Australia
IGF-II, receptor grade	GroPep Ltd, Adelaide, SA, Australia
IGF-IICI (IGF-II with IGF-I C domain chimera)	Dr. A. Denley, The University of Adelaide, Australia
Insulin, media grade	GroPep Ltd, Adelaide, SA, Australia
Iodoacetamide	Sigma, St.Louis, MO, USA
Isopropanol	BDH Chemicals, Vic, Australia
KCl	Sigma, St.Louis, MO, USA
Lipofectamine 2000	Life Technologies Inc., NY, USA
MagicMark™XP marker	Invitrogen Corporation, CA, USA
Mammalian cocktail protease inhibitor (for use with mammalian cell and tissue extracts) product code: P8340	Sigma, St Louis, MO, USA
Marker12™ (protein size marker)	Invitrogen, CA, USA
MDP Adjuvant (N-Acetyl-Muramyl-L-Ala-D-Iso-Gln-OH)	Auspep Pty. Ltd., Parkville, Australia
Methanol	BDH Chemicals, Vic, Australia
Methionine sulfoximine (MSX)	Sigma, St Louis, MO, USA
$MgCl_2$	Sigma, St.Louis, MO, USA
N-butyric acid sodium salt (butyrate)	Sigma, St Louis, MO, USA
Oxalacetic acid	Sigma, St.Louis, MO, USA
Papain	Boehringer Mannheim GmbH, Mannheim, Germany
Paraformaldehyde	Sigma, St Louis, MO, USA
PEG (polyethylene glycol) 1500	Roche, Germany
Penicillin/streptomycin	Gibco, Melbourne, Australia
Phenol	Novachem,Vic, Australia
Pronase solution (1%)	Sigma, St Louis, MO, USA

Protein G column (Bulk)	Sigma, St Louis, MO, USA
Protein G-agarose beads	Santa Cruz Biotechnology, Inc., CA, USA
Rat serum (Normal)	The University of Adelaide, Adelaide, Australia
RNase-Free DNase I	Roche, Basel, Switzerland
RPMI medium 1640	Gibco-BRL, Grand Island, NY, USA
Safsolvent	APS Chemicals, Seven Hills, Australia
Skim milk powder	Diploma
Sodium azide (Na-Azide)	Sigma, St.Louis, MO, USA
Sodium pyruvate	Sigma, St.Louis, MO, USA
Streptavidin CY3/FITC	Jakson ImmunoResearch laboratories, Inc. West Grove, PA, USA
Streptavidin-HRP conjugate	CHEMICON, Melbourne, Australia
SuperIn RNase Inhibitor	Ambion, Austin, TX, USA
SuperScript III Reverse Transcriptase	Invitrogen, Melbourne, Australia
Taq DNA Polymerase	New England Biolabs, MA, USA
TEMED	Bio-Rad Laboratories Inc., Hercules, CA, USA
Thermopol buffer (10× concentrate)	New England Biolabs, MA, USA
Tissue-Tek OCT compound (embedding medium for frozen tissue specimen)	Miles Inc., Elkhart, IN, USA
Trehalose	Sigma, St Louis, MO, USA
Triton-X100	Sigma, St Louis, MO, USA
TRIZOL Reagent	GibcoBRL, Melbourne, Australia
Trypan blue	Sigma, St Louis, MO, USA
Trypsin/EDTA	Gibco-BRL, Grand Island, NY, USA
Tween-20 (polyoxyethylene-sorbitan monolaurate)	Sigma, St.Louis, MO, USA
Xylene Cyanole	Sigma, St.Louis, MO, USA

2.1.3. Antibodies

All antibodies were diluted according to manufacturer's recommendations. The following antibodies were obtained from these sources

Name	**Address to Access**
Anti- human IGF-1R polyclonal (C-20)	Santa Cruz Biotechnology Inc., CA, USA
Anti-β-actin monoclonal	Sigma, St.Louis, MO, USA
Anti-human IGF-1R monoclonal (αIR-3)	Calbiochem, San Diego, CA
Anti-human IGF-1R monoclonal (24-31)	Professor K. Siddle, Cambridge, UK
Anti-human IGF-1R monoclonal (24-55)	GroPep Ltd, Adelaide, SA, Australia
Anti-human IGF-1R monoclonal (24-60)	Professor K. Siddle, Cambridge, UK
Anti-human IGF-1R monoclonal (IGFR 1-2)	GroPep Ltd, Adelaide, SA, Australia
Anti-mouse IgG fluorescein FITC conjugate, sheep polyclonal	CHEMICON, Melbourne, Australia
Anti-mouse IgG1 polyclonal, rabbit antibody	Biacore, Uppsala, Sweden
Anti-mouse immunoglobulin HRP conjugate, sheep antibody	CHEMICON, Melbourne, Australia
Anti-rabbit antibody HRP conjugate, donkey antibody	Rockland, Gilbertsville, PA, USA

Biotinylated anti-mouse immunoglobulin, goat antibody	DakoCytomation, Glostrup, Denmark
Biotinylated anti-human IGF-1R monoclonal (16-13), 1mg/ml	F. Occhiodoro, The University of Adelaide, Adelaide, Australia
Biotinylated anti-human IGF-1R monoclonal (24-60), 1mg/ml	F. Occhiodoro, The University of Adelaide, Adelaide, Australia
Biotinylated anti-mouse IgG, donkey antibody	Jackson ImmunoResearch laboratories, Inc. West Grove, PA, USA
IgG1 antibody negative control	CHEMICON, Melbourne, Australia

2.1.4. Bacterial Strains

DH5α: The *E. coli* DH5α strain was used in transformations and was a host for all recombinant plasmids.

2.1.5. Tissue Culture Cell Lines

The following cell lines have been used throughout the course of this study;

Name	**Address to Access**
293 EBNA cells	Invitrogen, San Diego, CA
BHK21 cells recombinantly producing the soluble extracellular part of the human IGF-1R (amino acids 1-906) (s-IGF-1R)	Dr. Kathy Surinya, The University of Adelaide, Adelaide, Australia
HT-29 cells (epithelial) from human colorectal adenocarcinoma	ATCC No: HTB-38, VA, USA
MCF-7 from human breast adenocarcinoma	ATCC No: HTB-22, VA, USA
NIH 3T3 cells stably expressing human IGF-1R/IR C1 receptor	Cell bank No: 624, provided by Prof. A. Ullrich, Martinsried, Germany
NIH 3T3 cells stably expressing human IR/IGF-1R C12 receptor	Cell bank No: 629, provided by Prof. A. Ullrich, Martinsried, Germany
NIH 3T3 cells stably expressing human IR/IGF-1R C2 receptor	Cell bank No: 163, provided by Prof. A. Ullrich, Martinsried, Germany
P6 cells (BALB/c3T3 cells overexpressing the human IGF-1R)	Professor R. Baserga, Philadelphia, USA
R^- cells (Mouse 3T3-like cells with a targeted oblation of the IGF-1R gene)	Professor R. Baserga, Philadelphia, USA
R^-IR-A cells (R^- cells expressing human IR-A)	Eric R. Bonython, The University of Adelaide, Adelaide, Australia
R^-IR-B cells (R^- cells expressing human IR-B)	Eric R.Bonython, The University of Adelaide, Adelaide, Australia
SP2/0 (BALB/c mouse lymphoblast-like myeloma cells)	ATCC No: CRL 1581, VA, USA

2.1.6. Tissue Culture Solutions

Name	Content
Cloning medium (for hybridomas)	10% (v/v) FCS, 1% (v/v) Penicillin/streptomycin, 1mM hypoxanthine and 1mM thymidine in DMEM.
DMEM/FCS	10% (v/v) FCS and 1% (v/v) penicillin/streptomycin in DMEM media
Freezing medium	10% (v/v) DMSO and 90% (v/v) FCS
Fusion medium (for hybridomas)	20% (v/v) FCS, 1mM sodium pyruvate, 1.1mM oxalacetic acid, 0.5 U/ml insulin and gentamicin 50 µg/ml in 40% (v/v) F-12 Nutrient mixture (HAM) and 40% (v/v) DMEM

2.1.7. Media for Growing Cells *in vitro*

Cell line	Related growth medium
293 EBNA cells	DMEM, 10% (v/v) FCS, 1% (v/v) penicillin/streptomycin and 0.5% (v/v) geneticin (G418)
HT-29 cells	47% (v/v) DMEM, 47% (v/v) F-12 Nutrient Mixture (HAM), 1% (v/v) dilution of penicillin/streptomycin and 5% (v/v) FCS
MCF-7 cells	DMEM, 10% (v/v) FCS, 1% (v/v) penicillin/streptomycin
NIH 3T3 cells stably expressing chimeric IGF-1R/IR receptors	DMEM, 10% (v/v) FCS, 1% (v/v) penicillin/streptomycin and 0.5% (v/v) geneticin (G418)
P6 cells	DMEM, 10% (v/v) FCS and 1% (v/v) penicillin/streptomycin
R^- cells	DMEM, 10% (v/v) FCS, and 1% (v/v) penicillin/streptomycin
R^-IR-A cells	DMEM, 10% (v/v) FCS, 0.25 mg/ml geneticin (G418) and 1% (v/v) penicillin/streptomycin
R^-IR-B cells	DMEM, 10% (v/v) FCS, 0.25 mg/ml geneticin (G418) and 1% (v/v) penicillin/streptomycin
SP2/0 (mouse myeloma) cells	DMEM 40% (v/v), F-12 Nutrient Mixture 40% (v/v), 20% (v/v) FCS

2.1.8. Primers

-Primer aIR3KR-AA for sequencing the cDNAs of the IGF-1R mutants or the chimeric IGF-1R/256-266IR in pcDNA3-zeo (+) plasmids:

aIR3KR-AA : **5′ CCAAGCACGTGTGGG<u>GCGGCC</u>GCGTGCACCGAGAAC 3′**
Oligonucleotide is complementary to the human IGF-1R sequence between amino acids 235-274 of the IGF-1R. The underlined nucleotides are not exactly complementary to this part of the IGF-1R.

-Primers RSP and USP for sequencing the pGEM-T Easy plasmids:

RSP: **5′- CAC ACA GGA AAC AGC TAT GAC CAT C –3′**
Oligonucleotide is complementary to a DNA sequence located within the pGEM-T Easy vector.

USP: **5′- CGC CAG GGT TTT CCC AGT CAC GAC –3′**
Oligonucleotide is complementary to a DNA sequence located within the pGEM-T Easy vector.

2.1.9. Commercial Kits

Name	Address to Access
Cell-Titer Glo™ Luminescent Cell Viability Assay Kit	Promega, WI, USA
DELFIA® Eu-labelling kit	PerkinElmer, Turku, Finland
Mouse Ig-Primer Set	Novagen, Madison, WI, USA
Mouse Typer®-Mouse Sub- Isotyping Panel	BIO-RAD, California, USA
pGEM-T Easy Vector System I Kit	Promega, NSW, Australia
QIAquick Gel Extraction Kit	QIAGEN, GmbH, Germany
Ultraclean Mini Plasmid Prep Kit	Mo Bio Laboratories, CA, USA
VECTOR® NovaRED ™ substrate kit for peroxidase	Vector Laboratories, Inc., Burlingame, CA, USA

2.1.10. Solutions

All solutions were made with Milli-Q water. These solutions were sterilized by autoclaving or filtering through a 0.45 μm filter when necessary. Solutions used in these experiments are listed below:

Name	Content
ABTS® reagent	Citric acid buffer (pH 4), 0.12% (v/v) H_2O_2 and 0.5 mg/ml ABTS
Agarose gel loading buffer (5×)	50% (v/v) glycerol, 0.05% (w/v) Bromophenol Blue, 0.05% (w/v) Xylene Cyanol
Antibody diluent solution (for immunohistochemistry)	0.55 M sodium chloride and 10 mM sodium phosphate (pH 7.1)
Binding buffer (for europium binding assay)	100 mM HEPES, 100mM NaCl, 0.05% (v/v) Tween 20 and 2 μM DTPA
Binding buffer (for MAb fragmentation)	20 mM sodium phosphate (pH 7)
Citric acid buffer	60 mM Citric Acid, 80 mM di-sodium hydrogen orthophosphate (pH 4)
Coomassie Blue R stain solution	0.1% (w/v) Coomassie Brilliant Blue R, 30% (v/v) methanol and 10% (v/v) acetic acid
DEPC-milli-Q H_2O	0.01% v/v DEPC in milli-Q H_2O
Destain solution (for Coomassie Gel)	20% (v/v) ethanol and 10% (v/v) glacial acetic acid

Digestion buffer (for MAbs digestion with papain)	PBS (pH 7.5), 0.02 M cysteine and 0.02 M EDTA (disodium salt)
ECL solution 1	2.5 mM luminol, 0.4mM coumaric acid and 0.1M Tris (PH 8.5)
ECL solution 2	0.0192% (v/v) H_2O_2 and 0.1 M Tris (PH 8.5)
Elution buffer (for PD-10 column)	50 mM Tris-HCl pH 7.8 containing 0.9% (w/v) NaCl and 0.05% (w/v) Na-Azide.
Elution buffer (for s-IGF-1R or MAb purification)	0.1 M glycine, 0.15M NaCl (pH 2.6)
Gel Drying Solution	5% (v/v) glycerol, 30% (v/v) ethanol
Glycerol 80%	80% (v/v) glycerol in milli-Q H2O
HBS buffer	10 mM HEPES, 0.15M NaCl (pH 7.4)
HBS running buffer (for BIAcore)	10 mM HEPES, 150 mM NaCl, 3.4 mM EDTA, 0.005% (v/v) Tween20 (pH 7.4)
Hypertonic phosphate-buffered saline or (hPBS)	10 mM sodium/potassium phosphate with 0.274 M NaCl, 5 mM KCl (pH 7.2)
IP Binding buffer	10 mM Tris (pH 7.5), 1mM PMSF, 0.1% (v/v) Triton-X100, 2 mM EDTA (pH 8), 150 mM KCl
IP Wash buffer	10 mM Tris (pH 7.5), 1 mM PMSF, 0.1% (v/v) Triton-X100, 2.5 mM EDTA (pH 8), 150 mM KCl
Luria Agar/Ampicillin Plates	2.5% (w/v) Luria Broth Base, 1.5% (w/v) Bacteriological Agar, 100µg/ml ampicillin)
Luria Broth (LB)	Luria Broth Base 2.5% (w/v)
Lysis buffer	20mM HEPES, 150 mM NaCl, 1.5mM MgCl2, 10% (v/v) glycerol, 1% (v/v) Triton X-100, 1 mM EGTA (pH 7.5)
PBS (Phosphate buffered saline)	0.137 M NaCl, 2.7 mM KCl, 1.46 mM KH_2PO4, 8.1 mM Na_2HPO_4, (pH 7.4)
PBS-T	PBS containing 0.1% (v/v) Tween-20
Regeneration solution (for BIAcore)	10 mM glycine-HCl (pH 1.7)
Resolving-gel	18-25% (v/v) acrylamide (40% stock solution), 13% (v/v) bis (2% stock solution), 0.25% (v/v) TEMED and 0.02% (w/v) ASP, in resolving gel buffer.
Resolving-gel buffer	1.5 M Tris and 0.4% (w/v) SDS (pH 8.8)
SDS-Page load buffer (5×)	0.25 M Tris (pH 6.8), 10% (w/v) SDS, 0.5% (w/v) bromophenol blue and 50% (v/v) glycerol.
Stacking-gel	11% (v/v) acrylamide (40% stock solution) 6% (v/v) bis (2% stock solution), 0.1% (v/v) TEMED and 0.05% (w/v) ASP in stacking gel buffer.
Stacking-gel buffer	0.5 M Tris and 0.4% (w/v) SDS (pH 6.8)
TAE buffer	40mM Tris, 40mM Glacial acetic acid, 1mM EDTA (pH 8.0), made in DEPC milli-Q H_2O
TBS	25 mM Tris (pH 7.4), 137 mM NaCl, 2.7 mM KCl
TBS-T	TBS, 0.05% (v/v) Tween-20
Transformation Buffer 1	30 mM KAc, 100 mM RbCl, 10 mM $CaCl_2$, 50 mM $MnCl_2$ and 18.7% (v/v) glycerol
Transformation Buffer 2	10 mM MOPS, 10 mM RbCl, 75 mM $CaCl_2$, 15% (v/v) glycerol
Western transfer buffer (wet method)	0.8% (v/v) 3M Tris (pH 8.3), 1.87% (w/v) glycine and 20% (v/v) methanol

2.1.11. Computer Applications

IMGT

IMGT/V-QUEST is used to analyse the immunoglobulin (Ig) nucleotide sequence and identify the CDR part of the V_L or V_H and to make comparisons with the IMGT reference directory.

Address: http://imgt.cines.fr

ClustalW

ClustalW™ is used to align DNA or protein sequences in order to identify homologous or conserved regions or residues (Thompson *et al.*, 1994).

Address: http://www.ebi.ac.uk/ClustalW

UCSF Chimera molecular graphics program

UCSF Chimera is used for modelling the IGF-1R and IGF-I.

Address: http://www.cgl.ucsf.edu/chimera

Chromas

Chromas 1.45 (Queensland, Australia) used to view the ab1 sequencing files.

Prism

Prism 3.03 (San Diego, CA) is used for calculating IC_{50} values and also statistical analysis.

2.2. General Methods

General methods, which have been used several times in this thesis, are explained in this section. Specific methods are described in the relevant chapter.

2.2.1. Culture of Mammalian Cells

Standard tissue culture techniques were used in the culture of mammalian cells. These included thawing, subculturing and freezing which are briefly described as follows. Cells in a vial stored in liquid N_2 were thawed rapidly in a 37°C water bath before dilution in 10 ml media, centrifugation (200×g for 2 min) and resuspension in fresh medium for culture at 37°C in a 5% (v/v) CO_2 environment. To passage cells, when the cells become 80% confluence, adherent cell monolayers were washed twice with PBS and trypsinized (1 ml trypsin/EDTA per 75 cm^2) for 2 min at 37°C in 5% (v/v). Detached cells were resuspended in medium containing 10% (v/v) fetal calf serum (FCS), centrifuged (200 × g for 3 min) and resuspended in fresh medium. The viable cell counts were determined with a 1:2 (v/v) dilution of trypan blue, and a haemocytometer grid prior to subculturing. Non-adherent cells were centrifuged, resuspended in fresh medium and counted before subculturing. The cell lines were cultured in their related medium (see Section 2.1.7). To freeze cells, healthy cells in exponential growth phase were washed, harvested and resuspended in freezing medium before immediate transfer into vials and storage at -80°C. After 2-3 days the vials moved to liquid N_2 for long-term storage.

2.2.2. Protein Chemistry Techniques

2.2.2.1. ELISA Test for Detection of s-IGF-1R

In this thesis, the soluble extracellular part of the IGF-1R (amino acids 1-906) is referred to as the soluble receptor (s-IGF-1R). An ELISA (enzyme linked immunosorbent assay) was conducted to identify and quantitate secreted or purified s-IGF-1R. Each well of a Nunc MaxiSorp™ flat-bottom 96 well plate was coated with 100 µl MAb 24-55 solution (2.5 µg/ml in PBS) overnight at 4°C and blocked with 2% (w/v) BSA in PBS overnight at 4°C. After washing the plate once in PBS-T, 100 µl of solution containing s-IGF-1R was added to the plate (100 µl/well) and incubated at room temperature (RT) for 2 h. Then the plate was

washed 3 times in PBS-T and incubated for 1 h at RT with 100 µl biotinylated-MAb 24-60 (stock: 1mg/ml) diluted 1:5000 (v/v) in PBS containing 1% (w/v) BSA. After washing the plate as above, the 1:400 (v/v) diluted streptavidin-HRP conjugate in PBS was added to the plate (100 µl/well) and incubated for 1 h at RT and rewashed as above. The bound HRP was detected by adding 100 µl ABTS® reagent to each well of the plate. After 20-30 min the absorbance at 405 nm was measured with a microplate reader (Molecular Device E_{Max} precision).

2.2.2.2. ELISA Test for Detection of Antibodies Against IGF-1R

Each well of a Nunc MaxiSorp™ flat-bottom 96 well plate was coated with 100 µl of s-IGF-1R solution (0.5 µg/ml) in PBS for overnight at 4°C and then blocked with 200 µl of 2% (w/v) BSA in PBS for 2 h at RT. Plates were washed once with PBS-T. Then, 100 µl of solution containing the antibodies against the IGF-1R were added to each well and incubated for 2 h at RT. The positive control was anti-IGF-1R MAb 24-60 (Soos *et al.,* 1992) and the negative control was mouse IgG1, both diluted in PBS to a final concentration of 0.02 mg/ml. Then the plate was washed three times with PBS-T followed by incubation with 100 µl secondary MAb, which was anti-mouse immunoglobulin HRP conjugate, diluted 1:500 (v/v) in PBS containing 1% (w/v) BSA, for 1 h at RT. After washing the plate as above, the bound MAbs were detected using ABTS® reagent as described in Section 2.2.2.1.

2.2.2.3. Protein Concentration

The protein concentration was determined by using either Bradford (Bradford, 1976) or BCA protein assay reagent (Stoscheck, 1990) as per the manufacturers' instructions. 10-25 µl BSA standards (in the range of 0-1.0 mg/ml) and sample (neat or diluted) were added to a 96-well plate with either 200 µl of 25% (v/v) Bradford's reagent or BCA mixture. The OD_{600nm} was

measured on a 96-well Emax™ microplate reader (Molecular Devices). The standard curve was calculated and used to determine the sample concentration.

2.2.2.4. Flow Cytometry

To determine the binding of different antibodies to the receptors, which are expressed on the cell surface, flow cytometry analysis was performed.

Initially cells expressing the desired receptor underwent cell sorting to isolate cells expressing similar levels of receptors. The cells were grown in their specific medium (see Section 2.1.7) in a T175 cm^3 flask to reach 80% confluence. Then the cells were washed with PBS and trypsinized with 2ml trypsin/EDTA for 2 min at 37°C and in a 5% (v/v) CO_2 incubator. Detached cells were resuspended in 10 ml medium containing 10% (v/v) fetal calf serum (FCS), centrifuged at 1,000 rpm in a GT-175 centrifuge (Spintron) (200 × g) for 3 min and resuspended in ice-cold PBS. The cells were then washed twice with and resuspended in ice-cold PBS. Between each step of washing the cells were pelleted by centrifuging at 200 × g for 2 min. Then 10^5 to 10^6 cells were resuspended in 100 µl of the solution containing the primary antibody against the receptor on the surface of the cells. Positive and negative control MAbs were made at a final concentration of 0.02 mg/ml. The cell suspensions were incubated on ice for 40 min then washed three times with 3 ml wash solution (PBS containing 1% (w/v) BSA and 0.01% (w/v) Na-Azide). Anti-mouse IgG FITC conjugated antibody was diluted 1:50 (v/v) in PBS containing 10% (v/v) normal rat serum and used as a secondary antibody in a volume of 50 µl. After incubating the cells with the secondary antibody on ice for 1 h, the cells were washed three times in wash solution by centrifugation and aspiration as described before. The cells were fixed in 500 µl of 1% (w/v) paraformaldehyde in PBS and stored in the dark on ice until flow cytometry acquisition in a FACScan Flow Cytometer using CellQuest Pro software (Becton Dickinson, CA, USA).

2.2.2.5. SDS-PAGE Electrophoresis and Gel Staining

Denaturing SDS-PAGE gels composed of tris-tricine and 8-10% (v/v) acrylamide were prepared using a Hoefer™ gel pouring apparatus. The resolving-gel was allowed to polymerise followed by the stacking-gel. Protein samples were loaded onto the gel under reducing or non-reducing conditions. For non-reducing conditions the lysate and loading buffer mixture (lysate-Lb) loaded to the gel directly. For reducing conditions, 5% (v/v) beta-mercaptoethanol (BME) was added to the lysate-Lb mixture and the solution was heated on a heating block (90 °C) for 3 min followed by cooling on ice before loading into the gel. Gels then were electrophoresed at 60 mA per gel until the ion front reached the bottom of the gel. Next the gels were stained for 30 min at 37°C in Coomassie Blue R™ stain solution to visualise the protein content. The excess stain was removed by extensive washing in Destain solution. After 30 min in Gel Drying solution, the gels were dried overnight at RT. A digital image of the gel was recorded using a Canon laser scanner and UMAX® MagicscanII software.

2.2.2.6. Electroblot and Western Immuno-Detection

Protein bands were separated by SDS-PAGE and detected using the standard Western immunodetection method (Ausubel *et al.,* 1995). This involved a Tris-tricine SDS-PAGE gel aligned onto a BioTrace™ nitrocellulose membrane or PVDF membrane (Hybond P) within a Whatmann™ paper sandwich. Prior to sandwich assembly, the gel, nitrocellulose and Whatmann™ paper were equilibrated in Western transfer buffer (wet), for 10 min to allow current conduction. Transfer of the protein from the gel to the nitrocellulose was performed at 80 mA per gel in a wet electro-blot apparatus (BIO-RAD California, U.S.A). Upon completion of the transfer, membranes were blocked in 5% (w/v) skim milk in PBS for 2 h at RT. After washing in PBS-T, membranes were probed for 1-24 h at 4°C with a primary diluted in blocking solution (dilution and incubation time were antibody dependent). After

five successive PBS-T washes, the membrane was incubated for 1h at RT with a 1:5000 (v/v) dilution HRP conjugated secondary antibody in blocking solution. Another series of PBS-T washes was performed before the membrane was blotted dry and covered with a fresh mix of equal volumes of the ECL detection solutions. Membranes were exposed to X-ray film (1sec-15 mins) and the film developed using a CURIX® 60 x-Ray developer. Digital images were recorded using a Canon laser scanner and UMAX® MagicscanII software.

2.2.2.7. Immunoprecipitation of Proteins from Cell Lysates

The cells which were the source of the protein (receptor) to immunoprecipitate, were lysed as described in (Denley *et al.*, 2004) in lysis buffer containing 1% (v/v) mammalian cocktail protease inhibitor (Sigma P8340). The total protein concentration was quantitated with BCA reagent as described in Section 2.2.2.3 as Triton-X100 is tolerated in this assay. Then 10 μg antibodies against the specific protein to immunoprecipitate were incubated overnight at 4°C (on gentle rocking) with cell lysate containing 850 μg total protein diluted 1:3 (v/v) in the IP binding buffer. No antibody was the negative control for the immunoprecipitation. Immune complexes were obtained by adding 15μl of the Protein G-agarose beads for 2 h at 4°C. Then the beads were pelleted by centrifugation at 2000 rpm in 5415D centrifuge (eppendorf) (400 × g) for 5 min at 4°C. The beads were washed 3 times with ice-cold IP wash buffer. The antibody-bound receptors were removed from the beads by boiling in 30 μl of 2 × SDS-PAGE loading buffer containing 2% (v/v) BME. Then 25 μl of each sample was loaded onto a 10% SDS-PAGE gel for electrophoresis and Western blot analysis. Protein bands were separated by SDS-PAGE and detected using the standard Western immunodetection method as described in Section 2.2.2.5 and Section 2.2.2.6 (Ausubel *et al.*, 1995).

2.2.3. Molecular Biology Techniques

The following methods were performed essentially as described in the manual "Molecular Cloning: A laboratory Manual"(Sambrook *et al.,* 1989).

2.2.3.1. Agarose Gel Electrophoresis

Mini-gels were prepared by dissolving 1-1.5%(w/v) agarose in 1× TAE buffer. Gels were allowed to set in an appropriate tray and then submerged in 1× TAE buffer in an electrophoresis tank (Bio-Rad Sub-cell GT WIDE MINI running chamber). RNA or DNA samples were mixed to a final concentration of 1× agarose gel loading buffer. The marker was 1µl 2-Log DNA Ladder (New England Biolabs). The samples and marker were electrophoresed in 1% (w/v) agarose gels submerged in 1× TAE running buffer at 100 V. Then the gels were stained in ethidium bromide solution (5µg/ml) for 5 min followed by de-staining in DEPC-milli-Q H_2O for 2 min. Then the bands were visualised by exposure to UV light on a Chromato-vue transilluminator (Ultra-violet Products®) and photographed.

2.2.3.2. Preparation of DH5-α Competent Cells

Competent cells used to transform plasmid DNA were prepared as follows. A small scale bacterial culture was set up in Luria Broth (LB) from a single *E. coli* DH5α colony and grown overnight at 37°C with shaking. The following morning, 330µl of the overnight culture was subcultured in 10 ml of LB and the culture expanded until it reached an OD_{600nm} reading of 0.5-0.6. Then a 5% (v/v) subculture was made in 100ml pre-warmed LB and incubated at 37°C for 1.5 hr. Then the culture was split into 4 × 50 ml centrifuge tubes and chilled on ice for 5 min before the bacterial cells were collected by centrifugation at 4000 rpm, in a GT-175 centrifuge (Spintron) (3,200 × g) for 5 min at 4°C. The cells then were resuspended in transformation buffer 1 and chilled on ice for 5 min, and then collected by centrifugation as above for 5 min at 4°C. The cells were then resuspended in 1ml transformation buffer 2 per

tube (4ml total) and placed on ice for 5 min. Approximately 200 µl aliquots in eppendorf tubes were stored at -80°C until required.

2.2.3.3. Transformation of Bacteria by Heat Shock

Competent cells were transformed with circular plasmids using a heat shock method. Briefly, plasmid DNA was mixed with 100 µl DH5-α competent cells and incubated on ice for 20 min before heat shock at 42°C for 2 min and then incubation on ice for a further 5 min. Cells were then plated on pre-warmed 90 mm Luria Agar plates containing the appropriate selection antibiotic and incubated overnight at 37°C. Colonies were picked and small-scale DNA preps made for each.

2.2.3.4. Glycerol Stocks

A small-scale bacterial culture was set up in selective LB media from a single *E. coli* transformed colony and grown overnight shaking at 37°C. The following morning, duplicate 500 µL samples were diluted 1:1 (v/v) with 80% (v/v) glycerol, mixed and stored at –80°C.

2.2.3.5. Bacterial Culture

Single colonies of bacteria, obtained by streaking the glycerol stock onto LB agar plates, were used to inoculate liquid growth medium. The bacterial cultures were grown at 37°C with continuous shaking to provide adequate aeration. The agar plates or liquid medium were supplemented with the appropriate antibiotic when required.

2.2.3.6. Purification of Plasmid DNA

The Ultraclean mini plasmid prep kit was used for purifying the plasmid DNA from overnight cultures as described in the manufacturer's instructions. By using a Cary 3 Bio UV-visible Spectrophotometer (Varian, Vic, Australia), total purified plasmid was quantified. Plasmids

were diluted 1:100 (v/v) in milli-Q H_2O, and the absorbance of the sample measured at a wavelength of 260 nm (A_{260}). This absorbance was used to determine the concentration of plasmids in each sample using the following equation:

$$\text{Concentration } (\mu g/\mu l) = A_{260} \times \text{Dilution factor} \times 0.05.$$

2.2.3.7. DNA Sequencing

Purified plasmid DNA was used for sequencing. A reaction mix was set up containing 1 to 4 µg of plasmid DNA, 100 ng sequencing primer and 4 µl of Big Dye (version 3) sequencing mix. The volume of the reaction mix was made up to 20 µl total with autoclaved milli-Q H_2O. The sequencing primer for the pGEM-T Easy Vector was USP or RSP and for the pcDNA3-zeo (+) plasmid was Primer aIR3KR-AA. The mixture then was subjected to polymerase chain reaction (PCR) for 30 cycles of denaturation at 96°C for 30 sec, annealing at 50°C for 15 sec and extension at 60°C for 4 min and lowering the temperature to 15°C terminated the reaction. After the PCR reaction, each mixture was transferred to a 1.5 ml microcentrifuge tube containing 80 µl isopropanol 75% (v/v) and 1 µl of glycogen (20 µg/µl) and briefly vortexed. Then the tube was incubated at RT for 30 min and the DNA was pelleted by centrifugation at 13,200 rpm in 5415D centrifuge (eppendorf) (17,500× g) for 20 min. The supernatant of the tube was carefully aspirated and discarded. The pellet was then washed with 250 µl 75% (v/v) isopropanol by vortexing thoroughly. The tube was centrifuged as above for 5 min to pellet the DNA and the supernatant was discarded again. The DNA pellet was dried in a 37°C heating block. The pellet was sent to the sequencing service at the Institute of Medical and Veterinary Science, Adelaide, Australia and the ab1 sequencing files were viewed using the chromas 1.45 software application.

Chapter 3

Production, Characterisation and Sequencing of the Variable Regions of Mouse Monoclonal Antibodies

3. Production, Characterisation and Sequencing of the Variable Regions of Mouse Monoclonal Antibodies

3.1. Introduction

The generation of monoclonal antibodies (MAbs) has been widely used in scientific research for 30 years (Kohler and Milstein, 1975). Using laboratory mice, the natural immune response is harnessed in order to obtain antibody-secreting cells. Injection of the immunogenic protein into the animal stimulates antigen-presenting cells to phagocytose the immunogen and display fragments of it on their cell surface in combination with major histocompatibility complex (MHC) molecules (Roitt *et al.,* 1989).

Immunogenic proteins are recognized by the immune system and interact with two different classes of antigen receptors, antibodies and T-cell receptors, made by two major cell types of the immune system. An antigen stimulates those B cells, which have antibody molecules on their surfaces that can recognize and bind the antigen. This binding activates production of a clone of identical B cells that secrete soluble antigen-binding antibodies into the bloodstream. T cells identify foreign antigens through a T-cell receptor that can bind degraded fragments of the antigen when they are associated with a MHC molecule (Branden and Tooze, 1999).

Hybridoma cells are a pure source of monoclonal antibody (MAb) of a desired specificity and they are most commonly of rodent origin. The clinical potential of these MAbs is limited because therapeutic mouse antibodies can cause an immune response in humans. To overcome this problem, mouse/human chimeric antibodies have been constructed by substitution of all but the murine variable regions (Poul *et al.,* 1995) or by grafting murine complementarity determining regions (CDR) with human framework regions (FR) (Jones *et al.,* 1986). In addition, bioactive paratope-derived peptides (PDP) designed from mouse MAbs are also a powerful tool to achieve minimal antibody-like structure (Laune *et al.,* 1997; Monnet *et al.,* 1999) presenting the lowest human anti-mouse antibody reaction.

Such humanisation of a mouse MAb or identification of PDPs relies on efficient amplification and sequencing of mouse variable regions from the MAb under study. Different strategies have been used for this purpose so far. Murine V genes have been classified into 15 V_H and 18 Vκ gene families, based on amino acid and/or nucleotide sequence similarities (Potter *et al.,* 1982; Strohal *et al.,* 1989; Kofler *et al.,* 1992; Mainville *et al.,* 1996). A one-side polymerase chain reaction (PCR) using a 3′ primer directed to the constant region has been described and is independent of the sequence of the variable segment (Heinrichs *et al.,* 1995). The most common methods, however, employ 5′ primers that take advantage of conserved features of the antibody framework (FR) (Orlandi *et al.,* 1989; Chaudhary *et al.,* 1990; Kettleborough *et al.,* 1993) or signal (S) sequences (Gavilondo-Cowley *et al.*, 1990; Coloma *et al.*, 1991; Jones and Bendig, 1991; Coloma *et al.*, 1992) within antibody variable areas, in conjunction with a 3′ primer directed to the constant region of the MAb. An approach employing FR primers can lead to the replacement of amino acids in the frame affecting antigen binding (Panka *et al.,* 1988; Chien *et al.,* 1989). Priming in the conserved motifs from the immunoglobulin (Ig) signal region is a powerful way to achieve entire sequences of antibody variable regions. In attempts to potentially amplify Ig genes from all V gene families, various sets of signal sequence primers have been constructed and described (Gavilondo-Cowley *et al.*, 1990; Coloma *et al.*, 1991; Jones and Bendig, 1991; Coloma *et al.*, 1992; Chardes *et al.*, 1999).

In this study, to determine the sequences of the variable regions of the generated MAbs, the oligonucleotides provided by the Mouse Ig-Primer Set (Novagen) were utilised to specifically amplify the hypervariable regions using PCR (Larrick *et al.*, 1989; Chaudhary *et al.*, 1990; Coloma *et al.*, 1991; Jones and Bendig, 1991). In this Ig-Primer set, there are sets of 5′ primers, which are complementary to the upstream signal sequence and 3′ primers directed to the constant region for light or heavy chains (Figure 3.1). These primers have been listed in Table 3-1. Details of the techniques will be described in Section 3.3.

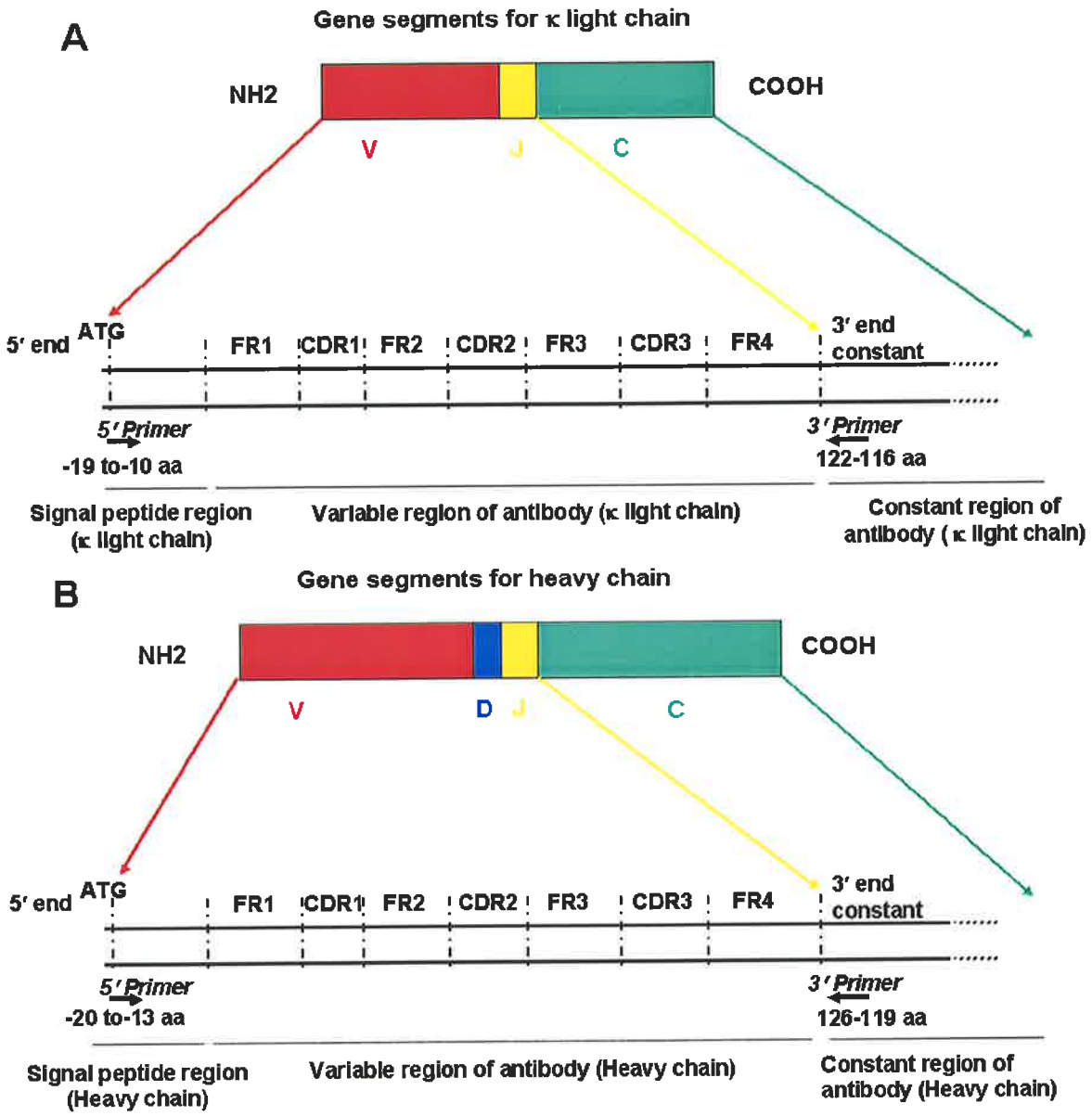

Figure 3.1 The strategy for PCR cloning of mouse rearranged immunoglobulin variable light (A) or heavy (B) regions.

Annealing sites for the primer combinations are shown in this figure; 5′ end in the leader sequence and 3′ end in the constant domain for both light and heavy chains. aa=amino acid

After sequencing the variable regions of MAb, the CDRs and FRs can be determined. Several methods for numbering the sequences of the variable domains have been described including the Kabat numbering scheme (Kabat *et al.,* 1991), Chothia numbering Scheme (Chothia *et al.,* 1989; Al-Lazikani *et al.,* 1997) and the IMGT unique numbering scheme (Lefranc *et al.,* 2003; Giudicelli *et al.,* 2004; Pommie *et al.,* 2004). In this study the sequences were analysed with the IMGT/V-Quest application, which is based on the IMGT unique numbering and its reference directory.

3.2. Methods for General Characterisation of MAbs

The general methods have been described in Chapter 2 and the specific methods are described as follows.

3.2.1. Animal Ethics

All animal procedures were carried out in accordance with the guidelines of the National Health and Medical Research Council of Australia. The Animal Ethics Committee of the University of Adelaide approved antibody production in mice.

3.2.2. Antigen Production and Purification

3.2.2.1. Culture and Purification of s-IGF-1R

The soluble extracellular part of the IGF-1R (amino acids 1-906), often referred to as the soluble receptor (s-IGF-1R), was used as the immunogen to immunise BALB/C mice in order to raise antibodies against IGF-1R. The s-IGF-1R antigen was purified from the culture medium of stably transfected BHK21 cells expressing the extracellular part of the IGF-1R into their medium. The recombinant cells were made in-house by Dr. Kathy Surinya (The University of Adelaide, Australia) using the same method as utilised for making recombinant soluble insulin receptor extracellular domain (Cosgrove *et al.,* 1995; Hoyne *et al.,* 2000a).The cells were grown at 37°C and 5% (v/v) CO_2 until 80-90% confluent in GMEM-S medium containing 10% (v/v) dFBS (Dialyzed fetal bovine serum), 2% (v/v) Glutamine synthetase (GS) Supplement (50×) and 25 μM MSX (Methionine sulfoximine). Then, for the purification of the s-IGF-1R, the culture medium was collected, centrifuged at 1,000 rpm (200 × g) for 5 min in GT-175 centrifuge (Spintron) and filtered through a 1 μm filter (GMF 150).

The s-IGF-1R was purified by affinity chromatography using MAb 24-55, specific for the IGF-1R, which was coupled to Affi-Gel® 10 Gel. The column was washed with filtered PBS for 40-50 min (Flow rate: 1 ml/min), and then the filtered culture medium containing

s-IGF-1R was loaded onto the column. The column was washed with filtered PBS for 40-50 min again and then the s-IGF-1R was eluted using elution buffer. The eluate containing s-IGF-1R was collected in tubes in 1 ml fractions and neutralized immediately by adding 80µl 1M Tris (pH 9.0). The elution profile was recorded at A_{280} nm. Purified s-IGF-1R, was dialyzed against PBS buffer in Cellu.Sep®T2 cellulose tubular membrane. The protein (s-IGF-1R) concentration was determined by using BCA protein assay reagent (Stoscheck, 1990) as described in the manufacturers' instructions.

3.2.2.2. ELISA Test for Detection of Purified s-IGF-1R

An ELISA was conducted to identify fractions from the s-IGF-1R purification that contain s-IGF-1R as generally described in Section 2.2.2.1. For this experiment, the Nunc MaxiSorp™ flat-bottom 96 well plate coated with MAb 24-55 and blocked with 2% (w/v) BSA solution in PBS was used. 100 µl of purified and neutralized s-IGF-1R solution (from each 1 ml fraction) was added to each well of the plate and the bound s-IGF-1R was detected by biotinylated-MAb 24-60 and streptavidin-HRP conjugate as described before.

3.2.3. Hybridoma Production

3.2.3.1. Immunisation of the Mice

Four female BALB/C mice were injected intraperitoneally with different immunogens several times with different intervals as follows:

- **Mouse No. 1**: was given 3 intraperitoneal injections of 30 or 50 µg of purified s-IGF-1R in PBS plus 50 µg MDP adjuvants (Auspep), 3 to 5 weeks apart. Three days before being sacrificed the mouse was boosted with 20 µg s-IGF-1R.
- **Mouse No. 2:** was immunised similar to the mouse No.1 but with two further immunisations.

- **Mouse No. 3:** was given 4 intraperitoneal injections of 10^6 P6 cells 4 to 10 weeks apart, and 5 days before being sacrificed it was boosted with 10^6 P6 cells.
- **Mouse No. 4:** was given 5 intraperitoneal injections of 10^6 or 8×10^6 P6 cells 4 to 10 weeks apart followed by two immunisations with 40 μg of purified s-IGF-1R in PBS plus 50 μg MDP adjuvants, 3 to 5 weeks apart. The mouse was boosted with 30 μg of purified s-IGF-1R plus 50 μg MDP adjuvants four days before being sacrificed.

3.2.3.2. ELISA Test for Detection of Antibodies in Plasma from Immunised Mice

Seven days after each immunisation, mice were bled and the sera were obtained and tested for anti-IGF-1R antibody.

The ELISA assay of anti-IGF-1R immunoglobulin titre in mouse plasma was performed as generally described in Section 2.2.2.2. In brief, each well of a Nunc MaxiSorp™ flat-bottom 96 well plate was coated with s-IGF-1R solution and blocked with 2% (w/v) BSA in PBS. 100 μl of the mouse sera at different dilutions, 1:10, 1:100, 1:1,000, 1:10,000 and 1:100,000 (v/v) in PBS-3% (w/v) BSA were added to each well (in triplicate) and incubated for 2 h at room temperature (RT). The positive control was MAb 24-60 (0.02 mg/ml) (Soos *et al.,* 1992) and the negative control was mouse IgG1 (0.02mg/ml) diluted in PBS. The bound anti-IGF-1R MAbs were detected by anti-mouse immunoglobulin HRP conjugate as described before. When each mouse developed anti-receptor antibodies, detectable at 1:10,000 dilution of serum, it was sacrificed for MAb production.

3.2.3.3. Preparation of Lymphocytes from Mouse Spleen

Having reached a desirable titer of anti-s-IGF-1R, the immunised animal was sacrificed by cervical dislocation and the spleen was removed aseptically and placed in a sterile dish containing DMEM. Fat and other tissues were trimmed from the surface of the spleen. The organ was washed again with DMEM medium in a fresh sterile dish. The spleen was cut, then gently disrupted and homogenised into 10 ml of DMEM between the frosted ends of sterile glass microscope slides. A normal mouse spleen was homogenised in the same way in a separate dish to provide feeder cells. Each cell suspension was transferred into a 50 ml tube with care to not transfer any pieces of connective tissue along with the cells. The immune and normal spleen cells were washed and centrifuged at 1,000 rpm (200 × g) for 4 min in GT-175 centrifuge (Spintron) and resuspended in 5 ml of DMEM. The immunised mouse spleen cells and normal mouse (feeder) spleen cells were counted.

3.2.3.4. Preparation of Myeloma Cells for Fusion

SP2/0 mouse myeloma cells were used to produce hybridomas (Ozato and Sachs, 1981) employing a standard methodology (Harlow and Lane, 1988).

SP2/0 cells were grown in DMEM/F12 medium containing 20% (v/v) FCS in flasks at 37°C in 5% (v/v) CO_2. The myeloma cells were in the exponential phase of growth and 90% viable before fusion. On the day of fusion, the cells were counted and washed twice with 50 ml DMEM, centrifuged at 1,000 rpm (200 × g) for 4 min in GT-175 centrifuge (Spintron) and each one resuspended in DMEM.

3.2.3.5. Fusion of Myeloma Cells with Spleen Lymphocytes

The fusion protocol was a modification of that described by (Harlow and Lane, 1988). Here the protocol for the first fusion (mouse No.1 immunised against s-IGF-1R) is described. The

protocol for the other three fusions was very much the same with minor differences in the number of spleen cells and SP2/0 cells used[#].

In the first fusion, 2×10^8 spleen cells from the immunised mouse were mixed with 4.0×10^7 SP2/0 myeloma cells in 50 ml DMEM (ratio of 5:1 spleen cells to SP2/0) and centrifuged at 1,000 rpm (200 × g) for 4 min in GT-175 centrifuge (Spintron) at RT. The supernatant was carefully discarded and the cells were maintained at 37°C in a water bath for further manipulations. One ml of pre warmed 50% PEG 1500 (w/v) in 75 mM Hepes buffer (pH 8.0), was added gradually to the cell suspension over a one min period with slight agitation. The suspension was then gently stirred with a pipette for an additional minute. To stop the fusion, 2 ml of DMEM was added gradually over a 2 min interval with gentle stirring. A further 7 ml of the same medium was then added over 3 min with gentle stirring. The cell suspension was then centrifuged at 1,000 rpm (200 × g) for 5 min in GT-175 centrifuge (Spintron) and at RT. The supernatant was discarded and the cell pellet was resuspended in 162 ml of fusion medium containing 1.1×10^8 normal spleen lymphocytes prepared from a non-immunised mouse as described in Section 3.2.3.3. One hundred µl of this mixed cell suspension (~2×10^6 cells/ml) was added into each well of ten 96-well culture plates and maintained at 37°C in 5% (v/v) CO_2. The following day, 100 µl of the selection medium, which was fusion medium containing 200 µM hypoxanthine and 2 µg/ml azaserine, was added to each well of the plates. HAT selection medium (Gibco-BRL) was added after 3 days and changed every 4 to 5 days until the monolayers reached greater than or equal to 50% confluence (10-20 days after fusion). At this stage cultures were screened for antibody production.

[#] Injection of mice, bleeding and generation of myeloma line was performed by Mr John Mackrill, The University of Adelaide.

3.2.3.6. Detection of Antibodies Against s-IGF-1R in the Hybridoma Culture Mediums

Viable hybridomas were obtained after each fusion. Depending on when individual cultures reached greater than or equal to 50% confluence they were screened for production of anti-s-IGF-1R immunoglobulins using the ELISA assay as described in Section 2.2.2.2. However, in this assay 100 µl of neat conditioned media was applied to each well of the plates.

The clones that expressed antibodies against s-IGF-1R, were expanded in 24-well plates containing hybridoma culture growth medium with the azaserine-free hybridoma selection medium. To determine the specificity of the antibodies secreted in the conditioned media, a control ELISA test was conducted on uncoated but blocked plates. Based on the strength of their reactions in the ELISA test, the consistency of production of antibodies that reacted with the s-IGF-1R and the ability of the cultures to survive, some of the positive hybridomas were selected for cloning using the limiting dilution technique (Section 3.2.3.7).

3.2.3.7. Cloning by Limiting Dilution of Hybridoma

The hybridoma cell cultures specifically positive against the s-IGF-1R in the ELISA test, were selected and subcultured at limiting dilutions to produce monoclonal cultures of antibody producing hybridoma cells. The cells were diluted to 60 cells/ml, 30 cells/ml, 15 cells/ml and 7.5 cells/ml and following addition of 100 µl per well resulted in a concentration of 6, 3, 1.5 and 0.75 cells/well. For each hybridoma culture, four viable potential clones, which produced antibodies that reacted positively with s-IGF-1R coated plates (using ELISA as described in Section 2.2.2.2), were obtained from the 0.75 or 1.5 cell/well dilution. The selected clones were cultured in 25 cm^3 and 75 cm^3 flasks and gradually (during two weeks) the culture medium was changed to the medium containing DMEM/FCS. Cloned cells were also stored frozen in liquid nitrogen at -196 °C.

3.2.3.8. Freezing and Thawing of Hybridoma Cells

Freezing of Hybridoma Cells

Only hybridoma cultures, which were in log phase growth, were used for freezing. The cells were suspended, centrifuged at 1,000 rpm (200 × g) for 5 min in GT-175 centrifuge (Spintron) and resuspended at 10^6-10^7 cells/ml in freezing medium (see Section 2.1.6). One ml aliquots of this suspension were pipetted into cryotube vials and sealed. The sealed cryotubes were placed immediately in a -80°C freezer. After 24 h, the cells were removed and stored in a liquid nitrogen tank.

Thawing of Hybridoma Cells

The cryotubes containing frozen cells were thawed in a 37°C water bath. The cells were transferred into a 24-well plate in DMEM/FCS. After 24 h, the medium was replaced with fresh medium. The cell cultures were then expanded gradually to 25 cm^3, 75 cm^3 or 175 cm^3 flasks.

3.2.4. Determination of Immunoglobulin Isotypes

The Mouse Typer® Sub- Isotyping Panel was used to determine the isotypes of the sub clones for the selected MAbs. The method was similar to previous ELISA tests for antibodies against s-IGF-1R (Section 2.2.2.2). The plates were coated with s-IGF-1R, blocked with 2% (w/v) BSA in PBS and the test was conducted as per the manufacturer's specifications. Briefly, hybridoma culture media were added neat (100 µl/well) and incubated at RT for 1 h. After washing the plate 3 times with PBS-T, 50 µl of each rabbit anti-isotype antibody (provided by Mouse Typer® Sub- Isotyping Panel) was added to each well and incubated at RT for 30 min. The plate was then washed 3 times with PBS-T. The anti-rabbit antibody HRP conjugate (donkey) was diluted 1:400 (v/v) in PBS containing 1% (w/v) BSA, and 50 µl was added to each well of the plate. After 1 h incubation at RT, the plate was washed three times with

PBS-T and the isotype of antibodies detected by using ABTS reagent and reading the plate at 405 nm after 20-30 min as described in Section 2.2.2.1.

3.2.5. Screening of Positive Hybridomas for Binding to the IGF-1R Cell Surface Using Flow Cytometry

To determine the specificity of generated antibodies and their ability to bind to the intact IGF-1R on the cell surface, flow cytometry analysis was conducted. The method was generally described in Section 2.2.2.4.

Cells expressing the IGF-1R (P6 cells) and the two IR isotypes (R^-IR-A and R^-IR-B) (Denley *et al.*, 2004), were used for flow cytometry analyses. The R^- cell line was the negative control as it does not express IGF-1R (Sell *et al.*, 1994). Each of the P6, R^-IR-A, R^-IR-B and R^- cells were grown in a T175 cm^3 flask. Then 10^5 to 10^6 cells were resuspended in 100 µl of culture medium of selected positive hybridomas, which could contain the primary antibody against the IGF-1R. Positive controls were anti-IGF-1R MAb 24-60 and anti-IR MAb 83-7 and negative control was IgG1 (CHEMICON) all at a final concentration of 0.02 mg/ml. The MAbs bound to the cells were detected by anti-mouse IgG FITC conjugated antibody as explained in Section 2.2.2.4.

3.2.6. Large-Scale Production of the Selected MAbs

The selected hybridoma clones were grown for large-Scale production of the MAbs. The concentration of the FCS in the hybridoma medium was gradually reduced from 10% (v/v) to 2.5% (v/v) before inoculation in the spinner flask. For each hybridoma clone, the hybridoma cells were grown from an inoculum of 1.3×10^8 cells in a spinner flask packed with 10 g of Fibra-cel® disc cell carriers (Figure 3.2) and filled with 500 ml of DMEM medium containing 2.5% (v/v) FCS and 1% (v/v) penicillin/streptomycin. The spinner was operated at 5% (v/v) CO_2 and 37°C on a magnetic stirrer, and the medium was harvested after two weeks.

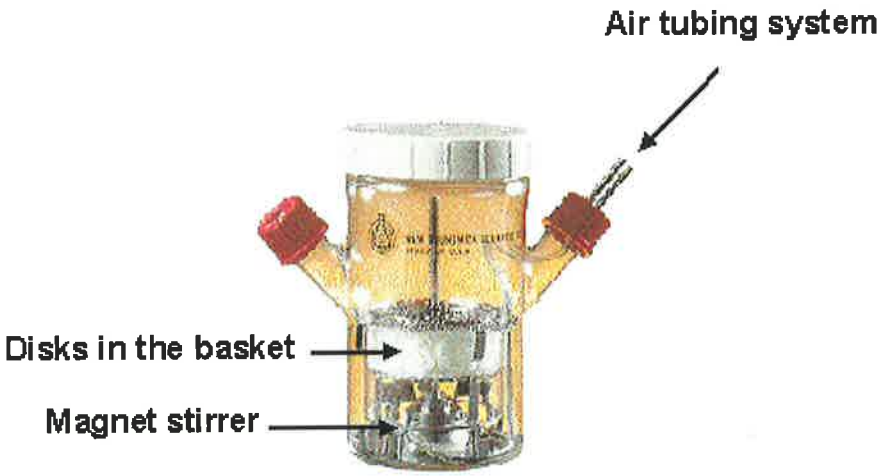

Figure 3.2 Spinner flask filled with Fibra-cel® discs for large-scale production of MAbs.
Figure is adapted from (New Brunswick Scientific Co, 2003).

3.2.7. Purification of Antibody and Determination of the Antibody Concentration

For the purification of IgGl monoclonal antibodies by Protein G column, the protocol described in (Andrew and Titus, 2004) was used with some modifications as follows. For each hybridoma clone, the hybridoma culture medium was collected from the spinner flask, centrifuged at 1,000 rpm (200 × g) for 10 min in 50 ml tubes and in GT-175 centrifuge (Spintron). Then filtered through a 1 μm filter (GMF 150) to remove any precipitate and cell debris. To purify each MAb, a 10 ml protein G column (Sigma, St Louis, MO, USA) was equilibrated in filtered PBS (pH 7.4) at 1 ml/min flow rate, and 500 ml of the hybridoma culture medium was loaded onto the column at the same flow rate. The rest of the purification procedure was the same as that described above for antigen purification (Section 3.2.2.1). The 1 ml neutralized fractions with maximum $A_{280\ nm}$ were collected, pooled and dialysed against HBS buffer. The concentration of MAbs was determined using UV detection. A 1 mg/ml solution of MAbs has an absorbance of 1.35 at 280 nm (Harlow and Lane, 1999).

3.2.8. SDS-PAGE Electrophoresis and Gel Staining of Purified MAbs

The purity of these MAb solutions were subsequently analysed by SDS-PAGE electrophoresis and gel staining as generally described in Section 2.2.2.5. Briefly the light and heavy chains of 1 μg of each purified MAbs was separated by SDS-PAGE in 10% acrylamide gel under reducing condition and the gel was then stained in Coomassie Brilliant Blue R^{TM}.

3.2.9. Freeze-Drying of the Purified MAbs

To determine the effect of freeze-drying on the MAbs' binding to the s-IGF-1R, the solutions of the selected MAbs in HBS buffer or in HBS buffer containing 60 mM trehalose (Cleland *et al.,* 2001) in a final concentration of 0.23 mg/ml for both MAbs 7C2 and 9E11 were lyophilised on a Virtis Benchtop 4K freeze-dryer (Virtis, Gardiner, NY, USA). After freeze-drying, they were dissolved in milli-Q H_2O, to reach the previous concentrations. Then serial dilutions of each one were made in HBS buffer and their activity against s-IGF-1R was determined by ELISA test as described in Section 2.2.2.2. The results were compared with the respective original solutions not subjected to lyophilization.

3.2.10. Immunoprecipitation and Western Blot Analysis

To demonstrate the ability of the obtained MAbs to immunoprecipitate the IGF-1R the following experiment was conducted. The method was generally as described in Section 2.2.2.7. In this experiment, P6 cells were used as a source of IGF-1R and the cells were lysed as described by (Denley *et al.,* 2004) in lysis buffer containing 1% (v/v) mammalian cocktail protease inhibitor (sigma P8340). In brief, the IGF-1R was immunoprecipitated from 250 μl P6 lysate containing 850 μg total protein diluted (1:3) (v/v) in the IP binding buffer using the primary anti-IGF-1R antibodies; 9E11, 7C2, 24-55 (positive control) (Soos *et al.,* 1992) or no antibody (negative control) overnight at 4°C with gentle rocking. Immune complexes were obtained by adding 15 μl of the Protein G-agarose beads for 2 h at 4°C. Then the beads were

pelleted and the antibody-bound receptors were removed from the beads by boiling in 30 µl of 2 × SDS-PAGE loading buffer containing 2% (v/v) µl of beta-mercaptoethanol. Then 25 µl of each sample was loaded onto a 10% SDS-PAGE gel for electrophoresis and Western blot analysis. Full range rainbow recombinant protein molecular weight markers (Amersham Biosciences) (10 µl) were also loaded onto a well of the gel.

Protein bands were separated by SDS-PAGE and transferred onto a BioTrace™ nitrocellulose membrane using the standard Western immunodetection method (Ausubel *et al.,* 1995) as generally described in Section 2.2.2.6. Upon completion of the transfer, the protein bands were detected with a primary antibody IGFR 1-2 solution (Soos *et al.,* 1993) diluted 1:1,000 (v/v) in PBS solution containing 1% (w/v) BSA. Antibody IGFR 1-2 is directed against the β subunit of the IGF-1R. Then anti-mouse immunoglobulin HRP conjugate was used as a secondary antibody. Then, the HRP was visualised with ECL detection solutions and exposure to X-Ray film.

3.2.11. Immunoblotting of the IGF-1R Using the Generated MAbs

To determine the ability of the obtained MAbs to detect the IGF-1R in Western blot, these MAbs were used as a primary antibody to probe the reduced or non-reduced IGF-1R derived from P6 cells lysate. The method was generally described in Section 2.2.2.6.

In brief, 20 µl of cell lysate containing 16 or 8 µg total protein was loaded into 7.5% SDS-PAGE gel (under reducing or non-reducing conditions) and electrophoresed. The P6 cells lysate was obtained as described in Section 3.2.10. Under reducing condition, beta-mercaptoethanol (BME) acts as a reducing agent to break disulphide bonds and separates the α and β subunits of IGF-1R. The proteins were electrophoresed and transferred to PVDF membrane for immunoblotting with the generated MAbs, 7C2 and 9E11. The final concentration for the primary antibodies was 0.4 µg/ml. The mouse MAbs IgG1 and IGFR 1-2 were applied as negative and positive controls respectively. The MAb IGFR 1-2 has

been developed against the β subunit of the receptor. The membrane was incubated with anti-mouse immunoglobulin HRP conjugate antibody solution and the HRP was visualised with ECL detection solutions and exposing to X-Ray film.

For the reducing blot, the uniform loading was assessed by monoclonal anti-β-actin antibody. The dried PVDF membrane containing reduced IGF-1R was used for this experiment. The membrane was soaked in methanol for 30 sec followed by 3 washes in milli-Q H_2O and once in PBS for 5 min each. The membrane then blocked in 5% (w/v) skim milk in PBS for 1 h at RT. The anti-β-actin antibody was applied to the membrane in 1:20,000 (v/v) dilution in the blocking solution. After washing the membrane 3 times for 5 min each in PBS-T, it was incubated for 1 h at RT with a 1:5000 (v/v) dilution of anti-mouse immunoglobulin HRP conjugate antibody in PBS-T. The HRP was visualised with ECL detection solutions and exposing to X-Ray film.

3.2.12. Using the MAbs in Immunohistochemistry

To assess whether MAbs 7C2 and 9E11 would be useful in immunohistochemistry, three series of experiments were conducted on frozen cells, frozen skin sections or paraffin-embedded skin sections. The human skin was selected because *in vitro* analyses revealed the IGF-1R expression in all layers of the epidermis (Rudman *et al.,* 1997). For frozen cells or sections, the indirect immunofluorescence method described in (Irving-Rodgers *et al.,* 2004) was used with modifications. For paraffin-embedded tissue sections, the technique demonstrated in (White *et al.,* 2004) was utilised with some changes. These methods are discussed in the following sections.

3.2.12.1. Immunohistochemistry on Frozen Cells

The cell suspensions of 25×10^5 cell/ml were made in PBS for each cell line. Then 50 µl of cell suspension was added to each slide and centrifuged for 5 min at 80 rpm in Cytospin 2

centrifuge (Shandon Instruments, Astmoor, UK). The slides with cytospin cell preparations of P6, R⁻IR-A or R⁻IR-B cells were dried under vacuum for 5 min followed by fixation in acetone for 5 min. Optimising experiments showed that the use of acetone for fixation provides less background than ethanol or paraformaldehyde. Slides were washed in hypertonic phosphate-buffered saline (hPBS) 3 times for 5 min each. Next, the blocking solution (10% (v/v) donkey serum (normal) in antibody diluent solution) was applied to slides for 30 min at RT. The primary antibodies against the IGF-1R (7C2, 9E11, 24-31 and IgG1) were diluted to 1 μg/ml in the blocking solution and 200 μl were added to each slide, followed by overnight incubation in a humid chamber and at RT. The negative and positive controls were unrelated IgG1 antibody and MAb 24-31, respectively. The slides were then washed as above followed by incubation with biotinylated donkey anti-mouse IgG at 1:100 (v/v) dilution in antibody diluent solution for 2 h at RT in a humid chamber. After rewashing the slides, they were incubated with Streptavidin CY3/FITC in 1:100 (v/v) dilution in antibody diluent solution for 1 h at RT, rewashed as above for the last time and wet mounted in the fluorescent mounting medium. The slides were observed with an Olympus B×51 microscope with epifluorescence attachment (Olympus Australia) and images captured with a stop RT digital camera (Diagnostic Instruments Inc., Sterling Heights, MI, USA).

3.2.12.2. Immunohistochemistry on Frozen Skin Sections

Human skin embedded in Tissue-Tek OCT compound was cut using a CM1800 Leica cryostat, into 10 μm sections which were collected on glass slides and stored at -20°C in a sealed container until required. Details for the immunofluorescence assay was the same as Section 3.2.12.1.

3.2.12.3. Immunohistochemistry on Paraffin-Embedded Skin Sections

Human skin embedded in paraffin was cut using a microtome into 5-10 μm sections which were floated on a warm water bath (45°C), before being picked up onto glass microscope slides and allowed to drain. Paraffin was removed from the sections by putting them in Safsolvent twice for 5 min, followed by rehydration of them in a series of ethanol concentrations: absolute ethanol, 90% (v/v) ethanol, 70% (v/v) ethanol, 50% (v/v) ethanol and then water all for 2 min and finally the sections were washed with PBS for 3 min. For antigen retrieval, the sections were incubated with 100 μl of a 0.033% (w/v) pronase solution at 37°C for 10 min (in a humid chamber). After washing the sections 3 times for 5min in PBS, endogenous peroxidase was blocked with 200μl of 3% (v/v) hydrogen peroxide solution for 30 min at RT. The sections were rewashed as above and blocked with 100 μl PBS containing 1% (w/v) BSA and 10% (v/v) goat serum for 30 min at RT. After washing the slides as above, they were immuno-labelled by incubating each slide with 100 μl primary MAb solutions overnight at 4°C and in a humid chamber. The primary antibodies against the IGF-1R (7C2, 9E11, 24-31 and IgG1) were diluted to make 3 μg/ml of each MAb in PBS containing 10% (v/v) goat serum and added to the slides, followed by incubation in a humid chamber at 4°C overnight. The negative and positive controls were mouse IgG1 antibody negative control and anti-IGF-1R MAb 24-31 respectively. Then the sections were rinsed in milli-Q H_2O followed by a 3-times wash in PBS for 5 min. Reactivity was detected by incubating the sections with biotinylated goat anti-mouse immunoglobulin diluted 1:500 (v/v) in PBS for 40 min at RT. After rewashing the sections with PBS as above, the slides were incubated with 1:500 (v/v) diluted streptavidin conjugated horseradish peroxidase (HRP) in PBS for 40 min at RT. The sections were washed again and 100 μl of VECTOR ® solution (VECTOR® NovaRED ™ substrate kit) was applied to each slide as described in the manufacturer's instructions to visualise the HRP label. Development time was generally 15-20 min at RT. Then the sections were washed in water for 5 min and for counterstaining they were incubated in hematoxylin

for 1 min and then washed in running tap water followed by incubation in 0.5% (v/v) ammonia water for 10-30 sec. After rewashing the sections in running tap water they were incubated in absolute ethanol twice for 2 min followed by incubation in Safsolvent three times for 5 min. Finally the sections were mounted in DPX mounting medium and left at RT overnight to dry. The slides were observed with an Olympus BH-2 microscope (Olympus Australia) and images captured with an Olympus DP12 digital camera (Olympus Australia).

3.3. Method for CDR Sequencing of MAbs Heavy and Light Chains

For the CDR sequencing of MAbs 7C2 and 9E11 heavy and light chains, the Ig-Primer Set (Novagen) (Table 3-1) was used for amplification of immunoglobulins (Ig) variable region cDNAs as described below.

Name	Bases	Degeneracy	aa position	Sequence (5'-3')
MuIgV$_H$5'-A	33	512	-20 to -13	GGGAATTCATGRASTTSKGGYTMARCTKGRTTT
MuIgV$_H$5'-B	34	64	-20 to -13	GGGAATTCATGRAATGSASCTGGGTYWTYCTCTT
MuIgV$_H$5'-C	39	–	-20 to -11	ACTAGTCGACATGGACTCCAGGCTCAATTTAGTTTTCCT
	36	48	-20 to -12	ACTAGTCGACATGGCTGTCYTRGBGCTGYTCYTCTG
	39	24	-20 to -11	ACTAGTCGACATGGVTTGGSTGTGGAMCTTGCYATTCCT
MuIgV$_H$5'-D	36	8	-20 to -12	ACTAGTCGACATGAAATGCAGCTGGRTYATSTTCTT
	36	32	-20 to -12	ACTAGTCGACATGGRCAGRCTTACWTYYTCATTCCT
	36	–	-20 to -12	ACTAGTCGACATGATGGTGTTAAGTCTTCTGTACCT
MuIgV$_H$5'-E	36	8	-20 to -12	ACTAGTCGACATGGGATGGAGCTRTATCATSYTCTT
	33	24	-20 to -13	ACTAGTCGACATGAAGWTGTGGBTRAACTGGRT
	35	64	-20 to -13	ACTAGTCGACATGGRATGGASCKKIRTCTTTMTCT
MuIgV$_H$5'-F	35	32	-20 to -13	ACTAGTCGACATGAACTTYGGGYTSAGMTTGRTTT
	35	–	-20 to -13	ACTAGTCGACATGTACTTGGGACTGAGCTGTGTAT
	33	–	-20 to -13	ACTAGTCGACATGAGAGTGCTGATTCTTTTGTG
	38	–	-20 to -12	ACTAGTCGACATGGATTTTGGGCTGATTTTTTTTATTG
MuIgMV$_H$3'-1	32	–	125 to 118	CCCAAGCTTACGAGGGGGAAGACATTTGGGAA
MuIgGV$_H$3'-2	35	32	126 to 119	CCCAAGCTTCCAGGGRCCARKGGATARACIGRTGG
MuIgκV$_L$5'-A	32	32	-20 to -13	GGGAATTCATGRAGWCACAKWCYCAGGTCTTT
MuIgκV$_L$5'-B	33	–	-20 to -13	GGGAATTCATGGAGACAGACACACTCCTGCTAT
MuIgκV$_L$5'-C	39	8	-20 to -11	ACTAGTCGACATGGAGWCAGACACACTSCTGYTATGGGT
MuIgκV$_L$5'-D	42	16	-20 to -10	ACTAGTCGACATGAGGRCCCCTGCTCAGWTTYTTGGIWTCTT
	41	128	-24 to -14	ACTAGTCGACATGGGCWTCAAGATGRAGTCACAKWYYCWGG
MuIgκV$_L$5'-E	39	4	-20 to -11	ACTAGTCGACATGAGTGTGCYCACTCAGGTCCTGGSGTT
	41	32	-15 to -5	ACTAGTCGACATGTGGGGAYCGKTTTYAMMCTTTTCAATTG
	38	–	-20 to -11	ACTAGTCGACATGGAAGCCCCAGCTCAGCTTCTCTTCC
MuIgκV$_L$5'-F	36	32	-20 to -12	ACTAGTCGACATGAGIMMKTCIMTTCAITTCYTGGG
	36	96	-20 to -12	ACTAGTCGACATGAKGTHCYCIGCTCAGYTYCTIRG
	35	8	-20 to -12	ACTAGTCGACATGGTRTCCWCASCTCAGTTCCTTG
	37	–	-16 to -8	ACTAGTCGACATGTATATATGTTTGTTGTCTATTTCT
MuIgκV$_L$5'-G	39	–	-19 to -10	ACTAGTCGACATGAAGTTGCCTGTTAGGCTGTTGGTGCT
	39	8	-22 to -13	ACTAGTCGACATGGATTTWCARGTGCAGATTWTCAGCTT
	37	12	-15 to -7	ACTAGTCGACATGGTYCTYATVTCCTTGCTGTTCTGG
	37	24	-15 to -7	ACTAGTCGACATGGTYCTYATVTTRCTGCTGCTATGG
MuIgκV$_L$3'-1	30	–	122 to 116	CCCAAGCTTACTGGATGGTGGGAAGATGGA
MuIgλV$_L$5'-A	33	128	-20 to -13	GGGAATTCATGGCCTGGAYTYCWCTYWTMYTCT
MuIgλV$_L$3'-1	32	32	125 to 118	CCCAAGCTTAGCTCYTCWGWGGAIGGYGGRAA

Table 3-1 Primer position, sequences and degeneracy.

The above chart shows position, degeneracy and sequence of the primers provided by the Mouse Ig-primer Set. The 5′ primers are complementary to the upstream signal sequence. The amino acid position refers to the position of the primer relative to the start codon of the IgG. The box around the triplet in each sequence indicates the open reading frame (ORF) in each of these 5′-sense or 3′-antisense primers. Table is adopted from (Novagen, 2004).

I=inosine, R=A or G, W=A or T, Y=C or T, D=A or G or T, K=G or T, H=A or C or T, S=C or G, V=A or C or G, M=A or C, B=C or G or T

3.3.1. Extraction of Total Cellular RNA

Total RNA was isolated from 10^6 hybridoma cells of 9E11 or 7C2 using TRIZOL reagent according to the manufacturer's instructions. After isolation, the total RNA was stored at -20°C.

3.3.2. Purification of RNA Samples

To remove any contaminating genomic DNA from RNA samples, a 50 µl reaction was set up containing 20 µl RNA, 20 units SuperInRNase inhibitor, 10 units RNase-free DNase I, 5 µl of 0.1M Tris-Cl pH 8.3, 5 µl of 0.5M KCl, 5 µl of 15 mM $MgCl_2$, 1.85 µl of DEPC-milli-Q H_2O. The reactions were incubated for 30 min at 37°C. Then, 50 µl phenol/chloroform (3:1) was added and the reaction was mixed by vortexing and centrifuged at 13,200 rpm in 5415D centrifuge (eppendorf) (17,500 × g) for 2 min to obtain two phases. Following this, the upper phase of the reaction was transferred to a new microcentrifuge tube, which contained 200 µl 100% ethanol and 5µl 3M sodium acetate (pH 5.2). After precipitation at –80°C, centrifugation at 17,500 × g for 4 min pelleted the RNA. The purified RNA was dissolved in 20 µl DEPC-milli-Q H_2O and stored at –20°C until required.

3.3.3. Electrophoresis of Purified RNA Samples on Agarose Gel

To determine the purity of the purified RNA samples, one µl of purified RNA was loaded into a 1% (w/v) agarose gel and electrophoresed, stained and visualised as described in Section 2.2.3.1.

3.3.4. Quantification of Purified RNA

By using a Cary 3 Bio UV-visible Spectrophotometer (Varian, Vic, Australia), total cellular RNA was quantified. RNA was diluted 1:60 (v/v) in DEPC-milli-Q H_2O, and the absorbance of the sample measured at a wavelength of 260 nm and 280 nm. To assess the purity of RNA, the ratio of absorbance at 260 nm and 280 nm (the A_{260}/A_{280} ratio) was used. The ratio of 1.8-2.1 is indicative of highly purified RNA (Wilfinger *et al.*, 1997). To determine the concentration of RNA in each sample, the following equation was used:

$$\text{RNA concentration } (\mu g/\mu l) = A_{260} \times \text{Dilution factor} \times 0.04$$

3.3.5. Synthesis of cDNA

For the cDNA synthesis, the Ig-3′ constant region primer (provided by Mouse Ig-Primer Set) was utilised as follows for each heavy and light chain of the MAb. In addition, SuperScript III reverse transcriptase was used. The following components were added to a nuclease-free microcentrifuge tube: 5μg purified RNA, 1 μl of 10 mM dNTP Mix containing 10 mM of each dATP, dGTP, dCTP and dTTP in DEPC-milli-Q H_2O, 2 pmol of gene-specific primer (MuIgGV_H 3′-2 for heavy chain or MuIgκV_L3′1 for light chain provided by Ig-Primer Set) DEPC-milli-Q H_2O to a final volume of 13 μl. The IgG and Igκ 3′ constant region primers were used because both MAbs are IgG1κ (as determined in Section 3.4.1). The mixture was heated then to 65°C for 5 min and incubated on ice for 1 min. The contents of the reaction tubes were collected by brief centrifugation then 4 μl of 5 × First-Strand Buffer, 1 μl of 0.1M DTT and 1 μl of SuperScript III reverse transcriptase (200 Units/μl) were added to each tube and gently mixed, and incubated at 25°C for 5 min. Then the tubes were incubated at 55°C for 55 min followed by inactivation of the reaction by heating at 70°C for 15 min and stored at -20°C until required.

3.3.6. PCR Amplification of cDNA Encoding the Variable Region of Heavy or Light Chain of the MAbs

PCR was employed to amplify specific segments of DNA between two oligonucleotide primers, provided by the Ig-Primer Sets that flank the variable part of the heavy or light chains of the MAbs. A reaction mixture was made for each 5′ leader (non-coding region) primer directed towards the heavy or light chain. Six different 5′ primers for IgG heavy chain (MuIgV_H5′-A to -F) and seven different 5′ primers for IgG kappa light chains (MuIgκV_L5′-A to -G) are provided by the Mouse Ig-Primer Sets (Novagen) listed in Table 3-1. The 50 μl reaction mixtures contained 2.5 units of Taq DNA polymerase, 5 μl of thermopol buffer (10 ×), 0.5 μl of 10 mM dNTP mix, 0.5 μl of either MuIgGV_H 3′-2 for heavy chain or

MuIgκV_L3′1 for light chain, 2.5 µl of heavy or light chain cDNA (see Section 3.3.5), and 1µl of just one of either the six 5′ primers for IgG heavy chain or the seven 5′ primers for IgG kappa light chains. The total volume of each reaction mixture was adjusted to 50 µl by adding milli-Q H_2O. All PCR reactions for heavy chains were conducted under the following conditions in a PTC-200 Peltier Thermal Cycler (Geneworks, Adelaide, SA): denature for 1 min at 92°C: 35 cycles of denaturation for 30 sec at 92°C, annealing for 30 sec at 60°C and extension for 30 sec at 72°C. Then a final extension carried out for 1 min at 72°C. The reactions were kept at 4-8°C until required. The PCR reactions for light chains were exactly the same as above except they were for 30 instead of 35 cycles.

3.3.7. Agarose Gel Electrophoresis of PCR Products

To determine which set of primers successfully amplified the cDNA encoding the variable region of heavy or light chain of the MAbs, 2 µl of PCR products for each set of primer were mixed with 5 × agarose gel loading buffer to a final concentration of 1 × and electrophoresed in 1.5% (w/v) agarose gels as described in Section 2.2.3.1.

3.3.8. Purification of DNA Fragments from the Positive PCR Products

QIAquick Gel Extraction kit was used to purify the DNA from the selected PCR product (which was amplified successfully) as described in the manufacturer's instructions.

3.3.9. Ligation of Variable Region cDNAs of MAbs into pGEM-T Easy Vector

The PCR products were ligated into pGEM-T Easy vector at a molar ratio of 3:1 respectively, using the pGEM-T Easy Vector System I kit as described in the instructions provided by the manufacturer (Figure 3.3). As a negative control, milli-Q H_2O was added instead of PCR products, and all were incubated overnight at 16°C.

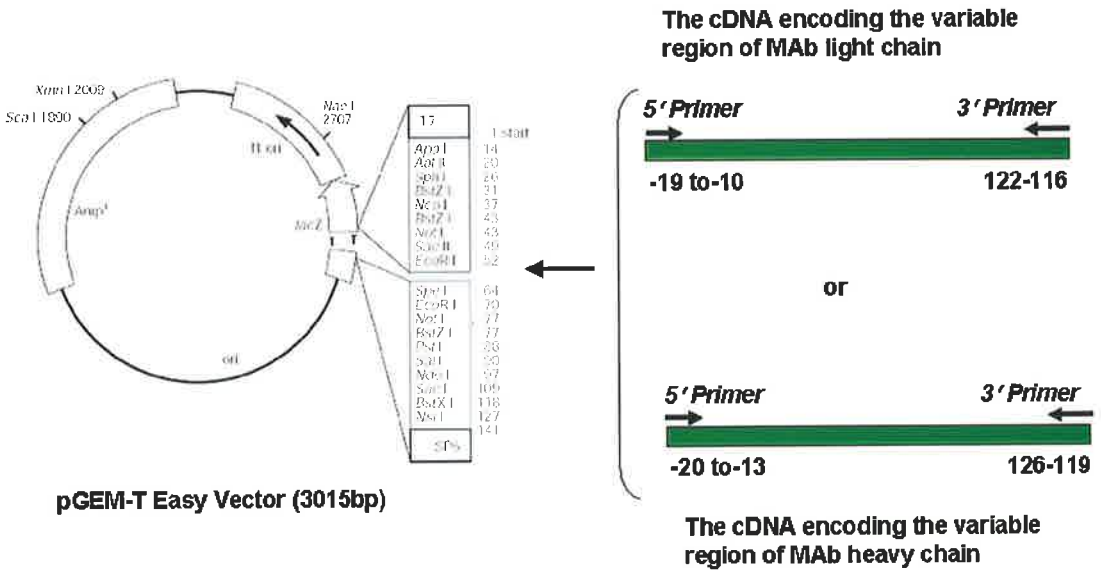

Figure 3.3 Cloning of the cDNA encoding the variable region of the MAbs heavy or light chains into pGEM-T Easy Vector.

The cDNA encoding amino acid residues of the variable part of the MAbs heavy or light chains was amplified by PCR, using the selected forward primers and the reverse primer (Figure 3.1 and Table 3-1). The oligonucleotide primers schematically represented as arrows. The resultant PCR product for each heavy or light chain was cloned into the pGEM-T Easy Vector. The figure for the vector is adapted from (Promega, 2005).

3.3.10. Transformation of the Ligated Plasmids into *E. coli* DH5α

Five µl of each ligation reaction was transformed to 100 µl of prepared competent DH5α cells as described in Section 2.2.3.2 and Section 2.2.3.3. The appropriate selection antibiotic for growing these transfected cells was 100 µg /ml ampicillin.

3.3.11. Small-Scale Production of Plasmid DNA

Three colonies were selected from each plate and each one inoculated in 2 ml of Luria broth (LB) containing 100 µg /ml ampicillin using a sterile toothpick. The cultures were incubated overnight at 37°C. The plasmid DNAs were purified from the overnight cultures and quantified as described in Section 2.2.3.6. For each colony, a glycerol stock was made as described in Section 2.2.3.4.

3.3.12. Digestion of Purified Plasmid DNA

To confirm the existence of the insert (variable part of the MAbs), 10 µl of the purified plasmids (0.5 µg/µl) (PGEM-T Easy vectors containing the insert) were digested in a solution of *Eco*RI buffer containing 6 units of *Eco*RI Restriction enzyme. The total volume of the reaction was adjusted to 20 µl by adding milli-Q H_2O. The reaction solutions were digested for 60 min at 37°C. The solutions were left at -20°C to terminate the digestion. For each sample, 10 µl of digested plasmid DNA were electrophoresed in a 1.5% (w/v) agarose gel as previously described in Section 2.2.3.1 and the pGEM-T Easy Vector and insert were separated and visualized.

3.3.13. DNA Sequencing

The purified pGEM-T Easy Vectors containing the inserted DNA were used for sequencing. The method was described in Section 2.2.3.7 with RSP and USP sequencing primers.

The sequence of V_H or V_L for each MAb were analysed by IMGT/V-QUEST (Giudicelli *et al.,* 2004). This software identifies the V, D and J genes and alleles by alignment with the germline IG gene and allele sequences of the IMGT reference directory. The software numbers the translated amino acids of the IG variable region on the basis of the IMGT unique numbering (Lefranc *et al.,* 2003) and shows the region's structurally important features, which are the three frameworks according to the IMGT unique numbering (FR-IMGT) (Pommie *et al.,* 2004) and the three CDRs according to the IMGT unique numbering (CDR-IMGT).

3.4. Results and Discussion for General Characterisation of MAbs

3.4.1. Hybridoma Screening and Isotyping

For all four fusions, the number of screened hybridomas, positive hybridomas detected by ELISA and hybridomas specific for binding to s-IGF-1R coated plates have been summarized

in Table 3-2. Among all initial 62 positive hybridomas, only four of them produced antibodies, which were negative when screened against uncoated wells. Different blocking reagent, casein 1% (w/v), or higher concentration of the same blocking reagent, BSA 4% (w/v), were used to inhibit the non-specific binding of the rest of the antibodies to the plate in ELISA. However, these strategies were not able to inhibit the non-specific binding.

Hybridomas 4C6, 5B6, 7C2, and 9E11 were found specific. All these four MAbs were obtained from the first fusion and they were selected for further characterisations. These hybridomas were cloned using the limiting dilution technique and the following positive clones (secreting MAbs against s-IGF-1R) were chosen for each hybridoma cell from the 0.75 or 1.5 cell/well dilution: 4C6 (H8, H9, H10 and H2), 5B6 (D11, E5, F2 and G12), 7C2 (F12, G10, G1 and H10) and 9E11 (H2, H6, H4 and G12). The ELISA isotyping showed the isotype for the all sub-clones of these MAbs were IgG1κ (Figure 3.4.).

	Immunogen	**Number of screened hybridomas**	**Number of positives**	**Number of specifics**
Mouse No.1	s-IGF-1R	97	4	4
Mouse No.2	s-IGF_1R	946	18	0
Mouse No.3	P6 cells	904	26	0
Mouse No.4	P6 cells and s-IGF-1R	1513	14	0

Table 3-2 Summary of hybridoma screening.

The number of screened hybridomas for each fusion, the number of positive hybridomas against s-IGF-1R in the ELISA test and the number of specific hybridoma are shown.

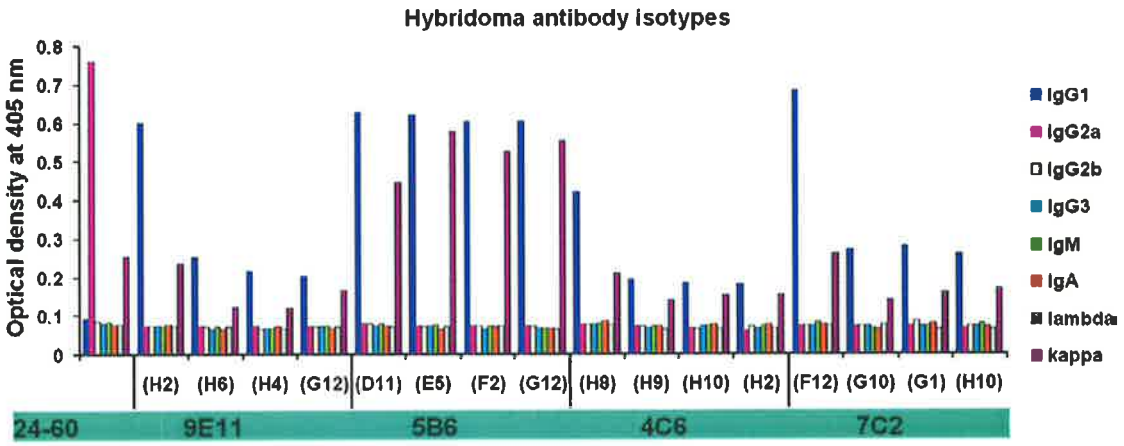

Figure 3.4 The isotype of MAbs expressed by hybridoma clones.

The isotype of antibodies found within neat hybridoma culture medium from four sub-clones of parental hybridoma lines 9E11, 5B6, 4C6 and 7C2 was determined. The MAb 24-60 (IgG2a) (Soos *et al.*, 1992) was employed as a positive control for this assay. The graph shown is a representative of three experiments.

3.4.2. Flow Cytometry Results

As mentioned earlier and showed in Table 3-2, 58 positive hybridomas screened against s-IGF-1Rnon-specifically bound to the plate in ELISA. To make sure none of the positive hybridomas, which appeared to bind to the receptor, were missed the supernatants were tested against cells expressing IGF-1R in flow cytometry. The results showed none of these hybridomas was positive against the cells expressing IGF-1R. Therefore they were not further characterised.

For the four specific MAbs (4C6, 5B6, 7C2 and 9E11) the results for the flow cytometry experiment were as follows. The hybridoma culture media of 7C2 and 9E11 were positive for the whole IGF-1R on the surface of P6 cells (Figure 3.5) but 5B6 and 4C6 were negative (data not shown). In addition, none of the MAbs had cross reactivity with IR-A or IR-B (Figure 3.5). All of the antibodies were negative against R^- cells (data not shown). These results suggest that 7C2 and 9E11 are able to bind to whole receptor on the surface of the cells and interestingly their binding is specific due to the lack of interaction with IR-A or IR-B and also the R^- cells. Because the structures of the IGF-1R and IR are very similar, the specific binding to the IGF-1R and not to IR is an important property for the MAbs.

The ELISA against s-IGF-1R showed 4C6 and 5B6 bind to the extracellular part of the receptor but flow cytometry revealed they do not bind to the whole receptor on P6 cells.

These results suggest that the MAbs 4C6 and 5B6 could bind to a part of the s-IGF-1R, which is not accessible when the whole receptor is attached to the cells. Hence, they were not characterised further.

In this study we aimed for generation of MAbs that interact with the natural form of human IGF-1R on cells, hence MAbs 7C2 and 9E11 were selected for further characterisation (Figure 3.5). In addition, the sub-clones for each antibody appeared identical because the ELISA, flow cytometry and isotyping results were very similar. One sub-clone for each hybridoma clone MAb 7C2 (F12) and MAb 9E11 (H6) were chosen for further study.

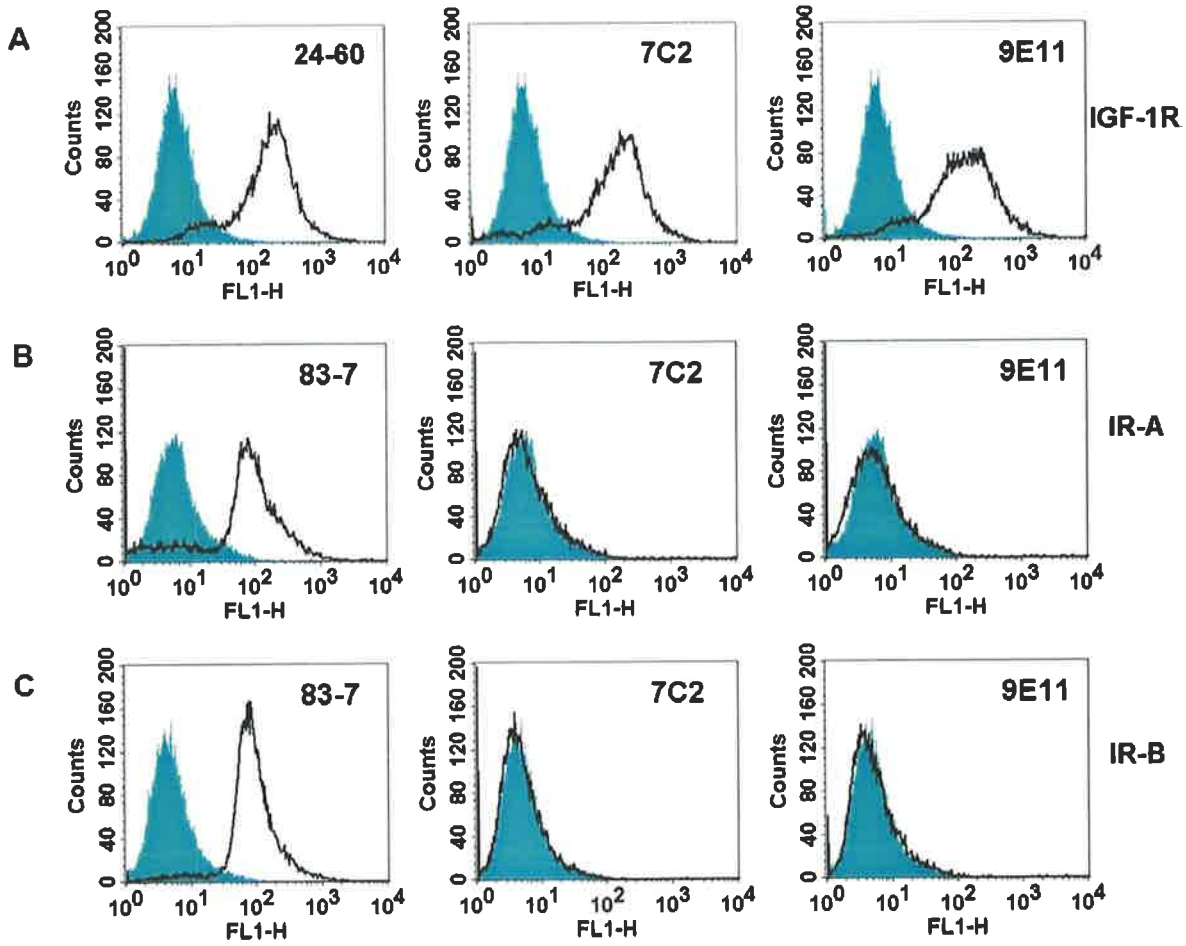

Figure 3.5 Flow cytometric analysis of the reactivity of MAbs 7C2 and 9E11 with IGF-1R, IR-A or IR-B.

Series A) Shows the results of the experiment on IGF-1R expressing cells, Series B) on IR-A expressing cells and Series C) on IR-B expressing cells. These cell lines were incubated with different primary antibodies. The green curves indicate the fluorescence of the cells stained with negative control (IgG1) and black curves indicate the fluorescence of the cells stained with positive controls or 7C2 and 9E11. The results for all sub-clones of MAbs were the same. This figure shows 7C2 (F12) and 9E11 (H6). The results are representative of three separate experiments.

3.4.3. Large Scale Production and Purification of MAbs

The MAbs were purified from spinner flask cultures in media containing 2.5% (v/v) FCS for both 7C2 (F12) and 9E11 (H6). The SDS-PAGE analysis for the purified MAbs followed by Coomassie Brilliant Blue R^{TM} staining showed two distinct protein bands of molecular weights ~55 and ~25 kDa. These bands indicate the presence of the heavy and light immunoglobulin chains for IgG respectively (Figure 3.6). The yield for the purification of MAbs from the culture media was between 7-15 mg/litre.

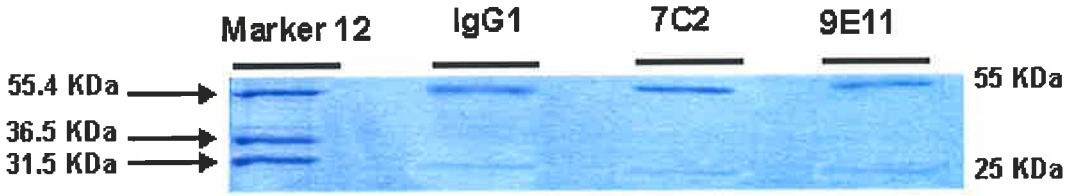

Figure 3.6 The SDS-PAGE analysis of purified MAbs (IgG1).

The mouse IgG1 negative control was used as a control. The molecular weight marker was Marker12^{TM} (Invitrogen).

3.4.4. The Activity of Freeze-Dried Monoclonal Antibodies

A comparison of the binding activities of the MAbs in the HBS buffer with reconstituted lyophilised formulations was made in an ELISA assay using s-IGF-1R. Both 7C2 and 9E11 freeze-dried in either the presence or absence of trehalose were equally stable and had similar activities in this experiment (Figure 3.7). As a result either freeze-drying procedures can be chosen for long-term storage of the MAbs.

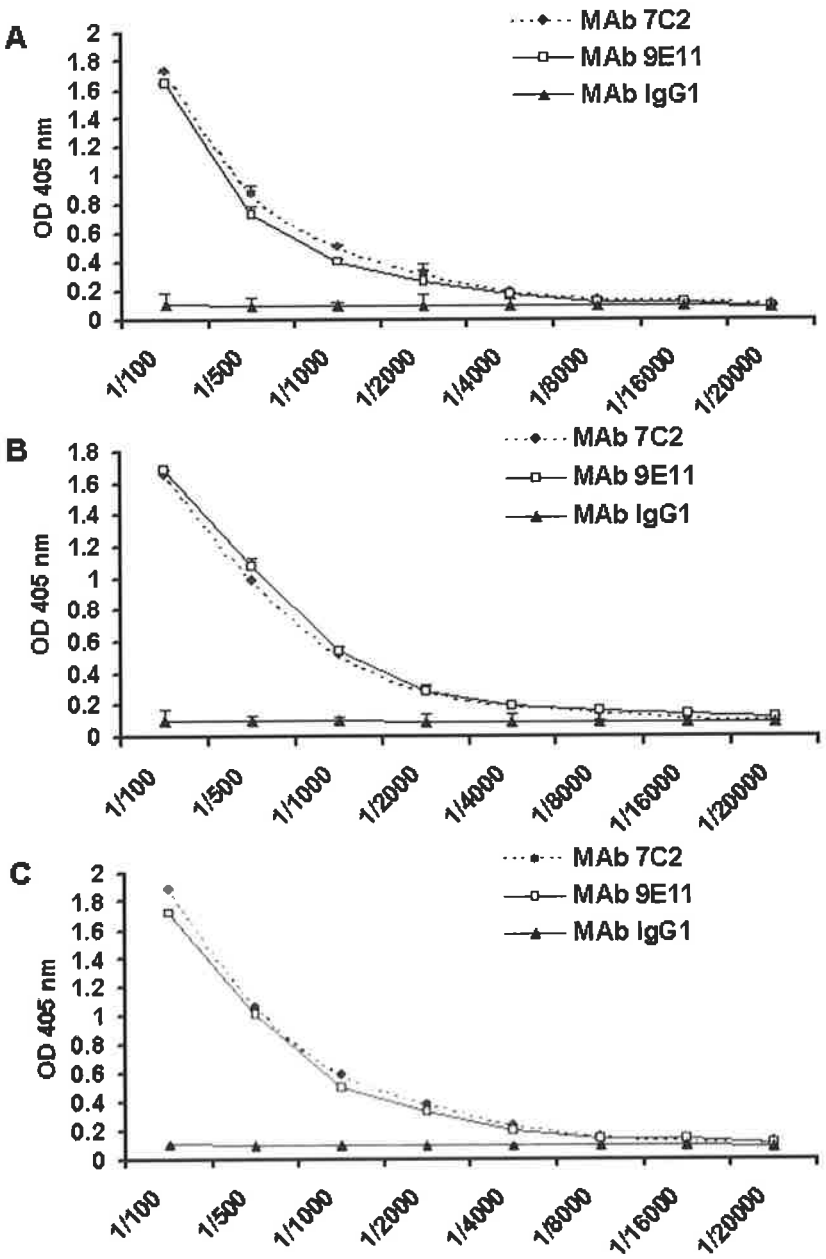

Figure 3.7 ELISA results for binding of MAbs 7C2 and 9E11 to s-IGF-1R.

A) MAbs 7C2 and 9E11 were in HBS solution, B) Freeze-dried 7C2 and 9E11 reconstituted in HBS buffer. C) Freeze-dried 7C2 and 9E11 reconstituted in HBS buffer containing 60 mM trehalose. Dilutions were made from stock solutions of each MAb (all at 0.23 mg/ml concentration). Bars are means ± SD of triplicate points. Errors are shown when greater than the size of the symbols.

3.4.5. Immunoprecipitation and Immunoblotting of the IGF-1R

Immunoprecipitation was carried out to determine whether the MAbs could react with native IGF-1R. The MAbs 9E11 and 7C2 successfully immunoprecipitated the IGF-1R from P6 cells lysates. Both immunoprecipitated the β subunit and pro-IGF-1R (αβ) was detected by the IGFR 1-2 as described in Section 2.2.2.7. The results show that MAbs 7C2 and 9E11 can bind to the IGF-1R on P6 cells and immunoprecipitate the receptor to a similar extent as MAb

24-55 as a positive control (Figure 3.8). In addition, it seems that all bands for MAbs 7C2 and 9E11 are more slowly migrated than those for 24-55. This could be the effect of the buffer since MAb 24-55 was in PBS and MAbs 9E11 and 7C2 were in HBS buffer. In addition, it could be due to the differences in the loading.

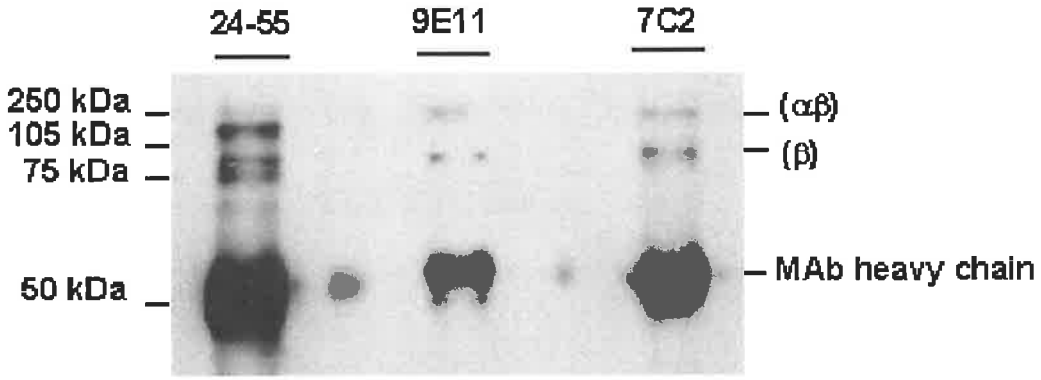

Figure 3.8 Immunoprecipitation analysis of the IGF-1R by MAb 24-55, 9E11 and 7C2.

The IGF-1R β subunit (~95kDa) and the pro-IGF-1R (shown as αβ) (~200 kDa) were detected with IGFR 1-2 as described in Section 2.2.2.7. Molecular weight was estimated in kilodaltons using the full range rainbow recombinant protein molecular weight marker (Amersham Biosciences).

Immunoblotting experiments showed neither the MAb 9E11 nor 7C2 detected the α or β subunits of the reduced IGF-1R on immunoblots (Figure 3.9). In contrast, two bands were detected with IGFR 1-2. The second band is ~ 95 kDa that corresponds to the β subunit of the receptor and the first band is a non-specific band, which has also appeared in R^- cell lysate (Figure 3.10).

Immunoblotting experiments under non-reducing conditions showed both 7C2 and 9E11 reacted with whole receptor under these conditions (Figure 3.11).

Under reducing conditions the receptor is broken into α and β subunits. Therefore if the epitope of the MAbs is conformational, it is no longer available for antigen antibody interaction when the receptor is reduced.

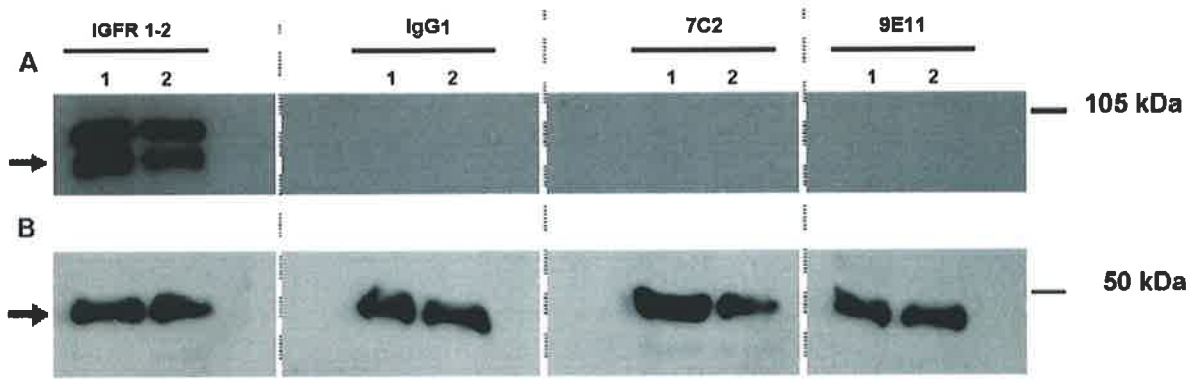

Figure 3.9 Western blot analysis of P6 cell lysate under reducing conditions.

A) Detection of IGF-1R by MAbs IGFR 1-2, IgG1 7C2 and 9E11.The 95KDa β subunit of the IGF-1R (arrow) was detected with IGFR 1-2. The upper band is a non-specific band for this MAb. B) The 42kDa β-actin (arrow) was detected as an internal protein loading control. Lanes 1 and 2 contain 16 and 8 μg total protein (from P6 cell lysate) respectively. The method was described in Section 3.2.11. A representative experiment is shown.

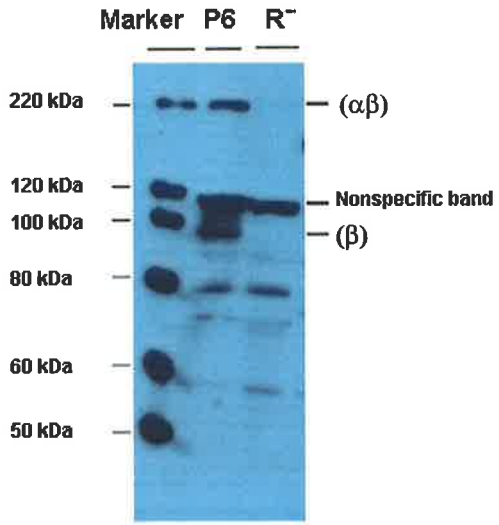

Figure 3.10 Western blot analysis of P6 cell and R⁻ cell lysates under reducing conditions.

The primary MAb IGF-R1-2 was used as primary antibody. The Marker was MagicMark™XP. The Western blot analysis performed by Chareeporn Akekawatchai (The University of Adelaide, Australia). The method was described in Section 3.2.11.

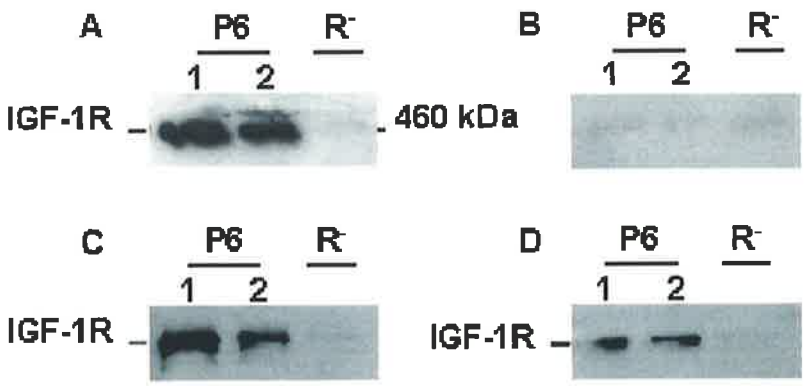

Figure 3.11 Western blot analysis of P6 cell lysates under non-reducing conditions.

Blots were probed with MAbs IGFR 1-2 (A), IgG1 negative control (B), 7C2 (C) and 9E11(D). The IGF-1R was detected with IGFR 1-2, 7C2 and 9E11(~ 460 kDa). Lanes 1 and 2 contain 16 and 8 μg of total protein from P6 cell lysate. 8 μg total protein from R⁻ cell lysate was loaded as a negative control. Method was as described in Section 3.2.11. A representative experiment is shown.

3.4.6. Immunohistochemistry Results

As shown in Figure 3.12, immunohistological analysis of frozen cells revealed that the IGF-1R on P6 cells stained positive with 7C2 and 9E11 to the similar extent as seen with MAb 24-31 as positive control. In this experiment, R$^-$IR-A, R$^-$IR-B and R$^-$ cells did not stain with MAbs 9E11 and 7C2. R$^-$IR-A and R$^-$IR-B were detected with 83-7 as positive control for the insulin receptor. Unrelated IgG1 did not come up positive in all cell lines (Figure 3.12). These data demonstrate the specific binding of 7C2 and 9E11 to the IGF-1R with no cross reaction to IR isoforms in immunohistochemistry.

Immunohistological analysis on the frozen human skin sections revealed intense specific staining of 7C2 and 9E11 compared to an unrelated IgG1 as a negative control for detecting the IGF-1R in the epidermis. However, for these sections the background fluorescence for IgG1 was detectable, though modest (Figure 3.13). In paraffin-embedded human skin sections, immunohistological analysis showed specific staining of both 7C2 and 9E11 in epidermis (Figure 3.14) and the background staining for IgG1 was minimal. Hence, using the MAbs in paraffin-embedded tissues and HRP labelling is preferable due to the lower background compared with fluorescence labelling on frozen sections.

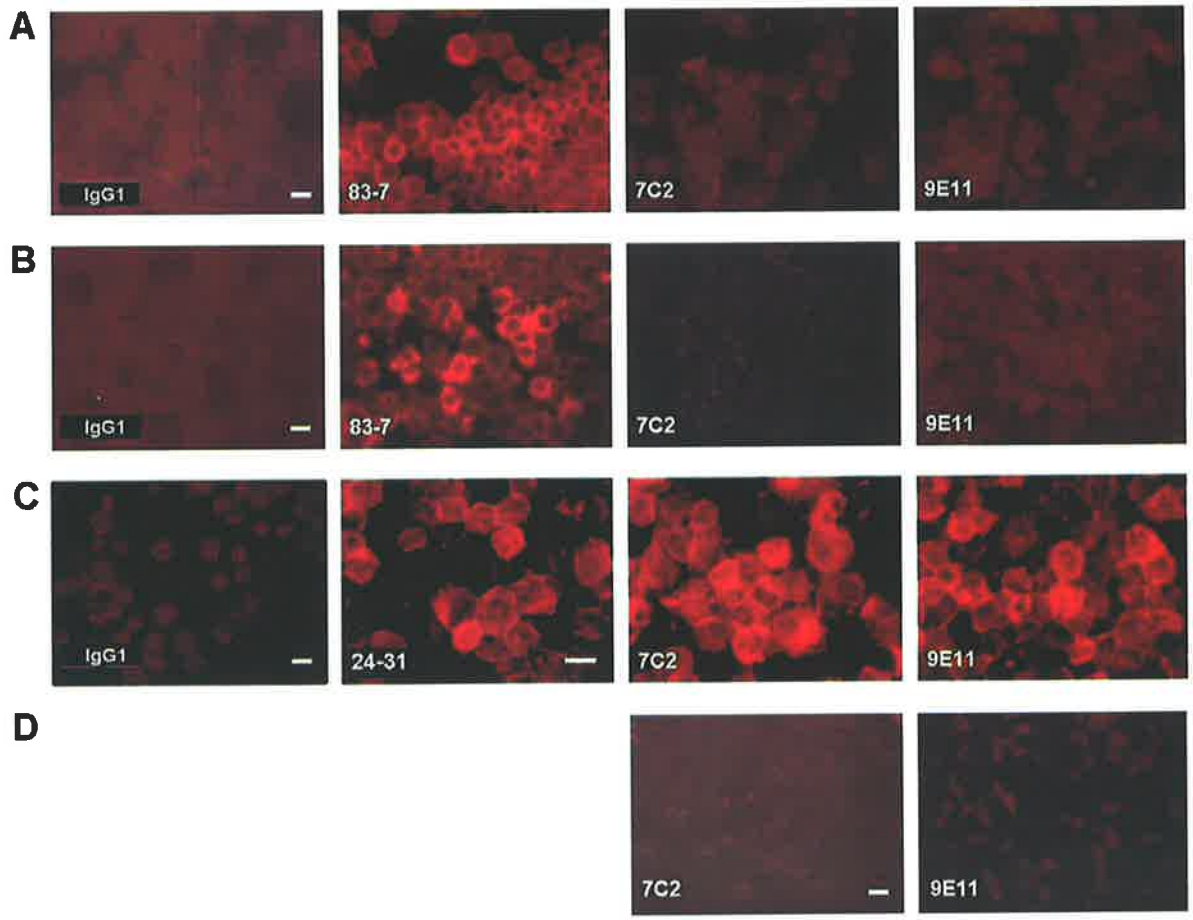

Figure 3.12 Immunohistochemistry assay detecting the IGF-1R, IR-A and IR-B expressed on frozen cells using MAbs 7C2, 9E11, 83-7, 24-31 and IgG1 negative control.

A) R⁻IRA cells B) R⁻IRB cells C) P6 cells D) R⁻ cells. Scale bar = 20 μm. Representative experiments are shown. Staining was performed as described in Section 3.2.12.1.

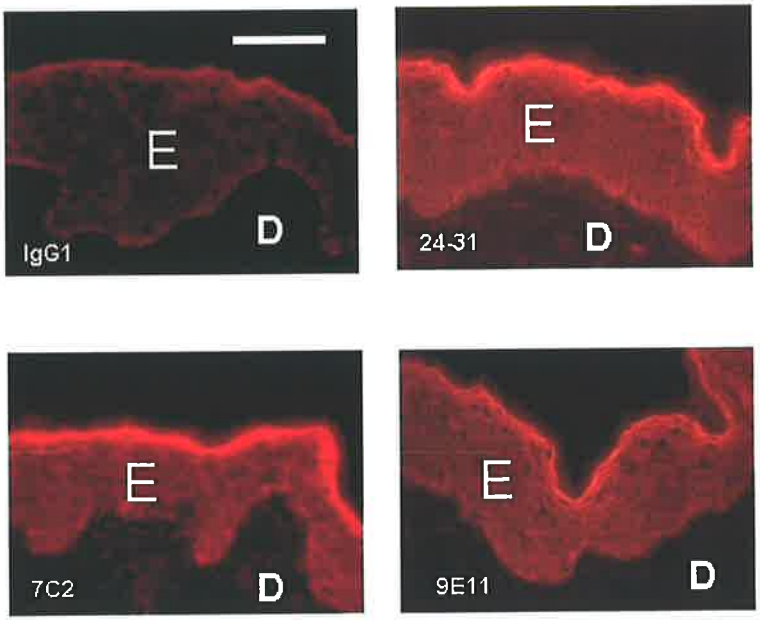

Figure 3.13 Immunostaining of IGF-1R in epidermis (E) of frozen human skin using different primary MAbs.

D stands for the underlying papillary layer of the dermis. Staining can be seen as bright red. Scale bar = 50 μm. Representative experiments are shown. Staining was performed as described in Section 3.2.12.2.

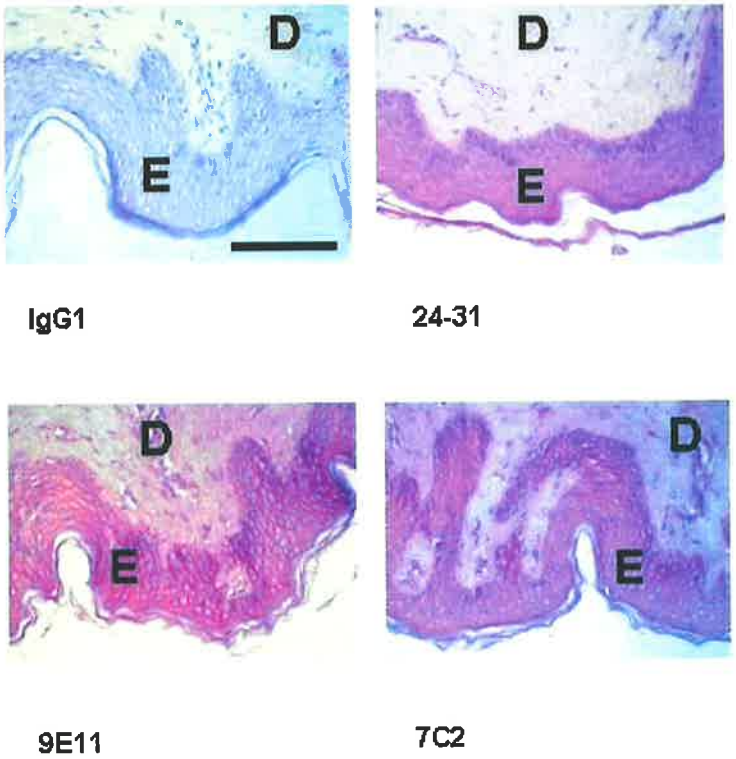

Figure 3.14 Immunostaining of IGF-1R in epidermis (E) of paraffin-embedded human skin using different primary MAbs as indicated.

D stands for the underlying papillary layer of the dermis. Staining can be seen as red. Scale bar = 50 µm. Representative experiments are shown. Staining was performed as described in Section 3.2.12.3.

The positive and specific interaction of the MAbs (7C2 and 9E11) with the IGF-1R shows the potential use of these MAbs to detect IGF-1R in human tissues by immunohistochemical experiments. Furthermore, due to the overexpression of IGF-1R in certain cancers, these MAbs can be employed to detect the IGF-1R in tumour samples thereby providing useful data in staging the tumour for planning a therapeutic strategy.

3.5. Results for CDR Sequencing

3.5.1. RNA Extraction

Total cellular RNA was successfully extracted from cultured hybridoma cells using TRIZOL as shown by strong bands that correspond to the 18S and 28S ribosomal RNA observed on ethidium bromide stained agarose gels (Figure 3.15).

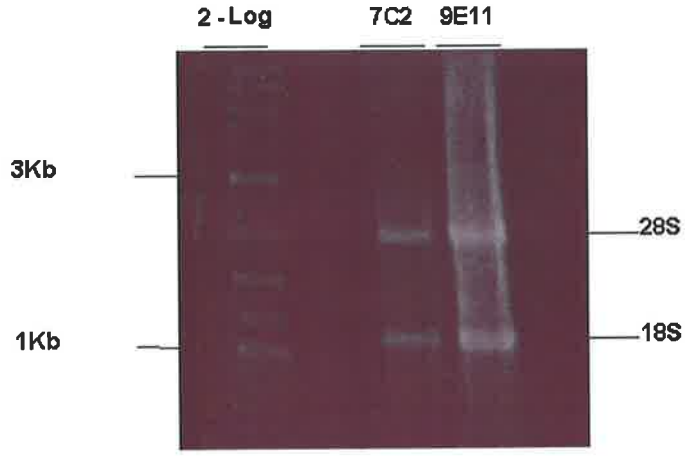

Figure 3.15 RNA extraction from 7C2 and 9E11 hybridomas.

UV visualisation of ethidium bromide stained 1% (w/v) agarose-TAE gels after electrophoresis of RNA samples (1µl) extracted from the hybridomas. The 18S and 28S ribosomal bands are visible.

3.5.2. PCR Amplification

PCR amplification of the V_H and V_L was performed using different primers provided by the kit. Amplification of PCR products for V_H region of cDNA was achieved using MuIgV$_H$5′-F and MuIgGV$_H$3′-2 for 7C2 and MuIgV$_H$5′-A and MuIgGV$_H$3′-2 for 9E11. MuIgκV$_L$5′-G and MuIgκV$_L$3′-1 amplified the V_L region of cDNA for both MAbs 7C2 and 9E11. Figure 3.16 shows the bands for PCR amplified light (V_L) and heavy (V_H) chains of 7C2 on an agarose gel.

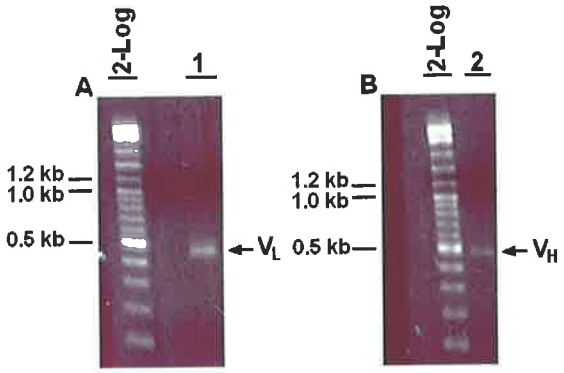

Figure 3.16 Immunoglobulin heavy (V_H) and kappa light (V_L) chain PCR products derived from first-strand cDNA of 7C2 on agarose gels.

Lane 1) V_H amplified with MuIgV$_H$5′-F and MuIgGV$_H$3′-2 primers. Lane 2) V_L amplified with MuIgκV$_L$5′-G and MuIgκV$_L$3′-1 primers.

3.5.3. Ligation

The variable parts of the MAbs (for both heavy and light chains) were successfully ligated into the pGEM-T Easy vector. Electrophoresis of *Eco*RI digested plasmid DNA samples on the agarose gel (Figure 3.17) showed two bands, one for plasmid (~3 kb) and one for the insert corresponding to the amplified V_L (~ 420 kb) or V_H cDNA (~440 kb).

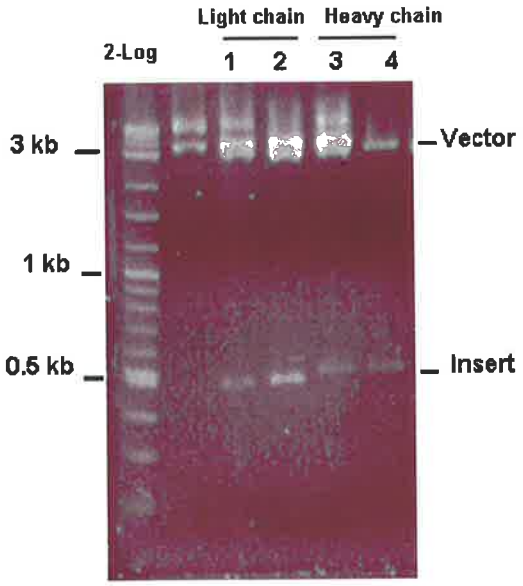

Figure 3.17 Digested pGEM-T Easy vectors containing the cDNA for V_L or V_H part of the MAbs

Lane 1) 7C2 V_L, lane 2) 9E11 V_L, lane 3) 7C2 V_H, lane 4) 9E11 V_H. The DNA marker was 2-Log DNA Ladder (New England Biolabs).

3.5.4. Sequencing Results

Three clones for each MAb 7C2 or 9E11 were sequenced and the results showed all three 7C2 clones were identical in V_L or V_H parts as were all three 9E11 clones. However, the 7C2 sequence differed from the 9E11 sequence (Figure 3.18).

The cDNA sequences were analysed with IMGT/V-Quest and the output aligned with the most similar five V and D genes and alleles, and the most closely related three J genes and alleles of the IMGT reference directory. From this sequence alignment it can be concluded that for both 7C2 and 9E11 light chain sequences, the V-J rearrangement involves the variable IGKV1-117*01 allele and the joining IGKJ1*01 allele. Furthermore, for both 7C2 and 9E11

heavy chain sequences, The V-D-J rearrangement involves the variable IGHV5S10*01 allele, the diversity IGHD-FL16.1*01 allele and the joining IGHJ1*01 allele.

This software also translated the nucleotide sequence to an amino acid sequence and delimited the CDRs and FRs for the MAb variable regions as shown in Figure 3.18. None of the sequences from the reference directory was exactly the same as the sequence of either 7C2 or 9E11, particularly in the CDR. Comparing the sequence of these two MAbs to each other shows that although their sequences are very similar, there are some differences particularly in the CDR1 (V_L), CDR2 (V_L), CDR1 (V_H) and CDR2 (V_H) regions Table 3-3.

	CDR1 (V_L)	**CDR2 (V_L)**	**CDR3 (V_L)**	**CDR1 (V_H)**	**CDR2 (V_H)**	**CDR3 (V_H)**
7C2	QSIVHSNGNTY	QVS	FQGSHVPWT	GFTFSSYY	VNSYGGGT	VRQAPDYYGSNRWYFDV
9E11	QTIVHSNGNTY	KVS	FQGSHVPWT	GFTFSNFY	INSYGGST	VRQAPDYYGSNRWYFDV

Table 3-3 Comparison of the CDR sequences of 7C2 and 9E11.

The differences in CDRs are shown in red.

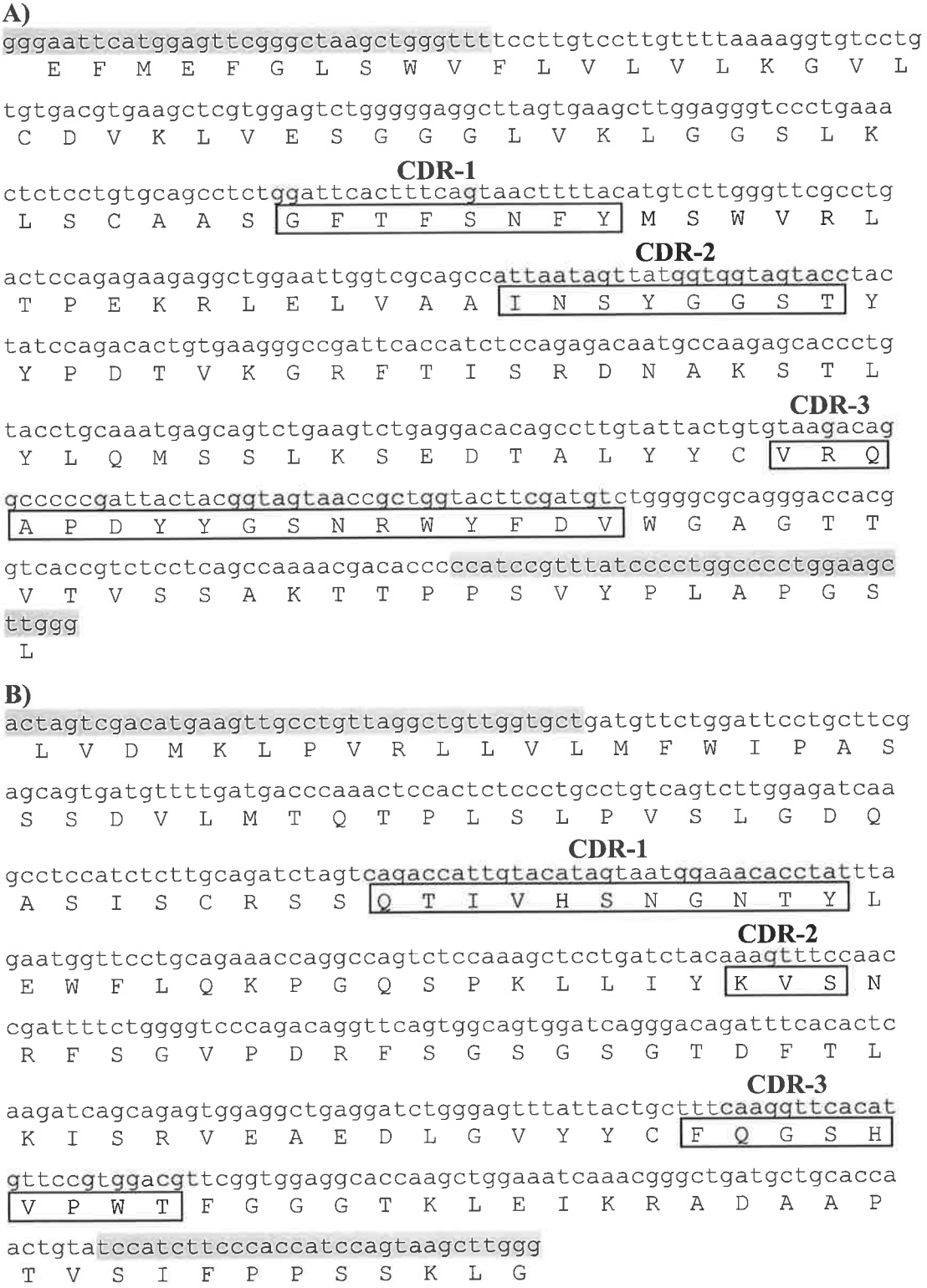

Figure 3.18 Nucleotide sequence of genes encoding the MAbs 9E11 and 7C2 variable regions and the deduced amino acid sequence.

A) The V_H sequence for 9E11; B) The V_L sequence for 9E11; C) The V_H sequence for 7C2; D) The V_L sequence for 7C2. The sequences are 5′ to 3′ and the primers are highlighted in grey. The CDR parts following the definition of IMGT/V-QUEST (Giudicelli *et al.*, 2004) are shown in boxes. The sequences correspond to clone No.1 for 7C2 and 9E11 (V_L or V_H).

To be continued on the next page.

C)

actagtcgacatgaacttcgggctgagcttggttttccttgtccttgttttaaaaggtgtc
L V D M N F G L S L V F L V L V L K G V

ctgtgtgacgtgaagctcgtggagtctgggggaggcttagtgaagcttggagggtccctg
L C D V K L V E S G G G L V K L G G S L

CDR-1

aaactctcctgtgcagcctctggattcactttcagtagttattacatgtcttgggttcgc
K L S C A A A S G F T F S S Y Y M S W V R

CDR-2

cagactccagagaagaggctggagttggtcgcagccgttaatagttatggtggtggcacc
Q T P E K R L E L V A A V N S Y G G G T

tactatccagacactgtgaagggccgattcaccatctccagagacaatgccaagaacacc
Y Y P D T V K G R F T I S R D N A K N T

CDR-3

ctgtacctgcaaatgagcagtctgaagtctgaggacacagccttgtatcactgtgtaaga
L Y L Q M S S L K S E D T A L Y H C V R

caggcccccgattactacggtagtaaccgctggtacttcgatgtctggggcgcagggacc
Q A P D Y Y G S N R W Y F D V W G A G T

acggtcaccgtctcctcagccaaaacgacacccccatccgtctatcccttggcccctgga
T V T V S S A K T T P P S V Y P L A P G

agcttggg
S L

D)

actagtcgacatgaagttgcctgttaggctgttggtgctgatgttctggattcctgcttcc
L V D M K L P V R L L V L M F W I P A S

agcagtgatgttttgatgacccaaagtccactctccctgcctgtcagtcttggagatcaa
S S D V L M T Q S P L S L P V S L G D Q

CDR-1

gcctccatctcttgcagatctagtcagagtattgtacatagtaatggaaacacctattta
A S I S C R S S Q S I V H S N G N T Y L

CDR-2

gaatggttcctgcagaaaccaggccagtctccaaagctcctgatctaccaagtttccaac
E W F L Q K P G Q S P K L L I Y Q V S N

cgattttctggggtcccagacaggttcagtggcagtggatcagggacagatttcacactc
R F S G V P D R F S G S G S G T D F T L

CDR-3

aagatcagcagagtggaggctgaggatctgggagtttattactgctttcaaggttcacat
K I S R V E A E D L G V Y Y C F Q G S H

gttccgtggacgttcggtggaggcaccaagctggaaatcaagcgggctgatgctgcacca
V P W T F G G G T K L E I K R A D A A P

actgtatccatcttcccaccatccagtaagcttggg
T V S I F P P S S K L G

Continued from previous page.

3.6. Summary and Final Discussion

For production of MAbs against human IGF-1R, the extracellular part of the receptor (s-IGF-1R) or transfected mouse fibroblasts expressing a high level of human IGF-1R (P6 cells) were used as immunogens alone or in combination. During this thesis four IgG1κ MAbs (4C6, 5B6, 7C2 and 9E11) were obtained recognizing the human s-IGF-1R specifically. All these four MAbs were generated from the first mouse immunised with s-IGF-1R. The isotype for these MAbs were IgG1κ. Among these MAbs only two of them (7C2 and 9E11) detected the intact human IGF-1R on the surface of P6 cells in flow cytometry. Although the other two MAbs 4C6 and 5B6 detected the s-IGF-1R in ELISA test they did not detect the receptor on the cells. It is possible that the epitopes for these MAbs are on the part of the s-IGF-1R that is not accessible when the receptor is attached to the cell in the intact form. For example the epitope might be on a part of the receptor that is usually attached to the membrane. Interestingly the flow cytometry results showed MAbs 7C2 and 9E11 did not interact with IR-A and IR-B expressing or R^- cells, hence they are specific for the IGF-1R.The specificity of the MAbs is important because of the high degree of sequence homology between IR and IGF-1R.

MAbs 7C2 and 9E11 were selected for further characterisations in different immunoassays and the most suitable applications for them were found. The results have been summarized in Table 3-4.

MAb	**Isotype**	**ELISA**	**WB** (reducing)	**WB** (non-reducing)	**IP**	**IH** (frozen cells)	**IH** (frozen sections)	**IH** (paraffin-embedded sections)
9E11	IgG1κ	+	-	+	+	+	+	+
7C2	IgG1κ	+	-	+	+	+	+	+

Table 3-4 Reactivity of MAbs 7C2 and 9E11 in different immunoassays

+ = reacting, – = not reacting
WB= Western blot, IP= Immunoprecipitation, IH=Immunohistochemistry

The immunohistochemical experiments showed 7C2 and 9E11 stained positive against the IGF-1R on frozen cells or tissue sections and also paraffin-embedded tissue sections. In addition, their staining was specific due to no staining against the IR-A or IR-B expressing cells and R^- cells.

According to the flow cytometry and immunohistochemistry results, MAbs 7C2 and 9E11 can be utilised to detect IGF-1R in different tissues or cells. More importantly the MAbs may be useful in diagnosis of malignant tumours or metastatic cells due to the overexpression of the IGF-1R in certain cancer cells such as in breast cancer (Cullen *et al.,* 1990). In addition, in some cancers it has been shown that there is a correlation between the increased expression of the IGF-1R and metastasis (Goyal *et al.,* 1998) and also both higher grade and higher-stage of tumour (Hakam *et al.,* 1999). Hence, the utilisation of the MAbs in immunohistochemistry or flow cytometry as diagnostic reagents may lead to predicting the stage of the malignancy in some cancer tissues. In addition, if the tumour shows IGF-1R overexpression, anti-IGF-1R therapy could be a beneficial method of treatment.

MAbs 7C2 and 9E11 could immunoprecipitate IGF-1R from P6 cell lysates. Both 7C2 and 9E11 reacted in Western blots with intact IGF-1R while none of them bound to the reduced IGF-1R. Therefore it could be concluded that these MAbs recognize a conformational epitope (Harlow and Lane, 1999). For the conformational epitopes, the folding of proteins in larger domains form the epitopes. These epitopes show interactions with side chains that are close together in the folded protein but may be widely separated in the linear sequence (Harlow and Lane, 1999). As expected the linear epitopes that are formed by contiguous or nearly contiguous amino acids are stable through denaturation or reduction whereas the conformational epitopes formed by noncontiguous amino acids are disrupted when the protein unfolds or the disulphide binds are broken.

There are existing mouse MAbs against the IGF-1R as mentioned in Chapter 1. Although they are not fully characterised, there are some differences from and similarities with 7C2 and 9E11. Soos *et al.* (1992) obtained 20 MAbs against the IGF-1R and their

isotypes fell into three different isotypes: IgG1, IgG2b and IgG2a. The IgG1 antibodies generated by Soos *et al.* are 24-31, 17-66, 17-69, 24-50, 24-51, 24-30, 24-55, 24-57, 4-52, 4-59, 17-20, 24-47, 26-11 and 26-3. The IgG2b MAbs were 17-54 and 16-13. The IgG2a MAbs were 24-32, 24-53, 24-58 and 24-60 (Soos *et al.,* 1992). None of these MAbs made by Soos *et al.* gave a strong reaction on immunoblots however, 17-66, 24-55, 24-60 and 24-57 reacted very weakly with the α subunit of the receptor (Soos *et al.,* 1992). Among these MAbs, MAb 24-31 was used in immunohistochemical analysis (Singer *et al.,* 2004). Hence, the epitopes for these MAbs might also be conformational as is seen with 7C2 and 9E11.

The MAb IGFR 1-2 has been developed against the β subunit of the receptor and can detect the β subunit in Western blot (recommended by the vendor: GroPep Ltd, Adelaide, SA, Australia), so it might have a linear (continuous) epitope. Other reported IgG1 mouse MAbs include 1H7 (Li *et al.,* 1993), αIR-3 (Kull *et al.,* 1983), 7C10 (Goetsch *et al.,* 2005) and EM164 (Maloney *et al.,* 2003). MAb EM164 specifically stained positive in flow cytometry analysis against the IGF-1R and it showed no cross reaction with IR (Singh *et al.,* 2003).

Generation of MAbs against the human IGF-1R allows the development of the necessary immunochemical methods to study the structure and function of the receptor as well as to investigate involvement of this receptor in cancer.

The amplification of specific cDNA using the combination of 5′ leader (signal peptide) and 3′ constant region oligonucleotides from the Ig-Primer Set was successful for both MAbs 7C2 and 9E11. In addition, both light and heavy chains for 7C2 and 9E11 were sequenced and the IMGT/V-Quest software program delimited the CDR regions. The results showed a unique sequence in the variable region for each of these MAbs compared to the reference directory of IMGT.

The variable regions of some other MAbs against the IGF-1R have been sequenced (Cohen *et al.,* 2002; Goetsch *et al.,* 2003; Singh *et al.,* 2003; Graus *et al.,* 2005). Among these antibodies, those designated 22, 18, 2.13.2 and 2.12.1 are human MAbs which were generated

in transgenic mice. MAbs 7C10 and EM164 are mouse MAbs. ClustalW was used to align amino acid sequences of the 7C2 and 9E11 against other MAbs in order to identify homologous and different regions or residues in the sequence (Figure 3.19). A summary of this comparison is listed in Table 3-5. The table shows that none of these MAbs against the IGF-1R, has exactly the same CDR sequences when compared to 7C2 or 9E11 in all their CDR regions.

For both MAbs 7C2 and 9E11, the CDR1 (V_L) and CDR3 (V_L) sequences are identical to each other and to the corresponding regions of 7C10. In addition, the CDR2 (VL) sequence for 9E11 is the same as a related region in EM164. Neither of the CDR regions in V_H of 7C2 or 9E11 was similar to each other nor to the other MAbs Figure 3.19. Hence, it is concluded that both MAbs 7C2 and 9E11 have unique sequences.

Light chain					
Identical to 7C2			**Identical to 9E11**		
CDR1	CDR2	CDR3	CDR1	CDR2	CDR3
9E11, 7C10	-	9E11, 7C10	7C2, 7C10	EM164	7C2, 7C10

Heavy chain					
Identical to 7C2			**Identical to 9E11**		
CDR1	CDR2	CDR3	CDR1	CDR2	CDR3
-	-	-	-	-	-

Table 3-5 Homologous CDRs of the aligned MAbs to 7C2 and 9E11

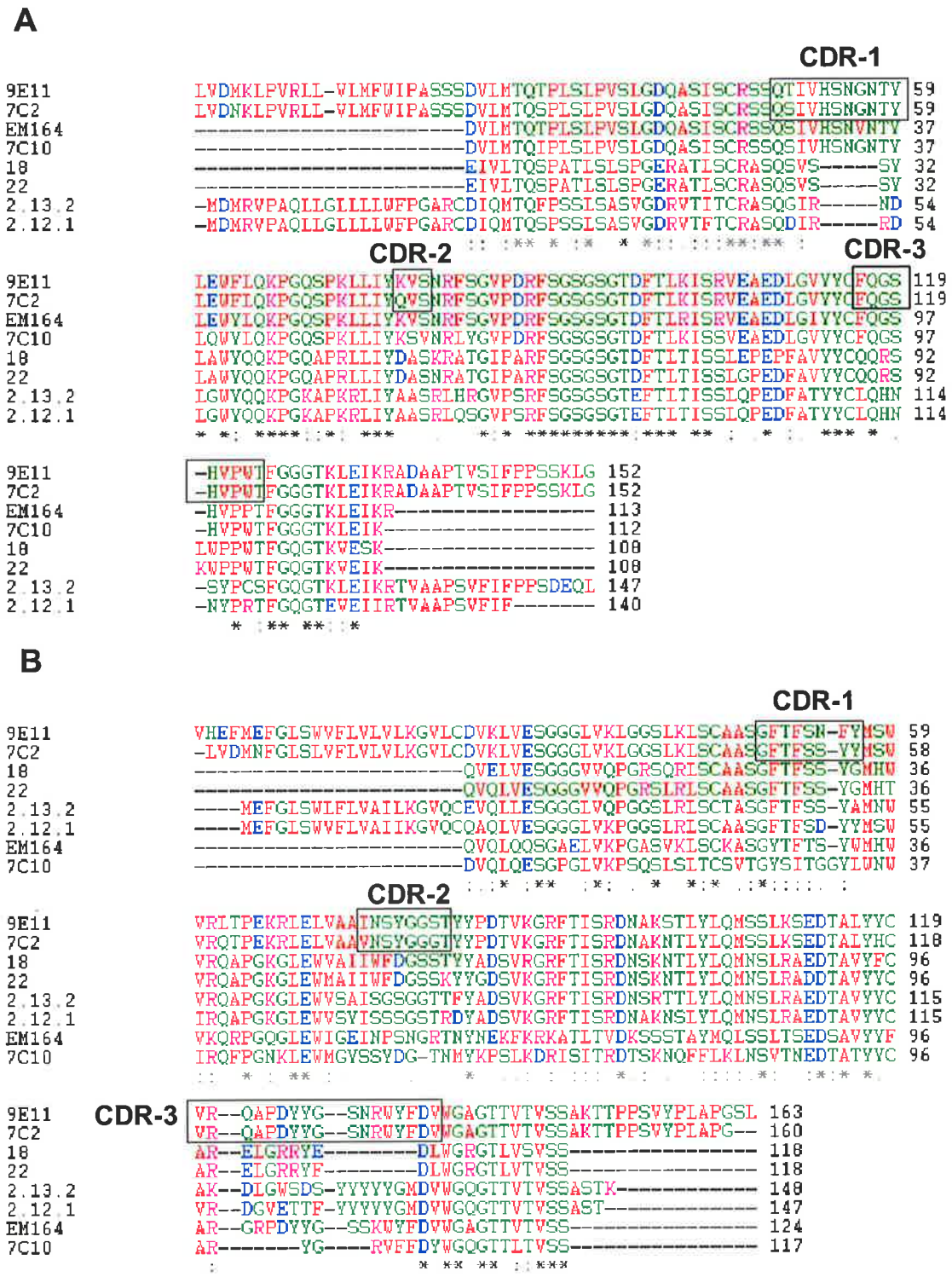

Figure 3.19 Sequence alignment of the variable regions of light (A) and heavy (B) chains for 7C2 and 9E11 against the sequences of the other antibodies against the IGF-1R.

The boxes show the CDRs according to IMGT unique numbering system for 7C2 and 9E11.
MAbs 18 and 22 (Graus *et al.*, 2005), 2.12.1 and 2.13.2 (Cohen *et al.*, 2002), EM164 (Singh *et al.*, 2003), 7C10 (Goetsch *et al.*, 2003).

Chapter 4

Binding Analysis and Epitope Mapping of MAbs 7C2 and 9E11 to IGF-1R

4. Binding Analysis and Epitope Mapping of MAbs 7C2 and 9E11 to IGF-1R

4.1. Introduction

To date, the role of the IGF-1R in cancer has been widely known as discussed in Section 1.6.5. The IGF-1R is activated by IGF-I and IGF-II, and promotes cell growth, survival and migration (Pollak *et al.,* 2004). A variety of experimental strategies have been employed to block either IGF-1R function or expression (Pollak *et al.,* 2004). Among these methods using MAbs against the IGF-1R can inhibit the ligand binding and neutralise the receptor activity (Pollak *et al.,* 2004). In addition, these MAbs could down-regulate the IGF-1R (Jackson-Booth *et al.,* 2003).

To determine the blocking effects of MAbs 7C2 and 9E11 on ligand binding, competition assays between the antibodies and ligands were conducted. These are traditionally done by competition assays using ligands that have been labelled with radioactive isotopes such as ^{125}I or ^{3}H. However, there are some disadvantages to these radioactive ligands such as short shelf life, high production expense, complex handling procedures when couriered and safety hazards during use (Pelizzola *et al.,* 1995). Due to these disadvantages, non-radioactive labelling has become an attractive alternative for use in receptor binding assays. Lanthanide chelates such as samarium (Sm^{3+}), europium (Eu^{3+}) or terbium (Tb^{3+}) have long decay fluorescence properties. When they are used in conjunction with time-resolved detection, these fluorescence tracers exhibit comparable sensitivity to radioactively labelled ligands. The principle of time-resolved fluorescence measurement is as follows. If a mixture of short-lived and long-lived (lanthanide chelates) fluorescent compounds are excited with a short pulse of light lasting less than 1 μs, the excited molecules will emit fluorescence, which is either short-lived or long-lived. In both cases, the fluorescence decay follows an exponential curve, but short-lived fluorescence will dissipate to almost zero very quickly. Thus, the long-lived fluorescence signals arising from the

lanthanide chelate can be measured with very high sensitivity under conditions of nearly zero background. Other important fluorescent properties of the lanthanides are large Stoke's shift, narrow emission peaks and optimal excitation and emission wavelengths for use with biological material such as serum (Dickson *et al.,* 1995).

While fluorescent labelling is far from ubiquitous in binding assays, a variety of ligands have been labelled with europium such as IL-2 (Stenroos *et al.,* 1997), IL-8 (Stenroos *et al.,* 1998), EGF (Mazor *et al.,* 2002) and neurotensin (Mazor *et al.,* 2002) as well as antibodies (Okada *et al.,* 1998; Amir-Zaltsman *et al.,* 2000; Maple *et al.,* 2001; Chen *et al.,* 2003; Gazi *et al.,* 2003) and nanoparticles (Harma *et al.,* 2000).

In this chapter, IGF-1R competition binding assays using europium labelled IGF-I and IGF-II are detailed. The development of this IGF-1R binding assay was first undertaken by Dr. Colin Ward, Dr. Tim Adams and Mr. Peter Hoyne (CSIRO Health Science and Nutrition, Parkville, Australia) and is based on the assay for the analysis of EGF and neurotensin binding previously described by (Mazor *et al.,* 2002).

In addition, a surface plasmon resonance measurement, using a BIAcore™ 2000 biosensor (Pharmacia biosensor AB, Uppsala, Sweden), was developed for interaction of MAbs and soluble extracellular part of the IGF-1R (amino acids 1-906) (s-IGF-1R) that allows kinetic analysis of this interaction. In addition, this BIAcore technique can be utilised to determine the effect of IGF-I and IGF-II or their chimeras (IGF-ICII and IGF-IICI) (Denley *et al.,* 2004) on binding of the antibodies to the receptor.

The BIAcore technology enables the real time analysis of antigen-antibody interactions in an automated system (Canziani *et al.,* 1999; Nice and Catimel, 1999). According to the manufacturer's (BIAcore 2000 instrument) handbook the BIAcore monitors the change in surface plasmon resonance (SPR) upon binding of a molecule in solution (the 'analyte') to a second molecule attached to the biosensor surface covalently or indirectly (the 'ligand') (Figure 4.1). SPR detects changes in the refractive index of the surface layer of a solution in contact with the sensor chip. Plotting the response against time during the course

of an interaction provides a quantitative measure of the progress of the interaction. This plot is called a sensorgram and SPR response values are expressed in resonance units (RU) (Figure 4.1).

The change in resonance units on the surface of a gold chip is a measure of the association of the two interacting molecules. The dissociation phase of the interaction can be determined by passage of analyte-free solution over the ligand (Figure 4.1).

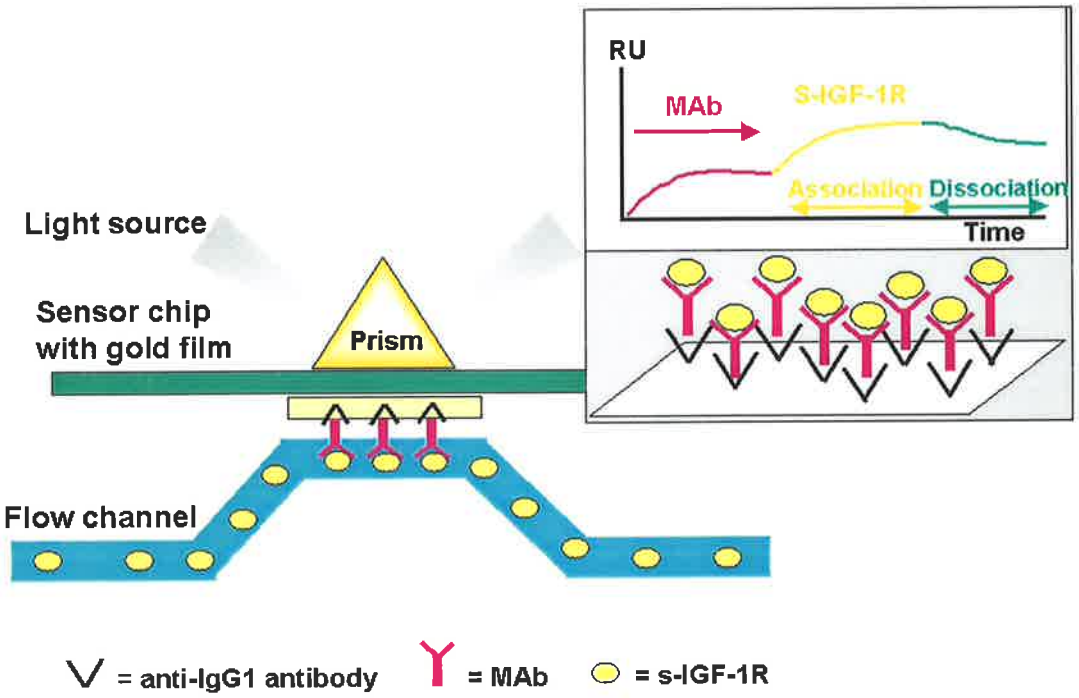

Figure 4.1 BIAcore analysis of the interaction between MAb and s-IGF-1R

In this study, the anti-mouse IgG1 antibody was immobilised on the BIAcore sensorchip surface. The sensorchip was then used to capture the anti-IGF-1R antibodies of the present study. Following this, the analyte in solution (s-IGF-1R) was passed over the sensor surface and the interaction of each MAb and s-IGF-1R was analysed. The subsequent change in surface mass upon binding of the analyte to the ligand is detected by diffraction of a light source. The change in the angle of light diffraction is recorded in resonance units (RU) over time and is presented as a chromatogram with association and dissociation phases defined.

Epitope mapping

The epitope is a specific region on an antigen molecule that is involved in recognition by an antibody (Harlow and Lane, 1999). Epitope mapping generally refers to defining the region recognised by a particular antibody and it is a methodology to study the specificity of antibodies or to distinguish between different antibodies (Harlow and Lane, 1999). Although simple chemical molecules such as carbohydrates and nucleic acids can act as antigens, the

term "epitope" generally refers to a region on a protein antigen (Morris, 1996). It is important to distinguish between conformational ("discontinuous", "assembled") epitopes, in which protein folding brings together amino acids far apart in the protein sequence and linear ("continuous", "sequential") epitopes, which can be mapped to small linear peptide sequences (Morris, 1996). Although the surface involved in binding antibodies to proteins is not known in various antigen-antibody interactions, it is likely that all epitope-paratope interfaces in proteins engage a surface of about 700 $Å^2$, as revealed in the case of lysozyme (Amit *et al.*, 1986; Sheriff *et al.*, 1987; Van Regenmortel, 1989).

There are several methods for epitope mapping of MAbs, which provide different levels of information (Morris, 1996). Among them, X-ray crystallography is often regarded as practically the only method for exact definition of an epitope by recognition of all the amino acids involved in the epitope. Nuclear magnetic resonance (NMR) spectroscopy techniques are limited by the size of the antigen that can be studied and are generally used for peptide antigens. Competition methods are applied to determine whether two different MAbs can bind to separate epitopes or whether they compete with each other for binding to the same or partially overlapping epitope. Chemical modification of amino acid side-chains is a method that is possibly less widely used. In this technique the addition of modifying groups specifically to amino acids prevents antibody binding to epitopes. This method could be particularly useful for conformational epitopes (Morris, 1996). However, such epitopes are also the most sensitive to indirect disruption by chemicals that cause even small conformational changes and great care is required to avoid false positives. New possibilities for mapping occur if the antigen can be expressed from recombinant cDNA. This allows the mutation of amino acids in the epitope and new methods of generating and identifying antigen fragments containing the epitope (Morris, 1996). The choice of a method for epitope mapping mainly depends on whether the antibody recognizes an assembled or a sequential epitope (Morris, 1996).

In this study the epitopes of MAbs 7C2 and 9E11 were mapped using a number of methods. Initially the epitopes were broadly studied with a competition technique to establish that the MAbs recognize different or overlapping epitopes compared with each other or other MAbs against the IGF-1R. Then, for further localization of the epitope, the interactions of the MAbs with chimeric receptors of IGF-1R and IR were examined. Next, the critical amino acids involved in the interaction of these MAbs with the IGF-1R were determined using alanine mutants of the IGF-1R (Whittaker *et al.,* 2001). In this method, a series of IGF-1R mutants with single amino acids substituted to alanine were used to identify individual residues involved in MAbs 7C2 and 9E11 binding.

4.2. Methods

The general methods are shown in Chapter 2 and the specific methods are described as follows.

4.2.1. IGF-1R Competition Binding Assay

To determine the effects of the MAbs on inhibition of binding of Eu-IGF-I or Eu-IGF-II to the solubilized IGF-1R, a competition assay was conducted as follows.

Europium-labelled receptor grade human IGF-I and IGF-II were prepared by Peter A. Hoyne (CSIRO Health Sciences and Nutrition, Parkville, Australia) as outlined by the manufacturer and as described in (Denley *et al.,* 2004).

As described in the manufacturer's instruction (PerkinElmer), the labelling reagent was the Eu-chelate of N^1-(p-isothiocyanatobenzyl)-diethylenetriamine N^1,N^2,N^3,N^3 tetraacetic acid (DTTA). The DTTA group forms a stable complex with Eu^{3+} and the isothiocyanate group reacts with a primary aliphatic amino group on the protein at alkaline pH to form a stable, covalent thiourea bond (Figure 4.2).

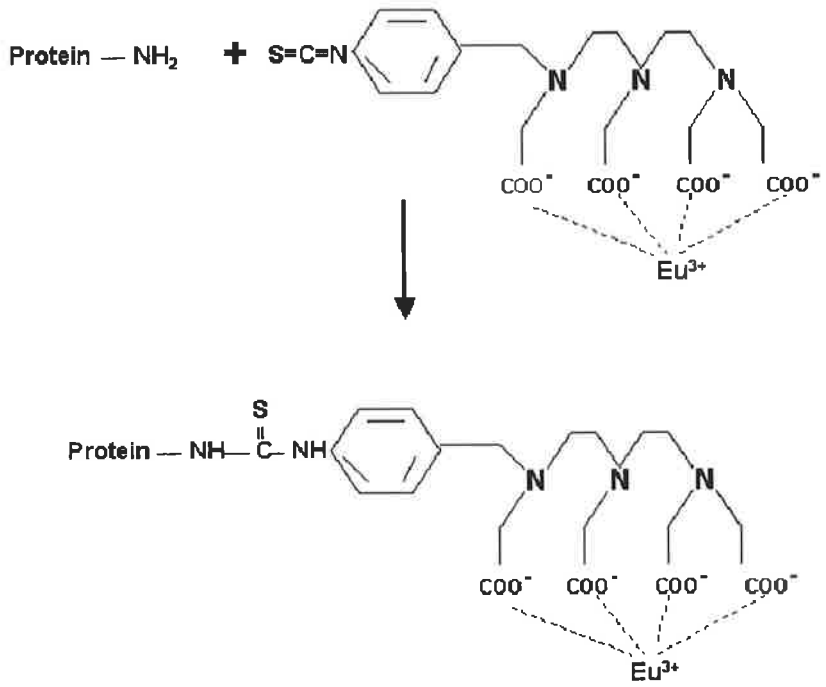

Figure 4.2 Protein labelling with Europium

The Eu-chelate of N-(p-isothiocyanatobenzyl)-diethylenetriamine N^1, N^2, N^3, N^3 tetraacetic acid used for protein labelling .

For the competition assay 96-well white Greiner Lumitrac 600 plates were coated with 100 µl MAb 24-31 solution (2.5 µg/ml in bicarbonate buffer) overnight at 4°C and blocked with 0.5% (w/v) BSA in TBS-T for 2 h at room temperature (RT). The MAb 24-31 does not interfere with receptor binding to IGF-I (Soos *et al.,* 1992) or IGF-II (Leah J Cosgrove, unpublished results).

P6 cells were used as a source of IGF-1R. The cells were lysed as described in (Denley *et al.,* 2004). The plate was then washed once with TBS-T solution and 100 µl of the lysate was added to each well and incubated overnight at 4°C. The solutions of IGF-I or IGF-II (both at 10 nM final concentration) and MAbs at serial concentrations were made in HBS buffer containing 0.05% (v/v) Tween 20. The solutions of Eu-IGF-I or Eu-IGF-II containing approximately 300,000 fluorescence (time-resolved) counts per 50 µl were prepared in Eu-binding buffer. The final concentration of the Eu-IGF-I or -II solutions was ~10 nM in each well of the plate. The plate was then washed once with TBS-T and incubated with 50 µl of the Eu-IGF-I or -II solution in each well along with 50 µl of various

concentrations of unlabelled competitors (antibody or ligand) at 4°C, overnight in the dark. The plate was then washed 4 times with TBS-T and once with Milli-Q H_2O. Afterward 100 µl of DELFIA® enhancement solution was added to each well of the plate and time-resolved fluorescence was measured. In this thesis the time-resolved fluorescence was measured using 340 nm excitation and 612 nm emission filters with a POLARstar Galaxy microplate reader (BMG Lab Technologies) and FLUOstar Galaxy PC software. The gain setting was at 127 (which is the maximum sensitivity). The background fluorescence detected in wells containing no P6 cell lysate was subtracted from all other fluorescence counts. Prism 3.03 software was used to calculate IC_{50} values employing curve-fitting with a one-site competition model (Denley *et al.*, 2004). The baseline used to calculate all IC_{50} values was set at the percent bound/total value, corresponding to that had no MAb added.

4.2.2. BIAcore Analysis of MAbs and s-IGF-1R Interactions

4.2.2.1. Surface Preparation

The anti-mouse IgG1 polyclonal antibody (Biacore) was immobilised to the Sensor chip CM5 using the protocol described by the manufacturer. Briefly, the anti-mouse IgG1 polyclonal antibody to be coupled was prepared in 10mM sodium acetate pH 5.0 at 30 µg/ml and injected over the activated chip surface in HBS running buffer. The surfaces were then deactivated by 1 M ethanolamine. A deactivated flow cell was left uncoupled as a reference on all chips. The anti-mouse IgG1 was coupled to the biosensor surface to give a final resonance value of ~8000 resonance units (RU).

4.2.2.2. Kinetic Assays of Anti-IGF-1R MAbs (7C2, 9E11 and αIR-3) Binding to the s-IGF-1R

The BIAcore measurements for interaction of the anti-IGF-1R MAbs and IGF-1R were performed basically as described by (Fagerstam *et al.*, 1990) with modifications. As briefly

described in Figure 4.1 the anti-mouse IgG1 polyclonal antibody coupled CM5 chip (Section 4.2.2.1) was used to capture the anti-IGF-1R MAbs. Solutions of the purified MAbs (7C2, 9E11 or αIR-3) at 0.002 mg/ml were made in HBS running buffer. For each MAb, 5 µl of this solution was injected over the chip at 3 µl/min flow rate to give a response of ~50 RU. Then, immediately after injection of the MAb, decreasing concentrations of s-IGF-1R (12.5 nM, 6.25 nM, 3.12 nM, 1.56 nM and 0 nM) were passed over at the same flow rate for 3.3 min. Dissociation of bound analyte (s-IGF-1R) in HBS buffer alone was measured at the same flow rate for about 50 min. All flow cells were regenerated by injection of 12 µl regeneration solution at 3 µl/min flow rate. Reference flow cell data was subtracted from all runs to account for bulk refractive index due to the buffer. Then the cycle for injection of HBS (0 nM s-IGF-1R) over the MAb was subtracted from all runs to account for bulk refractive index due to the buffer in the second injection. The association and dissociation phases obtained by the interactions of a MAb and different concentrations of s-IGF-1R was then analysed. All kinetic data were analysed using the BIAevaluation 3.2 software. Models were fitted globally across all concentrations. All interactions were fitted to a 1:1 Langmuir binding model and the kinetics of interactions between the anti-IGF-1R MAbs and the s-IGF-1R were analysed. The 1:1 Langmuir binding interaction describes 1:1 binding between analyte (A) and ligand (B) ($A+B \leftrightarrow AB$).

4.2.2.3. BIAcore Analysis of s-IGF-1R and MAbs Interaction in Presence of IGF-I or IGF-II

The ability of IGF-I and IGF-II to inhibit the binding of s-IGF-1R to the MAbs was determined by BIAcore.

Solutions containing a fixed concentration of s-IGF-1R (12.5 nM) and a range of concentrations of IGF-I or IGF-II (0.01 nM, 0.1 nM, 1 nM, 10 nM, 100 nM and 250 nM) were made in HBS running buffer and equilibrated for 3 h at RT. The anti-mouse IgG1 coupled

chip was employed to capture the anti-IGF-1R MAbs and then the solutions containing s-IGF-1R and different concentrations of IGF-I or IGF-II were passed over the chip as described in Section 4.2.2.2. Reference flow cell data was subtracted from all runs to account for bulk refractive index due to the buffer. In one cycle, HBS buffer was injected over the MAbs and this cycle was subtracted from all runs to account for bulk refractive index due to the buffer in the second injection. The association and dissociation phases for the MAbs and s-IGF-1R interaction, in the presence of ligands (IGF-I or IGF-II) were obtained.

4.2.2.4. BIAcore Analysis of s-IGF-1R and MAbs Interaction in the Presence of IGF Chimeras (IGF-ICII and IGF-IICI).

The C domain and to a lesser extent the D domain of IGF-I and IGF-II represent the principal determinants of the binding differences between these ligands to IGF-1R (Denley *et al.*, 2004). In this experiment the ability of IGF chimeras to inhibit the binding of s-IGF-1R to the MAbs was studied by BIAcore to determine the effect of the C domain of the IGF-I or IGF-II on the binding of the s-IGF-1R to the MAbs.

The details of this experiment were generally the same as above (Section 4.2.2.3), but instead of the IGFs, different concentrations of the chimeras IGF-ICII or IGF-IICI (0.01 nM, 0.1 nM, 1 nM, 10 nM and 100 nM) were pre-incubated with 6.25 nM s-IGF-1R (for 3 h) before injection.

4.2.2.5. Mass Transfer Control Experiment

Because in the kinetic studies using BIAcore the flow rate was low (3 μl/min) and the s-IGF-1R is a big molecule (~380 kDa), the existence of mass transfer is possible. If mass transfer limitations are serious, the apparent kinetic constants automatically calculated using BIAevaluation 3.2 software bear no relation to the kinetic constants for the interaction itself. To determine whether there are any mass transfer limitations for the interaction between

s-IGF-1R and MAb, the mass transfer control experiment was conducted according to the manufacturer's (BIAcore 2000 instrument) handbook. This experiment measures the association rate at one concentration of analyte (s-IGF-1R) at three different flow rates (3, 15 and 75 µl/min), using a 2-minute injection. In this experiment, 5 µl of the MAb 7C2 solution was injected over the chip in 3 µl/min flow rate but s-IGF-1R (50 nM) was injected at the three different flow rates for 2 min. This method was generally the same as the technique described in Section 4.2.2.2. This provided more RU after 2 min than did concentrations of 12.5 nM or less used in the BIAcore experiments (Section 4.2.2). Obviously, if there is no mass transfer effect for higher concentrations of s-IGF-1R, there is not any for lower concentrations.

4.2.3. Epitope Mapping by Flow Cytometry Analysis Using Chimeric Receptors

Flow cytometry analysis was carried out on MAbs 7C2 and 9E11 to test their reactions with chimeric IGF-1R/IR receptors. Chimeric receptors were generated in which sub-domains of the IR and IGF-1R α subunits were exchanged between their respective receptor backbone structures (Schumacher *et al.,* 1991; Schumacher *et al.,* 1993) and were expressed on the surface of NIH 3T3 cells. In this study three cell lines expressing three of these chimeras, kindly provided by Prof. A. Ullrich (Germany), were used to determine the interaction of MAbs 7C2 and 9E11 with different sub-domains of the IGF-1R. These three chimeric receptors are called IR/IGF-1R C2, IR/IGF-1R C12 and IGF-1R/IR C1 (Schumacher *et al.,* 1991; Schumacher *et al.,* 1993). In Figure 4.3, a schematic of these chimeric receptors is shown comparing them to their parental IR and IGF-1R.

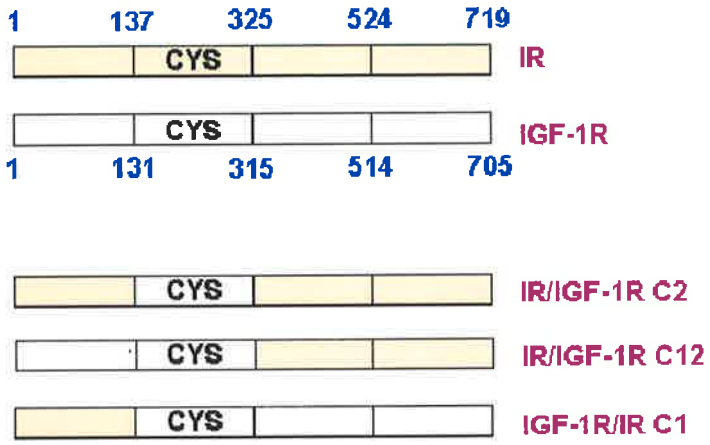

Figure 4.3 Schematic representation of the wild type (wt) IGF-lR, wt IR and IGF-1R/IR chimeric receptors.

The numbering system of the amino acids is as described in (Ullrich *et al.*, 1985) and (Ullrich *et al.*, 1986). The schematics show the composite structure of the chimeric receptors (IR, light orange; IGF-lR, white). IR/IGF-1R C2, is the insulin receptor containing amino acids 131-315 of IGF-1R, IR/IGF-1R C12 is the insulin receptor containing the signal peptide and the first 315 amino acids of the IGF-1R and IGF-1R/IR C1 is the IGF-1R containing the signal peptide and the first 137 amino acids of the IR (Schumacher *et al.*, 1991; Schumacher *et al.*, 1993). The cells stably expressing these chimeric receptors were kindly provided by Prof. A. Ullrich (Martinsried, Germany).

The cell lines expressing chimeric receptors were grown in DMEM, 10% (v/v) FCS, 1% (v/v) penicillin/streptomycin and 0.5% (v/v) geneticin (G418) in T175 flasks. The general method for flow cytometry analysis was described in Section 3.2.5. However, in this assay, the purified forms of MAbs 7C2 and 9E11 were used at a concentration of 10 µg/ml as primary antibody for binding to the chimeric receptor. This concentration was chosen to be similar to the concentration of MAbs in the hybridoma culture medium (~10 µg/ml). In this experiment, IgG1 was used as a negative isotype control. The MAbs 24-60 and 24-55 (against the IGF-1R) were applied as positive controls at the same concentration as MAbs 7C2 and 9E11. The MAbs bound to the chimeric receptors were detected by anti-mouse IgG FITC conjugated antibody as explained in Section 2.2.2.4.

4.2.4. Epitope Mapping by Competition Assay Between Different MAbs to IGF-1R

4.2.4.1. The Fragmentation of IgG to Fab Using Papain

The enzyme papain digests the IgG molecule into two Fab fragments and one Fc fragment (Porter, 1973) (Branden and Tooze, 1991). Pilot experiments were carried out where both the concentration of papain and the time of digestion were varied to determine the optimal conditions. Then, purified MAbs 7C2 and 9E11 were digested with papain in the presence of the reducing agent cysteine. The methods described by (Raychaudhuri *et al.,* 1985) and (Lutomski *et al.*, 1995) with some modifications were used. For each MAbs (7C2 or 9E11) the reaction was performed in a total volume of 10 ml containing 5 ml of 0.4 mg/ml purified MAb in PBS and 0.5 ml of 0.2 mg/ml papain (Boehringer Mannheim GmbH) in digestion buffer (see Section 2.1.10). The ratio of papain:antibody was 1:20 (w/w) and the antibody was digested for 7 h at 37°C. Iodoacetamide was added to a final concentration of 30 mM to stop the reaction. The digested antibody was dialysed into PBS at 4°C overnight, and the Fab and Fc fragments were separated by protein A-Sepharose chromatography.

The protein A-Sepharose column was washed with at least five-column volumes of binding buffer (20 mM sodium phosphate (pH 7)). Then for each 7C2 or 9E11 MAb, the dialysed solution of digested MAb (10 ml) was loaded onto the column at 1 ml/min flow rate. The flow through contains the Fab fragment and was collected while the Fc fragment and any undigested IgG remained bound to the column. Protein A binds specifically to the Fc region of mice immunoglobulin molecules (especially IgG) and it is totally non-reactive with the Fab region of mouse IgG (Aybay, 2003). The Fc fragment was eluted with 5 ml 0.1 M sodium citrate pH 6.0. The column was washed in 20% (v/v) ethanol in milli-Q H_2O for storage.

The preparation of Fab fragments was quantitated by the Bradford method as described in Section 2.2.2.3. To determine the success of Fab production and purification, a 6 μg aliquot of the Fab obtained from MAbs 7C2 or 9E11 was loaded onto a SDS-PAGE gel

and electrophoresed. Then the gel was stained in Coomassie Brilliant Blue R^{TM} as explained in Section 2.2.2.5.

4.2.4.2. Europium Labelling of Fab

The Fab fragments of each MAbs 7C2 and 9E11 were labelled with europium according to the protocol of DELFIA® Eu-labelling kit. The labelling reagent was Eu-chelate of N^1-(p-isothiocyanatobenzyl)-diethylenetriamine-N^1,N^2,N^3,N^3-tetraacetic acid as explained before (Section 4.2.1). Briefly, 0.35 mg of Fab (7C2 or 9E11) in 0.1 M sodium carbonate (pH 9.3) was mixed with 70 µg of europium labelling reagent (provided by DELFIA® Eu-labelling kit) at a europium to antibody ratio of 1:5 (w/w) to make the final volume 150 µl. The reaction was incubated overnight at 4°C. Separation of the labelled antibody from free Eu^{3+} chelate was performed by gel filtration on a PD-10 column. The mixture was applied directly into the column equilibrated with elution buffer (50 mM Tris-HCl pH 7.8 containing 0.9% (w/v) NaCl and 0.05% (w/v) Na-Azide) and 0.5 ml fractions were collected with the same buffer. The fractions from the first peak with the highest Eu^{3+} counts were pooled and characterised. Protein concentration in the pooled fractions was calculated by Bradford assay as generally described in Section 2.2.2.3.

To determine the activity of europium labelled Fab part of MAbs 7C2 (Eu-7C2 (Fab)) and 9E11 (Eu-9E11 (Fab)) against the IGF-1R the following experiment was performed. White Greiner Lumitrac 600 96-well plates were coated with 100 µl of anti-IGF-1R antibody MAb 24-31 solution (2.5 µg/ml in bicarbonate buffer) overnight at 4°C and blocked with 0.5% (w/v) BSA in TBS-T for 2 h at RT. Then after washing the plate 3 times with TBS-T, 100 µl of culture medium containing s-IGF-1R (prepared as described in Section 3.2.2.1) were added to each well of the plate as a source of the receptor and incubated overnight at 4°C. The plate was then washed 3 times in TBS-T and 100 µl of a range of concentrations for Eu-7C2 (Fab) or Eu-9E11 (Fab) were added to each well (each one in triplicate) and the plate

was incubated overnight at 4°C. For each of the Eu-7C2 (Fab) or Eu-9E11 (Fab), serial concentrations were made in europium binding buffer which contained approximately 300,000, 150,000, 30,000 and 3000 fluorescent counts per 100 µl. After washing the plate 4 times with TBS-T followed by once with milli-Q H_2O, 100 µl DELFIA® enhancement solution was added to each well of the plate. The time-resolved fluorescence was measured using 340 nm excitation and 612 nm emission filters with a BMG lab technologies Polarstar ™ Fluorimeter. The measured fluorescence represents Eu-7C2 (Fab) or Eu-9E11 (Fab) bound to the captured s-IGF-1R. The background fluorescence determined in wells containing no s-IGF-1R was subtracted from all other fluorescence counts.

4.2.4.3. Competition Binding Analysis Between MAbs Against the IGF-1R

To determine whether the two MAbs 7C2 and 9E11 and also other MAbs against the IGF-1R (24-60 and αIR-3) bind to distinct sites on the IGF-1R, a competition assay was carried out to determine the capacity of one antibody to inhibit the binding of another antibody. Briefly, white Greiner Lumitrac 600 96-well plates were coated with 100 µl of anti-IGF-1R antibody MAb 24-55 solution (2.5 µg/ml in bicarbonate buffer) overnight at 4°C and blocked with 0.5% (w/v) BSA in TBS-T for 2 h at RT. This 'capture' antibody binds to amino acids 440-586 of the IGF-1R, which are not in the same binding region as for 24-60 and αIR-3 (cysteine-rich domain). The epitope for MAbs 24-60 and αIR-3 are between amino acids 184-283 and 223-274 respectively (Gustafson and Rutter, 1990; Soos *et al.*, 1992). Then after washing the plate 3 times with TBS-T, 100 µl of cultured media containing s-IGF-1R was added to each well of the plate and incubated for overnight at 4°C. The plate was then washed 3 times in TBS-T. Approximately 300,000 fluorescent counts of Eu-7C2 (Fab) or Eu-9E11 (Fab) in 50 µl (each ~ 16.5 ng MAb (Fab)) were then added to each well of the plate along with 50 µl of 25 nM solution of unlabelled competitor and incubated for 16 h at 4°C. Afterwards, wells were washed 4 times with TBS-T followed by once with milli-Q H_2O. Then

DELFIA® enhancement solution was added (100µl/well) and the time-resolved fluorescence was measured as described in Section 4.2.1. The background fluorescence determined in wells containing no s-IGF-1R was subtracted from all other fluorescence counts.

4.2.5. Epitope Mapping Using Alanine Mutants of the IGF-1R

4.2.5.1. Transfection Methods

Recombinant cDNAs which encode mutant secreted IGF-1R, which were constructed in the plasmid pcDNA3-zeo (+) for expression (Figure 4.4), were kindly provided by Prof. J. Whittaker, Case Western Reserve University, Cleveland, Ohio, USA (Whittaker *et al.*, 2001).

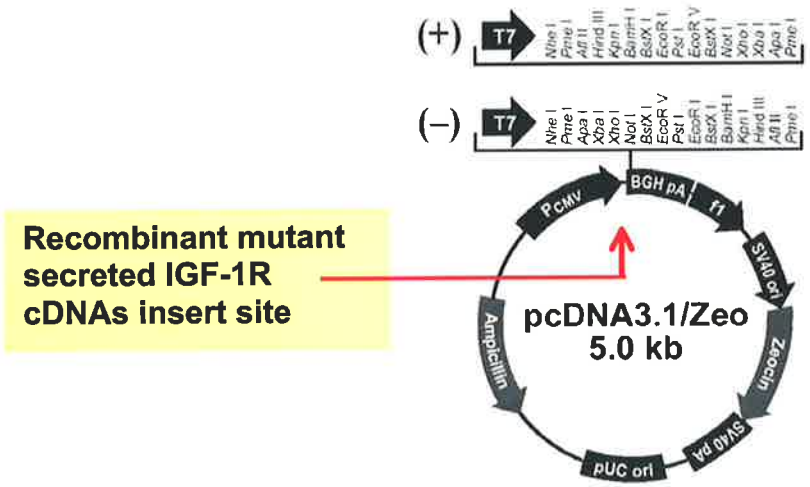

Figure 4.4 The pcDNA3.1/Zeo mammalian expression vector.

The vector carries the Zeocin resistance and ampicillin resistance genes. The figure for the vector is adapted from (Invitrogen, 2005). The site of insertion of the recombinant cDNAs encoding mutant secreted IGF-1R is indicated.

The mutants used in this study are listed in Table 4-1. As there is an ampicillin resistance gene in the expression vector, the plasmids were transformed into competent DH5α cells and grown on Luria Agar plates containing 100 µg/ml ampicillin, and the plasmid DNAs were also produced in culture containing 100 µg/ml ampicillin. For each one, the plasmid DNAs were purified from a 5 ml overnight culture using the Ultraclean mini plasmid prep kit. Subsequently the plasmids for these constructs were transiently transfected into 293 EBNA cells (an adenovirus-transformed human kidney cell line expressing Epstein-Barr virus

nuclear antigen). For each construct 4 μg of plasmid DNA was transfected using the commercially available lipofection 2000 reagent according to the manufacturer's instructions (Mynarcik *et al.,* 1997). The culture supernatants were harvested after 72 h of culturing the cells at 37°C in an atmosphere containing 5% (v/v) CO_2. For the details of the above experiments see Section 2.2.3.

No.	Construct	Description
1	Chimeric IGF-1R/256-266IR	The amino acids 256-266 of the IGF-1R replaced with the corresponding amino acids of IR-A (262-277).
2	IGF-1R R240A	The amino acid Arginine (240) replaced with Alanine.
3	IGF-1R F241A	The amino acid Phenylalanine (241) replaced with Alanine.
4	IGF-1R E242A	The amino acid Glutamic acid (242) replaced with Alanine.
5	IGF-1R F251A	The amino acid Phenylalanine (251) replaced with Alanine.
6	IGF-1R I255A	The amino acid Isoleucine (255) replaced with Alanine.
7	IGF-1R S257A	The amino acid Serine (257) replaced with Alanine.
8	IGF-1R E259A	The amino acid Glutamic acid (259) replaced with Alanine.
9	IGF-1R S260A	The amino acid Serine (260) replaced with Alanine.
10	IGF-1R D262A	The amino acid Aspartic acid (262) replaced with Alanine.
11	IGF-1R S263A	The amino acid Serine (263) replaced with Alanine.
12	IGF-1R E264A	The amino acid Glutamic acid (264) replaced with Alanine.
13	IGF-1R F266A	The amino acid Phenylalanine (266) replaced with Alanine.
14	IGF-1R H269A	The amino acid Histidine (269) replaced with Alanine.
15	IGF-1R E272A	The amino acid Glutamic acid (272) replaced with Alanine.
16	IGF-1R M274A	The amino acid Methionine (274) replaced with Alanine.
17	IGF-1R Q275A	The amino acid Glutamine (275) replaced with Alanine.
18	IGF-1R E276A	The amino acid Glutamic acid (276) replaced with Alanine.
19	IGF-1R S279A	The amino acid Serine (279) replaced with Alanine.
20	IGF-1R I282A	The amino acid Isoleucine (282) replaced with Alanine.
21	IGF-1R R283A	The amino acid Arginine (283) replaced with Alanine.
22	IGF-1R N284A	The amino acid Asparagine (284) replaced with Alanine.

Table 4-1 Alanine mutants of the IGF-1R.

These constructs have been described in (Whittaker *et al.,* 2001).

4.2.5.2. ELISA to Determine the Expression of the Recombinant Receptors

The production of the secreted recombinant receptors was assessed by ELISA. The principle of this test is the same as the ELISA on purified s-IGF-1R explained earlier (Section 2.2.2.1) with some modifications.

Briefly, a 96 well MaxiSorp plate was coated with MAb 24-55 (0.25 μg/well) and blocked with 200 μl of 2% (w/v) BSA in PBS. For the secreted alanine mutants and chimeric

IGF-1R/256-266IR, 100 µl of the harvested culture supernatant were added to each well of the plate in triplicate. In this experiment, 100 µl of 1:20 (v/v) dilution of culture supernatants from cells secreting s-IGF-1R (as explained in Section 3.2.2.1) were used as a positive control. The harvested supernatant of untransfected cells was used as negative control. The same batch of harvested supernatant containing the s-IGF-1R was used in all experiments for consistency between different experiments. The plate was then incubated overnight at 4°C, and after washing the plate with PBS-T, 100 µl of 1:200 (v/v) diluted Bt-16-13 (biotinylated MAb 16-13) in PBS–T containing 1% (w/v) BSA were added to each well of the plate, and incubated for two h at RT. In this experiment the antibody Bt-16-13 was used to detect the secreted receptors from the transfected cells. The epitope for the MAb 16-13 is near the N-terminus of the IGF-1R (between amino acids 62-184) (Soos *et al.,* 1992) and this part of the IGF-1R was intact in all of the recombinant constructs. The plate was then washed and 100 µl of 1:200 (v/v) diluted Streptavidin-HRP (CHEMICON) in PBS-T was added to each well of the plate followed by incubation for one h at RT. After another washing step, the bound receptors were detected using ABTS reagent.

To determine the concentration of s-IGF-1R in the 1:20 (v/v) dilution of culture supernatants from cell secreting s-IGF-1R in PBS, a standard curve was obtained from the same ELISA test on different concentrations of purified s-IGF-1R. The s-IGF-1R was purified from supernatant as described in Section 3.2.2.1.

4.2.5.3. Europium Binding Assay for Epitope Mapping of the MAbs by Alanine Mutants of the IGF-1R

To determine the binding of Eu-7C2 (Fab) and Eu-9E11 (Fab) to different alanine mutants of the IGF-1R, the europium binding assay was conducted. The principle for this experiment was similar to the competition binding assay described in Section 4.2.1.

The supernatant for each mutant of IGF-1R was diluted to give the same absorbance as a 1:20 dilution of culture supernatants from cell secreting s-IGF-1R (containing 0.28 mg/ml s-IGF-1R) as detected in the ELISA (Section 4.2.5.2). This allowed the same concentrations of secreted receptors to be applied in Europium binding assay for the different secreted receptors. Then, 100 µl of each diluted supernatant were added to each well of the Greiner Lumitrac white 96-well plate (in triplicate), previously coated with MAb 24-55, and incubated overnight at 4°C. The plate was then washed 3 times with TBS-T and approximately 300,000 fluorescent counts of Eu-7C2 (Fab) or Eu-9E11 (Fab) in 50 µl (each ~ 16.5 ng MAb (Fab)) were added to each well of the plate and incubated for 16 h at 4°C. The Eu-9E11 (Fab) and Eu-7C2 (Fab) were generated as described in Section 4.2.4.2. After washing the plates 4 times with TBS-T and once with milli-Q H_2O, 100µl DELFIA® enhancement solution was added to each well and the time-resolved fluorescence was measured as explained in Section 4.2.1. The background fluorescence, for the wells containing no s-IGF-1R, was subtracted from all other fluorescence counts.

4.2.5.4. Sequencing the Plasmids Containing cDNAs for Alanine Mutants of IGF-1R

For the selected constructs, the plasmids (pcDNA3-zeo (+)) containing cDNAs were sequenced. The method was generally as described in Section 2.2.3.7. A reaction mix was set up containing 12 µl of plasmid DNA (0.5µg/µl), 1 µl of DNA primer aIR3KR-AA (100ng/µl) and 4 µl of Big Dye (version 3) sequencing mix. The primer sequence is shown in Section 2.1.8. Ms. Carlie Delaine (The University of Adelaide, Australia) kindly sequenced the selected plasmids.

4.3. Results

4.3.1. Effect of the MAbs on IGF-1R Competition Binding Assay

The result of binding analysis revealed that MAbs 9E11 and 7C2 significantly ($P < 0.05$) competed with the Eu-IGF-I for binding to the captured solubilized IGF-1R as shown in (Figure 4.5 A). The maximum inhibition was obtained with highest concentration of the MAbs (200 nM). The MAbs 9E11 and 7C2 inhibited the Eu-IGF-I binding to the receptor by approximately 25% and 60% respectively (Figure 4.5 A). The unlabelled IGF-I (10nM), which was used as a control also competed with the Eu-IGF-I binding to the receptor. In this experiment, MAb 24-60 had no significant inhibiting effect. The isotype control IgG1 also did not show any significant inhibition of binding.

The binding curves shown in (Figure 4.6 A) were obtained from the same results as (Figure 4.5 A). The average blocking activity (IC_{50}±SD) for each MAb 7C2 and 9E11 to inhibit Eu-IGF-I binding to the IGF-1R were estimated as 1.9 ± 1 nM and 3.4 ± 2.4 nM, respectively, although the curve fitting was poor. Data from three separate experiments was used to obtain these values.

These results showed that MAbs 7C2 and 9E11 possessed a high and similar blocking activity (IC_{50}) to each other. Although MAb 7C2 shows higher affinity (smaller IC_{50}) than MAb 9E11, the difference between the values for MAbs 7C2 and 9E11 was not significant ($P > 0.05$). The P value was calculated by comparing the data using unpaired t-tests (Confidence Intervals 95%) by the Prism 3.03 software.

Surprisingly, none of the MAbs inhibited the Eu-IGF-II binding significantly (Figure 4.5 B and Figure 4.6 B). The unlabelled IGF-II (10 nM), which was a control, inhibited the binding of the Eu-IGF-II to the receptor by ~ 80%.

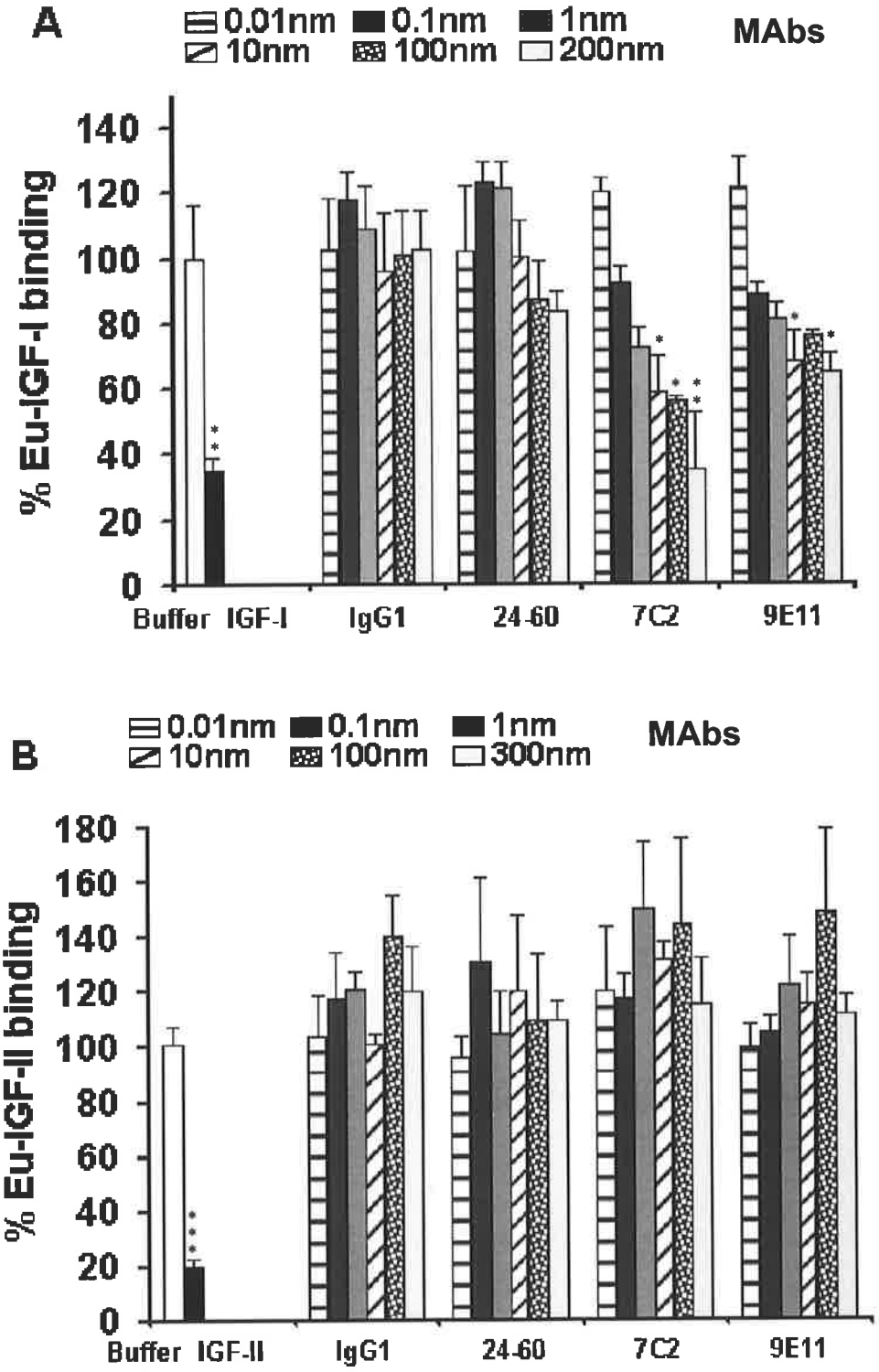

Figure 4.5 Percentage of binding the Eu-IGF-I (A) or Eu-IGF-II (B) to solubilized IGF-1R captured on the plate by MAb 24-31 in the presence of different anti-IGF-1R MAbs and IgG1 (negative control).

Results are expressed as a percentage of Eu-IGF-I or Eu-IGF-II binding in the absence of competing MAb (Buffer) and the data points are means ± SD of triplicate samples. 10 nM of unlabelled IGF-I or IGF-II were used as control to compete with Eu-IGF-I (A) or Eu-IGF-II (B) respectively for binding to the receptor. The graphs are the representative of three separate experiments.
The P values were calculated by comparing the data for no treatment (Buffer) with other data using unpaired t-tests (Confidence Intervals 95%) by the Prism 3.03 software.
P value 0.01 to 0.05 = *, P value 0.001 to 0.01 =**, P value < 0.001=***.

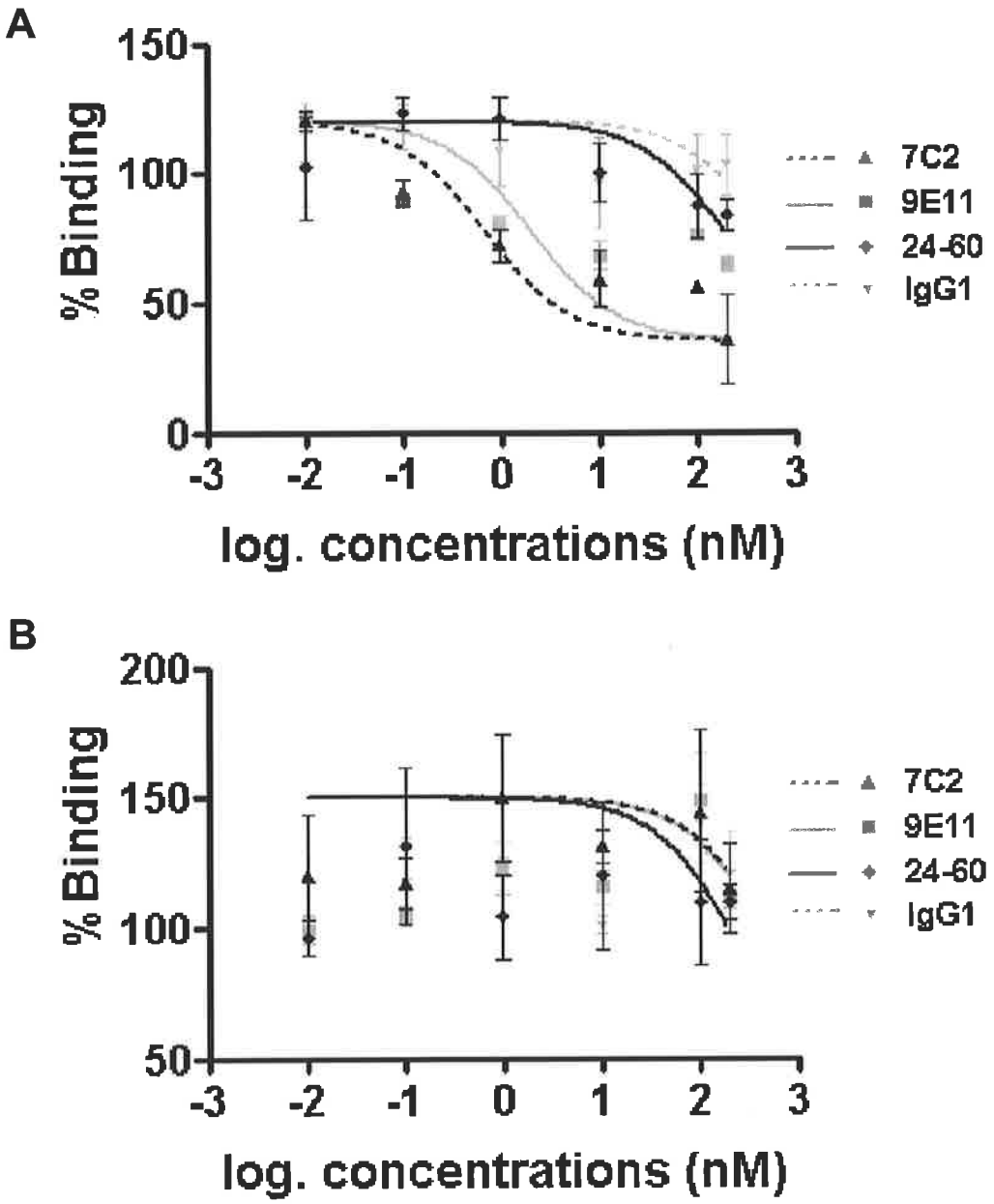

Figure 4.6 The isotherm curves for competition of Eu-IGF-I (A) or Eu-IGF-II (B) with different concentrations of various MAbs for binding to solubilized human IGF-1R from P6 cells.

Results are expressed as a percentage of Eu-IGF-I (A) or Eu-IGF-II (B) bound to the receptor in the absence of competing MAb. These graphs are the representative of three separate experiments and data points are means of triplicates ± SD. The curves were generated using the Prism 3.03 software employing curve-fitting with a one-site competition model. Curve fitting constants were the minimum and maximum percentage of binding the Eu-IGF-I (A) or Eu-IGF-II (B) to the receptor.

4.3.2. BIAcore Results

The BIAcore provided insight into the kinetics of the association and dissociation phases of s-IGF-1R with captured MAbs on the chip. The MAbs, which were IgG1 isotypes, were captured with immobilised polyclonal α-mouse IgG1 antibody. The BIAcore curves for capturing the MAb 7C2 followed by different concentrations of s-IGF-1R in each cycle are

shown in Figure 4.7. The same experiments were conducted for 9E11 and αIR-3. The association and dissociation phase for their binding to s-IGF-1R is shown in Figure 4.8.

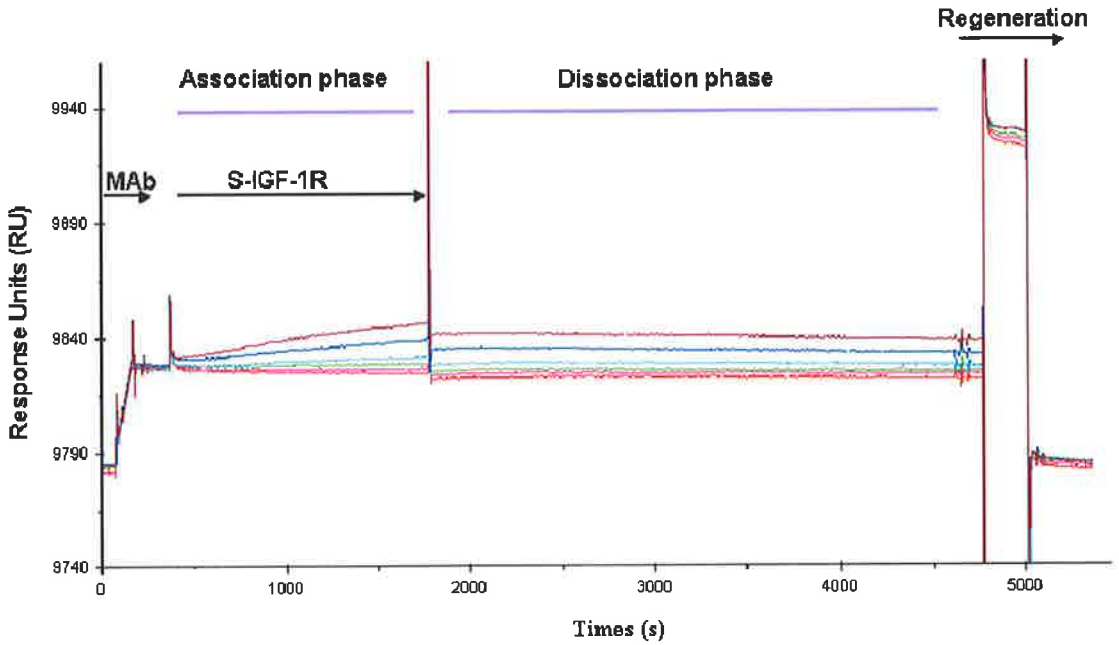

Figure 4.7 Overlays of a series of sensorgrams where the concentration of s-IGF-1R was varied from 0 to 12.5 nM.

In each curve the MAb 7C2 was injected over the chip followed by the s-IGF-1R solutions at different concentrations. The chip was then regenerated after each cycle.
— 0 nM s-IGF-1R, — 0.76 nM s-IGF-1R, — 1.56 nM s-IGF-1R, — 3.12 nM s-IGF-1R, — 6.25 nM s-IGF-1R, — 12.5 nM s-IGF-1R

4.3.2.1. Kinetic Analysis of the MAb and s-IGF-1R Binding

By fitting the binding curves globally to a 1:1 Langmuir binding model, the association and dissociation kinetics of the interaction between the MAbs and s-IGF-1R were initially assessed (Figure 4.8). The s-IGF-1R exhibited a fast association rate with both MAbs 7C2 and 9E11 (k_a shown in Table 4-2). The resultant complexes between the MAbs and s-IGF-1R were stable as illustrated by the slow dissociation rates (k_d shown in Table 4-2). Kinetic analysis of the biosensorgram curves suggests 7C2 and 9E11 both have slightly better affinity than αIR-3 for binding to the receptor and also the affinity of 7C2 is higher than 9E11 (K_D shown in Table 4-2). However, the K_D values for these three MAbs are not significantly different ($P > 0.05$). The P values were calculated by comparing the data using unpaired t-tests (Confidence Intervals 95%) by the Prism 3.03 software.

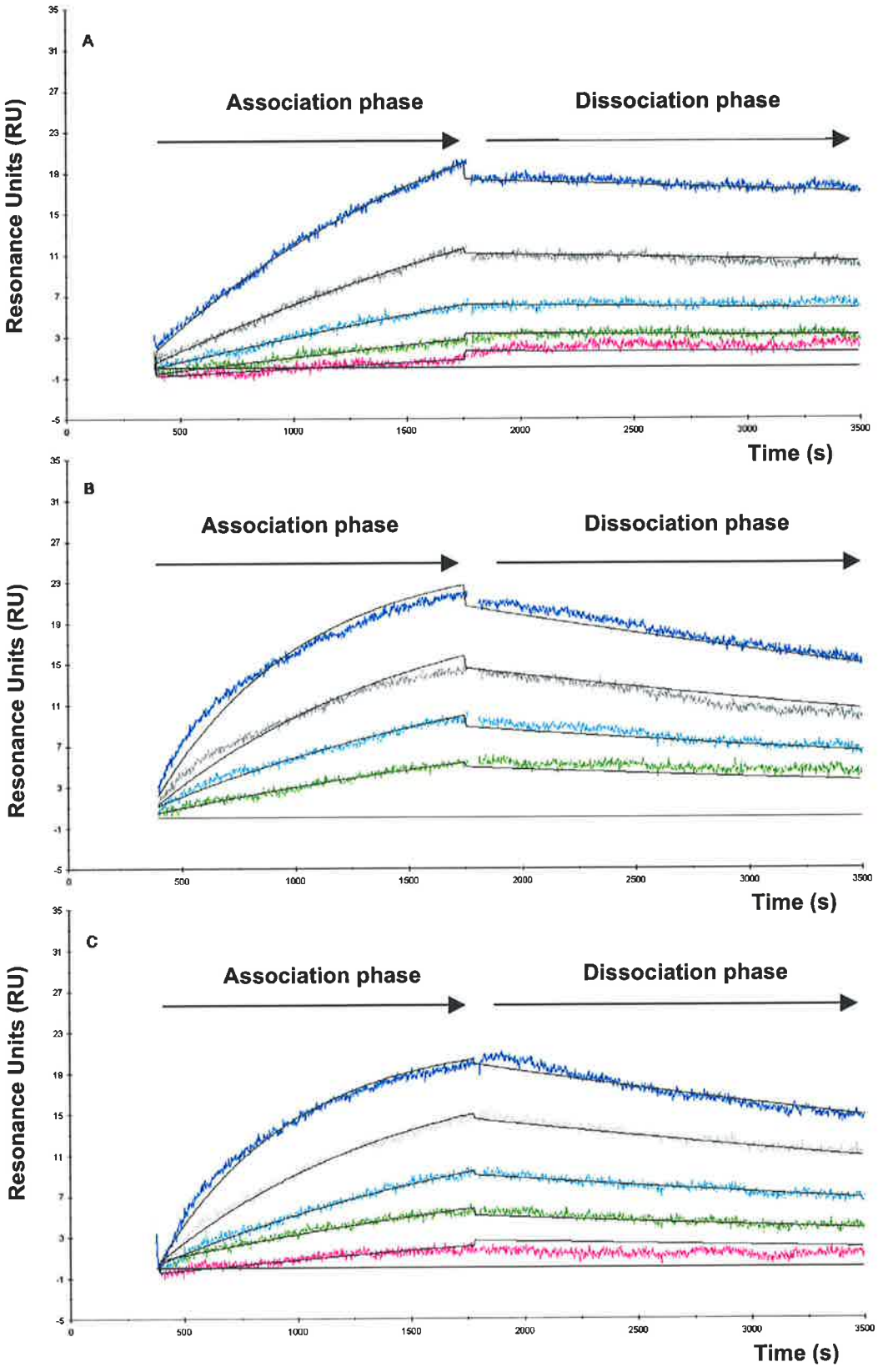

Figure 4.8 BIAcore binding the captured MAbs to s-IGF-1R

A) MAb 7C2 B) MAb 9E11 C) MAb αIR-3.
— 0.76 nM s-IGF-1R, — 1.56 nM s-IGF-1R, — 3.12 nM s-IGF-1R, — 6.25 nM s-IGF-1R, — 12.5 nM s-IGF-1R
The interaction curves and globally fitted to a 1:1 Langmuir binding model. The graphs are a representative of three experiments. Kinetic analysis results are shown in Table 4-2.

MAbs	Ka	kd	K_D (M)
7C2	$(6.6\pm1.8)\times 10^{4}$	$(3.1\pm0.2)\times 10^{-5}$	$(0.5\pm1.6)\times 10^{-9}$
9E11	$(0.8\pm0.2)\times 10^{5}$	$(1.7\pm0.1)\times 10^{-4}$	$(2.1\pm0.4)\times 10^{-9}$
αIR-3	$(1.0\pm0.3)\times 10^{5}$	$(1.2\pm0.5)\times 10^{-4}$	$(1.3\pm0.5)\times 10^{-9}$

Table 4-2 BIAcore kinetic analysis of binding of MAbs to s-IGF-1R.

The 1:1 Langmuir binding model was used to fit the kinetic data and ultimately derive the dissociation constant (K_D). The results generated are from three separate runs and the average of ka, kd and K_D for each MAb is shown. Values are the means ± SD from three independent experiments. The dissociation constant (KD)=kd/ka, kd= dissociation rate and ka=association rate.

4.3.2.2. Mass Transfer Control

Mass transfer effect is limitations on the rate of transport analyte between bulk solution and the sensor chip surface. If there is any mass transfer effect, it will be deleterious to kinetic measurements (Myszka *et al.*, 1998). The mass transfer control experiment, which analyses association rates at three different analyte flow rates, revealed no significant difference between curves obtained from injection of s-IGF-1R at different flow rates (3, 15 and 75 µl/min) over captured MAb 7C2 (Figure 4.9). It means that the kinetic interactions are independent of flow rate. Therefore, using 3 µl/min flow rate to analyse the interaction of the MAbs and s-IGF-1R caused no mass transfer effect.

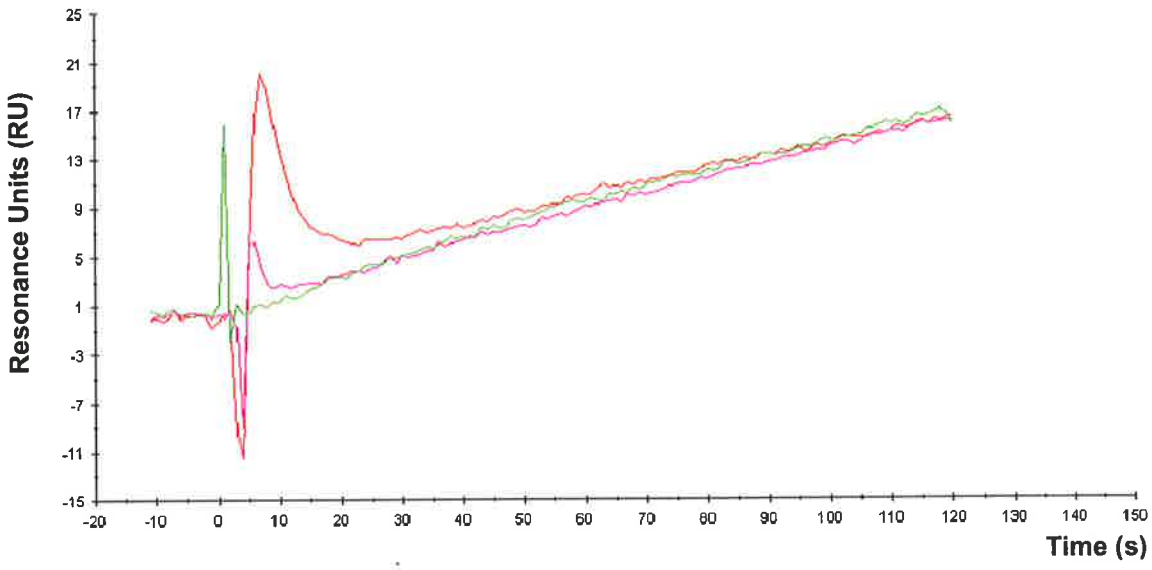

Figure 4.9 Mass transfer control curves.

The s-IGF-1R (50nM) was injected over the captured MAb 7C2 on the CM5 chip at three different flow rates as described in Section 4.2.2.5.The association phase for the interaction between s-IGF-1R and MAb 7C2 is shown in this figure for the three flow rates. — 3 µl/min — 15µl/min — 75µl/min

4.3.2.3. The Effects of IGF-I and IGF-II on Binding s-IGF-1R to the MAbs

The BIAcore results for passing the s-IGF-1R pre-incubated with different concentrations of IGFs over the captured MAbs on the chip showed that the IGF-I also concentration-dependently caused a reduction in the Resonance Units (RU) for binding the s-IGF-1R to MAbs 7C2, 9E11 and αIR-3 (Figure 4.10, Figure 4.11 and Figure 4.12). Interestingly, IGF-II did not cause any reduction in the Resonance Units (RU) for binding of s-IGF-1R to any of these three MAbs. Hence, IGF-I inhibited the binding of the s-IGF-1R to the captured MAbs but IGF-II had no inhibiting effect. The values for RU measured immediately after injection of the solutions containing s-IGF-1R and either IGF-I or IGF-II, at t=1810 (s), are shown in Table 4-3.

	7C2 (RU)		9E11 (RU)		αIR-3 (RU)	
Concentration	**IGF-I**	**IGF-II**	**IGF-I**	**IGF-II**	**IGF-I**	**IGF-II**
0 nM	29.9	29.9	26.1	25.9	25.5	25.5
0.1 nM	27.3	27.5	26.1	26.3	24.5	26.2
1 nM	27.3	27.8	26.1	26.3	24.7	25.3
10 nM	26.5	27.5	24.3	25.0	23.6	25.5
100 nM	23.3	28.3	18.5	26.5	19.5	25.5
250 nM	14.1	28.1	16.4	26.7	17.5	26.5

Table 4-3 The Resonance Units (RU) after injection of s-IGF-1R and either IGF-I or IGF-II over the captured MAbs

The values for (RU) were measured at t= 1810 (s).
Data obtained from Figure 4.10, Figure 4.11 and Figure 4.12.

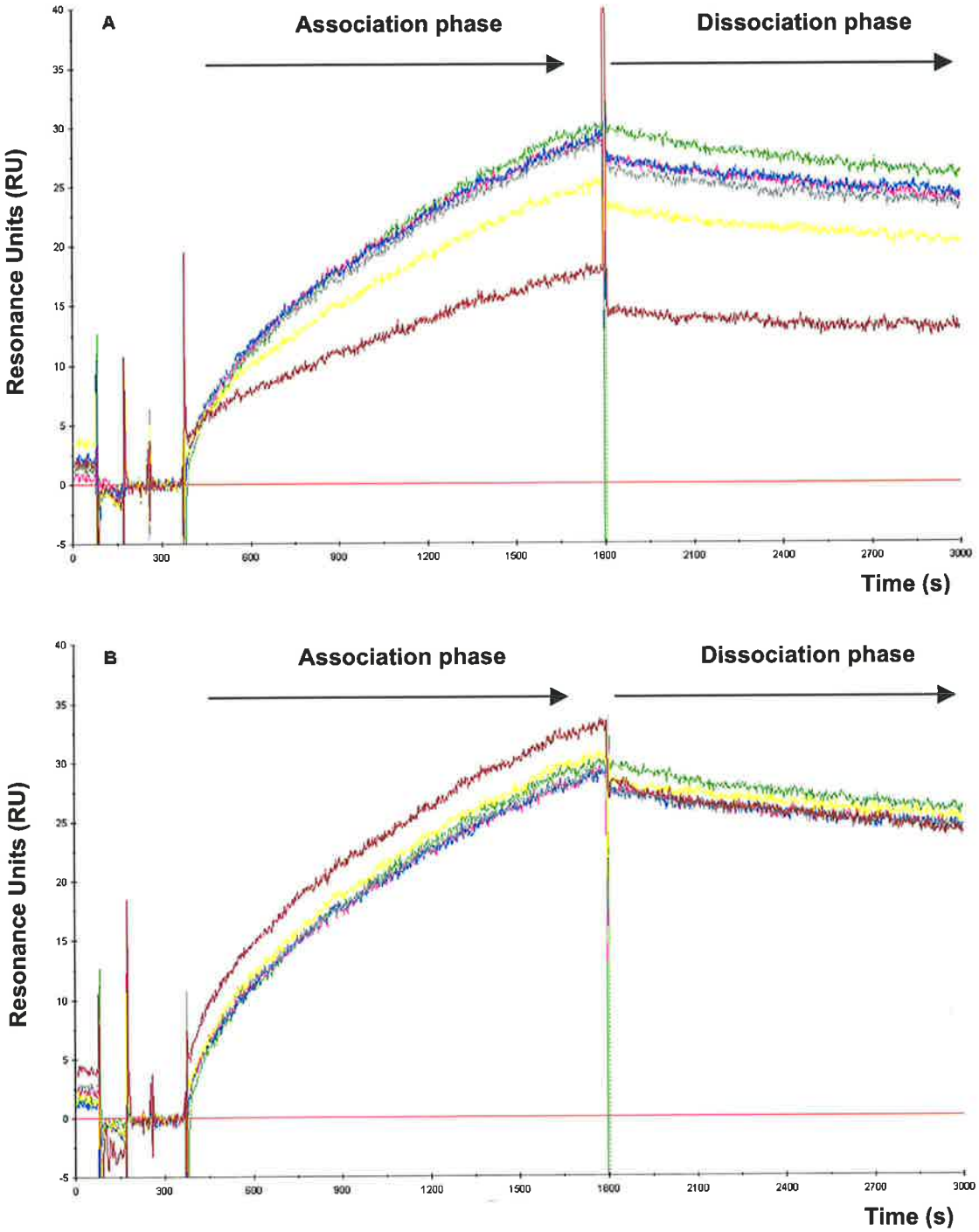

Figure 4.10 The association and dissociation phases for binding of s-IGF-1R pre-incubated with IGF-I (A) or IGF-II (B) to captured MAb (7C2).

0 nM s-IGF-1R, 12.5 nM s-IGF-1R + 0 nM ligand, 12.5 nM s-IGF-1R + 0.1 nM ligand, 12.5 nM s-IGF-1R + 1 nM ligand, 12.5 nM s-IGF-1R + 10 nM ligand, 12.5 nM s-IGF-1R + 100 nM ligand, 12.5 nM s-IGF-1R + 250 nM ligand. Representative experiments are shown.

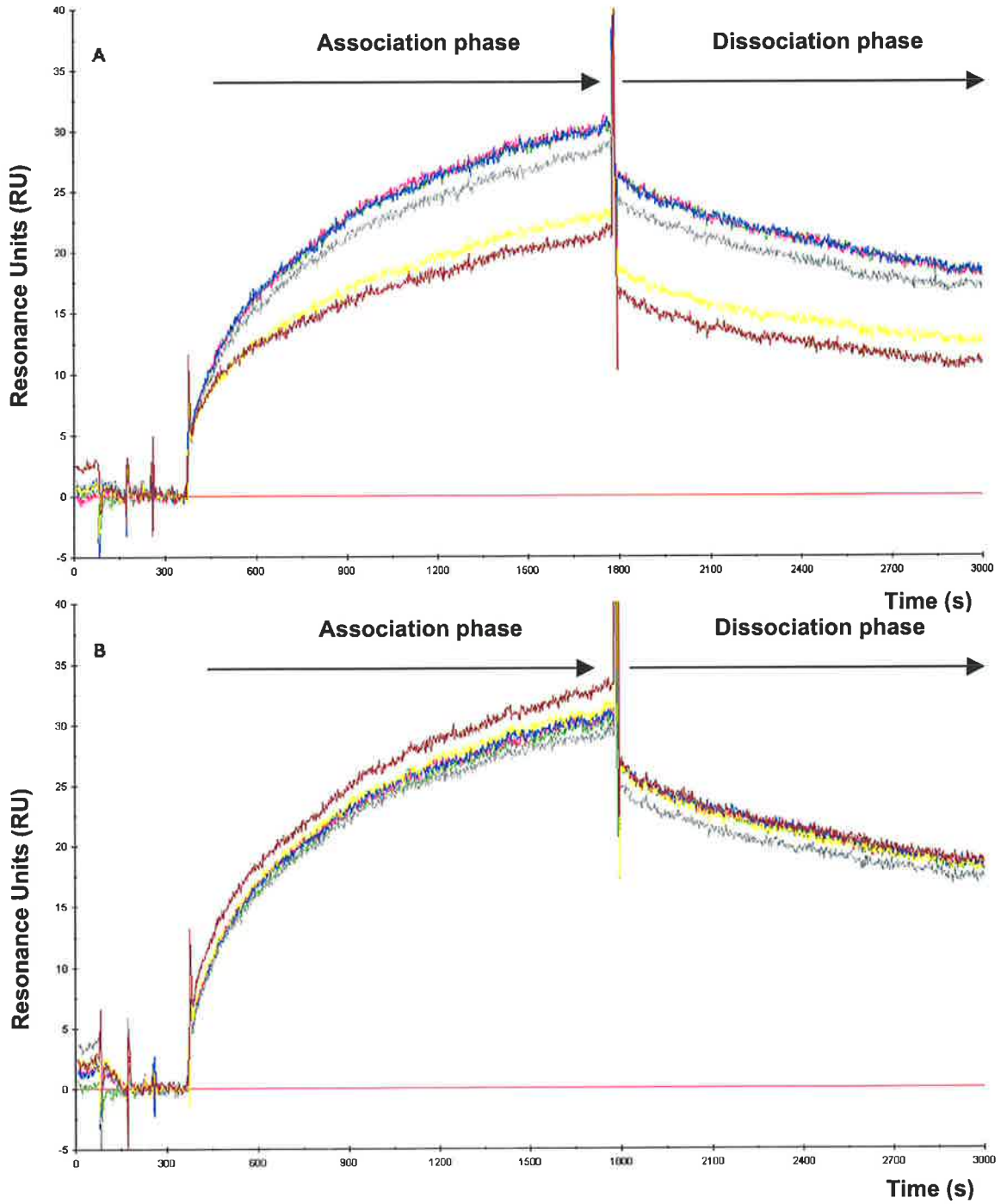

Figure 4.11 The association and dissociation phases for binding of s-IGF-1R pre-incubated with IGF-I (A) or IGF-II (B) to captured MAb (9E11).

0 nM s-IGF-1R, 12.5 nM s-IGF-1R + 0 nM ligand, 12.5 nM s-IGF-1R + 0.1 nM ligand, 12.5 nM s-IGF-1R + 1 nM ligand, 12.5 nM s-IGF-1R + 10 nM ligand, 12.5 nM s-IGF-1R + 100 nM ligand, 12.5 nM s-IGF-1R + 250 nM ligand. Representative experiments are shown.

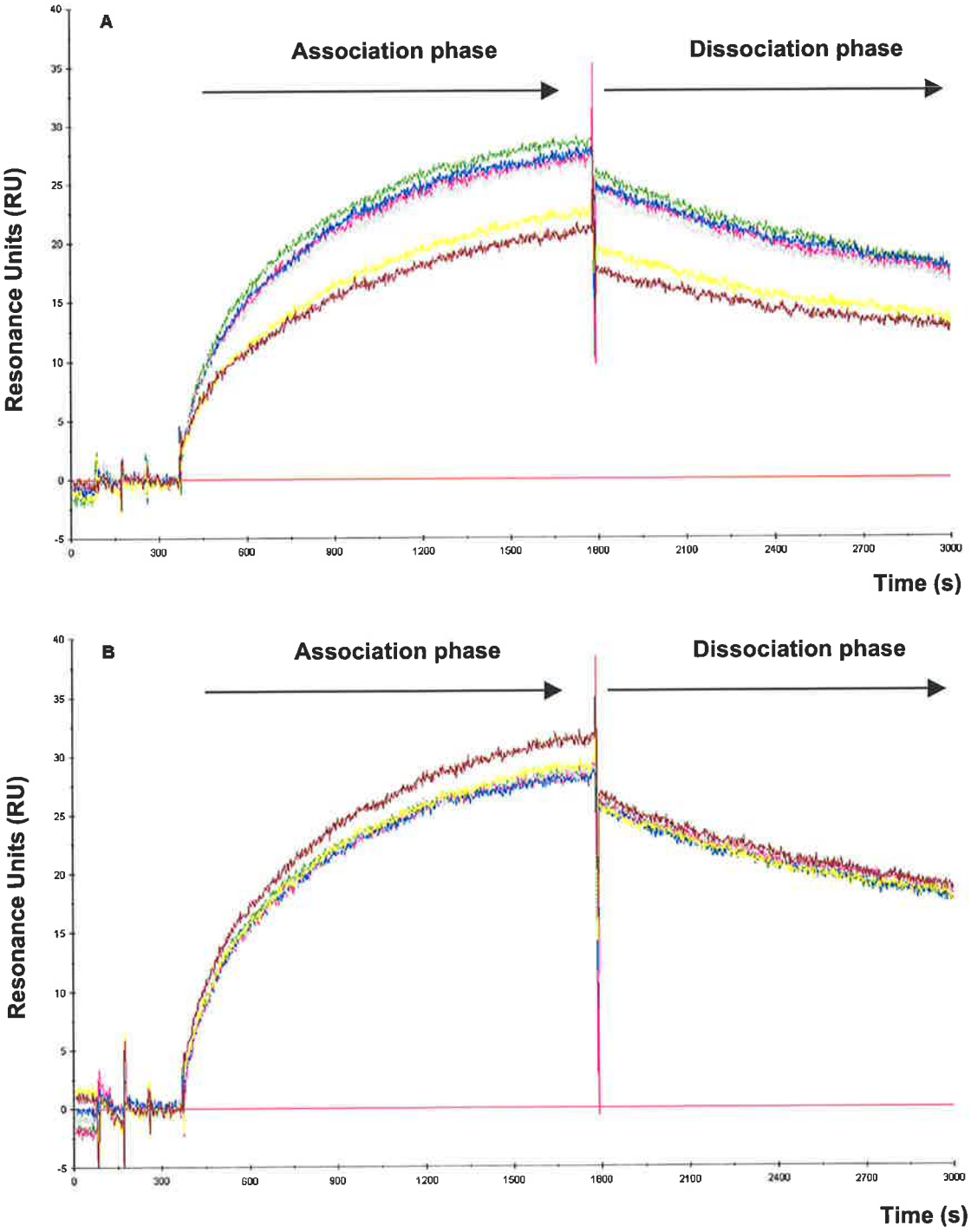

Figure 4.12 The association and dissociation phases for binding of s-IGF-1R pre-incubated with IGF-I (A) or IGF-II (B) to captured MAb (αIR-3).

— 0 nM s-IGF-1R, — 12.5 nM s-IGF-1R + 0 nM ligand, — 12.5 nM s-IGF-1R + 0.1 nM ligand, — 12.5 nM s-IGF-1R + 1 nM ligand, — 12.5 nM s-IGF-1R + 10 nM ligand, — 12.5nM s-IGF-1R + 100 nM ligand, — 12.5 nM s-IGF-1R + 250 nM ligand. Representative experiments are shown.

4.3.2.4. The Effects of IGF Chimeras (IGF-ICII and IGF-IICI) on Binding s-IGF-1R to the MAbs

The BIAcore results for passing the s-IGF-1R pre-incubated with chimeric IGFs over the captured MAbs on the chip showed that the IGF-IICI caused reduction in the Resonance Units (RU) for binding the s-IGF-1R to MAbs 7C2 and 9E11 (Figure 4.13 and Figure 4.14). Interestingly, IGF-ICII did not cause any reduction in the Resonance Units (RU) for binding of s-IGF-1R to either of these two MAbs. Hence, IGF-IICI inhibited the binding of the s-IGF-1R to the captured MAbs but IGF-ICII had no inhibiting effect. The values for RU measured immediately after injection of the solution containing s-IGF-1R and either IGF-IICI or IGF-ICII, at t=1810 (s), are shown in Table 4-4.

	7C2 (RU)		9E11 (RU)	
Concentration	**IGF-IICI**	**IGF-ICII**	**IGF-IICI**	**IGF-ICII**
0 nM	15.5	15.4	16.9	17.3
0.1 nM	15.3	15.1	15.8	17.1
1 nM	15.1	15.9	15.8	17
10 nM	14.0	14.7	14.6	17.1
100 nM	9.6	14.5	11.6	16.5

Table 4-4 The Resonance Units (RU) after injection of solutions containing s-IGF-1R and different concentrations of either IGF-IICI or IGF-ICII over the captured MAbs.

The Resonance Units were measured at t = 1810 (s).
Data obtained from Figure 4.13 and Figure 4.14.

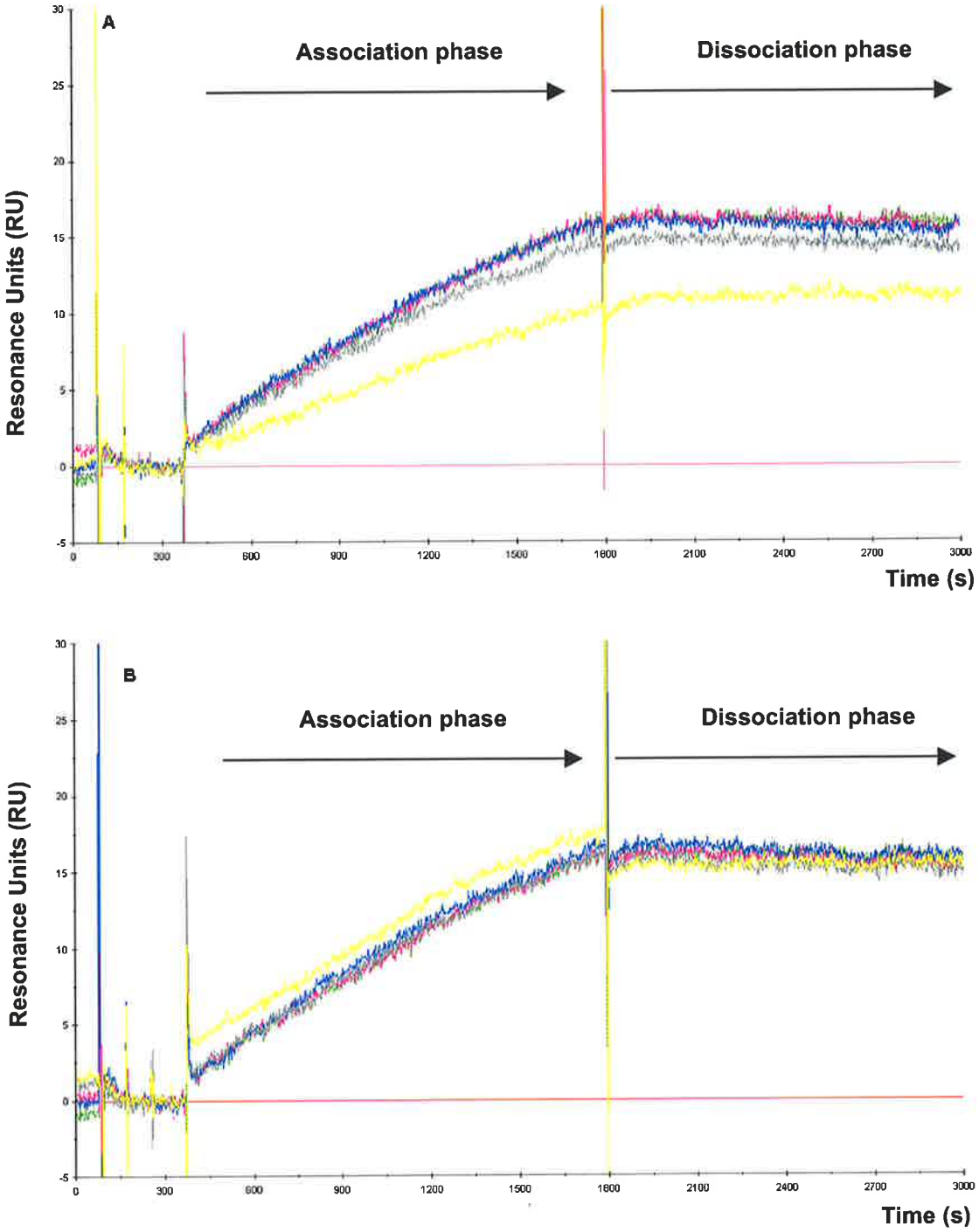

Figure 4.13 The association and dissociation phases for binding the captured MAb (7C2) to s-IGF-1R pre-incubated with IGF-IICI (A) or IGF-ICII (B).

— 0 nM s-IGF-1R, — 12.5 nM s-IGF-1R + 0 nM ligand, — 12.5 nM s-IGF-1R + 0.1 nM ligand, — 12.5 nM s-IGF-1R + 1 nM ligand, — 12.5 nM s-IGF-1R + 10 nM ligand, — 12.5 nM s-IGF-1R + 100 nM ligand. Representative experiments are shown.

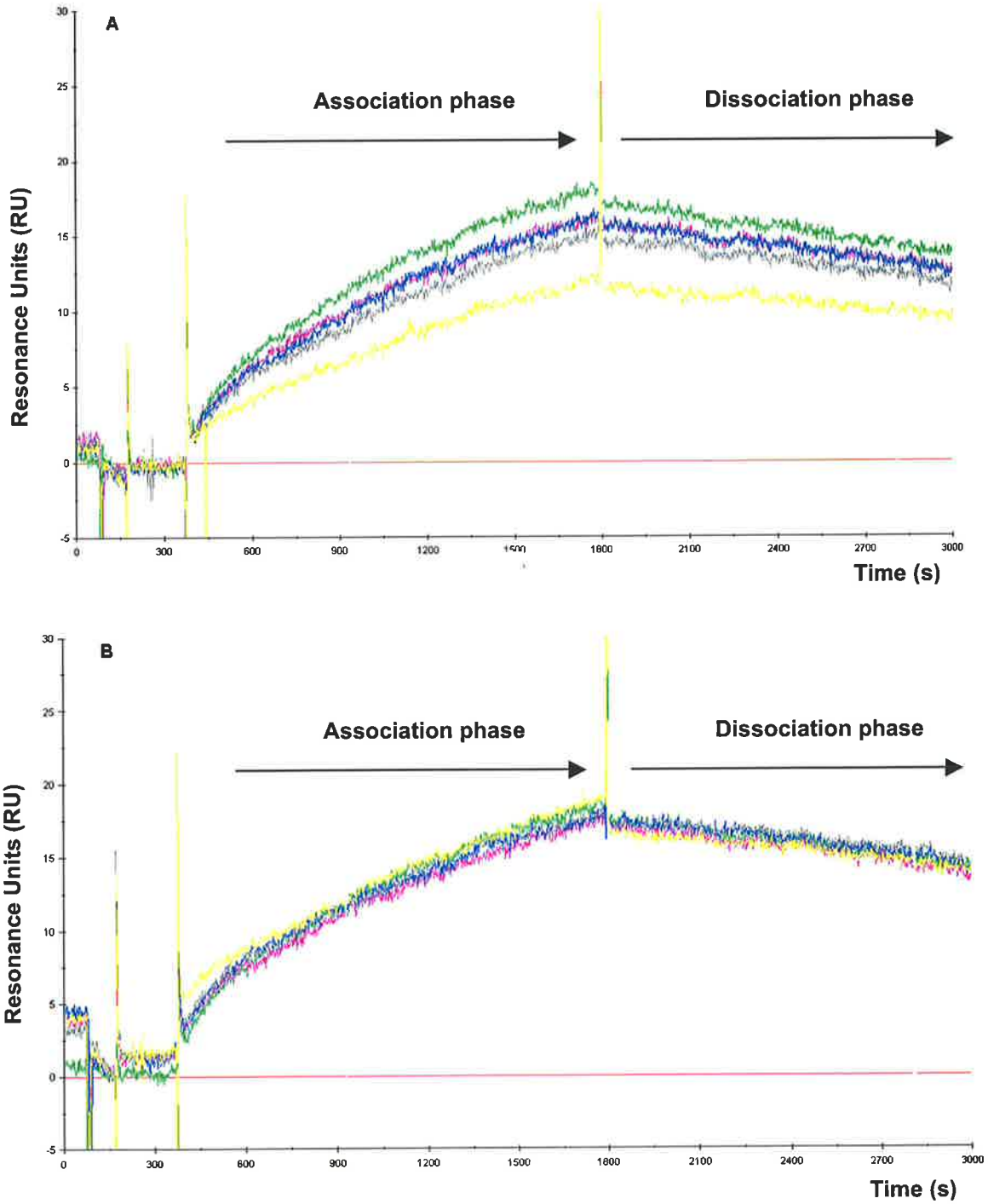

Figure 4.14 The association and dissociation phases for binding the captured MAb (9E11) to s-IGF-1R pre-incubated with IGF-IICI (A) or IGF-ICII (B).

— 0 nM s-IGF-1R, — 6.25 nM s-IGF-1R + 0 nM ligand, — 6.25 nM s-IGF-1R + 0.1 nM ligand, — 6.25 nM s-IGF-1R + 1 nM ligand, — 6.25 nM s-IGF-1R + 10 nM ligand, — 6.25 nM s-IGF-1R + 100 nM ligand. Representative experiments are shown.

4.3.3. Results for Flow Cytometry Analysis on Chimeric Receptors

In this experiment, the MAbs 24-60 and 24-55 raised against the IGF-1R were used as positive controls. The epitope of MAbs 24-60 and 24-55 are between amino acids 184-283 and 440-586 of the IGF-1R respectively (Soos *et al.*, 1992). The binding of the positive

control MAbs to the different chimeric receptors is predictable due to their epitope (see Table 1-5). As amino acids 184-283 of the IGF-1R are present in all three chimeric receptors, the binding of MAb 24-60 to all of them was expected and measured in these experiments. In addition, the binding of the MAb 24-55 to the IGF-1R/IR C1 was expected because of the presence of the IGF-1R amino acids 440-586 in this construct. These experiments showed that MAbs 7C2, 9E11 and 24-60 bound to all three chimeras of IGF-1R/IR but the MAb 24-55 only binds to the IGF-1R/IR C1 expressing cells (Figure 4.15). In the all tested cell lines, unrelated IgG1 (the negative control) did not come up positive. The results for binding the MAbs to the chimeric receptor expressing cells are summarized and compared to the results obtained for IGF-1R or IR (Section 3.4.2) in Figure 4.16. These results suggest that the epitope for the MAbs 24-60, 7C2 and 9E11 are in the cysteine-rich domain of the IGF-1R between residues 137-315.

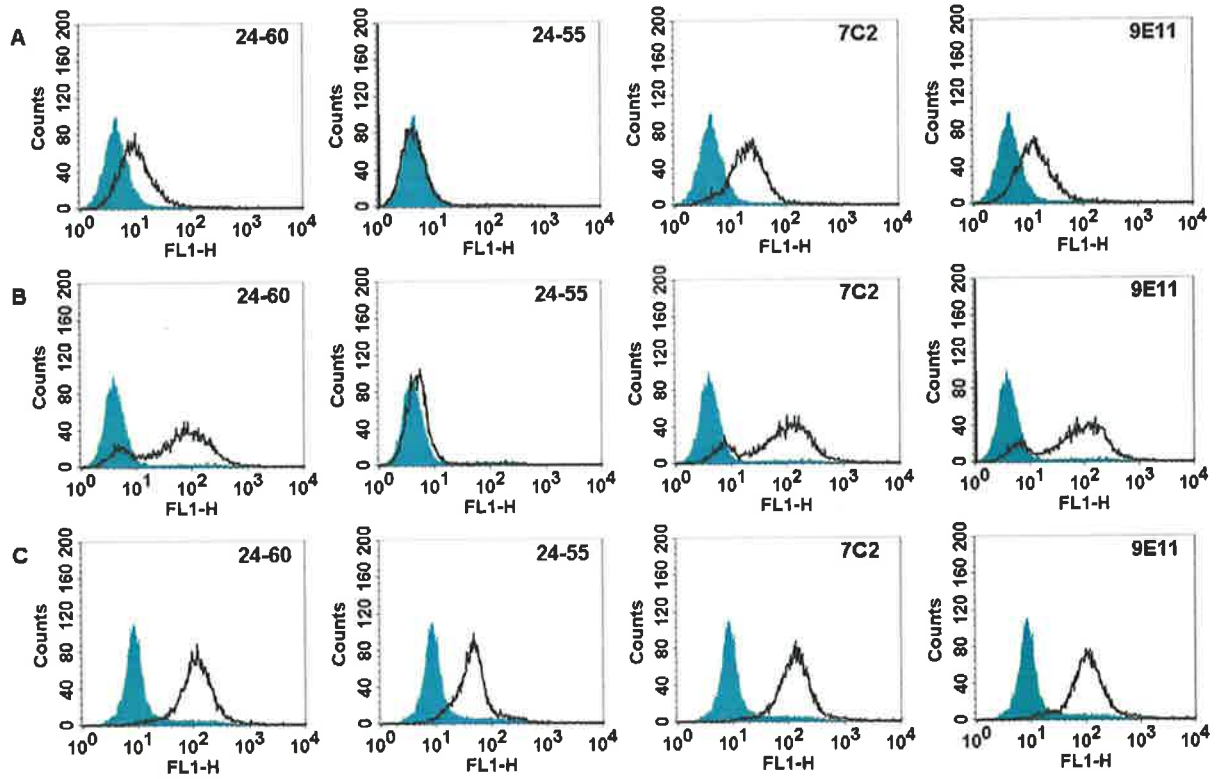

Figure 4.15 Flow cytometric analysis of MAbs 7C2 and 9E11 binding to chimeric IGF-1R/IR receptors.

Series A) Shows the results of the experiment on IR/IGF-1R C2 expressing cells, Series B) on IR/IGF-1R C12 expressing cells and Series C) on IGF-1R/IR C1 expressing cells as described in Figure 4.3. These cell lines were incubated with the different primary antibodies indicated. The green curves indicate the fluorescence of the cells stained with negative control (IgG1) and black curves indicate the fluorescence of the cells stained with positive controls or MAbs 7C2 and 9E11. Representative experiments are shown.

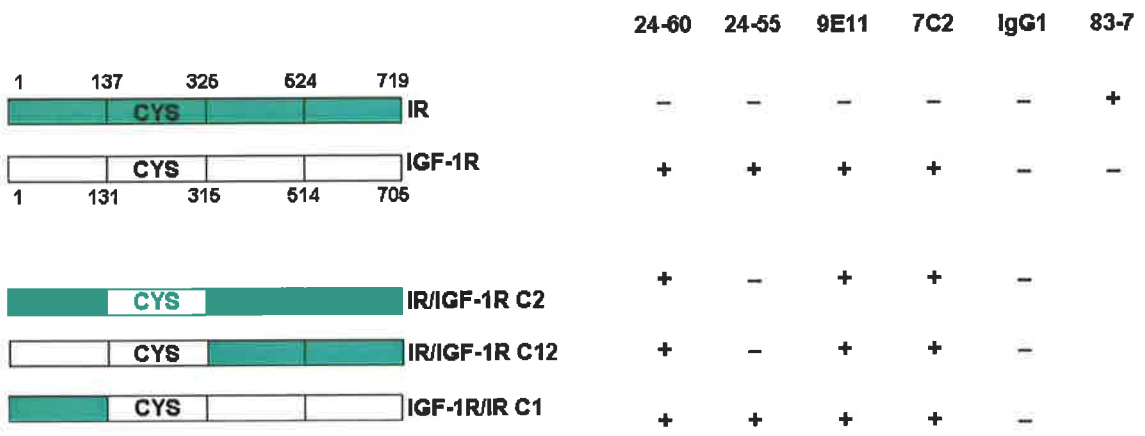

Figure 4.16 The summary of the flow cytometry results for interaction of MAbs with different chimeric receptors and their parental IR or IGF-1R.

In the figure, + represents binding and – represents no binding. The results for intact IGF-1R and IR are from Section 3.4.2.

4.3.4. Fragmentation of MAbs and Europium Labelling of the Fab

The MAbs were successfully fragmented using papain and the Fab domains purified using protein A-Sepharose chromatography. Purity of the fragments was assessed by SDS-page gel. The 50 kDa Fab fragment derived from papain digestion of MAb molecules is shown in Figure 4.17 on a Coomassie Blue stained gel. The results showed that the digestion and the purification were successful.

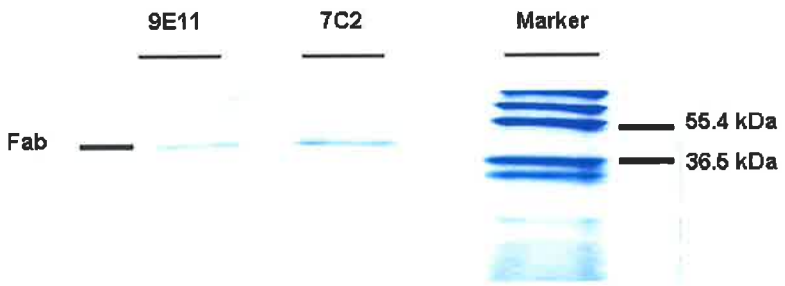

Figure 4.17 The purified Fab (50 kDa) fragment of the digested MAbs 9E11 and 7C2.

The purified Fab domains of the MAbs on SDS-Page gel and Coomassie stained. The marker was Marker12™ (Invitrogen).

Furthermore the Eu-7C2 (Fab) and Eu-9E11 (Fab) were successfully labelled and purified. The europium binding experiment showed that both these Eu-7C2 and Eu-9E11

were able to bind to the s-IGF-1R (Figure 4.18). The background fluorescence, for the wells containing no s-IGF-1R, was subtracted from all other fluorescence counts.

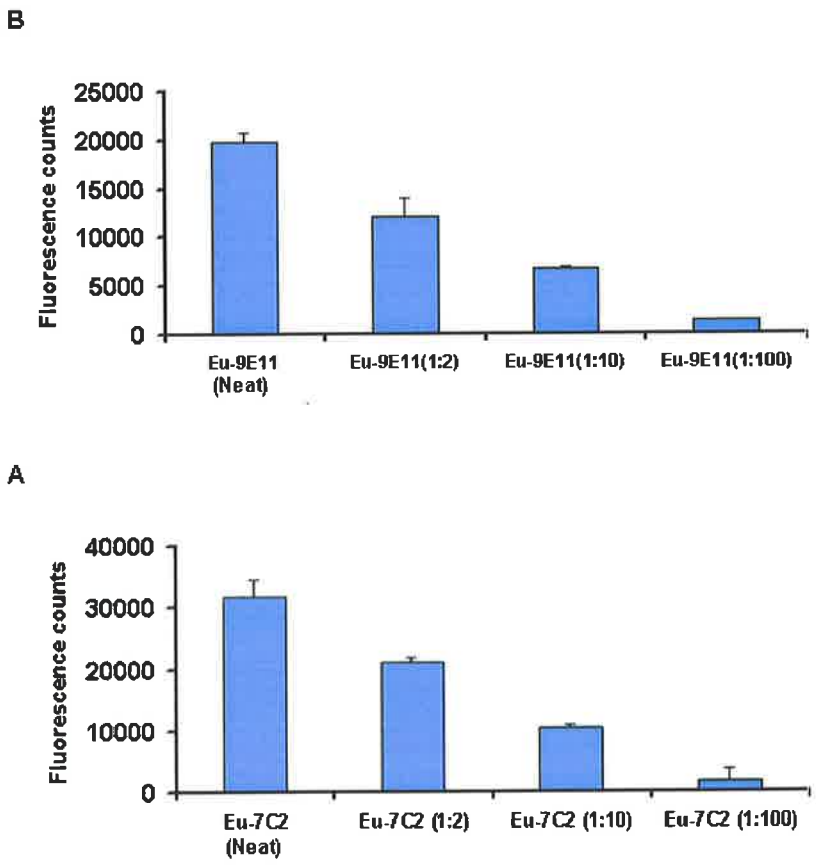

Figure 4.18 Binding of Eu-9E11 (Fab) (A) or Eu-7C2 (Fab) (B) to the s-IGF-1R.
Bars are means ± SD of triplicates.

4.3.5. Competition of Eu-7C2 and Eu-9E11 with other MAbs

Because the flow cytometry analysis on chimeric receptors showed that the epitope for MAbs 7C2 and 9E11 is between residues 137-315, the MAb 25-55, which binds between residues 440-586 of the receptor, was used to capture s-IGF-1R.

The results of the competition assay (Figure 4.19) revealed that Eu-7C2 (Fab) and Eu-9E11 (Fab) both significantly compete with 24-60, αIR-3 and each other for binding to the IGF-1R. However, neither 7C2 nor 9E11 compete with 24-55 as expected.

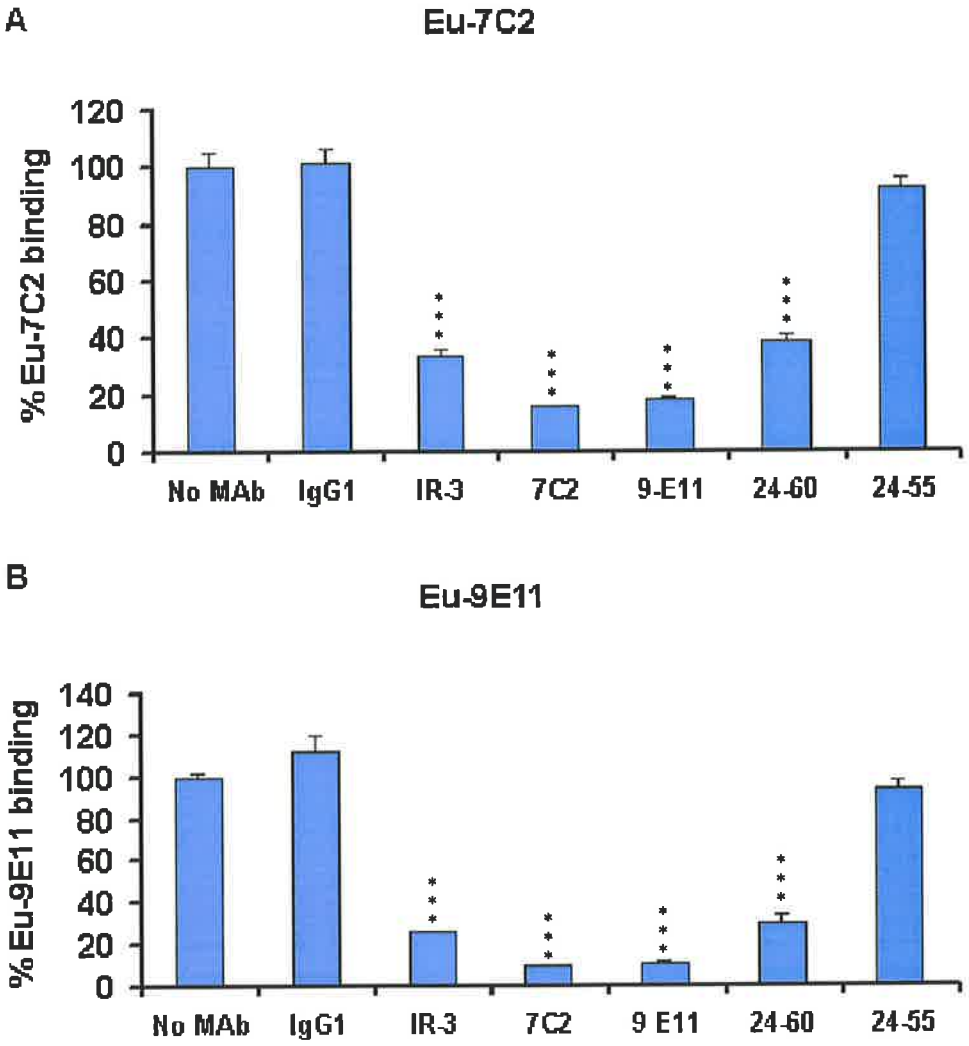

Figure 4.19 The competition of Eu-7C2 (A) and Eu-9E11 (B) with other MAbs for binding to the IGF-1R

The percentage of bound Eu-7C2 (Fab) or Eu-9E11 (Fab) was determined as a percentage of total binding (fluorescence) in the presence of no competitor. The P values were calculated by comparing the data for no treatment (No MAb) with other data using unpaired t-tests (Confidence Intervals 95%) by the Prism 3.03 software. The graphs are representative of three separate experiments.
P value 0.01 to 0.05 = *, P value 0.001 to 0.01 =**, P value < 0.001=***.

4.3.6. IGF-1R Alanine Mutant Expression

The plasmids containing the alanine mutants of the cysteine-rich domain of the receptor (Table 4-1) were transfected into 293 EBNA cells for transient receptor expression. These mutants were chosen because the flow cytometric analysis on chimeric IGF-1R/IR showed the epitope for MAbs 7C2 and 9E11 broadly localised on the cysteine-rich region of the receptor. The alanine mutants of the IGF-1R cysteine-rich domain were used for fine epitope mapping. The cDNAs of the IGF-1R mutants were successfully expressed transiently in 293 EBNA

cells for 21 out of 22 constructs. For all recombinant receptors except the IGF-1R I255A, the expression was successful and the ELISA detected secreted receptors in the supernatants. For the IGF-1R I255A, the transfection was repeated 3 times and each time with increased amount of plasmid DNA and the supernatant was 10-fold concentrated using Centricon YM-10. However, even in this 10-fold concentrated supernatant, no receptor was detected. The plasmid for this mutant of the receptor was sequenced, and it was shown that the plasmid contains an insert with correct mutation at position I255. The transfected cells with plasmids for IGF-1R I255A expression were lysed and the ELISA on cells lysate detected IGF-1R I255A production (Data not shown). Hence, it suggests that this receptor has probably folded incorrectly. This receptor mutant was not studied further. The ELISA test on the cell lysate was kindly performed by Ms. Carlie Delaine (The University of Adelaide, Australia).

4.3.7. ELISA on s-IGF-1R

An ELISA experiment was performed with different dilutions of s-IGF-1R to produce a standard curve. Plotting the absorbances against different concentrations of the s-IGF-1R resulted in a linear between 0.14 - 3.6 mg/ml s-IGF-1R (Figure 4.20). Using this standard curve, for each receptor mutant a dilution of the supernatants was made to contain the same concentration of the s-IGF-1R as in a 1:20 dilution of culture supernatants from cells secreting s-IGF-1R (0.28 mg/ml), and applied in the europium binding assay. In each experiment, ELISA was performed to compare the concentrations of expressed constructs with the concentration of s-IGF-1R in a 1:20 dilution of supernatant from cells expressing s-IGF-1R (Figure 4.21 A). This was performed at the same time as the binding assays.

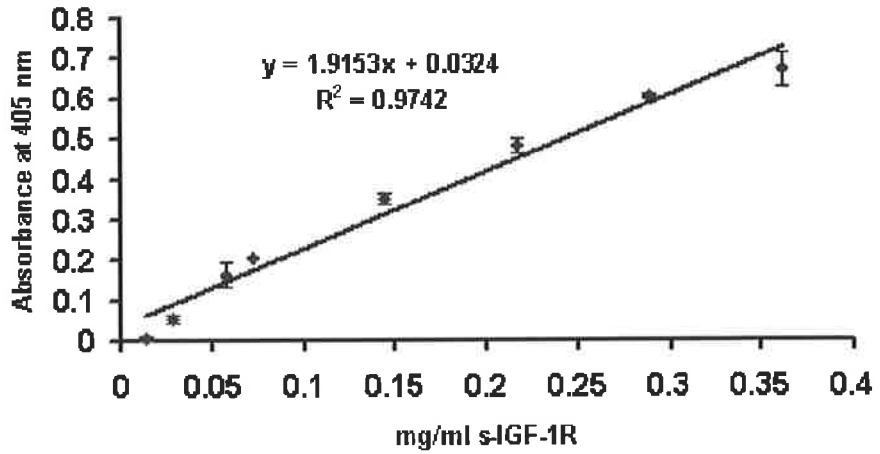

Figure 4.20 The standard curve obtained from ELISA on s-IGF-1R.

The graph shown is a representative of three experiments and data points are means of triplicates ± SD. Error bars are shown when greater than the size of symbols. The x-axis displays the concentration for the s-IGF-1R.

4.3.8. Identification of MAbs Binding Epitope

The secretion of IGF-1R constructs was detected by ELISA using MAb Bt-16-13 as a primary antibody as described in Section 4.2.5.2. Because all of the alanine substitutions are between amino acids 240-284 and the MAb 16-13 binds to the amino acids 62-184 of the IGF-1R, its binding to the receptor is not affected. This part of the receptor (amino acids 62-184) is also intact in the chimeric IGF-1R/256-266IR. The results for the ELISA showed that the recombinant receptors in their diluted supernatants have almost the same absorbances as the 1:20 dilution of culture supernatants from cell secreting s-IGF-1R (0.28 mg/ml) indicating the presence of a similar concentrations of expressed receptors (Figure 4.21 A). The mutations of 3 amino acids, phenylalanine 241, phenylalanine 251 and phenylalanine 266 to alanine have major effects on the binding of either Eu-7C2 (Fab) or Eu-9E11 (Fab) to the IGF-1R (Figure 4.21 B, C). Also, the chimeric secreted receptor IGF-1R/256-266IR, which is IGF-1R with replacement of the IR amino acids 262-277 into amino acids 256-266 of the IGF-1R, did not bind to either Eu-7C2 (Fab) or Eu-9E11 (Fab) (Figure 4.21 B, C) and this was consistent with the single alanine substitution at position 266.

4.3.9. Sequencing of the Plasmids Containing IGF-1R Mutants

The plasmids encoding the chimeric IGF-1R/256-266IR, IGF-1R F241A, IGF-1R F251A, IGF-1R F266A and IGF-1R I255A were sequenced and were found to contain the correct insert (data not shown) as mentioned in Table 4-1.

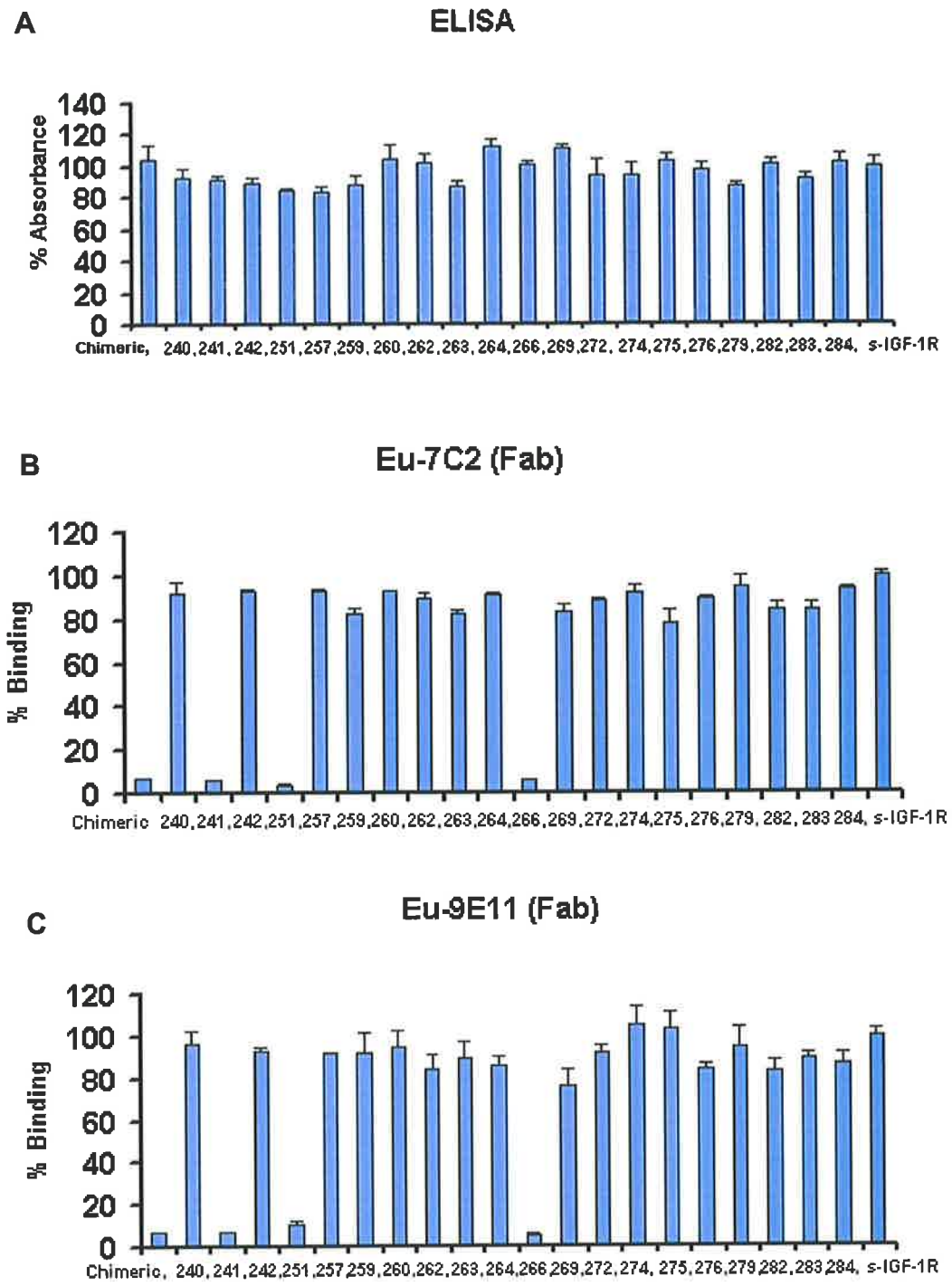

Figure 4.21 The effects of the alanine mutations or chimeric IGF-1R/256-266IR on binding the Fab domains of MAbs 7C2 and 9E11 to the IGF-1R

A) ELISA on the supernatants of the expressed receptor mutants. B) The binding of the Eu-7C2 (Fab) to each expressed receptor. C) The binding of the Eu-9E11 (Fab) to each expressed receptor. In (A) the absorbances are shown as a percentage of the absorbance for 1:20 dilution of culture supernatants from cell secreting s-IGF-1R (0.28 mg/ml). In (B) and (C), the fluorescence counts are shown as a percentage of the counts for binding Eu-7C2(Fab) and Eu-9E11(Fab) to 1:20 dilution of culture supernatants from cells secreting s-IGF-1R (containing 0.28 mg/ml s-IGF-1R). The numbers in the x-axis relate to the amino acid number in the IGF-1R mutated to alanine. Chimeric refers to the chimeric IGF-1R/256-266IR as described in Table 4-1. The graph shown is representative of three experiments and bars are means ± SD of triplicates.

4.4. Discussion

4.4.1. Binding Studies

The competition binding assays between Eu-IGF-I (Figure 4.5 A) or Eu-IGF-II (Figure 4.5 B) and the MAbs for binding to the IGF-1R showed that MAbs 7C2 and 9E11 significantly ($P < 0.05$) inhibited the binding of the Eu-IGF-I to the solubilized IGF-1R from the P6 cells. Although MAb 24-60 appeared to slightly inhibit Eu-IGF-I binding in this experiment, this effect was not significant. Another study on MAb 24-60 showed that it inhibited the binding of IGF-I to solubilized receptor by about 50% (Soos *et al.,* 1992). A possible explanation for the difference between these results and Soos *et al.*, (1992) could be due to our method of capturing solubilized IGF-1R. Since the epitopes of MAbs 24-31 and 24-60 are very close (see Table 1-5), capturing the IGF-1R by MAb 24-31 could affect binding of MAb 24-60 to the receptor.

Interestingly MAbs 24-60, 7C2 and 9E11 did not significantly inhibit the binding of the Eu-IGF-II to the solubilized IGF-1R from the P6 cells (Figure 4.5 B). The BIAcore study on MAbs 7C2, 9E11 and αIR-3 revealed similar results for the binding of the s-IGF-1R to these MAbs being inhibited by IGF-I but not by IGF-II (Figure 4.10, Figure 4.11 and Figure 4.12). Hence, the results of the europium competition assays and BIAcore studies suggest that the MAbs compete with IGF-I but not with IGF-II for binding to the s-IGF-1R. Comparable results for the MAb αIR-3 have been reported in other studies (Casella *et al.*, 1986; Graus *et al.*, 2005). For instance, it has been shown that this antibody inhibited the binding of ^{125}I-IGF-I to the purified IGF-1R by 62% while only 15% of ^{125}I-IGF-II (Casella *et al.*, 1986). Another study showed that αIR-3 did not inhibit the binding of the ^{125}I-IGF-II to HT-29 cancer cells, which express IGF-1R (Graus *et al.,* 2005).

These results imply that there are separate binding sites for IGF-I and IGF-II on IGF-1R. Furthermore, it seems that the binding sites of these MAbs (7C2, 9E11 and αIR-3) on IGF-1R could overlap with the IGF-I and not the IGF-II binding sites. Recently, the

existence of separate or more specific binding sites for IGF-I and IGF-II on the IGF-1R have been reported. Sorensen *et al.* (2004) showed that the IGF-1R cysteine-rich domain residues are critical for IGF-I binding but not for IGF-II binding. This group's study also revealed that the functional epitope for IGF-II contains residues in the N-terminal L1 domain and residues at the C-terminus of the α subunit (Sorensen *et al.,* 2004). This is consistent with the observation that the MAb αIR-3, which binds to the cysteine-rich domain of the receptor (Gustafson and Rutter, 1990), only inhibits IGF-I binding.

4.4.2. Epitope Mapping with Chimeric Receptors

The experiments on chimeric IGF-1R/IR (Figure 4.16) revealed that the epitope for the MAbs 24-60, 7C2 and 9E11 are in the cysteine-rich domain of the IGF-1R between residues 137-315. In addition, the competition experiments (Figure 4.19) showed that MAbs 7C2 and 9E11 significantly ($P < 0.05$) compete with both MAbs 24-60 and αIR-3. Hence, the epitope for 7C2 and 9E11 most likely overlap with the epitope for both αIR-3 and 24-60. The MAbs αIR-3 and 24-60 bind to the IGF-1R cysteine-rich domain between amino acids 223 to 274 (Gustafson and Rutter, 1990) and amino acids 184 to 283 (Soos *et al.,* 1992) respectively. The competition assay also revealed that MAbs 7C2 and 9E11 significantly ($P < 0.05$) compete with each other for binding to the IGF-1R (Figure 4.19), indicating that the epitopes for 7C2 and 9E11 are overlapping. This result supports the hypothesis that the epitopes for 7C2 and 9E11 are in cysteine-rich region of the receptor.

Other studies on IR/IGF-1R chimeras of both full-length receptor and ectodomain showed the cysteine-rich region of the IGF-1R plays an important role in controlling the specific binding of IGF-I but not insulin (Gustafson and Rutter, 1990; Hoyne *et al.*, 2000b). So, the specific binding of MAbs 7C2 and 9E11 to the IGF-1R and not to the IR (Figure 4.16) is also consistent with the fact that IGF-I but not insulin binds to the IGF-1R cysteine-rich domain.

Although the theory of direct binding of MAbs 7C2 and 9E11 to the cysteine-rich domain of the receptor seems very consistent with other studies, there are alternative explanations for the competition of the MAbs with IGF-I, MAb 24-60 and αIR-3. For example, binding MAbs 7C2 and 9E11 to the receptor could cause a change in the conformation of the receptor, thereby rendering the cysteine-rich domain inaccessible for IGF-I or other MAbs binding. Another possibility is that the MAbs are big molecules and may hinder the binding of IGF-I or the other MAbs to the receptor rather than bind exactly to the same epitope.

4.4.3. Epitope Mapping with Alanine-Scan Receptor Mutants

In the present study, further epitope mapping using the expressed alanine mutants in the cysteine-rich region of the IGF-1R revealed that the amino acids F241, F251 and F266 were critical for the binding of Eu-7C2 (Fab) and Eu-9E11 (Fab) to the IGF-1R due to the disruptive effect of these mutants on binding to the MAbs (Figure 4.21). The three amino acids are located in the cysteine-rich domain of IGF-1R and they are distinct from each other in the sequence. Mapping of these amino acids on the model of the IGF-1R domains from the crystal structure of the IGF-1R L1-cysteine-rich-L2 domains (Garrett *et al.,* 1998) revealed that these three amino acids are actually very close together in the folded form of the receptor. This confirms that, the epitopes for MAbs 7C2 and 9E11 are conformational (Figure 4.22).

The observation that the disruptive mutants in the cysteine-rich domain of the receptor form a patch on the protein surface surrounded by non-disruptive mutations suggests that they are contact sites for MAbs 7C2 and 9E11 (Figure 4.22).

Both MAbs 7C2 and 9E11 directly bind to residues F241, F251 and F266 of the IGF-1R. Hence, these two generated MAbs bind to the same epitope on the IGF-1R or at least share these three amino acids in their binding site. In addition, although it is possible that these three mutants of the IGF-1R could cause indirect intramolecular perturbation of the structure of the binding site for MAbs, this seems unlikely. Particularly for F266, because its

mutation to alanine had no effect on IGF-I (Whittaker *et al.*, 2001) or IGF-II binding (Sorensen *et al.*, 2004), the direct binding of the MAbs to F266 is very likely. Interestingly, the mutation of any one of these amino acids (F241, F251 and F266) was sufficient to disrupt the binding of the Eu-7C2 (Fab) or Eu-9E11 (Fab) to the s-IGF-1R (Figure 4.21). Hence, it could be concluded that these residues F241, F251 and F266 actually contribute to the binding energy for binding to MAbs 7C2 and 9E11.

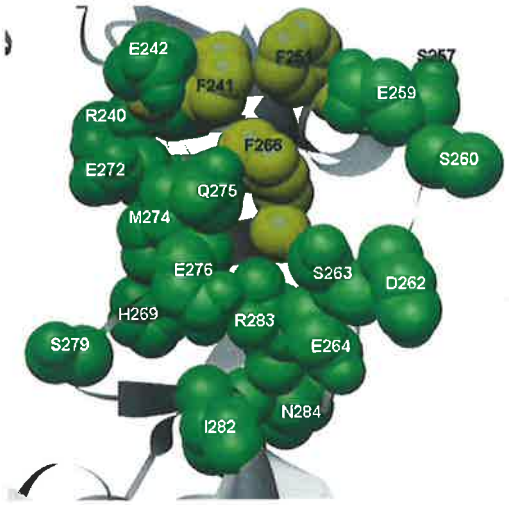

Figure 4.22 The structure of the functional epitopes of MAbs 7C2 and 9E11 on the cysteine-rich domain of the IGF-1R.

The Cα backbone of the IGF-1R cysteine-rich domain is shown as a ribbon and the amino acids mutated are shown in space-filling representation. Alanine mutants of amino acids showed in yellow had disruptive effect on the Eu-7C2 (Fab) and Eu-9E11 (Fab) binding. Alanine mutants of those amino acids shown in green had no effect on binding the MAbs. The figure was created using the UCSF Chimera molecular graphics program (Pettersen *et al.*, 2004).

4.4.4. Epitope Mapping with a Cysteine-Rich Domain Chimera

In addition, MAbs 7C2 and 9E11 did not bind to the chimeric receptor IGF-1R/256-266IR, which contains the amino acids 256-266 of the IGF-1R substituted with the corresponding amino acids of IR-A, residues 262-277. This effect could be due to the mutation of amino acid 266 of the IGF-1R, which was shown to be critical for binding MAbs 7C2 and 9E11. Since the amino acids L256, A258, S261 and G265 of the IGF-1R have not been tested individually for binding to the MAbs, their role in binding these two MAbs is not clear. It has been shown that mutation of L256 and S261 to alanine had no significant effect on IGF-I or IGF-II binding to the IGF-1R (Whittaker *et al.*, 2001; Sorensen *et al.*, 2004). Particularly, since the

position of the amino acid L256 is very close to the other amino acids involved in MAbs binding (Figure 4.23), its possible participation in the epitope of MAbs 7C2 and 9E11 cannot be ignored.

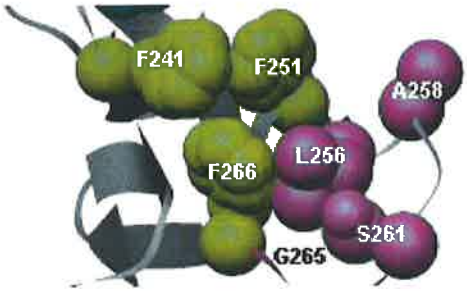

Figure 4.23 The amino acids in the chimeric IGF-1R/256-266IR that could be involved in MAbs 7C2 and 9E11 binding.

The Cα backbone of the IGF-1R cysteine-rich domain is shown as a ribbon representation. The amino acids mutated are shown in space-filling representation except G265. The epitope of MAbs 7C2 and 9E11 is shown in yellow. The amino acids mutated indirectly in chimeric IGF-1R/256-266IR are shown in pink. The figure was created using the UCSF Chimera molecular graphics program (Pettersen *et al.*, 2004) .

Furthermore, in the chimeric receptor IGF-1R/256-266IR, module 6 of the cysteine-rich region for the IGF-1R (residues 253-266) (Garrett *et al.*, 1998) is mostly substituted with IR (residues 262-277). In IGF-1R the modules 5 and 6 of the cysteine-rich domain are located on one side of the central cavity and possibly shape part of the ligand binding site (Hoyne *et al.*, 2000b). In module 6 of the IGF-1R there is a mobile loop (amino acids 255-265), which extends into the central cavity of the L1/cysteine-rich/L2 fragment and is the most different module in the cysteine-rich domain in terms of sequence identity compared to IR. The corresponding region in the IR is longer as it contains four additional residues and it also has a disulphide bond that does not exist in the IGF-1R (Ward *et al.*, 1995). In another study, the residues 260-277 of human IR were replaced with residues 253-266 (module 6 of the cysteine-rich region) of the human IGF-1R to produce an IR based, cysteine loop exchange chimera (Hoyne *et al.*, 2000b). This chimeric receptor was not different from IR in terms of insulin binding affinity but permitted displacement of ^{125}I-insulin by IGF-I more readily than did the IR (Hoyne *et al.*, 2000b). It was concluded that, this loop (residues 253-266) could make direct contact with IGF-I in the ligand/receptor

complex in the IGF-1R. Conversely, the weaker binding of IGF-I by IR could be explained by steric constraints imposed by the loop (Hoyne *et al.*, 2000b). In a similar way, the replacement of the IGF-1R mobile loop (amino acids 255-265) in chimeric IGF-1R/256-266IR could cause structural restriction for binding MAbs 7C2 and 9E11 to the IGF-1R. Moreover, the lack of binding by MAbs 7C2 and 9E11 to this chimeric receptor could also be due to the different length of the inserted region of the IR compared to the original part of the IGF-1R. As mentioned before, in this chimeric IGF-1R/256-266IR, 11 amino acids (256-266) of the IGF-1R were replaced by the 16 corresponding amino acids (262-277) of IR-A. So the chimeric receptor has 5 more amino acids in this region and this extra length could change the structure of the receptor toward making the epitope unavailable for MAbs 7C2 and 9E11.

The expression of the IGF-1R construct with the alanine mutation in the I255 position (IGF-1RI255A) was not successful despite the sequencing results showing the plasmid contained the correct insert. This amino acid could also be involved in binding to the MAbs because modelling of the IGF-1R revealed that the three amino acids in the epitope of the MAbs surrounded I255 (Figure 4.24). However, its effect on binding could not be tested.

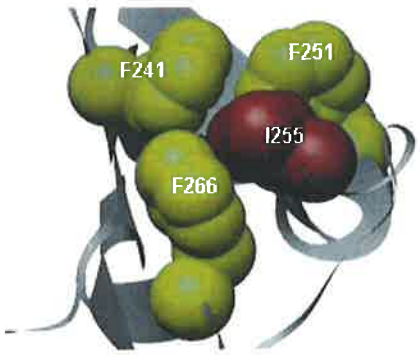

Figure 4.24 The structure of the epitope for MAbs 7C2 and 9E11 highlighting the amino acid I255.

The central carbon atom (Cα) backbone of the IGF-1R cysteine-rich domain is shown as a ribbon and the mutated amino acids are shown in space-filling representation. The binding sites of MAbs 7C2 and 9E11 are shown in yellow and the I255 is shown in red. The figure was created using the UCSF Chimera molecular graphics program (Pettersen *et al.*, 2004).

4.4.5. MAb Epitopes and IGF Binding to IGF-1R

By comparing the binding sites of the ligands and of MAbs 7C2 and 9E11 on IGF-1R, the selective inhibitory effects of MAbs 7C2 and 9E11 on IGF-I but not on IGF-II binding can be explained. In attempts to determine the residues of the IGF-1R involved in binding to ligands (IGF-I and IGF-II), several investigations have been carried out. Studies on chimeric IR/IGF-1R implied that the C-terminus of the cysteine-rich domain (amino acids 190-300) is a major determinant of IGF-I binding specificity (Kjeldsen *et al.*, 1991; Schumacher *et al.*, 1991; Zhang and Roth, 1991; Schumacher *et al.*, 1993) The location for the C-terminus of the cysteine-rich domain in the N-terminal fragment of the IGF-1R is consistent with it forming part of a ligand binding pocket (Garrett *et al.*, 1998; Whittaker *et al.*, 2001). Moreover, studies utilising alanine mutagenesis of residues in the L1 N-terminal domain of the receptor showed that this also forms part of the ligand binding site (Mynarcik *et al.*, 1997). Alanine mutants of residues in different regions were transiently expressed as secreted recombinant receptors and their affinity was determined (Whittaker *et al.*, 2001). This study revealed that in the L1 domain of the IGF-1R, alanine substitution of D8, N11, Y28, H30, L33, L56, F58, R59, W79 resulted in a 2- to 10-fold decrease, while the mutation of F90 to alanine caused a 23-fold reduction in affinity for binding to IGF-I (Whittaker *et al.*, 2001). In addition, alanine mutants in the cysteine-rich domain of the receptor revealed that mutation of R240, F241, E242 and F251 resulted in more than a 2-fold reduction in affinity for IGF-I (Figure 4.25) (Whittaker *et al.*, 2001). Among these amino acids, the mutation of F241 to alanine caused the largest decrease in affinity of 6-fold for binding IGF-I to the receptor (Sorensen *et al.*, 2004). In another study, the effect of these alanine mutants on the receptor affinity for IGF-II was compared with IGF-I (Sorensen *et al.*, 2004). For IGF-I and IGF-II, both functional epitopes in the L1 domain of the receptor were qualitatively very similar. However, the mutation of W79 to alanine compromised affinity for IGF-I but did not affect IGF-II binding. Mutation to alanine of L32, which is involved in IGF-II binding had no influence on binding IGF-I to the receptor (Figure 4.26) (Sorensen *et al.*, 2004). The most significant difference

between the IGF-I and IGF-II binding sites on the IGF-1R was that the cysteine-rich domain residues R240, F241, E242 and F251 were not involved in IGF-II binding (Figure 4.25 and Figure 4.26) (Sorensen *et al.*, 2004).

Comparison of the binding sites for the IGF-I, IGF-II and MAbs 7C2 and 9E11 on the IGF-1R showed there are overlapping residues between the MAbs and IGF-I binding sites in the cysteine-rich domain of the receptor but none of the binding sites for MAbs 7C2 and 9E11 in the cysteine-region of the receptor are involved in IGF-II binding (Figure 4.25 and Figure 4.26). Hence, it can be concluded that the interaction of MAbs 7C2 and 9E11 with the amino acids F241 and F251, which are only involved in IGF-I binding, accounts for the selective inhibitory effect of these MAbs on only IGF-I binding and not on IGF-II binding to the IGF-1R (Figure 4.25 and Figure 4.26).

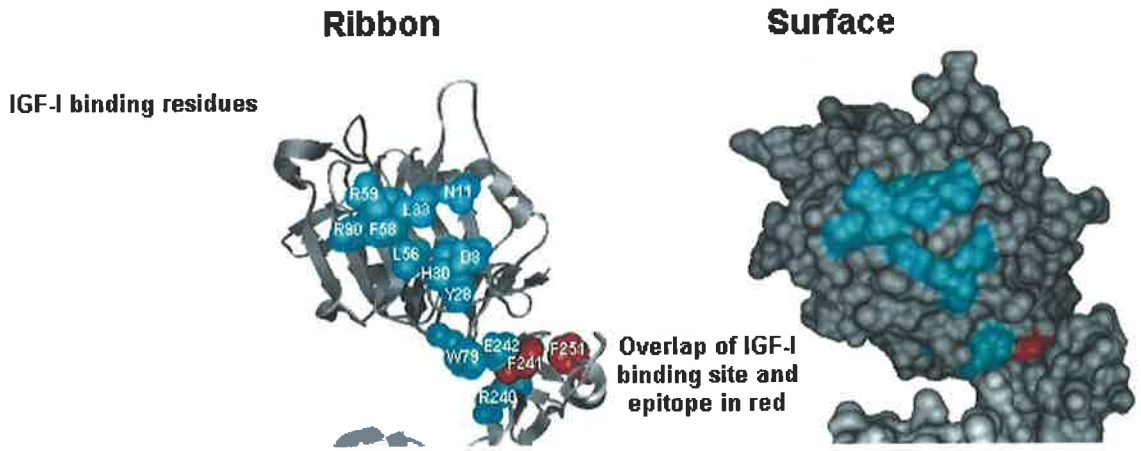

Figure 4.25 Structure of the functional binding sites for IGF-I on the L1 and cysteine- rich domains of the IGF-1R.

The Cα backbone of the L1 and cysteine-rich domains is shown as a ribbon (left) and surface representation (right). Alanine mutants of amino acids are shown in space-filling (left) or surface (right) representations. The mutants in blue or red produced a 2-fold or greater reduction in affinity for binding IGF-I to the IGF-1R. The amino acids shown in red are the binding site for both IGF-I and for MAbs 7C2 and 9E11. The figure was created using the UCSF Chimera molecular graphics program (Pettersen *et al.*, 2004).

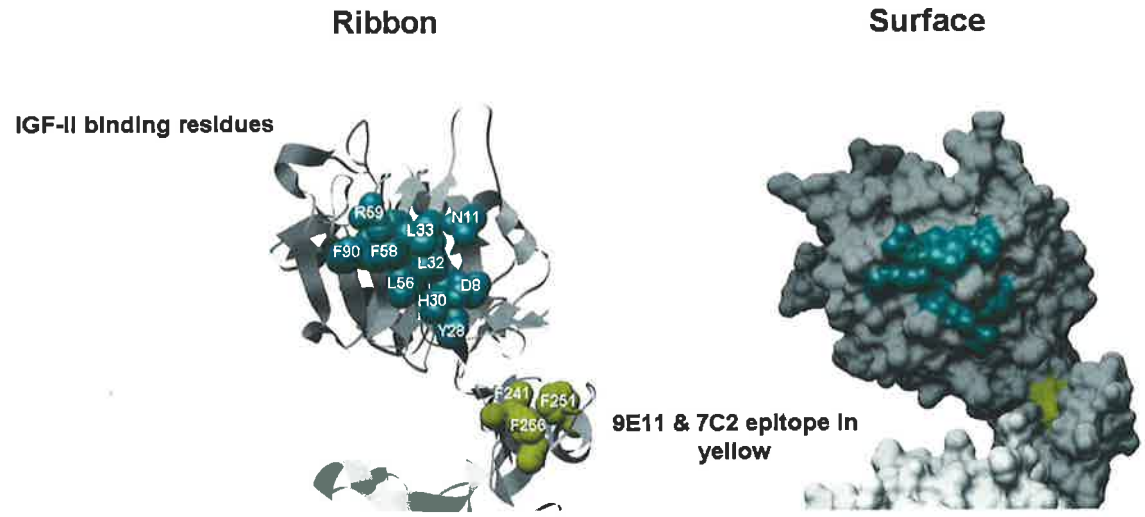

Figure 4.26 Structure of the functional binding sites for IGF-II on the L1 and cysteine-rich domains of the IGF-1R.

The Cα backbone of the L1 and cysteine-rich domains is shown as a ribbon (left) and surface representation (right). The amino acids are shown in space-filling (left) or surface representations (right). The mutation of amino acids shown in blue, produced a 2-fold or greater reduction in affinity for binding IGF-II to the IGF-1R. The amino acids shown in yellow are the binding site for MAbs 7C2 and 9E11. The figure was created using the UCSF Chimera molecular graphics program (Pettersen *et al.*, 2004).

Comparison of amino acid sequences of IGF-1R and IR showed that the lowest conservation between these two receptors could be seen in the cysteine-rich domain (Abbott *et al.*, 1992; Baserga *et al.*, 1997). Although the amino acids F241 and F251 which are involved in epitope of MAbs 7C2 and 9E11 are conserved in both receptors (Figure 4.27), MAbs 7C2 and 9E11 are both specific for the IGF-1R and do not interact with the IR. So, this suggests that the orientation of these amino acids in the structure of IGF-1R is important for the specific binding of MAbs 7C2 and 9E11 to these amino acids in IGF-1R only and not in IR. In addition, the amino acid F266 in the IGF-1R is also crucial for binding to MAbs 7C2 and 9E11 and this amino acid is not conserved in the IR (Figure 4.27). Hence, the specific binding of the MAbs to the IGF-1R could be due to F266. However, the mutation of F266 to alanine did not affect the IGF-I or IGF-II binding to the receptor (Whittaker *et al.*, 2001; Sorensen *et al.*, 2004). Therefore, it can be concluded that the steric structure of the IGF-1R is important for specific binding to the IGF-I. Another possibility is binding the MAbs to the proximity residues involved in IGF-I binding, resulted in destruction of the IGF-I binding to the receptor.

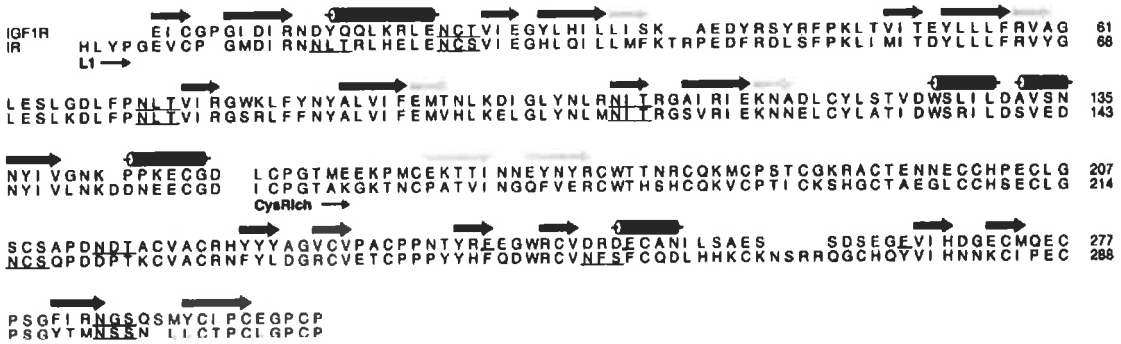

Figure 4.27 Amino acid sequences of L1/cysteine-rich domains of IGF-1R and IR.

The secondary structural assignments are drawn above the sequences as cylinders for α helices and arrows for β strands. The demarcation borders for the various domains and modules are shown under the sequences. Residues F241, F251 and 266 of the IGF-1R are underlined (red). Figure is adapted from (Adams *et al.*, 2000).

4.4.6. Structural and Functional Epitope on the IGF-1R

Although we have not tested all amino acids in the IGF-1R, the epitope mapping results showed there are at least three critical amino acids in IGF-1R for binding to MAbs 7C2 and 9E11. Epitope mapping using X-ray crystallography leads to the view that an epitope is comprised of approximately 15 antigen residues that are in contact with the paratope on the antibody, however, the residues in the interface that actually contribute to the binding energy could be 1-5 amino acids and are identifiable in binding measurements (Amit *et al.*, 1986; Sheriff *et al.*, 1987; Colman, 1988). Hence, some of the tested amino acids of IGF-1R (using the alanine mutants) could be in contact with MAbs 7C2 and 9E11 but because they did not have critical effect on binding to the MAbs, their binding has not been detectable in the binding experiments.

There could be additional residues that also contribute to the MAbs binding sites. For instance, although the role of amino acids L256 and I255 of the IGF-1R in binding to MAbs 7C2 and 9E11 was not tested, these residues could be involved in binding to the MAbs. These two amino acids (L256 and I255) are hydrophobic and also very close to the epitope of MAbs 7C2 and 9E11 in the IGF-1R structure (Figure 4.23 and Figure 4.24). Moreover, the amino acid W79 in the IGF-1R L1, which compromises affinity for IGF-I, is not involved in IGF-II binding and it forms a patch with R240, F241, E242 and F251 from the cysteine-rich domain

together for binding to IGF-I (Whittaker *et al.,* 2001). In our study, the involvement of amino acid W79 in the epitope of MAbs 7C2 and 9E11 was not available to be tested, but it could be a part of the epitope particularly because the position of W79 in the receptor is very close to the amino acids F241, F251 and F266 as shown in Figure 4.28. This amino acid (W79) could form a patch with the amino acids F241, F251 and F266 for binding to MAbs 7C2 and 9E11. On the other hand, our experiments revealed that MAbs 7C2 and 9E11 bound to the chimeric receptor IR/IGF-1R C2, the insulin receptor containing amino acids 131-315 of IGF-1R. So, although the amino acid W79 could be involved in binding to MAbs 7C2 and 9E11, it does not seem to be critical for binding to these MAbs.

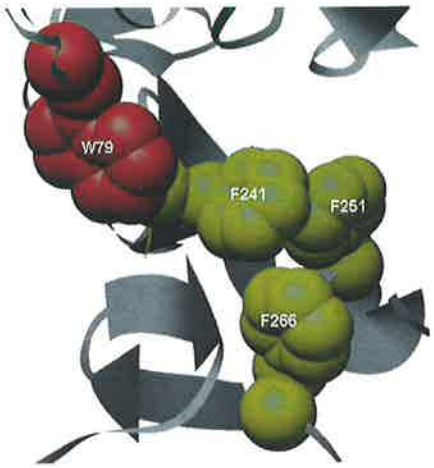

Figure 4.28 The structure of the epitope for MAbs 7C2 and 9E11, highlighting the amino acid W79.

The Cα backbone of the IGF-1R cysteine-rich domain and a part of L1 domain is shown as a ribbon and the amino acids are shown in space-filling representation. The binding sites of MAbs 7C2 and 9E11 are shown in yellow and the W79 is shown in red. The figure was created using the UCSF Chimera molecular graphics program (Pettersen *et al.,* 2004).

All three critical amino acids (F241, F251 and F266) in the epitope of MAbs 7C2 and 9E11 are phenylalanine, which is a hydrophobic amino acid (Branden and Tooze, 1991), suggesting that the interaction of MAbs 7C2 and 9E11 with the IGF-1R is through hydrophobic contacts. In addition, the MAbs bind the epitope through their CDR as described in Section 1.8. Hence, their interaction could be hydrophobic and the hydrophobic amino acids in the CDR part of MAbs 7C2 and 9E11 (Figure 3.18) could be involved in binding the MAbs to the receptor. Although CDRs for MAbs 7C2 and 9E11 have been sequenced, the

amino acids involved in their binding to IGF-1R is not known. Modeling of the MAbs could help to predict their binding sites but it was beyond the scope of this study.

4.4.7. Interaction of IGF-1R with IGF-I and IGF-II

Interestingly, the BIAcore experiments showed that the chimeric IGF-IICI had inhibitory effects on binding of the s-IGF-1R to the captured 7C2 and 9E11 but IGF-ICII had no significant effect. By comparing this result with the same experiment on IGF ligands, it can be deduced that IGF-IICI and IGF-ICII represented similar effects to IGF-I and IGF-II respectively. Hence, the C domain of the IGF-I might play a role in interfering with MAbs 7C2 and 9E11 binding to IGF-1R. It suggests that, the IGF-I C domain binds to the epitope for MAbs 7C2 and 9E11 or the nearby residues which were sterically affected by the presence of MAbs binding to the IGF-1R.

In other studies it has shown that the C domain of the IGF-I is critical for its high affinity binding to the IGF-1R. For example, linking the IGF-I C domain to the C-terminus of the insulin B chain caused a 67-fold increase in IGF-1R binding affinity compared to native human insulin (Cara *et al.,* 1990). Another study on these two chimeras (IGF-IICI and IGF-ICII) revealed that the C domain of IGF-I allows higher affinity binding to the IGF-1R than the analogous domains of IGF-II (Denley *et al.,* 2004). Substitution of the whole C domain, with a tetra-glycine bridge ([1-27, Gly4, 38-70] IGF-I) made to maintain the tertiary structure also caused a 30-fold reduction in the affinity for IGF-1R (Bayne *et al.,* 1989).

In the C domain of IGF-I, the amino acids R36 and R37 and also Y31 have been shown to be critical for binding to the IGF-1R and their substitution with alanine resulted in 5- to 15-fold reduction in IGF-1R affinity (Bayne *et al.,* 1990; Zhang *et al.,* 1994; Jansson *et al.,* 1998). Hence, it implies that the binding of the IGF-I C domain is mostly via binding these amino acids (Y31, R36 and R37). It has been shown that the positively charged residues in the IGF-I C domain (R36 and R37) bind to the N-terminal 283 amino acids of the α-subunit and more specifically to the cysteine-rich region 217-283 of the IGF-1R (Zhang *et*

al., 1994). Hence, electrostatic interactions could be involved in the IGF-I C domain binding to the IGF-1R. Also, in the IGF-I C domain, Y31 with no equivalent residues in the IGF-II C domain (Denley *et al.,* 2004) may involve steric or hydrophobic interactions.

Moreover, the crystal structure studies on the IGF-I in the presence of detergent suggested that the Y31 lies at the tip of the extended C-domain and its location places it in an ideal location to interact with a receptor molecule (Vajdos *et al.,* 2001). On the other hand, the 3D structure of the L1-cysteine-rich-L2 domain fragment of the IGF-1R shows that the molecule adopts an extended bilobal structure with the L domains at both ends. The cysteine-rich domain runs two-thirds the length of the molecule, making contact along the length of the L1 domain but showing very little contact with the L2 domain. This makes an approximately 24Å diameter space at the centre of the molecule of sufficient size to accommodate the ligands IGF-I or IGF-II as shown in Figure 4.29 (Garrett *et al.,* 1998; Adams *et al.,* 2000). Hence, the residues R36, R37 and particularly Y31 could bind to the space at the centre of the IGF-1R molecule.

Taken together, it could be concluded that the binding of the IGF-I C domain to the IGF-1R cysteine-rich domain involves these three amino acids (Y31, R36 and R37) binding to or in close proximity residues F241 and F251.

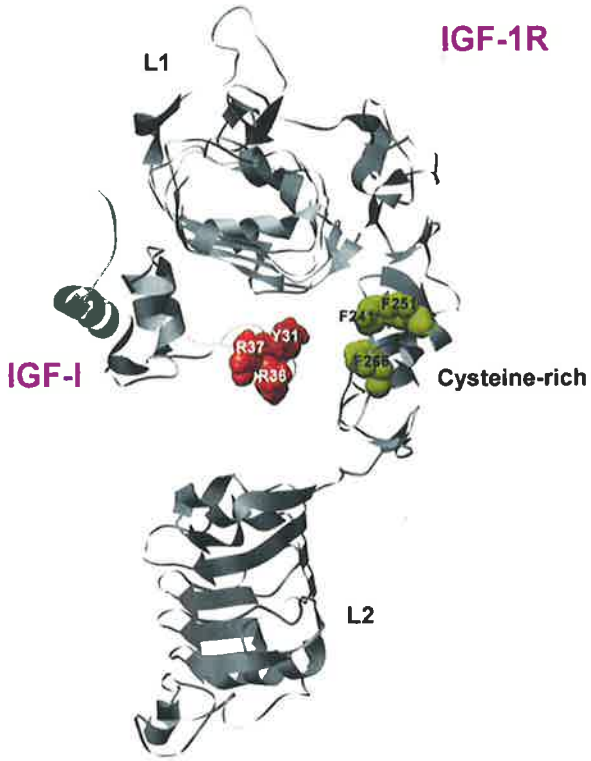

Figure 4.29 The structure of functional epitopes of MAbs 7C2 and 9E11 on the cysteine-rich domain of IGF-1R and the structure of residues of the IGF-I C domain involved in binding to IGF-1R.

Polypeptide fold for residues 1-478 of the human IGF-1R (right) and 1-70 of IGF-I (left) are shown based on (Garrett *et al.*, 1998; Vajdos *et al.*, 2001). The Cα backbone of IGF-I and IGF-1R is shown as a ribbon and the amino acids are shown in space-filling representation. The figure was created using the UCSF Chimera molecular graphics program. Yellow represents epitope of the MAbs and red IGF-I C domain residues.

4.4.8. Comparing the Affinity of MAbs 7C2 and 9E11 to other Antibodies Against the IGF-1R

The europium binding assay results showed slightly higher but not significant ($P > 0.05$) inhibitory activity for 7C2 (IC_{50} =1.9±1 nM) compared with 9E11 (IC_{50} =3.4±2.4 nM). The P value was calculated by comparing the data using unpaired t-tests (Confidence Intervals 95%) using the Prism 3.03 software. Furthermore, the kinetic analysis using the BIAcore showed that both MAbs 7C2 and 9E11 had high affinity for binding to the s-IGF-1R similar to αIR-3. The K_D values were as follows: K_D (7C2) = 0.5±1.6 nM, K_D (9E11) = 2.1±0.4 nM and K_D (αIR-3) = 1.3±0.5 nM (see Table 4-2 for details).

The affinity (K_D) and IGF inhibitory activity (IC_{50}) for some of the other MAbs against the IGF-1R have also been reported so far. The fully human A12 antibody inhibits IGF-I or IGF-II binding to cell surface IGF-1R with an IC_{50} of 0.6-1 nM (Burtrum *et al.*,

2003). The CP-751, 871, a fully human IgG2 binds to the receptor with K_D= 1.5 nM and it inhibits IGF-I binding with IC_{50}=1.8 nM (Cohen *et al.,* 2005). The mouse MAb EM-164 revealed a dissociation constant (K_D) of 0.1 nM (Maloney *et al.,* 2003). The humanised 7C10 or its murine parental form 7C10 displayed a similar IC_{50}, 4.2 nM $\pm$ 0.2 and 5.6 nM $\pm$ 0.59 respectively in IGF-I experiments (Goetsch *et al.,* 2005). For human MAbs 18 and 22 the K_D was 6.95×10^{-13} (M) and 6.56×10^{-10} (M) respectively (Graus *et al.,* 2005). These data suggest that although 7C2 and 9E11 only inhibit IGF-I binding, their inhibitory effect (IC_{50}) and affinity (k_D) are comparable with other MAbs to IGF-1R. These MAbs have higher affinity than most of other MAbs. Although the human MAbs 18 and 22 show an affinity even higher than 7C2 and 9E11 for the receptor with smaller K_D values, the standard errors for K_D of these two MAbs have not been shown and the accuracy of the K_D is not known.

Chapter 5

Biological Effects of the MAbs *in vitro*

5. Biological Effects of the MAbs *in vitro*

5.1. Introduction

In this chapter the biological effects of the generated MAbs (7C2 and 9E11) against the IGF-1R are explored on cancer cell lines *in vitro*. As described in Section 1.6.5, the involvement of the IGF system and particularly IGF-1R in cancer is well established due to the role of the IGF-1R to mediate the mitogenic effects of ligands such as IGF-I and IGF-II.

The IGF-1R is involved in promoting oncogenic transformation, growth, and survival of cancer cells (Kaleko *et al.,* 1990; Baserga *et al.,* 1997; Blakesley *et al.,* 1997; Khandwala *et al.,* 2000). Clinical and *in vitro* studies have revealed that the activation of the IGF-1R increased the proliferation and metastasis of cancer cells (Pollak *et al.,* 1990). High levels of IGF-1R expression have been reported in a wide range of human malignancies such as synovial sarcoma, breast, prostate, colon, ovarian, and pancreatic cancer (Khandwala *et al.,* 2000) (Bergmann *et al.*, 1995; Werner and LeRoith, 1996; Happerfield *et al.*, 1997; Xie *et al.*, 1999; Hellawell *et al.*, 2002; Weber *et al.*, 2002). Moreover, IGF-1R protects cells from apoptosis induced by growth factor deprivation or cytotoxic drug treatment (Harrington *et al.*, 1994; Baserga *et al.*, 1997; Navarro and Baserga, 2001). For example, it has showed that IGF-1R activation by IGF-I blocked the expected cytotoxic effects of 5-fluorouracil and external beam radiation in SW 480 colon cancer cells (Perer *et al.,* 2000). In another study combination therapy with tamoxifen and a chimeric humanised single chain antibody, scFv-Fc (generated from the parental 1H7 MAb against the IGF-1R), was more effective in inhibiting the T61 human breast tumour model (in athymic mice) growth than scFv-Fc or tamoxifen treatment alone *in vivo* (Ye *et al.,* 2003). The IGF-1R is thus a potential therapeutic target based on the theory that inhibition of IGF-1R function would cause selective growth inhibition and apoptosis of tumour cells (Baserga, 1995; Resnicoff *et al.*, 1995a).

Down-regulation of IGF-1R action by different methods such as antisense and dominant negative techniques caused reduction in the growth and tumourigenicity of several

cancer cell lines *in vivo* and *in vitro*, including colon cancer, melanoma, lung carcinoma, ovarian cancer, neuroblastoma, glioblastoma, and rhabdomyosarcoma (Resnicoff *et al.*, 1994; Shapiro *et al.*, 1994; Lee *et al.*, 1996; Liu *et al.*, 1998; Muller *et al.*, 1998; Adachi *et al.*, 2002; Reinmuth *et al.*, 2002; Seely *et al.*, 2002). To inhibit the IGF-1R function in cancer cells, using anti-IGF-1R antibodies that bind to the receptor and inhibit its activation is an attractive strategy. Several antagonistic anti-IGF-1R MAbs have been generated and reported so far as described in Chapter 1. Among them, the αIR-3 MAb has been used in several studies to inhibit the activation of the IGF-1R stimulated with IGF-I (Rohlik *et al.,* 1987; Kalebic *et al.,* 1994; Zia *et al.,* 1996; Scotlandi *et al.,* 1998).

Metastatic cancers not responding to surgery, chemotherapy and radiotherapy are fatal since they interfere with the functions of affected organs such as liver, bone, lung, and brain. Lung and liver metastases, which are often associated with late-stage malignancies of breast, prostate, the gastrointestinal tract, osteosarcomas, and melanoma, are generally resistant to common treatments and often inaccessible to surgical resection (Boring *et al.,* 1994). The establishment of a metastasis is the result of a dynamic process that involves various interactions between the disseminating cancer cells and their swiftly changing microenvironments. It includes cell separation from the primary tumour, migration, invasion of host tissue barriers and intravasation (Brodt *et al.*, 2000). These multiple processes are mediated by a series of molecular interactions. Disruption of the molecular interactions could potentially cause termination of the entire process (Brodt *et al.*, 2000).

The involvement of the IGF-1R and IGF-I in metastasis has been reported in several studies. The IGF-1R was identified as a positive regulator of the invasive/metastatic phenotype and IGF-I as a paracrine growth-promoting factor in the liver (Long *et al.,* 1994; Long *et al.,* 1998b). Highly invasive murine Lewis lung carcinoma subline H-59 cells express a high level of IGF-1R and this was crucial for tumour cell ability to form metastases in the liver. H-59 cells expressing IGF-1R antisense RNA lost mitogenic responses to IGF-I, had decreased levels of the extracellular matrix-degrading metalloproteinase MMP-2, became

non-invasive, and failed to form metastases in the liver following intrasplenic/portal inoculation (Long *et al.,* 1995; Long *et al.,* 1998a). These studies identified IGF-1R as a potential biological target for antimetastatic therapy and are the basis of ongoing attempts to develop additional antimetastatic approaches based on suppression of IGF-1R expression and function (Brodt *et al.*, 2000).

5.2. Methods

The general methods have been described in Chapter 0, and the specific methods are as follows.

5.2.1. Cell Proliferation Assay

Viability of cells in culture was determined using the Cell-Titer Glo™ Luminescent Cell Viability Assay Kit (Promega). Cells were grown in Nuclon Delta white microwell S1 96-well plates and treated as per experimental conditions. Upon completion of cell culture, adenosine triphosphate (ATP) released from metabolically active cells was detected by addition of Cell-Titer Glo substrate (luciferin), added 1:1 into culture media, and its subsequent conversion into oxyluciferin and light. Following shaking the plate at 960 rpm for 2 min using a Multiskan Ascent microplate reader (Labsystems), the plate was allowed to stand at room temperature (RT) for 10 min and then luminescence emitted from the cells (between 240-740 nm) was recorded, for 0.5 seconds per well, on a POLARstar Galaxy microplate reader (BMG lab Technologies) and FLUOstar Galaxy PC software.

In the present study the colorectal cancer cell line (HT-29) was used as an experimental model to determine the effects of MAbs 7C2 and 9E11 on cell proliferation induced by IGF-I or IGF-II. The overexpression of the IGF-1R has been reported in colorectal cancer tumours compared to normal tissues (Guo *et al.,* 1992; Weber *et al.,* 2002). In this study a total number of 12000 HT-29 cells per well were seeded into 96-well flat bottom plates in their growth medium. After 48 h incubation at 37°C and 5% (v/v) CO_2, the cells

were washed and serum starved for 5 h under the same conditions. Different treatment solutions were made in the serum-free growth medium containing 0.5% (w/v) BSA. Then, after adding the treatments to the wells containing HT-29 cells (in triplicate), the plate was incubated for 48 h at 37°C and 5% (v/v) CO_2. Subsequently, the luminescent counts were measured by adding Cell-Titer Glo substrate as above.

5.2.2. Cell Migration Assays

Cell migration is one of the crucial aspects in metastatic spread of cancer cells. In this study, the anti-migration effects of the generated MAbs were studied in breast cancer MCF-7 cell line as a model due to the overexpression of the IGF-1R (up to 14-fold) in malignant breast tissue compared with its level in normal breast tissue (Resnik *et al.*, 1998). Using a highly metastatic murine lung carcinoma model, it has been shown that the IGF-1R regulates these cells migration (Brodt *et al.*, 2000).

Pilot proliferation experiments revealed that for MCF-7 cells, IGF-I acts as a chemoattractant for migration and dose-dependently stimulates cells' migration. For the migration assay, framed polycarbonate filters with a pore size of 12 μm were incubated in 25 μg/ml type 1 collagen in 10 mM acetic acid solution overnight at 4°C to prepare them for use in this assay. The lower wells of an AC96 NeuroProbe A Series 96 Well Chamber were filled with RPMI containing 0.5% (w/v) BSA and different concentrations of IGF-I (1,10 or 100nM) or no IGF-I. Filters were then washed in PBS and placed against the rubber gasket of the top plate of the chamber. The top plate was then gently lowered onto the lower wells of the chamber containing the IGF solutions and fastened with screws. MCF-7 cells from approximately 80% confluent monolayers in a T175 flask were trypsinized with 1 ml trypsin/EDTA solution for 2 min at 37°C in an atmosphere containing 5% (v/v) CO_2, and washed twice in RPMI medium containing 0.5% (w/v) BSA. Then, viable cell counts were determined with a 1:2 (v/v) final dilution of trypan blue and cells were diluted to 1.5×10^6 cells/ml in RPMI medium containing 0.5% (w/v) BSA. Afterwards, calcein was added into

the cell suspension at a final concentration of 1mg/ml and incubated at 37°C, 5% (v/v) CO_2 for 30 min. The cells then were washed 3 times in RPMI containing 0.5% (w/v) BSA and re-suspended to 1.5×10^6 cells/ml. Next, the cell suspensions were incubated for 1 h at 37°C, 5% (v/v) CO_2 with various MAbs 7C2, 9E11, αIR-3 or IgG1 (negative control) all at a final concentration of 25 nM. A series of cells was also incubated in no MAb. The upper wells of the chamber were loaded with 40 µl/ml cell suspension (60,000 cells/well). Then the chamber was wrapped in damp Teri® wipers, and the cells left to migrate for 5.5 h at 37°C in an atmosphere containing 5% (v/v) CO_2. Following the incubation, the chamber was disassembled and non-migrated cells on the upper surface of the polycarbonate filters were wiped off with Teri® wipers soaked in PBS. Then, the calcein-labelled migrated cells on the underside of the filters were measured as follows. The fluorescent intensity of the transmigrated cells on the lower surface was quantified using a Molecular Image® FX (Biorad Laboratories, USA) and expressed as a migration index, which represents the fluorescent signals of stimulated cells divided by that of non-stimulated cells.

5.2.3. Analysis of the IGF-1R Down-Regulation

To determine the effect of the MAbs on down-regulation of the IGF-1R in human breast cancer cells (MCF-7) *in vitro*, the method described in (Hailey *et al.*, 2002) was employed with modifications. MCF-7 cells were treated with different MAbs against the IGF-1R as well as IGF-I and no MAb. The cells (7×10^5) were seeded into each well of 6-well plates in MCF-7 growth medium, and incubated at 37°C in 5% (v/v) CO_2 to grow. Then the cells were incubated in serum-free growth medium for 20 h in the same conditions. Subsequently, the treatment solutions which were IGF-I at the 50nM final concentration and MAbs 9E11, 7C2 and αIR-3 all at 25 nM final concentration, were made in serum-free growth medium and added to each well of the plate (in triplicate). The cells in the plate were incubated for 24 h at 37°C in 5% (v/v) CO_2 with the various treatments. The effect of the MAbs treatment on the

IGF-1R down-regulation was studied by detecting IGF-1R by Western blot analysis. The various treated cells were lysed as described in (Denley *et al.,* 2004) and 15 μg cell lysates for each one and 15 μg of R^- cell lysates (as a negative control for IGF-1R) were loaded into a 10% SDS-PAGE gel and electrophoresed under reducing condition and then transferred to a nitrocellulose membrane (see Sections 2.2.2.5 and 2.2.2.6 for detail). The IGF-1R was detected using anti-IGF-1R antibody C-20 (polyclonal) directed to the β subunit of the IGF-1R by incubating the membrane overnight at 4°C in a 1:1,000 (v/v) dilution of this antibody in PBS containing 1% w/v BSA. Anti-rabbit HRP conjugate (Rockland) antibody diluted 1:10,000 (v/v) in PBS-T was applied to the membrane as a secondary antibody and incubated for one h at RT. The HRP was visualized using ECL (enhanced chemiluminescence reagent) detection solutions and exposed to X-Ray film. For more details refer to Section 2.2.2.6.

5.3. Results

5.3.1. Effect of the MAbs on HT-29 Cell Proliferation

It has been reported that butyrate (n-butyric acid sodium salt) has potent anti-tumourigenic effects on many cancer cell lines such as HT-29, by regulating differention, inducing apoptosis and inhibiting tumour cells' growth *in vitro* (Leng *et al.*, 2001; Kautenburger *et al.*, 2005). Butyrate is a short chain fatty acid, fermented from oligo- and polysaccharides by human colonic bacteria (Kautenburger *et al.*, 2005; Lim *et al.*, 2005).

Pilot proliferation experiments revealed that 5 mM butyrate significantly ($P < 0.05$) inhibited HT-29 cell proliferation compared to no butyrate (Figure 5.1). However, adding 10 nM IGF-I or 50 nM IGF-II along with butyrate (5mM) significantly ($P < 0.05$) rescued the cells from death induced by butyrate. The 10 nM IGF-I and 50 nM IGF-II had similar efficacy in neutralizing the anti-apoptotic effect of butyrate. Then to characterize the neutralizing effects of the MAbs 24-60, αIR-3, 7C2 and 9E11 on the induced cell proliferation by IGFs

in vitro, the proliferation assay was carried out as described in Section 5.2.1. HT-29 cells were treated with increasing concentrations of the MAbs (from 0.01 nM to 100 nM) in combination with butyrate (5mM) and IGF-I (10nM) or IGF-II (50nM). An unrelated IgG1 was used as negative control.

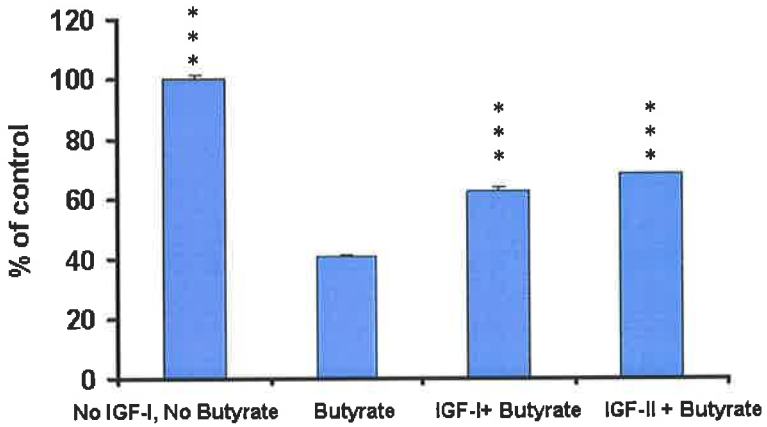

Figure 5.1 The effect of the butyrate alone or in combination with IGF-I or IGF-II on HT-29 cell proliferation.

The concentrations for butyrate, IGF-I and IGF-II were 5 mM, 10 nM and 50 nM respectively.
The P values were calculated by comparing the data for treatment with butyrate alone to other data using unpaired t-tests (Confidence Intervals 95%) by the Prism 3.03 software. Representative experiments are shown. Bars are means ± SD of triplicates.
P value 0.01 to 0.05 = *, P value 0.001 to 0.01 =**, P value < 0.001=***.

The results for these proliferation assays revealed that the MAbs αIR-3, 7C2 and 9E11 at a concentration equal or greater than 1nM could significantly ($P< 0.05$) inhibit survival of cultured cells induced by IGF-I (10nM) (Figure 5.2). In this experiment the maximum inhibition was obtained with the highest concentration of the MAbs (100 nM). The MAbs αIR-3, 9E11 and 7C2 (100nM) inhibited the IGF-I induced proliferation by approximately 25%, 25% and 30% respectively (Figure 5.2, A). In this experiment, MAb 24-60 had no significant effect on IGF-I mediated proliferation. The isotype control (IgG1) also had no effect on IGF-I (10nM) induced cell growth as expected. The IC_{50} for 7C2, 9E11 and αIR-3 are shown in Figure 5.3 (A).

None of the MAbs inhibited the effect of IGF-II (50 nM) as potently as they inhibited IGF-I (10 nM) induced proliferation (Figure 5.2 B). However, all the MAbs 24-60, αIR-3, 7C2 and 9E11 significantly ($P < 0.05$) inhibited the IGF-II induced proliferation by approximately 10% at their maximum concentration (100nM) (Figure 5.2 B). The inhibiting effects of the MAbs αIR-3, 7C2 and 9E11 were also significant ($P< 0.05$) at 10 nM concentration of these MAbs, but at this concentration MAb 24-60 had no significant effect.

For inhibition of IGF-II (50 nM) induced proliferation, the IC_{50} for 24-60, αIR-3, 7C2 and 9E11 are shown in (Figure 5.3 B). As expected, the isotype control (IgG1) revealed no effect on IGF-I induced cell growth.

The isotherm curves shown in (Figure 5.3) were obtained from the same results as Figure 5.2. The average inhibitory activity (IC_{50}±SD) for the tested MAbs to inhibit IGF-I or IGF-II induced HT-29 cell proliferation are shown in Figure 5.3. To obtain these values, data from three separate experiments were used. These results revealed that MAbs 7C2, 9E11 and αIR-3 possessed a high and similar blocking activity (IC_{50}) to each other to inhibit IGF-I induced cell proliferation. In this experiment, although MAbs 7C2 and 9E11 seem to have a better inhibitory effect (smaller IC_{50}) than MAb αIR-3, the difference between the IC_{50} values for these three MAbs were not significant ($P > 0.05$).

Interestingly, the MAbs 24-60, αIR-3, 7C2 and 9E11 significantly inhibited the IGF-II induced cell proliferation. However, the inhibitory effect (IC_{50}) of these MAbs was not as potent as their effect on IGF-I induced cell proliferation. The IC_{50} values for these four MAbs to inhibit IGF-II induced cell proliferation were not significantly different ($P > 0.05$). The P values were calculated by comparing the data using unpaired t-tests (Confidence Intervals 95%) by the Prism 3.03 software.

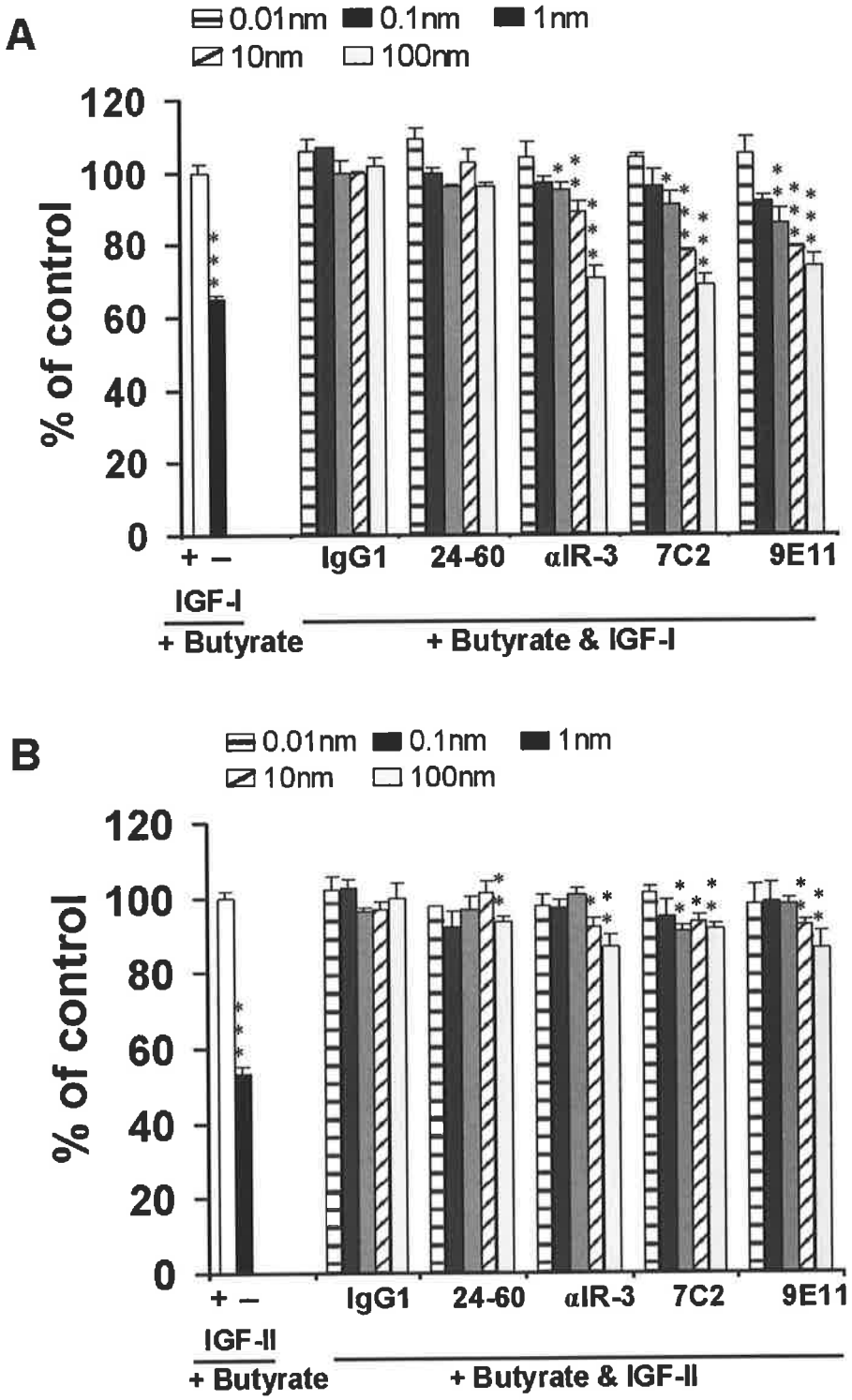

Figure 5.2 The effect of the MAbs on cell proliferation.

The HT-29 cells were treated with butyrate (5mM) as chemotherapeutic reagent. 10 nM IGF-I (A) or 50 nM IGF-II (B) rescued the cells from death induced by butyrate. Various concentrations of MAbs were applied to inhibit the cell survival as described in Section 5.2.1. These graphs are the representative of three separate experiments. Bars are means ± SD of triplicates. The P values were calculated by comparing the data for treating the cells with IGF-I or IGF-II (but not MAb) to other treatments using unpaired t-tests by the Prism 3.03 software.
$0.01 < P < 0.05$ = *, $0.001 < P < 0.01$ = **, $P < 0.001$ = ***.

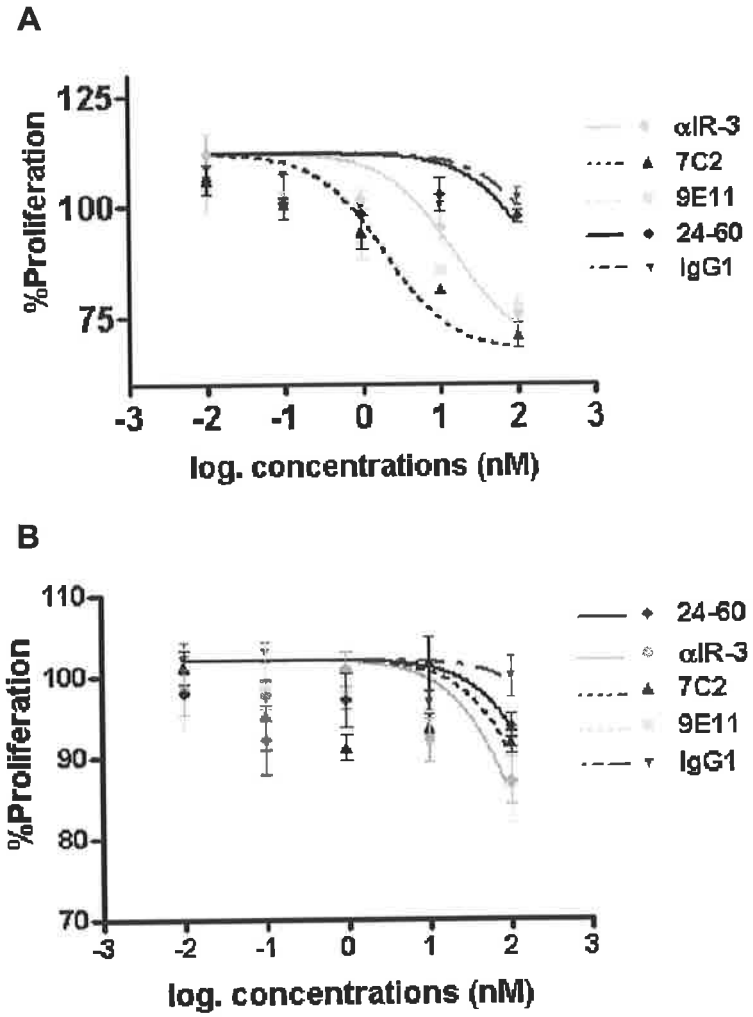

MAb	IC_{50} (nM)
αIR-3	11±6.6
7C2	1.3±1
9E11	1.5±1.1

MAb	IC_{50} (nM)
αIR-3	150.3±46
7C2	231.1±101.3
9E11	132.4±60.7
24-60	356.9±158.3

Figure 5.3 The isotherm curves and calculated IC_{50} for the inhibitory effects of different concentrations of various MAbs on the HT-29 proliferation induced by 10 nM IGF-I (A) or 50 nM IGF-II (B).

Results are expressed as a percentage of HT-29 cell proliferation in the absence of competing MAb. These graphs are the representative of three separate experiments and data points are means of triplicates ± SD. The curves and IC_{50} values were generated using the Prism 3.03 software employing curve-fitting with a one-site competition model. Curve fitting constants were the minimum and maximum percentage of HT-29 cells proliferation for each experiment. The IC_{50}± SD values were obtained from three separate experiments.

5.3.2. Effect of the MAbs on MCF-7 Cell Migration

For MCF-7 cells, the effect of the anti-human IGF-1R MAbs on IGF-I stimulated chemotaxis can be observed in Figure 5.4. Comparing the migration of MAb treated MCF-7 cells to no MAb shows that MAbs 9E11 (25 nM) and 7C2 (25 nM) inhibited the IGF-I induced migration significantly ($P < 0.05$) in the highest concentration of IGF-I (100 nM). MAbs αIR-3 (25 nM) and 24-60 (25nM) did not significantly inhibit the migration induced by 100 or 10 nM IGF-I however, they both inhibit the effect of 1 nM IGF-I (Figure 5.4). An unrelated

IgG1 antibody was employed as an isotype control and did not inhibit the migration, but rather it shows a slight stimulatory effect on the cells' migration.

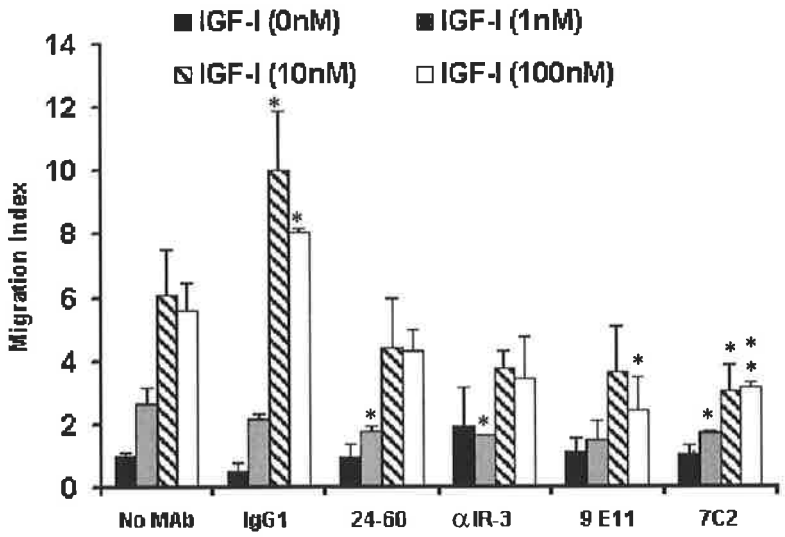

Figure 5.4 The effect of the MAbs on MCF-7 cell migration towards IGF-I as a chemoattractant.

The MCF-7 cells migration was induced by different concentrations of IGF-I and a constant concentration (25 nM) of various MAbs were used to inhibit the induced migration as described in Section 5.2.2.
The P values were calculated by comparing the data for no treatment (Buffer) with other data corresponding to relevant concentration of IGF-I using unpaired t-tests (Confidence Intervals 95%) by the Prism 3.03 software. The graph shown is a representative of three separate experiments and bars are means ± SD of triplicates.
P value 0.01 to 0.05 = *, P value 0.001 to 0.01 =**, P value < 0.001=***.

5.3.3. Effect of the MAbs on IGF-1R Down-Regulation in MCF-7Cells

In the lysate extracted from the P6 cells, the β subunit of the IGF-1R was detected with Western blot analysis and anti-IGF-1R antibody. Prolonged treatment of the MCF-7 cells with the MAbs revealed that compared to no treatment, the level of IGF-1R was dramatically reduced after 24 h treatment with 25 nM MAbs 7C2, 9E11, 24-60 or αIR-3. In contrast, the treatment with IGF-I (50 nM) did not down-regulate the IGF-1R compared to no treatment (Figure 5.5). A non-specific band was detected in P6 cells lysate as well as R^- cells lysate for the anti-IGF-1R antibody (C-20) at 55 kDa. These bands could be considered as loading controls.

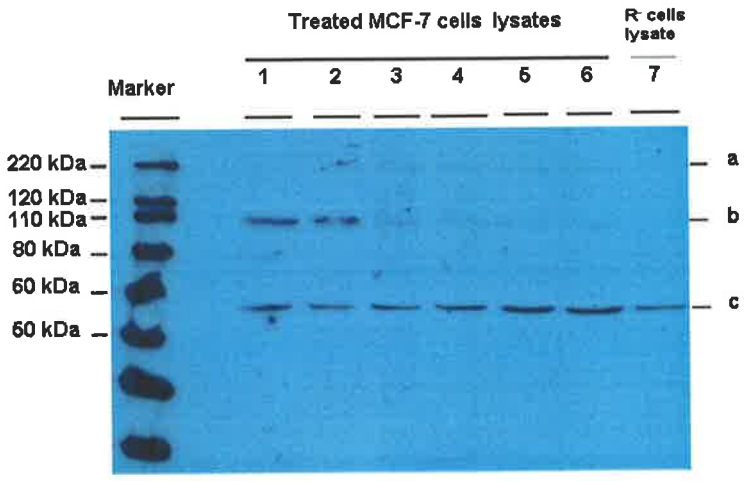

Figure 5.5 The IGF-1R down-regulation by the MAbs against the IGF-1R.

MCF-7 cells were treated with IGF-I or different MAbs against the IGF-1R as described in Section 5.2.3
Lane 1: No treatment, Lane 2: IGF-I treated, Lane 3: 9E11 treated, Lane 4: 7C2 treated, Lane 5: 24-60 treated, Lane 6: αIR-3 treated, Lane 7: R^- cells lysate (no treatment).
a) Pro-IGF-1R, b) IGF-1R β subunit, c) non-specific band (used here as loading control).
Molecular weight was estimated in kilodaltons using the MagicMark^{TM}XP marker. A representative experiment is shown.

5.4. Discussion

The cell proliferation experiment showed that MAbs 7C2, 9E11 and αIR-3 significantly ($P < 0.05$) inhibited the IGF-I induced HT-29 cell proliferation at concentrations equal or greater than 1nM. This effect of MAbs 7C2 and 9E11 was consistent with their inhibitory effects on IGF-I binding (Figure 4.5 A) since the IC_{50} values for the MAbs to inhibit the IGF-I induced cell proliferation (7C2 (IC_{50})= 1.28±1 nM, 9E11 (IC_{50})= 1.5±1.1 nM) were similar to the IC_{50} values for these MAbs to inhibit the IGF-I binding to IGF-1R, (7C2 (IC_{50})= 1.9±1 nM, 9E11 (IC_{50})= 3.4±2.4 nM). It could be concluded that the inhibitory effect of MAbs 7C2 and 9E11 on cell proliferation was due to their inhibiting effect on the IGF-I binding to the IGF-1R. Although a slight effect could be seen for MAb 24-60 to inhibit the IGF-I binding to the receptor in binding experiments (Figure 4.5 A) and cell proliferation induced by IGF-I, these effects were not statistically significant in either assay.

The proliferation assay also revealed that MAbs 24-60, αIR-3, 7C2 and 9E11 significantly ($P< 0.05$) inhibited the IGF-II induced HT-29 cell proliferation at their highest concentration (100nM). However, this inhibitory effect could not be considered as potent as

the effect of the MAbs (αIR-3, 7C2 and 9E11) on IGF-I induced proliferation particularly by comparing the IC_{50} values (Figure 5.3 A). The inhibitory effect of the anti-IGF-1R MAbs on IGF-II induced HT-29 cell proliferation was interesting particularly because MAbs 7C2, 9E11 and 24-60 did not show a significant inhibitory effect on binding IGF-II to the IGF-1R in competition experiments (Figure 4.5 B). So, it could be concluded that the inhibitory effect of MAbs 7C2, 9E11 and 24-60, on IGF-II induced proliferation was due to an indirect effect of the MAbs on the IGF-1R such as inactivation or down-regulation of the receptor. In this study the result for the receptor down-regulation experiment on MCF-7 cells showed that prolonged treatment with the anti-IGF-1R MAbs dramatically reduced the IGF-1R level. Hence, it suggests that the IGF-1R down-regulation could have happened in HT-29 and caused indirect inhibition of the IGF-II induced proliferation. Another possibility could be that MAbs 7C2, 9E11 and 24-60 slightly inhibited the binding of the IGF-II to the receptor but the method (europium binding assay) used in this study was not sensitive enough to detect it.

It has also been reported that neutralizing anti-IGF-1R antibodies MAB391 and αIR-3, inhibited the receptor function and also induced receptor degradation in MCF-7 breast, HT-29 colon and DU-145 prostate tumour cells (Hailey *et al.,* 2002). In addition, a humanised single-chain antibody scFv-Fc against the IGF-1R (originated from the parental mouse MAb 1H7) stimulated *in vitro* growth but inhibited *in vivo* tumour growth (Sachdev *et al.,* 2003). To explain the difference between *in vitro* and *in vivo* effects, Sachdev et al. showed that, both *in vitro* and in athymic mice with xenograft tumours, treatment with the scFv-Fc antibody down-regulated the IGF-1R. Hence, the IGF-1R down-regulation resulted in resistance of MCF-7 cells to additional IGF-I exposure (Sachdev *et al.,* 2003). Furthermore, it has shown that long-term treatment with anti-IGF-1R neutralizing antibody MAB391 caused receptor degradation in MCF-7 cells (Hailey *et al.,* 2002). In addition, the IGF-1R was internalized and degraded by a combination of both lysosome-dependent and lysosome-independent pathways. However, proteasome inhibitors did not affect the pathway (Hailey *et al.,* 2002). The mechanism of the anti-IGF-1R MAbs 24-60, αIR-3, 7C2 and 9E11 on IGF-1R

down-regulation, which was demonstrated in this study, could be similar to the reported mechanism for MAB391 (Hailey *et al.,* 2002). In conclusion, due to the importance of the receptor down-regulation to inhibit the tumour growth particularly *in vivo* the generated MAbs 7C2 and 9E11 are good candidates for further study *in vivo* as anti-tumour reagents.

Several studies revealed the antiproliferative effects of several MAbs against the IGF-1R on tumour cells, alone or in combination with chemotherapeutics *in vitro* and *in vivo*. For example the inhibitory effect of MAb αIR-3 on non-small cell lung cancer growth *in vitro* and *in vivo* has shown (Zia *et al.,* 1996). MAb αIR-3 also inhibited the growth of MCF-7 cells cultured in 5% (v/v) calf serum (Rohlik *et al.,* 1987). It has also been reported that treatment with MAb αIR-3 suppressed both progression of human rhabdomyosarcoma (RMS) tumour growth in tumour-bearing animals and formation of newly established tumours (Kalebic *et al.,* 1994). Kalebic et al. also showed histological analysis of tumours from animals treated with MAb αIR-3 did not reveal necrotic lesions. This suggests that the treatments had no cytotoxic effect (Kalebic *et al.,* 1994). In addition, in another study, MAb αIR-3 inhibited the growth of Ewing's sarcoma in athymic mice (Scotlandi *et al.,* 1998). MAb EM164 also inhibited IGF-I, IGF-II, and serum-stimulated survival and proliferation of various human cancer cell lines *in vitro*, including breast, lung, colon, ovarian, melanoma, pancreatic, prostate, cervical, neuroblastoma, rhabdomyosarcoma, and osteosarcoma cancer lines (Maloney *et al.,* 2003).

For MAb αIR-3, a number of studies revealed the antiproliferative effects of chemotherapeutics were increased in combination with this MAb. For instance, the cytotoxic response of chemoradiation therapy increased with the IGF-1R antagonism (MAb αIR-3) (Perer *et al.,* 2000). Adding MAb αIR-3 to breast cancer cell lines MCF-7 and MDA-231 also resulted in improved cytotoxicity of taxol or doxorubicin in IGF-I stimulated cells compared to the use of either taxol or doxorubicin alone (Beech *et al.,* 2001).

The cell proliferation assay on HT-29 revealed that, although the IC_{50} values for MAbs 7C2 and 9E11 to inhibit IGF-I or IGF-II induced cell proliferation were not

significantly different from αIR-3, they seem more potent than αIR-3 due to their lower IC_{50} (particularly for IGF-I induced proliferation) (Figure 5.3). Hence, MAbs 7C2 and 9E11 seem good candidates for further study as anti-cancer reagents *in vitro* and *in vivo*.

To determine the effect of the MAbs on metastasis, a cell migration assay was carried out. The results of this migration assay revealed that IGF-I induced cell migration in MCF-7 cells (dose-dependently). MAbs 7C2 and 9E11 (25 nM) significantly ($P < 0.05$) inhibited the IGF-I (100 nM) induced cell migration. Although MAbs 24-60 and αIR-3 inhibited the IGF-I (1nM) induced migration significantly ($P < 0.05$), and they were not able to inhibit the migration induced by IGF-I (100 nM). This suggests that the inhibiting effects of MAbs 24-60 and αIR-3 were not as potent as 9E11 and 7C2 because at the same concentration, MAbs 24-60 and αIR-3 were not able to inhibit the effect of the high concentration IGF-I (100 nM) on cell migration. These results demonstrated that IGF-I stimulated the migration of MCF-7 cells and this could be inhibited by targeting the IGF-1R with MAbs 7C2 and 9E11. The migration assay showed isotype IgG1 control slightly induced the migration of MCF-7 cells compared to no MAb and it was significant. This negative control MAb could have a non-specific effect to induce cell migration. Although the anti-mitogenic effects of blocking the IGF-1R in different methods such as using IGF-1R antisense RNA have been shown (Long *et al.,* 1995; Long *et al.,* 1998b), the effect of targeting IGF-1R with antibodies on cell migration has not been clarified. This study showed that the anti-IGF-1R antibodies (7C2 and 9E11) inhibited the MCF-7 cells migration induced by IGF-I. So, it can be concluded that these MAbs may have anti-metastatic effects.

Chapter 6

Final Discussion, Future Applications and Directions

6. Final Discussion, Future Applications and Directions

6.1. Discussion

Clear links between certain cancers and cellular signalling triggered by the IGF-1R and its ligands (IGF-I and IGF-II) have been widely reported. Therefore, the IGF-1R is becoming an attractive target for cancer therapy. The broad objective of this thesis was to generate specific monoclonal antibodies (MAbs) to inhibit the binding of IGFs to IGF-1R and thereby neutralising its function. In addition, due to the overexpression of the IGF-1R in several cancer cell lines, the antibodies can be used as diagnostic reagents in different biochemical studies.

The IGF-1R is expressed almost everywhere in the mammalian body (Khandwala *et al.,* 2000). Although using knock out technology, it has been shown that the IGF-1R is essential in early development (Baker *et al.,* 1993; Liu *et al.,* 1993), it is more difficult to define to what extent the receptor expression and function are necessary in the mature adult. IGF-1R inhibitors could cause toxicity to tissues that are rapidly proliferating (Bohula *et al.,* 2003a). However, large molecules such as antibodies may be less likely to cross the blood-brain barrier. Hence, using antibodies potentially protects against possible severe effects on peripheral or central nervous system function that could be caused by small molecules such as chemical inhibitors or oligonucleotides (Bohula *et al.,* 2003a).

Lack of information regarding the IGFs binding mechanism to the IGF-1R constitutes a considerable gap in our understanding of IGF-1R function. These MAbs could also be utilised to investigate the mechanism of ligand binding to the receptor and its activation.

6.2. Summary of Findings

During this research, two specific mouse MAbs against IGF-1R were generated by immunising a mouse with s-IGF-1R (the soluble extracellular part of the IGF-1R, amino acids 1-906). These MAbs were called 7C2 and 9E11, and both were IgG1 and κ isotype. They

were successfully utilised in a number of immunoassays. In ELISA (enzyme linked immunosorbent assay) these two MAbs detected s-IGF-1R. MAbs 7C2 and 9E11 also specifically detected the intact human IGF-1R on the surface of P6 cells in flow cytometry with no cross-reaction with IR-A or IR-B expressed in R^- cells. These MAbs also immunoprecipitated IGF-1R from lysates of cells overexpressing recombinant IGF-1R. In addition, although MAbs 7C2 and 9E11 were not able to detect the α or β subunits of the IGF-1R under reducing conditions, they bound to the whole receptor under non-reducing conditions. This suggests that the epitope for MAbs 7C2 and 9E11 are conformational (Harlow and Lane, 1999). This is consistent with our epitope mapping results that showed the epitopes for these MAbs are conformational. These MAbs also specifically detected the IGF-1R in immunohistochemistry assays in frozen human skin tissues, frozen P6 cells and paraffin-embedded skin tissues with no cross-reaction with IR-A or IR-B expressed in R^-cells.

The complementarity determining regions (CDRs) of MAbs 7C2 and 9E11 were sequenced. The sequences of the CDRs were compared with these of other MAbs against the IGF-1R, for which the variable region sequences have been reported. It showed that although the biochemical characteristics of MAbs 7C2 and 9E11 were similar, each one displayed a unique sequence.

6.2.1. The Selective Blocking Activity of the MAbs and Epitope Mapping

The binding analysis experiments revealed that MAbs 7C2 and 9E11 only inhibited IGF-I binding to the receptor and not IGF-II. These results suggest that there are two distinct binding sites for IGF-I and IGF-II on IGF-1R. Moreover, it can be concluded that the epitope of the MAbs only overlap the IGF-I binding site on the receptor and not therefore IGF-II. Recently, it has been revealed that the IGF-1R cysteine-rich domain is crucial for IGF-I binding but not IGF-II (Sorensen *et al.,* 2004). This is consistent with the epitope mapping results using chimeric IGF-1R/IR receptors that showed both MAbs 7C2 and 9E11 bound to the cysteine-rich domain of the receptor. More specific epitope mapping, using alanine

mutants in the cysteine-region of the IGF-1R, showed the epitopes for the MAbs were at least the residues F241, F251 and F266. The epitopes for MAbs 7C2 and 9E11 could be exactly the same or at least share these three residues in their binding sites. Because the mutation of only one of these three amino acids to alanine almost disrupted the binding of these MAbs to IGF-1R, it suggests that the three residues contribute to provide major energy for binding MAbs 7C2 and 9E11 to IGF-1R.

It has been shown that the mutation of residues F241 and F251 to alanine caused a major reduction in binding IGF-I to the receptor (Sorensen *et al.,* 2004). However, mutation of residues F241, F251 and F266 to alanine had no significant effect on binding IGF-II to the receptor (Sorensen *et al.,* 2004). Therefore, it can be concluded that binding of MAbs 7C2 and 9E11 particularly to amino acids F241 and F251 is responsible for specific inhibition of binding of IGF-I to the receptor.

Interestingly, in this thesis it was shown that chimeric IGF-I/IGF-II ligands, IGF-ICII (IGF-I with IGF-II C domain) and IGF-IICI (IGF-II with IGF-I C domain) represented similar effects to IGF-II and IGF-I, respectively. It means that the C domain of the IGF-I could interfere with the binding of MAbs 7C2 and 9E11 to IGF-1R. This finding also implies that out of all domains of the IGF-I, it is the C domain, which binds to the epitope for these MAbs or to nearby residues which were sterically affected by the presence of MAbs binding to the receptor. This binding is related to residues F241 and F251 of IGF-1R as mentioned earlier.

In the C domain of IGF-I, the amino acids R36 and R37 and also Y31 have been recognized as critical for binding to IGF-1R (Bayne *et al.,* 1990; Zhang *et al.,* 1994; Jansson *et al.,* 1998). Therefore, it suggests that the binding of the IGF-I C domain to the IGF-1R cysteine-rich domain involves these three amino acids (R36, R37 and Y31) binding to or in close proximity residues F241 and F251.

In addition, it has been shown that the positively charged residues, R36 and R37, bind to the N-terminal 283 amino acids of the IGF-1R α-subunit and more specifically to the

cysteine-rich region 217-283 of the IGF-1R (Zhang *et al.*, 1994). This suggests electrostatic interactions could be involved in the IGF-I C domain binding to the receptor.

6.2.2. Affinity of the MAbs

The europium competition assay results showed that MAbs 7C2 and 9E11 efficiently inhibit IGF-I binding to the IGF-1R. The IC_{50} values were as follows: IC_{50} (7C2) = 1.9±1 nM and IC_{50} (9E11) = 3.4±2.4 nM.

Moreover, the kinetic studies using BIAcore showed the affinity of MAbs 7C2 and 9E11 to IGF-1R to be high. The K_D values for these two MAbs were as follows: K_D (7C2) = 0.5±1.6 nM and K_D (9E11) = 2.1±0.4 nM.

These data suggest that although 7C2 and 9E11 only inhibit IGF-I binding, their inhibitory effect (IC_{50}) and affinity (k_D) are comparable with other MAbs to IGF-1R.

6.2.3. The Biological Effects of MAbs

The cell proliferation experiment showed that MAbs 7C2 and 9E11 inhibited IGF-I induced HT-29 cell proliferation. This effect of the MAbs was consistent with their inhibitory effects on IGF-I binding. The IC_{50} values for the MAbs to inhibit the IGF-I induced cell proliferation were as follows: IC_{50} (7C2) = 1.3±1 nM and IC_{50} (9E11) = 1.5±1.1 nM. These values were similar to the IC_{50} values for MAbs 7C2 and 9E11 to inhibit the IGF-I binding to IGF-1R that mentioned earlier. It suggests that the inhibitory effect of MAbs 7C2 and 9E11 on cell proliferation was due to their inhibiting effect on the IGF-I binding to the IGF-1R.

In addition, the proliferation assay revealed that MAbs 7C2 and 9E11 inhibited IGF-II induced HT-29 cell proliferation. However, this inhibitory effect could not be considered as potent as the effect of MAbs 7C2 and 9E11 on IGF-I induced proliferation. The IC_{50} values to inhibit the IGF-II induced cell proliferation were as follows: IC_{50} (7C2) = 231.1±101.3 nM and IC_{50} (9E11) = 132.4±60.7 nM. Because these MAbs did not inhibit IGF-II binding to the

receptor, their effects on IGF-II induced cell proliferation could be due to an indirect effect of the MAbs on the IGF-1R, such as inactivation or down-regulation of the receptor. This is consistent with the result for the receptor down-regulation experiment on MCF-7 cells, which showed that 24 h incubation with MAbs 7C2 and 9E11 dramatically reduced IGF-1R levels. So, it implies that in HT-29 cells, the IGF-1R is down-regulated resulting in indirect inhibition of the IGF-II induced proliferation.

This study also showed that MAbs 7C2 and 9E11 inhibited MCF-7 cells migration induced by IGF-I, indicating the potential anti-metastatic effects of these MAbs. Although the anti-metastatic effects of blocking the IGF-1R via different methods, such as by using IGF-1R antisense RNA have been revealed (Long *et al.,* 1995; Long *et al.,* 1998b), the effect of targeting IGF-1R with anti-IGF-1R antibodies on metastasis has not been clarified before.

6.3. Future Applications

In this section, some potential applications of Mabs 7C2 and 9E11 are discussed. MAbs 7C2 and 9E11 successfully detected IGF-1R in a range of immunoassays as mentioned earlier. It suggests that they can be used to detect the receptor in tumour samples. If the tumour shows IGF-1R overexpression, anti-IGF-1R therapy could be a beneficial method of treatment. In addition, in some cancers, there is a correlation between the increased expression of IGF-1R and metastasis and also higher grade and higher stage of tumour (Goyal *et al.,* 1998; Hakam *et al.,* 1999). So, the overexpression of the receptor can also bring insight to predicting the stage of progression in certain tumours.

Due to the anti-proliferative and anti-metastatic effect of MAbs 7C2 and 9E11 on cancer cell lines *in vitro*, and also because these two MAbs induced down-regulation of the IGF-1R, these antibodies could be appropriate for being tested *in vivo*. For this, a human tumour model can be established in mice (Maloney *et al.,* 2003). Then, the animal would be treated by intravenous injections with MAbs 7C2 or 9E11 alone or in combination with

chemotherapeutic drugs, appropriate to the type of tumour, to determine the anti-tumour effect in the established tumour.

Although some of the mouse antibodies such as Orthoclone OKT3 and Zevalin have been used as human therapeutics, there are side effects from using mouse antibodies, particularly due to patient immune response against mouse immunoglobulins (Hudson and Souriau, 2003). The murine MAbs are foreign proteins to the human immune system and induce anti-murine responses in the human body to form anti-mouse antibodies (Maynard and Georgiou, 2000; Hudson and Souriau, 2003).

Several strategies have been developed to avoid, mask or redirect the immune reaction of murine MAbs 7C2 and 9E11 (Figure 6.1). These strategies are fusion of mouse variable regions to human constant regions to generate 'chimeric antibodies', removal of T-cell epitopes for 'de-immunisation' of antibodies and grafting mouse surface residues onto human acceptor antibody frameworks for 'humanisation' (Hudson and Souriau, 2003). It has been shown that replacement of the murine constant regions with those from human antibodies resulted in chimeras with significantly reduced immunogenicity (Boulianne *et al.,* 1984; Morrison *et al.,* 1984; Knight *et al.,* 1995). Moreover, transplanting the murine CDR regions, which are primarily involved in antigen contact and binding, to a homologous human β-sheet framework can obtain a further reduction in immunogenicity (Jones *et al.,* 1986; Riechmann *et al.,* 1988).

The big size of the therapeutic MAbs restricts their access to tumour cells, especially in central regions of solid tumours (Russell *et al.,* 1992). Smaller fragments are being studied in an attempt to improve access and uptake of antibodies (Li *et al.,* 2000; Bohula *et al.,* 2003a; Sachdev *et al.,* 2003). In addition, antibody fragments can be designed for unique clinical applications. For receptor blockade, the Fc-induced effector functions are often unwanted and can be removed by proteolysis of intact antibodies to make monovalent Fab fragments. However, proteolysis does not simply yield molecules smaller than a Fab fragment, and microbial expression of single-chain Fv (scFv) is currently the preferred

method of production. In scFv, the variable regions of antibody heavy (V_H) and light (V_L) chains are stably joined together with a flexible polypeptide linker (Figure 6.1) (Desplancq *et al.*, 1994; Ayala *et al.*, 1995; Hudson and Souriau, 2001). Small antibody fragments such as Fab and scFv exhibit better pharmacokinetics than whole antibodies for tissue penetration. These antibody fragments also provide full binding specificity because the antigen-binding surface is unchanged. However, Fab and scFv are monovalent and often exhibit rapid off-rates and poor retention time on the target.

Moreover, Fab and scFv fragments can be engineered to make dimeric, trimeric or tetrameric conjugates to increase functional affinity through the use of either chemical or genetic cross-links (Carter, 2001; Hudson and Souriau, 2001; Hudson and Souriau, 2003).

The MAbs could be also utilised to make bispecific antibodies contain two different binding specificities fused together (Figure 6.1). These antibodies can bind to two adjacent epitopes on a single target antigen, thereby increasing the avidity or alternatively can cross-link two different antigens. For example, the bispecific antibodies, which bind to both IGF-1R and epidermal growth factor (EGF) receptor can be made to inhibit both receptors and enhance the anti-tumour activity of the generated MAbs (Hudson and Souriau, 2003; Lu *et al.*, 2005).

Another possibility is to fuse the MAbs to one or more of a vast range of molecules such as radionuclides and cytotoxic drugs that provide important additional functions after binding to the IGF-1R. It has been shown that radiolabeled antibodies can be used for both tumour imaging and therapy and also provide an effective evaluation of pharmacokinetics (Goldenberg, 2002).

In this study, interestingly the anti-IGF-1R antibodies (7C2 and 9E11) were shown to inhibit the MCF-7 cells migration induced by IGF-I. So, these MAbs could be used to inhibit cancer cells metastasis in certain cancers.

In addition, to obtain information about the molecular envelope and the arrangement of IGF-1R domains, the IGF-1R ectodomain in complex with Fabs (originated from MAbs

7C2 and 9E11) can be analysed by electron microscopy as performed by (Tulloch *et al.*, 1999) for the IR.

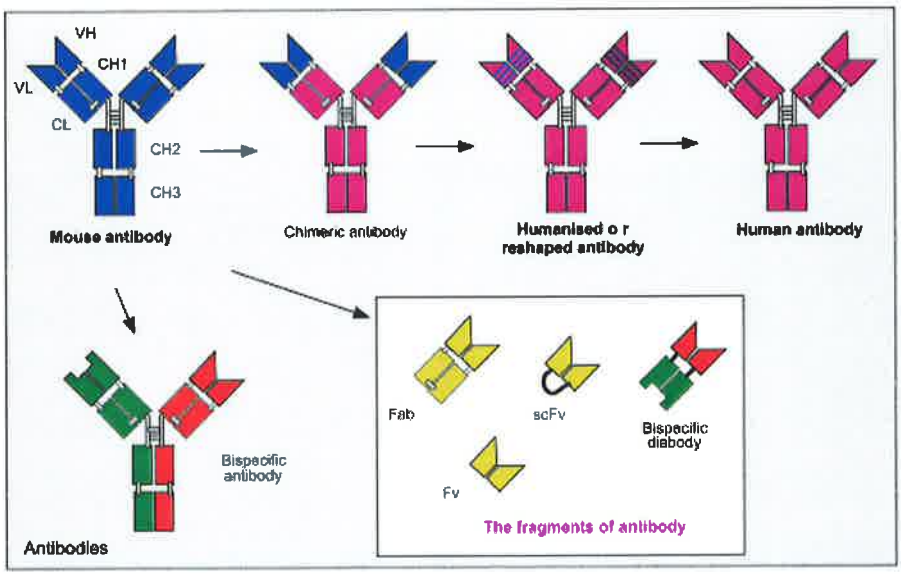

Figure 6.1 Schematic showing various antibody fragments of biotechnological and clinical interest.

Monoclonal antibodies from hybridomas are mouse antibodies. Recombinant chimeric antibodies are composed of mouse variable (V) regions attached to human constant (C) regions, but in humanised antibodies, only the CDR loops are from mouse antibodies. All-human antibodies can be assembled from human V regions (isolated by phage technology) and human C regions. Fv and scFv fragments, and diabodies include only V regions and can be cloned from hybridomas or obtained from phage libraries. Figure is adapted from (Holliger and Hoogenboom, 1998).

6.4. Future Directions

The work described here in this thesis also has raised several fundamental questions about the interaction of IGF-I and MAbs 7C2 and 9E11 with IGF-1R that could be investigated in future. The questions and the directions leading to possible answers are addressed as follows:

- *Are there any other residues in the IGF-1R that are involved in binding to the MAbs?*

Although the role of amino acids W79, L256 and I255 of the IGF-1R in binding to MAbs 7C2 and 9E11 were not tested in this study (we did not have the alanine mutants of these amino acids), they could be involved in binding to the MAbs. The amino acids L256 and I255 are very close to the epitope of MAbs 7C2 and 9E11 in the IGF-1R structure and the amino acid W79 could form a patch with the amino acids F241, F251 and F266 for binding to MAbs 7C2 and 9E11.

In addition to the amino acids in the epitope, which are involved in binding, there may be some other residues, which are in contact with the MAbs but are not critical for binding. These amino acids could be visualized using X-ray crystallography of antigen-Fab complexes (Van Regenmortel, 1989; Hewat *et al.*, 1997).

- *What are the specific factors, size or charge of the IGF-I C domain that regulates its binding to IGF-1R and what are the critical residues in the cysteine-rich domain of the IGF-1R and the IGF-I C domain for their interaction?*

Although our experiments indirectly showed that the C domain of IGF-I binds to F241 and F251or the nearby residues, additional experiments with a wider range of mutant IGFs can be designed to confirm this. Chimeric IGF-IICI and further mutants of it can be labelled with europium and their binding to each alanine mutants of the IGF-1R, kindly provided by Prof. J. Whittaker, Case Western Reserve University, Cleveland, Ohio, USA (Whittaker *et al.,* 2001), can be investigated individually. In addition, deletion of amino acids in IGF-I C domain to decrease the size and conversely the introduction of amino acids into the IGF-II C domain, will reveal whether domain size is important for regulating IGF-1R binding specificity. Moreover, to determine whether charge interactions are regulating binding specificity, the positively charged residues in the IGF-I C domain could be substituted with either neutral or negatively charged amino acids. On the other hand, the IGF-1R residues involved in the epitope of the MAbs can be replaced by positively charged amino acids. In addition, to investigate the contribution of the hydrophobic binding in the IGF-I C domain and IGF-1R interaction, the hydrophobic residues in the IGF-I C domain, such as A38 and P39,` can be mutated.

- *Which residues in the CDRs of MAbs 7C2 and 9E11 make contact to their epitope in IGF-1R cysteine-rich domain?*

Modelling of the MAbs could help to predict their binding sites. Particularly, since the three critical amino acids for binding the MAbs to IGF-1R are all phenylalanine, which is a hydrophobic amino acid, detection of the hydrophobic parts of the CDR on MAbs 7C2 and 9E11 molecule could lead to determining the binding sites.

- *Which residues in the IGF-1R are involved in binding to MAbs 5B6 and 4C6?*

As mentioned in Section 3.4.2, in addition to MAbs 7C2 and 9E11, two other IgG1κ MAbs were obtained in this study which were bound to the s-IGF-1R but did not detect the intact IGF-1R on P6 cells. It suggests that MAbs 4C6 and 5B6 could bind to a part of the s-IGF-1R, which is not accessible when the whole receptor is attached to the cell membrane. The epitope of these two MAbs could be mapped using alanine mutants of the IGF-1R (Whittaker *et al.*, 2001), which are secreted recombinant receptors. Determination of the binding sites for these MAbs could provide information about the organisation of the IGF-1R residues attached to the membrane.

- *Do MAbs 7C2 and 9E11 down-regulate the IGF-1R in the HT-29?*

As shown in Section 5.3.3, MAbs 7C2 and 9E11 down-regulated the IGF-1R in MCF-7 cells. In addition, it was shown that although these two MAbs inhibited the IGF-I but not IGF-II binding to the receptor (Figure 4.5), they inhibited the HT-29 cell proliferation induced by both IGF-I and IGF-II (Figure 5.2). It implies that MAbs 7C2 and 9E11 could down-regulate the IGF-1R in HT-29 cells as do in MCF-7 cells. This effect could be further studied as performed for MCF-7 cells.

6.5. Conclusion

The studies presented in this thesis were successful in developing two high affinity and specific mouse MAbs 7C2 and 9E11 against IGF-1R. The epitope of these MAbs on the IGF-1R were finely mapped and used in defining the IGFs and IGF-1R interaction.

MAbs 7C2 and 9E11 showed the potential to inhibit cancer cell proliferation and migration. They also induced the IGF-1R down-regulation in cancer cells. Based on these *in vitro* results, MAbs 7C2 and 9E11 are promising candidates for pre-clinical animal trials as anti-cancer agents to inhibit cancer cell growth and metastasis.

MAbs 7C2 and 9E11 were successfully utilised to detect the IGF-1R in a range of immunoassays. Therefore, they could be used as a diagnostic reagent to detect receptor expression in cells or tissue samples. Such agents will be important in the detection and treatment of IGF-responsive cancers in the future.

References

Abbott, A. M., Bueno, R., Pedrini, M. T., Murray, J. M. and Smith, R. J. (1992) Insulin-like growth factor I receptor gene structure. *J Biol Chem*, **267**(15): 10759-63.

Abuzzahab, M. J., Schneider, A., Goddard, A., Grigorescu, F., Lautier, C., Keller, E., Kiess, W., Klammt, J., Kratzsch, J., Osgood, D., Pfaffle, R., Raile, K., Seidel, B., Smith, R. J. and Chernausek, S. D. (2003) IGF-I receptor mutations resulting in intrauterine and postnatal growth retardation. *N Engl J Med*, **349**(23): 2211-22.

Adachi, Y., Lee, C. T., Coffee, K., Yamagata, N., Ohm, J. E., Park, K. H., Dikov, M. M., Nadaf, S. R., Arteaga, C. L. and Carbone, D. P. (2002) Effects of genetic blockade of the insulin-like growth factor receptor in human colon cancer cell lines. *Gastroenterology*, **123**(4): 1191-204.

Adams, T. E., Epa, V. C., Garrett, T. P. and Ward, C. W. (2000) Structure and function of the type 1 insulin-like growth factor receptor. *Cell Mol Life Sci*, **57**(7): 1050-93.

Adams, T. E., McKern, N. M. and Ward, C. W. (2004) Signalling by the type 1 insulin-like growth factor receptor: interplay with the epidermal growth factor receptor. *Growth Factors*, **22**(2): 89-95.

Allander, S. V., Illei, P. B., Chen, Y., Antonescu, C. R., Bittner, M., Ladanyi, M. and Meltzer, P. S. (2002) Expression profiling of synovial sarcoma by cDNA microarrays: association of ERBB2, IGFBP2, and ELF3 with epithelial differentiation. *Am J Pathol*, **161**(5): 1587-95.

Al-Lazikani, B., Lesk, A. M. and Chothia, C. (1997) Standard conformations for the canonical structures of immunoglobulins. *J Mol Biol*, **273**(4): 927-48.

Allen, N. E., Roddam, A. W., Allen, D. S., Fentiman, I. S., Dos Santos Silva, I., Peto, J., Holly, J. M. and Key, T. J. (2005) A prospective study of serum insulin-like growth factor-I (IGF-I), IGF-II, IGF-binding protein-3 and breast cancer risk. *Br J Cancer*, **92**(7): 1283-1287.

Amir-Zaltsman, Y., Mazor, O., Gayer, B., Scherz, A., Salomon, Y. and Kohen, F. (2000) Inhibitors of protein tyrosine phosphorylation: preliminary assessment of activity by time-resolved fluorescence. *Luminescence*, **15**(6): 377-80.

Amit, A. G., Mariuzza, R. A., Phillips, S. E. and Poljak, R. J. (1986) Three-dimensional structure of an antigen-antibody complex at 2.8 A resolution. *Science*, **233**(4765): 747-53.

Andersen, A. S., Kjeldsen, T., Wiberg, F. C., Christensen, P. M., Rasmussen, J. S., Norris, K., Moller, K. B. and Moller, N. P. (1990) Changing the insulin receptor to possess insulin-like growth factor I ligand specificity. *Biochemistry*, **29**(32): 7363-6.

Andrew, S. and Titus, J. (2004). Purification of immunoglobulin G. Current Protocols in Cell Biology. J. Bonifacino, M. Dasso, J. Lippincott-Schwartz, J. Harford and K. Yamada, John Wiley & Sons, Inc.

Armand, A. S., Lecolle, S., Launay, T., Pariset, C., Fiore, F., Della Gaspera, B., Birnbaum, D., Chanoine, C. and Charbonnier, F. (2004) IGF-II is up-regulated and myofibres are

hypertrophied in regenerating soleus of mice lacking FGF6. *Exp Cell Res*, **297**(1): 27-38.

Arteaga, C. and Osborne, C. (1989a) Growth inhibition of human breast cancer cells in vitro with an antibody against the type I somatomedin receptor. *Cancer Res*, **49(22)**: 6237-41.

Arteaga, C. L., Kitten, L. J., Coronado, E. B., Jacobs, S., Kull, F. C., Jr., Allred, D. C. and Osborne, C. K. (1989) Blockade of the type I somatomedin receptor inhibits growth of human breast cancer cells in athymic mice. *J Clin Invest*, **84**(5): 1418-23.

Arteaga, C. L. and Osborne, C. K. (1989b) Growth inhibition of human breast cancer cells in vitro with an antibody against the type I somatomedin receptor. *Cancer Res*, **49**(22): 6237-41.

Atassi, M. Z. (1984) Antigenic structures of proteins. Their determination has revealed important aspects of immune recognition and generated strategies for synthetic mimicking of protein binding sites. *Eur J Biochem*, **145**(1): 1-20.

Ausubel, F. M., Brent, R., Kingston, R. E., Moore, D. D., Seidman, J. G., Smith, J. A., Struhl, K., L.M., A., Coen, D. M., Varki, A. and Chanda, V. B. (1995). *Current protocols in molecular biology*. New York, John Wiley &sons, Inc.

Ayala, M., Balint, R. F., Fernandez-de-Cossio, L., Canaan-Haden, J. W., Larrick, J. W. and Gavilondo, J. V. (1995) Variable region sequence modulates periplasmic export of a single-chain Fv antibody fragment in Escherichia coli. *Biotechniques*, **18**(5): 832, 835-8, 840-2.

Aybay, C. (2003) Differential binding characteristics of protein G and protein A for Fc fragments of papain-digested mouse IgG. *Immunol Lett*, **85**(3): 231-5.

Bach, L. A., Hsieh, S., Sakano, K., Fujiwara, H., Perdue, J. F. and Rechler, M. M. (1993) Binding of mutants of human insulin-like growth factor II to insulin-like growth factor binding proteins 1-6. *J Biol Chem*, **268**(13): 9246-54.

Bahr, C. and Groner, B. (2004) The insulin like growth factor-1 receptor (IGF-1R) as a drug target: novel approaches to cancer therapy. *Growth Horm IGF Res*, **14**(4): 287-95.

Bajaj, M., Waterfield, M. D., Schlessinger, J., Taylor, W. R. and Blundell, T. (1987) On the tertiary structure of the extracellular domains of the epidermal growth factor and insulin receptors. *Biochim Biophys Acta*, **916**(2): 220-6.

Baker, J., Liu, J. P., Robertson, E. J. and Efstratiadis, A. (1993) Role of insulin-like growth factors in embryonic and postnatal growth. *Cell*, **75**(1): 73-82.

Banner, D. W., D'Arcy, A., Janes, W., Gentz, R., Schoenfeld, H. J., Broger, C., Loetscher, H. and Lesslauer, W. (1993) Crystal structure of the soluble human 55 kd TNF receptor-human TNF beta complex: implications for TNF receptor activation. *Cell*, **73**(3): 431-45.

Barbieri, M., Bonafe, M., Franceschi, C. and Paolisso, G. (2003) Insulin/IGF-I-signaling pathway: an evolutionarily conserved mechanism of longevity from yeast to humans. *Am J Physiol Endocrinol Metab*, **285**(5): E1064-71.

Baselga, J. (2001) Clinical trials of Herceptin(trastuzumab). *Eur J Cancer*, **37**(Suppl 1): S18-24.

Baselga, J., Tripathy, D., Mendelsohn, J., Baughman, S., Benz, C. C., Dantis, L., Sklarin, N. T., Seidman, A. D., Hudis, C. A., Moore, J., Rosen, P. P., Twaddell, T., Henderson, I. C. and Norton, L. (1996) Phase II study of weekly intravenous recombinant humanized anti-p185HER2 monoclonal antibody in patients with HER2/neu-overexpressing metastatic breast cancer. *J Clin Oncol*, **14**(3): 737-44.

Baserga, R. (1995) The insulin-like growth factor I receptor:a key to tumor growth ? *Cancer Res*, **55(2)**.

Baserga, R., Hongo, A., Rubini, M., Prisco, M. and Valentinis, B. (1997) The IGF-I receptor in cell growth, transformation and apoptosis. *Biochim Biophys Acta*, **1332(3)**: F105-26.

Baxter, R. C. (1995) Insulin-like growth factor binding proteins as glucoregulators. *Metabolism*, **44**(10 Suppl 4): 12-7.

Bayne, M. L., Applebaum, J., Chicchi, G. G., Hayes, N. S., Green, B. G. and Cascieri, M. A. (1988) Structural analogs of human insulin-like growth factor I with reduced affinity for serum binding proteins and the type 2 insulin-like growth factor receptor. *J Biol Chem*, **263**(13): 6233-9.

Bayne, M. L., Applebaum, J., Chicchi, G. G., Miller, R. E. and Cascieri, M. A. (1990) The roles of tyrosines 24, 31, and 60 in the high affinity binding of insulin-like growth factor-I to the type 1 insulin-like growth factor receptor. *J Biol Chem*, **265**(26): 15648-52.

Bayne, M. L., Applebaum, J., Underwood, D., Chicchi, G. G., Green, B. G., Hayes, N. S. and Cascieri, M. A. (1989) The C region of human insulin-like growth factor (IGF) I is required for high affinity binding to the type 1 IGF receptor. *J Biol Chem*, **264**(19): 11004-8.

Beech, D. J., Parekh, N. and Pang, Y. (2001) Insulin-like growth factor-I receptor antagonism results in increased cytotoxicity of breast cancer cells to doxorubicin and taxol. *Oncol Rep*, **8**(2): 325-9.

Belfiore, A., Pandini, G., Vella, V., Squatrito, S. and Vigneri, R. (1999) Insulin/IGF-I hybrid receptors play a major role in IGF-I signaling in thyroid cancer. *Biochimie*, **81**(4): 403-7.

Benini, S., Manara, M. C., Baldini, N., Cerisano, V., Massimo, S., Mercuri, M., Lollini, P. L., Nanni, P., Picci, P. and Scotlandi, K. (2001) Inhibition of insulin-like growth factor I receptor increases the antitumor activity of doxorubicin and vincristine against Ewing's sarcoma cells. *Clin Cancer Res*, **7**(6): 1790-7.

Benito, M., Valverde, A. M. and Lorenzo, M. (1996) IGF-I: a mitogen also involved in differentiation processes in mammalian cells. *Int J Biochem Cell Biol*, **28**(5): 499-510.

Benjamin, D. C., Berzofsky, J. A., East, I. J., Gurd, F. R., Hannum, C., Leach, S. J., Margoliash, E., Michael, J. G., Miller, A., Prager, E. M. and et al. (1984) The antigenic structure of proteins: a reappraisal. *Annu Rev Immunol 1984;2:67-101.*

Bentley, G., Dodson, E., Dodson, G., Hodgkin, D. and Mercola, D. (1976) Structure of insulin in 4-zinc insulin. *Nature*, **261**(5556): 166-8.

Bergmann, U., Funatomi, H., Yokoyama, M., Beger, H. G. and Korc, M. (1995) Insulin-like growth factor I overexpression in human pancreatic cancer: evidence for autocrine and paracrine roles. *Cancer Res*, **55**(10): 2007-11.

Biddle, C., Li, C. H., Schofield, P. N., Tate, V. E., Hopkins, B., Engstrom, W., Huskisson, N. S. and Graham, C. F. (1988) Insulin-like growth factors and the multiplication of Tera-2, a human teratoma-derived cell line. *J Cell Sci*, **90**(Pt 3): 475-84.

Blakesley, V. A., Stannard, B. S., Kalebic, T., Helman, L. J. and LeRoith, D. (1997) Role of the IGF-I receptor in mutagenesis and tumor promotion. *J Endocrinol*, **152**(3): 339-44.

Blum, G., Gazit, A. and Levitzki, A. (2000) Substrate competitive inhibitors of IGF-1 receptor kinase. *Biochemistry*, **39**(51): 15705-12.

Blum, G., Gazit, A. and Levitzki, A. (2003) Development of new insulin-like growth factor-1 receptor kinase inhibitors using catechol mimics. *J Biol Chem*, **278**(42): 40442-54.

Blundell, T. L., Bedarkar, S. and Humbel, R. E. (1983) Tertiary structures, receptor binding, and antigenicity of insulinlike growth factors. *Fed Proc*, **42**(9): 2592-7.

Blundell, T. L., Bedarkar, S., Rinderknecht, E. and Humbel, R. E. (1978) Insulin-like growth factor: a model for tertiary structure accounting for immunoreactivity and receptor binding. *Proc Natl Acad Sci U S A*, **75**(1): 180-4.

Bohula, E. A., Playford, M. P. and Macaulay, V. M. (2003a) Targeting the type 1 insulin-like growth factor receptor as anti-cancer treatment. *Anticancer Drugs*, **14**(9): 669-82.

Bohula, E. A., Salisbury, A. J., Sohail, M., Playford, M. P., Riedemann, J., Southern, E. M. and Macaulay, V. M. (2003b) The efficacy of small interfering RNAs targeted to the type 1 insulin-like growth factor receptor (IGF1R) is influenced by secondary structure in the IGF1R transcript. *J Biol Chem*, **278**(18): 15991-7.

Boring, C. C., Squires, T. S., Tong, T. and Montgomery, S. (1994) Cancer statistics, 1994. *CA Cancer J Clin*, **44**(1): 7-26.

Boulianne, G. L., Hozumi, N. and Shulman, M. J. (1984) Production of functional chimaeric mouse/human antibody. *Nature*, **312**(5995): 643-6.

Bradford, M. M. (1976) A rapid and sensitive method for the quantitation of microgram quantities of protein utilizing the principle of protein-dye binding. *Anal Biochem*, **72**: 248-54.

Branden, C. and Tooze, J. (1991). *Introduction to protein structure*. New York, Garland Publishing, Inc.

Branden, C. and Tooze, J. (1999). *Introduction to Protein Structure*. London, Garland publishing, Inc.

Brandt, J., Andersen, A. S. and Kristensen, C. (2001) Dimeric fragment of the insulin receptor alpha-subunit binds insulin with full holoreceptor affinity. *J Biol Chem*, **276**(15): 12378-84.

Brechbiel, M. W. and Waldmann, T. A. (1999) Anti-HER2 Radioimmunotherapy. *Breast Dis 1999;11:125-32.*

Brekke, O. H. and Sandlie, I. (2003) Therapeutic antibodies for human diseases at the dawn of the twenty-first century. *Nat Rev Drug Discov*, **2**(1): 52-62.

Brodt, P., Samani, A. and Navab, R. (2000) Inhibition of the type I insulin-like growth factor receptor expression and signaling: novel strategies for antimetastatic therapy. *Biochem Pharmacol*, **60**(8): 1101-7.

Brzozowski, A. M., Dodson, E. J., Dodson, G. G., Murshudov, G. N., Verma, C., Turkenburg, J. P., de Bree, F. M. and Dauter, Z. (2002) Structural origins of the functional divergence of human insulin-like growth factor-I and insulin. *Biochemistry*, **41**(30): 9389-97.

Bubendorf, L., Kolmer, M., Kononen, J., Koivisto, P., Mousses, S., Chen, Y., Mahlamaki, E., Schraml, P., Moch, H., Willi, N., Elkahloun, A. G., Pretlow, T. G., Gasser, T. C., Mihatsch, M. J., Sauter, G. and Kallioniemi, O. P. (1999) Hormone therapy failure in human prostate cancer: analysis by complementary DNA and tissue microarrays. *J Natl Cancer Inst*, **91**(20): 1758-64.

Burfeind, P., Chernicky, C. L., Rininsland, F. and Ilan, J. (1996) Antisense RNA to the type I insulin-like growth factor receptor suppresses tumor growth and prevents invasion by rat prostate cancer cells in vivo. *Proc Natl Acad Sci U S A*, **93**(14): 7263-8.

Burtrum, D., Zhu, Z., Lu, D., Anderson, D. M., Prewett, M., Pereira, D. S., Bassi, R., Abdullah, R., Hooper, A. T., Koo, H., Jimenez, X., Johnson, D., Apblett, R., Kussie, P., Bohlen, P., Witte, L., Hicklin, D. J. and Ludwig, D. L. (2003) A fully human monoclonal antibody to the insulin-like growth factor I receptor blocks ligand-dependent signaling and inhibits human tumor growth in vivo. *Cancer Res*, **63**(24): 8912-21.

Byrd, J. C., Devi, G. R., de Souza, A. T., Jirtle, R. L. and MacDonald, R. G. (1999) Disruption of ligand binding to the insulin-like growth factor II/mannose 6-phosphate receptor by cancer-associated missense mutations. *J Biol Chem*, **274**(34): 24408-16.

Cantrell, D. A. (2001) Phosphoinositide 3-kinase signalling pathways. *J Cell Sci*, **114**(Pt 8): 1439-45.

Canziani, G., Zhang, W., Cines, D., Rux, A., Willis, S., Cohen, G., Eisenberg, R. and Chaiken, I. (1999) Exploring biomolecular recognition using optical biosensors. *Methods*, **19**(2): 253-69.

Cara, J. F., Mirmira, R. G., Nakagawa, S. H. and Tager, H. S. (1990) An insulin-like growth factor I/insulin hybrid exhibiting high potency for interaction with the type I insulin-like growth factor and insulin receptors of placental plasma membranes. *J Biol Chem*, **265**(29): 17820-5.

Carrasquillo, J. A., Krohn, K. A., Beaumier, P., McGuffin, R. W., Brown, J. P., Hellstrom, K. E., Hellstrom, I. and Larson, S. M. (1984) Diagnosis of and therapy for solid tumors with radiolabeled antibodies and immune fragments. *Cancer Treat Rep*, **68**(1): 317-28.

Carter, P. (2001) Improving the efficacy of antibody-based cancer therapies. *Nat Rev Cancer*, **1**(2): 118-29.

Cascieri, M. A., Chicchi, G. G., Applebaum, J., Green, B. G., Hayes, N. S. and Bayne, M. L. (1989) Structural analogs of human insulin-like growth factor (IGF) I with altered affinity for type 2 IGF receptors. *J Biol Chem*, **264**(4): 2199-202.

Cascieri, M. A., Chicchi, G. G., Applebaum, J., Hayes, N. S., Green, B. G. and Bayne, M. L. (1988) Mutants of human insulin-like growth factor I with reduced affinity for the type 1 insulin-like growth factor receptor. *Biochemistry*, **27**(9): 3229-33.

Casella, S. J., Han, V. K., D'Ercole, A. J., Svoboda, M. E. and Van Wyk, J. J. (1986) Insulin-like growth factor II binding to the type I somatomedin receptor. Evidence for two high affinity binding sites. *J Biol Chem*, **261**(20): 9268-73.

Chakravarti, A., Loeffler, J. S. and Dyson, N. J. (2002) Insulin-like growth factor receptor I mediates resistance to anti-epidermal growth factor receptor therapy in primary human glioblastoma cells through continued activation of phosphoinositide 3-kinase signaling. *Cancer Res*, **62**(1): 200-7.

Chang, L. and Karin, M. (2001) Mammalian MAP kinase signalling cascades. *Nature*, **410**(6824): 37-40.

Chappell, S. A., Walsh, T., Walker, R. A. and Shaw, J. A. (1997) Loss of heterozygosity at the mannose 6-phosphate insulin-like growth factor 2 receptor gene correlates with poor differentiation in early breast carcinomas. *Br J Cancer*, **76**(12): 1558-61.

Chardes, T., Villard, S., Ferrieres, G., Piechaczyk, M., Cerutti, M., Devauchelle, G. and Pau, B. (1999) Efficient amplification and direct sequencing of mouse variable regions from any immunoglobulin gene family. *FEBS Lett*, **452**(3): 386-94.

Chaudhary, V. K., Batra, J. K., Gallo, M. G., Willingham, M. C., FitzGerald, D. J. and Pastan, I. (1990) A rapid method of cloning functional variable-region antibody genes in Escherichia coli as single-chain immunotoxins. *Proc Natl Acad Sci U S A*, **87**(3): 1066-70.

Chen, J. W., Ledet, T., Orskov, H., Jessen, N., Lund, S., Whittaker, J., De Meyts, P., Larsen, M. B., Christiansen, J. S. and Frystyk, J. (2003) A highly sensitive and specific assay for determination of IGF-I bioactivity in human serum. *Am J Physiol Endocrinol Metab*, **284**(6): E1149-55.

Chien, N. C., Roberts, V. A., Giusti, A. M., Scharff, M. D. and Getzoff, E. D. (1989) Significant structural and functional change of an antigen-binding site by a distant amino acid substitution: proposal of a structural mechanism. *Proc Natl Acad Sci U S A*, **86**(14): 5532-6.

Chothia, C., Lesk, A. M., Tramontano, A., Levitt, M., Smith-Gill, S. J., Air, G., Sheriff, S., Padlan, E. A., Davies, D., Tulip, W. R. and et al. (1989) Conformations of immunoglobulin hypervariable regions. *Nature*, **342**(6252): 877-83.

Cleland, J. L., Lam, X., Kendrick, B., Yang, J., Yang, T. H., Overcashier, D., Brooks, D., Hsu, C. and Carpenter, J. F. (2001) A specific molar ratio of stabilizer to protein is required for storage stability of a lyophilized monoclonal antibody. *J Pharm Sci*, **90**(3): 310-21.

Cohen, B. D., Baker, D. A., Soderstrom, C., Tkalcevic, G., Rossi, A. M., Miller, P. E., Tengowski, M. W., Wang, F., Gualberto, A., Beebe, J. S. and Moyer, J. D. (2005) Combination therapy enhances the inhibition of tumor growth with the fully human

anti-type 1 insulin-like growth factor receptor monoclonal antibody CP-751,871. *Clin Cancer Res*, **11**(5): 2063-73.

Cohen, B. D., Beebe, J., Miller, P. E., J.D., M., Corvalan, J. R. and Gallo, M. (2002). Antibodies to insulin-like growth facotr I receptor (WO 02/053596 A2). U.S.A.

Colman, P. M. (1988) Structure of antibody-antigen complexes: implications for immune recognition. *Adv Immunol 1988;43:99-132.*

Coloma, M. J., Hastings, A., Wims, L. A. and Morrison, S. L. (1992) Novel vectors for the expression of antibody molecules using variable regions generated by polymerase chain reaction. *J Immunol Methods*, **152**(1): 89-104.

Coloma, M. J., Larrick, J. W., Ayala, M. and Gavilondo-Cowley, J. V. (1991) Primer design for the cloning of immunoglobulin heavy-chain leader-variable regions from mouse hybridoma cells using the PCR. *Biotechniques*, **11**(2): 152-4, 156.

Condorelli, G., Bueno, R. and Smith, R. J. (1994) Two alternatively spliced forms of the human insulin-like growth factor I receptor have distinct biological activities and internalization kinetics. *J Biol Chem*, **269**(11): 8510-6.

Cooke, R. M., Harvey, T. S. and Campbell, I. D. (1991) Solution structure of human insulin-like growth factor 1: a nuclear magnetic resonance and restrained molecular dynamics study. *Biochemistry*, **30**(22): 5484-91.

Coppola, D., Ferber, A., Miura, M., Sell, C., D'Ambrosio, C., Rubin, R. and Baserga, R. (1994) A functional insulin-like growth factor I receptor is required for the mitogenic and transforming activities of the epidermal growth factor receptor. *Mol Cell Biol*, **14**(7): 4588-95.

Cosgrove, L., Lovrecz, G. O., Verkuylen, A., Cavaleri, L., Black, L. A., Bentley, J. D., Howlett, G. J., Gray, P. P., Ward, C. W. and McKern, N. M. (1995) Purification and properties of insulin receptor ectodomain from large-scale mammalian cell culture. *Protein Expr Purif*, **6**(6): 789-98.

Cullen, K. J., Yee, D., Sly, W. S., Perdue, J., Hampton, B., Lippman, M. E. and Rosen, N. (1990) Insulin-like growth factor receptor expression and function in human breast cancer. *Cancer Res*, **50**(1): 48-53.

Czech, M. P. (1982) Structural and functional homologies in the receptors for insulin and the insulin-like growth factors. *Cell*, **31**(1): 8-10.

Czech, M. P. (1989) Signal transmission by the insulin-like growth factors. *Cell*, **59**(2): 235-8.

D'Ambrosio, C., Ferber, A., Resnicoff, M. and Baserga, R. (1996) A soluble insulin-like growth factor I receptor that induces apoptosis of tumor cells in vivo and inhibits tumorigenesis. *Cancer Res*, **56**(17): 4013-20.

Daughaday, W. H. and Rotwein, P. (1989) Insulin-like growth factors I and II. Peptide, messenger ribonucleic acid and gene structures, serum, and tissue concentrations. *Endocr Rev*, **10**(1): 68-91.

De Meyts, P. and Whittaker, J. (2002) Structural biology of insulin and IGF1 receptors: implications for drug design. *Nat Rev Drug Discov*, **1**(10): 769-83.

de Pagter-Holthuizen, P., van Schaik, F. M., Verduijn, G. M., van Ommen, G. J., Bouma, B. N., Jansen, M. and Sussenbach, J. S. (1986) Organization of the human genes for insulin-like growth factors I and II. *FEBS Lett*, **195**(1-2): 179-84.

De Wolf, E., Gill, R., Geddes, S., Pitts, J., Wollmer, A. and Grotzinger, J. (1996) Solution structure of a mini IGF-1. *Protein Sci*, **5**(11): 2193-202.

DeChiara, T. M., Efstratiadis, A. and Robertson, E. J. (1990) A growth-deficiency phenotype in heterozygous mice carrying an insulin-like growth factor II gene disrupted by targeting. *Nature*, **345**(6270): 78-80.

Denley, A. (2004). Investigation into the molecular specificity of the IGFs: A chimeric approach. School of Molecular and Biomedical Science, The University of Adelaide.

Denley, A., Bonython, E. R., Booker, G. W., Cosgrove, L. J., Forbes, B. E., Ward, C. W. and Wallace, J. C. (2004) Structural determinants for high-affinity binding of insulin-like growth factor II to insulin receptor (IR)-A, the exon 11 minus isoform of the IR. *Mol Endocrinol*, **18**(10): 2502-12.

Denley, A., Cosgrove, L. J., Booker, G. W., Wallace, J. C. and Forbes, B. E. (2005a) Molecular interactions of the IGF system. *Cytokine Growth Factor Rev*, **16**(4-5): 421-39.

Denley, A., Wallace, J. C., Cosgrove, L. J. and Forbes, B. E. (2003) The insulin receptor isoform exon 11- (IR-A) in cancer and other diseases: a review. *Horm Metab Res*, **35**(11-12): 778-85.

Denley, A., Wang, C. C., McNeil, K. A., Walenkamp, M. J., van Duyvenvoorde, H., Wit, J. M., Wallace, J. C., Norton, R. S., Karperien, M. and Forbes, B. E. (2005b) Structural and functional characteristics of the Val44Met insulin-like growth factor I missense mutation: correlation with effects on growth and development. *Mol Endocrinol*, **19**(3): 711-21.

Desplancq, D., King, D. J., Lawson, A. D. and Mountain, A. (1994) Multimerization behaviour of single chain Fv variants for the tumour-binding antibody B72.3. *Protein Eng*, **7**(8): 1027-33.

Devi, G. R., De Souza, A. T., Byrd, J. C., Jirtle, R. L. and MacDonald, R. G. (1999) Altered ligand binding by insulin-like growth factor II/mannose 6-phosphate receptors bearing missense mutations in human cancers. *Cancer Res*, **59**(17): 4314-9.

Diamandis, E. P. and Christopoulos, T. K. (1996). *Immunoassay*. San Diego, Academic Press.

Dickinson, C. D., Veerapandian, B., Dai, X. P., Hamlin, R. C., Xuong, N. H., Ruoslahti, E. and Ely, K. R. (1994) Crystal structure of the tenth type III cell adhesion module of human fibronectin. *J Mol Biol*, **236**(4): 1079-92.

Dickson, E. F., Pollak, A. and Diamandis, E. P. (1995) Time-resolved detection of lanthanide luminescence for ultrasensitive bioanalytical assays. *J Photochem Photobiol B*, **27**(1): 3-19.

Dunn, S. E., Hardman, R. A., Kari, F. W. and Barrett, J. C. (1997) Insulin-like growth factor 1 (IGF-1) alters drug sensitivity of HBL100 human breast cancer cells by inhibition of apoptosis induced by diverse anticancer drugs. *Cancer Res*, **57**(13): 2687-93.

Dupont, J. and LeRoith, D. (2001) Insulin and insulin-like growth factor I receptors: similarities and differences in signal transduction. *Horm Res*, **55**(Suppl 2): 22-6.

Durai, R., Yang, W., Gupta, S., Seifalian, A. M. and Winslet, M. C. (2005) The role of the insulin-like growth factor system in colorectal cancer: review of current knowledge. *Int J Colorectal Dis*, **20**(3): 203-220.

Ebina, Y., Ellis, L., Jarnagin, K., Edery, M., Graf, L., Clauser, E., Ou, J. H., Masiarz, F., Kan, Y. W., Goldfine, I. D. and et al. (1985) The human insulin receptor cDNA: the structural basis for hormone-activated transmembrane signalling. *Cell*, **40**(4): 747-58.

Elleman, T. C., Frenkel, M. J., Hoyne, P. A., McKern, N. M., Cosgrove, L., Hewish, D. R., Jachno, K. M., Bentley, J. D., Sankovich, S. E. and Ward, C. W. (2000) Mutational analysis of the N-linked glycosylation sites of the human insulin receptor. *Biochem J*, **347**(Pt 3): 771-9.

Erbay, E., Park, I. H., Nuzzi, P. D., Schoenherr, C. J. and Chen, J. (2003) IGF-II transcription in skeletal myogenesis is controlled by mTOR and nutrients. *J Cell Biol*, **163**(5): 931-6.

Esteva, F. J. (2004) Monoclonal antibodies, small molecules, and vaccines in the treatment of breast cancer. *Oncologist*, **9**(Suppl 3): 4-9.

Estrov, Z., Meir, R., Barak, Y., Zaizov, R. and Zadik, Z. (1991) Human growth hormone and insulin-like growth factor-1 enhance the proliferation of human leukemic blasts. *J Clin Oncol*, **9**(3): 394-9.

Fagerstam, L. G., Frostell, A., Karlsson, R., Kullman, M., Larsson, A., Malmqvist, M. and Butt, H. (1990) Detection of antigen-antibody interactions by surface plasmon resonance. Application to epitope mapping. *J Mol Recognit*, **3**(5-6): 208-14.

Favelyukis, S., Till, J. H., Hubbard, S. R. and Miller, W. T. (2001) Structure and autoregulation of the insulin-like growth factor 1 receptor kinase. *Nat Struct Biol*, **8**(12): 1058-63.

Firth, S. M. and Baxter, R. C. (2002) Cellular actions of the insulin-like growth factor binding proteins. *Endocr Rev*, **23**(6): 824-54.

Forbes, B. E., McNeil, K. A., Scott, C. D., Surinya, K. H., Cosgrove, L. J. and Wallace, J. C. (2001) Contribution of residues A54 and L55 of the human insulin-like growth factor-II (IGF-II) A domain to Type 2 IGF receptor binding specificity. *Growth Factors*, **19**(3): 163-73.

Forbes, B. E., Turner, D., Hodge, S. J., McNeil, K. A., Forsberg, G. and Wallace, J. C. (1998) Localization of an insulin-like growth factor (IGF) binding site of bovine IGF binding protein-2 using disulfide mapping and deletion mutation analysis of the C-terminal domain. *J Biol Chem*, **273**(8): 4647-52.

Foulstone, E., Prince, S., Zaccheo, O., Burns, J., Harper, J., Jacobs, C., Church, D. and Hassan, A. (2005) Insulin-like growth factor ligands, receptors, and binding proteins in cancer. *J Pathol*, **205**(2): 145-153.

Frankel, A. E., Houston, L. L., Issell, B. F. and Fathman, G. Prospects for immunotoxin therapy in cancer. *Annu Rev Med 1986;37:125-42.*

Frasca, F., Pandini, G., Scalia, P., Sciacca, L., Mineo, R., Costantino, A., Goldfine, I. D., Belfiore, A. and Vigneri, R. (1999) Insulin receptor isoform A, a newly recognized, high-affinity insulin-like growth factor II receptor in fetal and cancer cells. *Mol Cell Biol*, **19**(5): 3278-88.

Fuller, G. N., Rhee, C. H., Hess, K. R., Caskey, L. S., Wang, R., Bruner, J. M., Yung, W. K. and Zhang, W. (1999) Reactivation of insulin-like growth factor binding protein 2 expression in glioblastoma multiforme: a revelation by parallel gene expression profiling. *Cancer Res*, **59**(17): 4228-32.

Furlanetto, R. W. and DiCarlo, J. N. (1984) Somatomedin-C receptors and growth effects in human breast cells maintained in long-term tissue culture. *Cancer Res*, **44**(5): 2122-8.

Furlanetto, R. W., Harwell, S. E. and Baggs, R. B. (1993) Effects of insulin-like growth factor receptor inhibition on human melanomas in culture and in athymic mice. *Cancer Res*, **53**(11): 2522-6.

Garcia-Echeverria, C., Pearson, M. A., Marti, A., Meyer, T., Mestan, J., Zimmermann, J., Gao, J., Brueggen, J., Capraro, H. G., Cozens, R., Evans, D. B., Fabbro, D., Furet, P., Porta, D. G., Liebetanz, J., Martiny-Baron, G., Ruetz, S. and Hofmann, F. (2004) In vivo antitumor activity of NVP-AEW541-A novel, potent, and selective inhibitor of the IGF-IR kinase. *Cancer Cell*, **5**(3): 231-9.

Garrett, T. P., McKern, N. M., Lou, M., Frenkel, M. J., Bentley, J. D., Lovrecz, G. O., Elleman, T. C., Cosgrove, L. J. and Ward, C. W. (1998) Crystal structure of the first three domains of the type-1 insulin-like growth factor receptor. *Nature*, **394**(6691): 395-9.

Garrouste, F. L., Remacle-Bonnet, M. M., Lehmann, M. M., Marvaldi, J. L. and Pommier, G. J. (1997) Up-regulation of insulin/insulin-like growth factor-I hybrid receptors during differentiation of HT29-D4 human colonic carcinoma cells. *Endocrinology*, **138**(5): 2021-32.

Gavilondo-Cowley, J. V., Coloma, M. J., Vazquez, J., Ayala, M., Macias, A., Fry, K. E. and Larrick, J. W. (1990) Specific amplification of rearranged immunoglobulin variable region genes from mouse hybridoma cells. *Hybridoma*, **9**(5): 407-17.

Gazi, L., Lopez-Gimenez, J. F., Rudiger, M. P. and Strange, P. G. (2003) Constitutive oligomerization of human D2 dopamine receptors expressed in Spodoptera frugiperda 9 (Sf9) and in HEK293 cells. Analysis using co-immunoprecipitation and time-resolved fluorescence resonance energy transfer. *Eur J Biochem*, **270**(19): 3928-38.

Gicquel, C., Bertagna, X., Schneid, H., Francillard-Leblond, M., Luton, J. P., Girard, F. and Le Bouc, Y. (1994) Rearrangements at the 11p15 locus and overexpression of insulin-like growth factor-II gene in sporadic adrenocortical tumors. *J Clin Endocrinol Metab*, **78**(6): 1444-53.

Gill, R., Wallach, B., Verma, C., Urso, B., De Wolf, E., Grotzinger, J., Murray-Rust, J., Pitts, J., Wollmer, A., De Meyts, P. and Wood, S. (1996) Engineering the C-region of human insulin-like growth factor-1: implications for receptor binding. *Protein Eng*, **9**(11): 1011-9.

Giovannucci, E., Pollak, M. N., Platz, E. A., Willett, W. C., Stampfer, M. J., Majeed, N., Colditz, G. A., Speizer, F. E. and Hankinson, S. E. (2000) A prospective study of

plasma insulin-like growth factor-1 and binding protein-3 and risk of colorectal neoplasia in women. *Cancer Epidemiol Biomarkers Prev*, **9**(4): 345-9.

Giudicelli, V., Chaume, D. and Lefranc, M. P. (2004) IMGT/V-QUEST, an integrated software program for immunoglobulin and T cell receptor V-J and V-D-J rearrangement analysis. *Nucleic Acids Res*, **32**(Web Server issue): W435-40.

Goetsch, L., Corvaia, N. and Leger, O. (2003). Novel anti-IGF-IR antibodies and uses thereof (WO 03/059951 A2). France.

Goetsch, L., Gonzalez, A., Leger, O., Beck, A., Pauwels, P. J., Haeuw, J. F. and Corvaia, N. (2005) A recombinant humanized anti-insulin-like growth factor receptor type I antibody (h7C10) enhances the antitumor activity of vinorelbine and anti-epidermal growth factor receptor therapy against human cancer xenografts. *Int J Cancer*, **113**(2): 316-28.

Goldenberg, D. M. (2002) Targeted therapy of cancer with radiolabeled antibodies. *J Nucl Med*, **43**(5): 693-713.

Gonzales, N. R., De Pascalis, R., Schlom, J. and Kashmiri, S. V. (2005) Minimizing the Immunogenicity of Antibodies for Clinical Application. *Tumour Biol*, **26**(1): 31-43.

Gooch, J. L., Van Den Berg, C. L. and Yee, D. (1999) Insulin-like growth factor (IGF)-I rescues breast cancer cells from chemotherapy-induced cell death--proliferative and anti-apoptotic effects. *Breast Cancer Res Treat*, **56**(1): 1-10.

Goyal, J., Smith, K. M., Cowan, J. M., Wazer, D. E., Lee, S. W. and Band, V. (1998) The role for NES1 serine protease as a novel tumor suppressor. *Cancer Res*, **58**(21): 4782-6.

Graus, Y., Kopetzki, E., Kuenkele, K. P., Mundigl, O., Parren, P., F., R., Schumacher, R., D., W. J. and Vugt, M. V. (2005). Antibodies against insulin-like growth factor 1 receptor and uses thereof (US 2005/0008642 A1). U.S.A.

Gray, S. G., Stenfeldt Mathiasen, I. and De Meyts, P. (2003) The insulin-like growth factors and insulin-signalling systems: an appealing target for breast cancer therapy? *Horm Metab Res*, **35**(11-12): 857-71.

Guler, H. P., Zapf, J., Schmid, C. and Froesch, E. R. (1989) Insulin-like growth factors I and II in healthy man. Estimations of half-lives and production rates. *Acta Endocrinol (Copenh)*, **121**(6): 753-8.

Guo, Y. S., Narayan, S., Yallampalli, C. and Singh, P. (1992) Characterization of insulinlike growth factor I receptors in human colon cancer. *Gastroenterology*, **102**(4 Pt 1): 1101-8.

Gustafson, T. A. and Rutter, W. J. (1990) The cysteine-rich domains of the insulin and insulin-like growth factor I receptors are primary determinants of hormone binding specificity. Evidence from receptor chimeras. *J Biol Chem*, **265**(30): 18663-7.

Hailey, J., Maxwell, E., Koukouras, K., Bishop, W. R., Pachter, J. A. and Wang, Y. (2002) Neutralizing anti-insulin-like growth factor receptor 1 antibodies inhibit receptor function and induce receptor degradation in tumor cells. *Mol Cancer Ther*, **1**(14): 1349-53.

Hakam, A., Yeatman, T. J., Lu, L., Mora, L., Marcet, G., Nicosia, S. V., Karl, R. C. and Coppola, D. (1999) Expression of insulin-like growth factor-1 receptor in human colorectal cancer. *Hum Pathol*, **30**(10): 1128-33.

Hampton, B., Burgess, W. H., Marshak, D. R., Cullen, K. J. and Perdue, J. F. (1989) Purification and characterization of an insulin-like growth factor II variant from human plasma. *J Biol Chem*, **264**(32): 19155-60.

Han, V. K., Lund, P. K., Lee, D. C. and D'Ercole, A. J. (1988) Expression of somatomedin/insulin-like growth factor messenger ribonucleic acids in the human fetus: identification, characterization, and tissue distribution. *J Clin Endocrinol Metab*, **66**(2): 422-9.

Hankinson, S. E., Willett, W. C., Colditz, G. A., Hunter, D. J., Michaud, D. S., Deroo, B., Rosner, B., Speizer, F. E. and Pollak, M. (1998) Circulating concentrations of insulin-like growth factor-I and risk of breast cancer. *Lancet*, **351**(9113): 1393-6.

Happerfield, L. C., Miles, D. W., Barnes, D. M., Thomsen, L. L., Smith, P. and Hanby, A. (1997) The localization of the insulin-like growth factor receptor 1 (IGFR-1) in benign and malignant breast tissue. *J Pathol*, **183**(4): 412-7.

Harlow, E. and Lane, D. (1988). *Antibodies: a laboratory manual*. NY, Cold Spring Harbor Laboratory.

Harlow, E. and Lane, D. (1999). *Using Antibodies: a laboratory manual*. Cold Spring Harbor, NY, Cold Spring Harbor Laboratory Press.

Harma, H., Soukka, T., Lonnberg, S., Paukkunen, J., Tarkkinen, P. and Lovgren, T. (2000) Zeptomole detection sensitivity of prostate-specific antigen in a rapid microtitre plate assay using time-resolved fluorescence. *Luminescence*, **15**(6): 351-5.

Harrington, E. A., Bennett, M. R., Fanidi, A. and Evan, G. I. (1994) c-Myc-induced apoptosis in fibroblasts is inhibited by specific cytokines. *EMBO J*, **13**(14): 3286-95.

Hashimoto, R., Fujiwara, H., Higashihashi, N., Enjoh-Kimura, T., Terasawa, H., Fujita-Yamaguchi, Y., Inagaki, F., Perdue, J. F. and Sakano, K. (1995) N-terminal deletion mutants of insulin-like growth factor-II (IGF-II) show Thr7 and Leu8 important for binding to insulin and IGF-I receptors and Leu8 critical for all IGF-II functions. *J Biol Chem*, **270**(30): 18013-8.

Heinrichs, A., Milstein, C. and Gherardi, E. (1995) Universal cloning and direct sequencing of rearranged antibody V genes using C region primers, biotin-captured cDNA and one-side PCR. *J Immunol Methods*, **178**(2): 241-51.

Hellawell, G. O., Turner, G. D., Davies, D. R., Poulsom, R., Brewster, S. F. and Macaulay, V. M. (2002) Expression of the type 1 insulin-like growth factor receptor is up-regulated in primary prostate cancer and commonly persists in metastatic disease. *Cancer Res*, **62**(10): 2942-50.

Hewat, E. A., Verdaguer, N., Fita, I., Blakemore, W., Brookes, S., King, A., Newman, J., Domingo, E., Mateu, M. G. and Stuart, D. I. (1997) Structure of the complex of an Fab fragment of a neutralizing antibody with foot-and-mouth disease virus: positioning of a highly mobile antigenic loop. *EMBO J*, **16**(7): 1492-500.

Hober, S., Forsberg, G., Palm, G., Hartmanis, M. and Nilsson, B. (1992) Disulfide exchange folding of insulin-like growth factor I. *Biochemistry*, **31**(6): 1749-56.

Hodgson, D. R., May, F. E. and Westley, B. R. (1995) Mutations at positions 11 and 60 of insulin-like growth factor 1 reveal differences between its interactions with the type I insulin-like-growth-factor receptor and the insulin receptor. *Eur J Biochem*, **233**(1): 299-309.

Hodgson, D. R., May, F. E. and Westley, B. R. (1996) Involvement of phenylalanine 23 in the binding of IGF-1 to the insulin and type I IGF receptor. *Regul Pept*, **66**(3): 191-6.

Hoeflich, A., Reisinger, R., Lahm, H., Kiess, W., Blum, W. F., Kolb, H. J., Weber, M. M. and Wolf, E. (2001) Insulin-like growth factor-binding protein 2 in tumorigenesis: protector or promoter? *Cancer Res*, **61**(24): 8601-10.

Hofmann, F. and Garcia-Echeverria, C. (2005) Blocking the insulin-like growth factor-I receptor as a strategy for targeting cancer. *Drug Discov Today*, **10**(15): 1041-7.

Holliger, P. and Hoogenboom, H. (1998) Antibodies come back from the brink. *Nat Biotechnol*, **16**(11): 1015-6.

Hong, J., Zhang, G., Dong, F. and Rechler, M. M. (2002) Insulin-like growth factor (IGF)-binding protein-3 mutants that do not bind IGF-I or IGF-II stimulate apoptosis in human prostate cancer cells. *J Biol Chem*, **277**(12): 10489-97.

Horak, E., Hartmann, F., Garmestani, K., Wu, C., Brechbiel, M., Gansow, O. A., Landolfi, N. F. and Waldmann, T. A. (1997) Radioimmunotherapy targeting of HER2/neu oncoprotein on ovarian tumor using lead-212-DOTA-AE1. *J Nucl Med*, **38**(12): 1944-50.

Hoyne, P. A., Cosgrove, L. J., McKern, N. M., Bentley, J. D., Ivancic, N., Elleman, T. C. and Ward, C. W. (2000a) High affinity insulin binding by soluble insulin receptor extracellular domain fused to a leucine zipper. *FEBS Lett*, **479**(1-2): 15-8.

Hoyne, P. A., Elleman, T. C., Adams, T. E., Richards, K. M. and Ward, C. W. (2000b) Properties of an insulin receptor with an IGF-1 receptor loop exchange in the cysteine-rich region. *FEBS Lett*, **469**(1): 57-60.

Hubbard, S. R. (1997) Crystal structure of the activated insulin receptor tyrosine kinase in complex with peptide substrate and ATP analog. *EMBO J*, **16**(18): 5572-81.

Hubbard, S. R. and Till, J. H. (2000) Protein tyrosine kinase structure and function. *Annu Rev Biochem*, **69**: 373-98.

Hubbard, S. R., Wei, L., Ellis, L. and Hendrickson, W. A. (1994) Crystal structure of the tyrosine kinase domain of the human insulin receptor. *Nature*, **372**(6508): 746-54.

Hudson, P. J. (1999) Recombinant antibody constructs in cancer therapy. *Curr Opin Immunol*, **11**(5): 548-57.

Hudson, P. J. and Souriau, C. (2001) Recombinant antibodies for cancer diagnosis and therapy. *Expert Opin Biol Ther*, **1**(5): 845-55.

Hudson, P. J. and Souriau, C. (2003) Engineered antibodies. *Nat Med*, **9**(1): 129-34.

Humbel, R. E. (1990) Insulin-like growth factors I and II. *Eur J Biochem*, **190**(3): 445-62.

Hwa, V., Oh, Y. and Rosenfeld, R. G. (1999) The insulin-like growth factor-binding protein (IGFBP) superfamily. *Endocr Rev*, **20**(6): 761-87.

Invitrogen (2005). pcDNA3.1/Zeo (+), http://www.invitrogen.com/content/sfs/vectors/pcdna3.1zeo_map.pdf.

Irving-Rodgers, H. F., Harland, M. L. and Rodgers, R. J. (2004) A novel basal lamina matrix of the stratified epithelium of the ovarian follicle. *Matrix Biol*, **23**(4): 207-17.

Jackson-Booth, P. G., Terry, C., Lackey, B., Lopaczynska, M. and Nissley, P. (2003) Inhibition of the biologic response to insulin-like growth factor I in MCF-7 breast cancer cells by a new monoclonal antibody to the insulin-like growth factor-I receptor. The importance of receptor down-regulation. *Horm Metab Res*, **35**(11-12): 850-6.

Janssen, J. A., Wildhagen, M. F., Ito, K., Blijenberg, B. G., Van Schaik, R. H., Roobol, M. J., Pols, H. A., Lamberts, S. W. and Schroder, F. H. (2004) Circulating free insulin-like growth factor (IGF)-I, total IGF-I, and IGF binding protein-3 levels do not predict the future risk to develop prostate cancer: results of a case-control study involving 201 patients within a population-based screening with a 4-year interval. *J Clin Endocrinol Metab*, **89**(9): 4391-6.

Jansson, M., Andersson, G., Uhlen, M., Nilsson, B. and Kordel, J. (1998) The insulin-like growth factor (IGF)binding protein 1 binding epitope on IGF-I probed by heteronuclear NMR spectroscopy and mutational analysis. *J Biol Chem*, **273**(38): 24701-7.

Jansson, M., Uhlen, M. and Nilsson, B. (1997) Structural changes in insulin-like growth factor (IGF) I mutant proteins affecting binding kinetic rates to IGF binding protein 1 and IGF-I receptor. *Biochemistry*, **36**(14): 4108-17.

Jaques, G., Rotsch, M., Wegmann, C., Worsch, U., Maasberg, M. and Havemann, K. (1988) Production of immunoreactive insulin-like growth factor I and response to exogenous IGF-I in small cell lung cancer cell lines. *Exp Cell Res*, **176**(2): 336-43.

Jerne, N. K. (1960) Immunological speculations. *Annu Rev Microbiol*, **14**: 341-58.

Jones, J. and Clemmons, D. (1995) Insulin-like growth factors and their binding proteins: biological actions. *Endocr Rev*, **16(1)**: 3-34.

Jones, P. T., Dear, P. H., Foote, J., Neuberger, M. S. and Winter, G. (1986) Replacing the complementarity-determining regions in a human antibody with those from a mouse. *Nature*, **321**(6069): 522-5.

Jones, S. T. and Bendig, M. M. (1991) Rapid PCR-cloning of full-length mouse immunoglobulin variable regions. *Biotechnology (N Y)*, **9**(1): 88-9.

Kabat, E. A., Wu, T. T., Perry, H. M., Gottesman, K. S. and Foeller, C. (1991). *Sequences of Proteins of Immunological Interest*. Bethesda, MD., National Institutes of Health.

Kalebic, T., Tsokos, M. and Helman, L. J. (1994) In vivo treatment with antibody against IGF-1 receptor suppresses growth of human rhabdomyosarcoma and down-regulates p34cdc2. *Cancer Res*, **54**(21): 5531-4.

Kaleko, M., Rutter, W. J. and Miller, A. D. (1990) Overexpression of the human insulinlike growth factor I receptor promotes ligand-dependent neoplastic transformation. *Mol Cell Biol*, **10**(2): 464-73.

Kalli, K. R., Falowo, O. I., Bale, L. K., Zschunke, M. A., Roche, P. C. and Conover, C. A. (2002) Functional insulin receptors on human epithelial ovarian carcinoma cells: implications for IGF-II mitogenic signaling. *Endocrinology*, **143**(9): 3259-67.

Kambhampati, S., Ray, G., Sengupta, K., Reddy, V. P., Banerjee, S. K. and Van Veldhuizen, P. J. (2005) Growth factors involved in prostate carcinogenesis. *Front Biosci*, **10**: 1355-67.

Karey, K. P. and Sirbasku, D. A. (1988) Differential responsiveness of human breast cancer cell lines MCF-7 and T47D to growth factors and 17 beta-estradiol. *Cancer Res*, **48**(14): 4083-92.

Kasuga, M., Karlsson, F. A. and Kahn, C. R. (1982) Insulin stimulates the phosphorylation of the 95,000-dalton subunit of its own receptor. *Science*, **215**(4529): 185-7.

Kato, H., Faria, T. N., Stannard, B., Roberts, C. T., Jr. and LeRoith, D. (1993) Role of tyrosine kinase activity in signal transduction by the insulin-like growth factor-I (IGF-I) receptor. Characterization of kinase-deficient IGF-I receptors and the action of an IGF-I-mimetic antibody (alpha IR-3). *J Biol Chem*, **268**(4): 2655-61.

Kato, H., Faria, T. N., Stannard, B., Roberts, C. T., Jr. and LeRoith, D. (1994) Essential role of tyrosine residues 1131, 1135, and 1136 of the insulin-like growth factor-I (IGF-I) receptor in IGF-I action. *Mol Endocrinol*, **8**(1): 40-50.

Kautenburger, T., Beyer-Sehlmeyer, G., Festag, G., Haag, N., Kuhler, S., Kuchler, A., Weise, A., Marian, B., Peters, W. H., Liehr, T., Claussen, U. and Pool-Zobel, B. L. (2005) The gut fermentation product butyrate, a chemopreventive agent, suppresses glutathione S-transferase theta (hGSTT1) and cell growth more in human colon adenoma (LT97) than tumor (HT29) cells. *J Cancer Res Clin Oncol*: 1-9.

Kehinde, E. O., Akanji, A. O., Mojiminiyi, O. A., Bashir, A. A., Daar, A. S. and Varghese, R. (2005) Putative role of serum insulin-like growth factor-1 (IGF-1) and IGF binding protein-3 (IGFBP-3) levels in the development of prostate cancer in Arab men. *Prostate Cancer Prostatic Dis*, **8**(1): 84-90.

Kettleborough, C. A., Saldanha, J., Ansell, K. H. and Bendig, M. M. (1993) Optimization of primers for cloning libraries of mouse immunoglobulin genes using the polymerase chain reaction. *Eur J Immunol*, **23**(1): 206-11.

Khandwala, H. M., McCutcheon, I. E., Flyvbjerg, A. and Friend, K. E. (2000) The effects of insulin-like growth factors on tumorigenesis and neoplastic growth. *Endocr Rev*, **21**(3): 215-44.

Khosravi, J., Diamandi, A., Mistry, J. and Scorilas, A. (2001) Insulin-like growth factor I (IGF-I) and IGF-binding protein-3 in benign prostatic hyperplasia and prostate cancer. *J Clin Endocrinol Metab*, **86**(2): 694-9.

Kim, J. J. and Accili, D. (2002) Signalling through IGF-I and insulin receptors: where is the specificity? *Growth Horm IGF Res*, **12**(2): 84-90.

Kishimoto, Y., Morisawa, T., Kitano, M., Shiota, G., Horie, Y., Suou, T., Ito, H., Kawasaki, H. and Hasegawa, J. (2001) Loss of heterozygosity of the mannose 6-phosphate/insulin-like growth factor II receptor and p53 genes in human hepatocellular carcinoma. *Hepatol Res*, **20**(1): 68-83.

Kjeldsen, T., Andersen, A. S., Wiberg, F. C., Rasmussen, J. S., Schaffer, L., Balschmidt, P., Moller, K. B. and Moller, N. P. (1991) The ligand specificities of the insulin receptor and the insulin-like growth factor I receptor reside in different regions of a common binding site. *Proc Natl Acad Sci U S A*, **88**(10): 4404-8.

Knight, D. M., Wagner, C., Jordan, R., McAleer, M. F., DeRita, R., Fass, D. N., Coller, B. S., Weisman, H. F. and Ghrayeb, J. (1995) The immunogenicity of the 7E3 murine monoclonal Fab antibody fragment variable region is dramatically reduced in humans by substitution of human for murine constant regions. *Mol Immunol*, **32**(16): 1271-81.

Kofler, R., Geley, S., Kofler, H. and Helmberg, A. (1992) Mouse variable-region gene families: complexity, polymorphism and use in non-autoimmune responses. *Immunol Rev*, **128**: 5-21.

Kohler, G. and Milstein, C. (1975) Continuous cultures of fused cells secreting antibody of predefined specificity. *Nature*, **256**: 495-7.

Kolar, G. R. and Capra, J. D. (2003). Immunoglobulins: Structure and Function. Fundamental immunology. W. E. Paul. Philadelphia, LIPPINCOTT WILLIAMS & WILKINS: 47-68.

Kornfeld, S. (1992) Structure and function of the mannose 6-phosphate/insulinlike growth factor II receptors. *Annu Rev Biochem*, **61**: 307-30.

Kotzke, G., Schutt, M., Missler, U., Moller, D. E., Fehm, H. L. and Klein, H. H. (1995) Binding of human, porcine and bovine insulin to insulin receptors from human brain, muscle and adipocytes and to expressed recombinant alternatively spliced insulin receptor isoforms. *Diabetologia*, **38**(7): 757-63.

Kreitman, R. J., Wilson, W. H., Bergeron, K., Raggio, M., Stetler-Stevenson, M., FitzGerald, D. J. and Pastan, I. (2001) Efficacy of the anti-CD22 recombinant immunotoxin BL22 in chemotherapy-resistant hairy-cell leukemia. *N Engl J Med*, **345**(4): 241-7.

Kristensen, C., Wiberg, F. C., Schaffer, L. and Andersen, A. S. (1998) Expression and characterization of a 70-kDa fragment of the insulin receptor that binds insulin. Minimizing ligand binding domain of the insulin receptor. *J Biol Chem*, **273**(28): 17780-6.

Kull, F. C., Jr., Jacobs, S., Su, Y. F., Svoboda, M. E., Van Wyk, J. J. and Cuatrecasas, P. (1983) Monoclonal antibodies to receptors for insulin and somatomedin-C. *J Biol Chem*, **258**(10): 6561-6.

Kurihara, M., Tokunaga, Y., Tsutsumi, K., Kawaguchi, T., Shigematsu, K., Niwa, M. and Mori, K. (1989) Characterization of insulin-like growth factor I and epidermal growth factor receptors in meningioma. *J Neurosurg*, **71**(4): 538-44.

Lahm, H., Suardet, L., Laurent, P. L., Fischer, J. R., Ceyhan, A., Givel, J. C. and Odartchenko, N. (1992) Growth regulation and co-stimulation of human colorectal cancer cell lines by insulin-like growth factor I, II and transforming growth factor alpha. *Br J Cancer*, **65**(3): 341-6.

Larrick, J. W., Danielsson, L., Brenner, C. A., Abrahamson, M., Fry, K. E. and Borrebaeck, C. A. (1989) Rapid cloning of rearranged immunoglobulin genes from human hybridoma cells using mixed primers and the polymerase chain reaction. *Biochem Biophys Res Commun*, **160**(3): 1250-6.

Laune, D., Molina, F., Ferrieres, G., Mani, J. C., Cohen, P., Simon, D., Bernardi, T., Piechaczyk, M., Pau, B. and Granier, C. (1997) Systematic exploration of the antigen binding activity of synthetic peptides isolated from the variable regions of immunoglobulins. *J Biol Chem*, **272**(49): 30937-44.

Leboulleux, S., Gaston, V., Boulle, N., Le Bouc, Y. and Gicquel, C. (2001) Loss of heterozygosity at the mannose 6-phosphate/insulin-like growth factor 2 receptor locus: a frequent but late event in adrenocortical tumorigenesis. *Eur J Endocrinol*, **144**(2): 163-8.

Lee, C. T., Wu, S., Gabrilovich, D., Chen, H., Nadaf-Rahrov, S., Ciernik, I. F. and Carbone, D. P. (1996) Antitumor effects of an adenovirus expressing antisense insulin-like growth factor I receptor on human lung cancer cell lines. *Cancer Res*, **56**(13): 3038-41.

Lee, H. Y., Chun, K. H., Liu, B., Wiehle, S. A., Cristiano, R. J., Hong, W. K., Cohen, P. and Kurie, J. M. (2002) Insulin-like growth factor binding protein-3 inhibits the growth of non-small cell lung cancer. *Cancer Res*, **62**(12): 3530-7.

Lefranc, M. P., Pommie, C., Ruiz, M., Giudicelli, V., Foulquier, E., Truong, L., Thouvenin-Contet, V. and Lefranc, G. (2003) IMGT unique numbering for immunoglobulin and T cell receptor variable domains and Ig superfamily V-like domains. *Dev Comp Immunol*, **27**(1): 55-77.

Leng, S. L., Leeding, K. S., Gibson, P. R. and Bach, L. A. (2001) Insulin-like growth factor-II renders LIM 2405 human colon cancer cells resistant to butyrate-induced apoptosis: a potential mechanism for colon cancer cell survival in vivo. *Carcinogenesis*, **22**(10): 1625-31.

LeRoith, D. and Roberts, C. T., Jr. (2003) The insulin-like growth factor system and cancer. *Cancer Lett*, **195**(2): 127-37.

Lewitt, M. S., Saunders, H., Phuyal, J. L. and Baxter, R. C. (1994) Complex formation by human insulin-like growth factor-binding protein-3 and human acid-labile subunit in growth hormone-deficient rats. *Endocrinology*, **134**(6): 2404-9.

Li, S. L., Kato, J., Paz, I. B., Kasuya, J. and Fujita-Yamaguchi, Y. (1993) Two new monoclonal antibodies against the alpha subunit of the human insulin-like growth factor-I receptor. *Biochem Biophys Res Commun*, **196**(1): 92-8.

Li, S. L., Liang, S. J., Guo, N., Wu, A. M. and Fujita-Yamaguchi, Y. (2000) Single-chain antibodies against human insulin-like growth factor I receptor: expression, purification, and effect on tumor growth. *Cancer Immunol Immunother*, **49**(4-5): 243-52.

Lim, C. C., Ferguson, L. R. and Tannock, G. W. (2005) Dietary fibres as "prebiotics": implications for colorectal cancer. *Mol Nutr Food Res*, **49**(6): 609-19.

Liu, J. L., Blakesley, V. A., Gutkind, J. S. and LeRoith, D. (1997) The constitutively active mutant Galpha13 transforms mouse fibroblast cells deficient in insulin-like growth factor-I receptor. *J Biol Chem*, **272**(47): 29438-41.

Liu, J. P., Baker, J., Perkins, A. S., Robertson, E. J. and Efstratiadis, A. (1993) Mice carrying null mutations of the genes encoding insulin-like growth factor I (Igf-1) and type 1 IGF receptor (Igf1r). *Cell*, **75**(1): 59-72.

Liu, X., Turbyville, T., Fritz, A. and Whitesell, L. (1998) Inhibition of insulin-like growth factor I receptor expression in neuroblastoma cells induces the regression of established tumors in mice. *Cancer Res*, **58**(23): 5432-8.

Long, L., Navab, R. and Brodt, P. (1998a) Regulation of the Mr 72,000 type IV collagenase by the type I insulin-like growth factor receptor. *Cancer Res*, **58**(15): 3243-7.

Long, L., Nip, J. and Brodt, P. (1994) Paracrine growth stimulation by hepatocyte-derived insulin-like growth factor-1: a regulatory mechanism for carcinoma cells metastatic to the liver. *Cancer Res*, **54**(14): 3732-7.

Long, L., Rubin, R., Baserga, R. and Brodt, P. (1995) Loss of the metastatic phenotype in murine carcinoma cells expressing an antisense RNA to the insulin-like growth factor receptor. *Cancer Res*, **55**(5): 1006-9.

Long, L., Rubin, R. and Brodt, P. (1998b) Enhanced invasion and liver colonization by lung carcinoma cells overexpressing the type 1 insulin-like growth factor receptor. *Exp Cell Res*, **238**(1): 116-21.

Louvi, A., Accili, D. and Efstratiadis, A. (1997) Growth-promoting interaction of IGF-II with the insulin receptor during mouse embryonic development. *Dev Biol*, **189**(1): 33-48.

Lu, D., Zhang, H., Koo, H., Tonra, J., Balderes, P., Prewett, M., Corcoran, E., Mangalampalli, V., Bassi, R., Anselma, D., Patel, D., Kang, X., Ludwig, D. L., Hicklin, D. J., Bohlen, P., Witte, L. and Zhu, Z. (2005) A fully human recombinant IgG-like bispecific antibody to both the epidermal growth factor receptor and the insulin-like growth factor receptor for enhanced antitumor activity. *J Biol Chem*, **280**(20): 19665-72.

Lu, D., Zhang, H., Ludwig, D., Persaud, A., Jimenez, X., Burtrum, D., Balderes, P., Liu, M., Bohlen, P., Witte, L. and Zhu, Z. (2004) Simultaneous blockade of both the epidermal growth factor receptor and the insulin-like growth factor receptor signaling pathways in cancer cells with a fully human recombinant bispecific antibody. *J Biol Chem*, **279**(4): 2856-65.

Lu, Y., Zi, X., Zhao, Y., Mascarenhas, D. and Pollak, M. (2001) Insulin-like growth factor-I receptor signaling and resistance to trastuzumab (Herceptin). *J Natl Cancer Inst*, **93**(24): 1852-7.

Ludwig, T., Eggenschwiler, J., Fisher, P., D'Ercole, A. J., Davenport, M. L. and Efstratiadis, A. (1996) Mouse mutants lacking the type 2 IGF receptor (IGF2R) are rescued from perinatal lethality in Igf2 and Igf1r null backgrounds. *Dev Biol*, **177**(2): 517-35.

Luo, R. Z., Beniac, D. R., Fernandes, A., Yip, C. C. and Ottensmeyer, F. P. (1999) Quaternary structure of the insulin-insulin receptor complex. *Science*, **285**(5430): 1077-80.

Lupu, F., Terwilliger, J. D., Lee, K., Segre, G. V. and Efstratiadis, A. (2001) Roles of growth hormone and insulin-like growth factor 1 in mouse postnatal growth. *Dev Biol*, **229**(1): 141-62.

Lutomski, D., Joubert-Caron, R., Bourin, P., Bladier, D. and Caron, M. (1995) Use of thiophilic adsorption in the purification of biotinylated Fab fragments. *J Chromatogr B Biomed Appl*, **664**(1): 79-82.

Ma, J., Pollak, M. N., Giovannucci, E., Chan, J. M., Tao, Y., Hennekens, C. H. and Stampfer, M. J. (1999) Prospective study of colorectal cancer risk in men and plasma levels of insulin-like growth factor (IGF)-I and IGF-binding protein-3. *J Natl Cancer Inst*, **91**(7): 620-5.

Macaulay, V. M., Salisbury, A. J., Bohula, E. A., Playford, M. P., Smorodinsky, N. I. and Shiloh, Y. (2001) Downregulation of the type 1 insulin-like growth factor receptor in mouse melanoma cells is associated with enhanced radiosensitivity and impaired activation of Atm kinase. *Oncogene*, **20**(30): 4029-40.

Magee, B. A., Shooter, G. K., Wallace, J. C. and Francis, G. L. (1999) Insulin-like growth factor I and its binding proteins: a study of the binding interface using B-domain analogues. *Biochemistry*, **38**(48): 15863-70.

Mainville, C. A., Sheehan, K. M., Klaman, L. D., Giorgetti, C. A., Press, J. L. and Brodeur, P. H. (1996) Deletional mapping of fifteen mouse VH gene families reveals a common organization for three Igh haplotypes. *J Immunol*, **156**(3): 1038-46.

Maloney, E. K., McLaughlin, J. L., Dagdigian, N. E., Garrett, L. M., Connors, K. M., Zhou, X. M., Blattler, W. A., Chittenden, T. and Singh, R. (2003) An anti-insulin-like growth factor I receptor antibody that is a potent inhibitor of cancer cell proliferation. *Cancer Res*, **63**(16): 5073-83.

Maple, P. A., Jones, C. S. and Andrews, N. J. (2001) Time resolved fluorometric immunoassay, using europium labelled antihuman IgG, for the detection of human tetanus antitoxin in serum. *J Clin Pathol*, **54**(10): 812-5.

Marino-Buslje, C., Mizuguchi, K., Siddle, K. and Blundell, T. L. (1998) A third fibronectin type III domain in the extracellular region of the insulin receptor family. *FEBS Lett*, **441**(2): 331-6.

Mathews, L. S., Norstedt, G. and Palmiter, R. D. (1986) Regulation of insulin-like growth factor I gene expression by growth hormone. *Proc Natl Acad Sci U S A*, **83**(24): 9343-7.

Maynard, J. and Georgiou, G. (2000) Antibody engineering. *Annu Rev Biomed Eng*, **2**: 339-76.

Mazor, O., Hillairet de Boisferon, M., Lombet, A., Gruaz-Guyon, A., Gayer, B., Skrzydelsky, D., Kohen, F., Forgez, P., Scherz, A., Rostene, W. and Salomon, Y. (2002) Europium-labeled epidermal growth factor and neurotensin: novel probes for receptor-binding studies. *Anal Biochem*, **301**(1): 75-81.

McClain, D. A. (1991) Different ligand affinities of the two human insulin receptor splice variants are reflected in parallel changes in sensitivity for insulin action. *Mol Endocrinol*, **5**(5): 734-9.

Megyesi, K., Kahn, C. R., Roth, J., Froesch, E. R., Humbel, R. E., Zapf, J. and Neville, D. M., Jr. (1974) Insulin and non-suppressible insulin-like activity (NSILA-s): evidence for separate plasma membrane receptor sites. *Biochem Biophys Res Commun*, **57**(1): 307-15.

Milner, S. J., Francis, G. L., Wallace, J. C., Magee, B. A. and Ballard, F. J. (1995) Mutations in the B-domain of insulin-like growth factor-I influence the oxidative folding to yield products with modified biological properties. *Biochem J*, **308**(Pt 3): 865-71.

Minuto, F., Del Monte, P., Barreca, A., Alama, A., Cariola, G. and Giordano, G. (1988) Evidence for autocrine mitogenic stimulation by somatomedin-C/insulin-like growth factor I on an established human lung cancer cell line. *Cancer Res*, **48**(13): 3716-9.

Mitsiades, C. S., Mitsiades, N. S., McMullan, C. J., Poulaki, V., Shringarpure, R., Akiyama, M., Hideshima, T., Chauhan, D., Joseph, M., Libermann, T. A., Garcia-Echeverria, C., Pearson, M. A., Hofmann, F., Anderson, K. C. and Kung, A. L. (2004) Inhibition of the insulin-like growth factor receptor-1 tyrosine kinase activity as a therapeutic strategy for multiple myeloma, other hematologic malignancies, and solid tumors. *Cancer Cell*, **5**(3): 221-30.

Molina, L., Marino-Buslje, C., Quinn, D. R. and Siddle, K. (2000) Structural domains of the insulin receptor and IGF receptor required for dimerisation and ligand binding. *FEBS Lett*, **467**(2-3): 226-30.

Molina, M. A., Codony-Servat, J., Albanell, J., Rojo, F., Arribas, J. and Baselga, J. (2001) Trastuzumab (herceptin), a humanized anti-Her2 receptor monoclonal antibody, inhibits basal and activated Her2 ectodomain cleavage in breast cancer cells. *Cancer Res*, **61**(12): 4744-9.

Moller, D. E., Yokota, A., Caro, J. F. and Flier, J. S. (1989) Tissue-specific expression of two alternatively spliced insulin receptor mRNAs in man. *Mol Endocrinol*, **3**(8): 1263-9.

Monnet, C., Laune, D., Laroche-Traineau, J., Biard-Piechaczyk, M., Briant, L., Bes, C., Pugniere, M., Mani, J. C., Pau, B., Cerutti, M., Devauchelle, G., Devaux, C., Granier, C. and Chardes, T. (1999) Synthetic peptides derived from the variable regions of an anti-CD4 monoclonal antibody bind to CD4 and inhibit HIV-1 promoter activation in virus-infected cells. *J Biol Chem*, **274**(6): 3789-96.

Moore, M. G., Wetterau, L. A., Francis, M. J., Peehl, D. M. and Cohen, P. (2003) Novel stimulatory role for insulin-like growth factor binding protein-2 in prostate cancer cells. *Int J Cancer*, **105**(1): 14-9.

Moriyama, S., Ayson, F. G. and Kawauchi, H. (2000) Growth regulation by insulin-like growth factor-I in fish. *Biosci Biotechnol Biochem*, **64**(8): 1553-62.

Morris, G. E. (1996). *Epitope Mapping Protocols*. Totowa, Human Press Inc.

Morrison, S. L., Johnson, M. J., Herzenberg, L. A. and Oi, V. T. (1984) Chimeric human antibody molecules: mouse antigen-binding domains with human constant region domains. *Proc Natl Acad Sci U S A*, **81**(21): 6851-5.

Morton, P. A., Arbuckle, J. A., Bailey, K. S., Nicastro, P. J. and Runnels, H. A. (2004). Antibodies to IGF-I receptor for the treatment of cancers (US 2004/0202655 A1). U.S.A.

Mosthaf, L., Grako, K., Dull, T. J., Coussens, L., Ullrich, A. and McClain, D. A. (1990) Functionally distinct insulin receptors generated by tissue-specific alternative splicing. *EMBO J*, **9**(8): 2409-13.

Mulhern, T. D., Booker, G. W. and Cosgrove, L. (1998) A third fibronectin-type-III domain in the insulin-family receptors. *Trends Biochem Sci*, **23**(12): 465-6.

Muller, M., Dietel, M., Turzynski, A. and Wiechen, K. (1998) Antisense phosphorothioate oligodeoxynucleotide down-regulation of the insulin-like growth factor I receptor in ovarian cancer cells. *Int J Cancer*, **77**(4): 567-71.

Munshi, S., Hall, D. L., Kornienko, M., Darke, P. L. and Kuo, L. C. (2003) Structure of apo, unactivated insulin-like growth factor-1 receptor kinase at 1.5 A resolution. *Acta Crystallogr D Biol Crystallogr*, **59**(Pt 10): 1725-30.

Munshi, S., Kornienko, M., Hall, D. L., Reid, J. C., Waxman, L., Stirdivant, S. M., Darke, P. L. and Kuo, L. C. (2002) Crystal structure of the Apo, unactivated insulin-like growth factor-1 receptor kinase. Implication for inhibitor specificity. *J Biol Chem*, **277**(41): 38797-802.

Murphy, L. J. (1998) Insulin-like growth factor-binding proteins: functional diversity or redundancy? *J Mol Endocrinol*, **21**(2): 97-107.

Mynarcik, D. C., Williams, P. F., Schaffer, L., Yu, G. Q. and Whittaker, J. (1997) Identification of common ligand binding determinants of the insulin and insulin-like growth factor 1 receptors. Insights into mechanisms of ligand binding. *J Biol Chem*, **272**(30): 18650-5.

Myszka, D. G., He, X., Dembo, M., Morton, T. A. and Goldstein, B. (1998) Extending the range of rate constants available from BIACORE: interpreting mass transport-influenced binding data. *Biophys J*, **75**(2): 583-94.

Nakae, J., Kido, Y. and Accili, D. (2001) Distinct and overlapping functions of insulin and IGF-I receptors. *Endocr Rev*, **22**(6): 818-35.

Nakamura, K., Hongo, A., Kodama, J., Miyagi, Y., Yoshinouchi, M. and Kudo, T. (2000) Down-regulation of the insulin-like growth factor I receptor by antisense RNA can reverse the transformed phenotype of human cervical cancer cell lines. *Cancer Res*, **60**(3): 760-5.

Nakanishi, Y., Mulshine, J. L., Kasprzyk, P. G., Natale, R. B., Maneckjee, R., Avis, I., Treston, A. M., Gazdar, A. F., Minna, J. D. and Cuttitta, F. (1988) Insulin-like growth factor-I can mediate autocrine proliferation of human small cell lung cancer cell lines in vitro. *J Clin Invest*, **82**(1): 354-9.

Navarro, M. and Baserga, R. (2001) Limited redundancy of survival signals from the type 1 insulin-like growth factor receptor. *Endocrinology*, **142**(3): 1073-81.

New Brunswick Scientific Co (2003). Spinner Basket with Fibra-cel Support, http://www.nbsc.com/products/spinner.htm.

Nice, E. C. and Catimel, B. (1999) Instrumental biosensors: new perspectives for the analysis of biomolecular interactions. *Bioessays*, **21**(4): 339-52.

Nielsen, F. C. (1992) The molecular and cellular biology of insulin-like growth factor II. *Prog Growth Factor Res*, **4**(3): 257-90.

Novagen (2004). Ig-Primer Sets, http://www.emdbiosciences.com/docs/docs/PROT/TB326.pdf.

O'Bryan, J. P., Frye, R. A., Cogswell, P. C., Neubauer, A., Kitch, B., Prokop, C., Espinosa, R., 3rd, Le Beau, M. M., Earp, H. S. and Liu, E. T. (1991) axl, a transforming gene isolated from primary human myeloid leukemia cells, encodes a novel receptor tyrosine kinase. *Mol Cell Biol*, **11**(10): 5016-31.

O'Connor, R. (2003) Regulation of IGF-I receptor signaling in tumor cells. *Horm Metab Res*, **35**(11-12): 771-7.

O'Dell, S. and Day, I. (1998) Insulin-like growth factor II (IGF-II). *Int J Biochem Cell Biol*, **30(7)**: 767-71.

Okada, Y., Yokono, K., Katsuta, A., Yoshida, M., Morita, S., Irino, H., Goto, T., Baba, S., Roth, R. A. and Shii, K. (1998) Development of an assay for bioactive insulin. *Anal Biochem*, **257**(2): 134-8.

Okubo, Y., Siddle, K., Firth, H., O'Rahilly, S., Wilson, L. C., Willatt, L., Fukushima, T., Takahashi, S., Petry, C. J., Saukkonen, T., Stanhope, R. and Dunger, D. B. (2003) Cell proliferation activities on skin fibroblasts from a short child with absence of one copy of the type 1 insulin-like growth factor receptor (IGF1R) gene and a tall child with three copies of the IGF1R gene. *J Clin Endocrinol Metab*, **88**(12): 5981-8.

Onoda, N., Ohmura, E., Tsushima, T., Ohba, Y., Emoto, N., Isozaki, O., Sato, Y., Shizume, K. and Demura, H. (1992) Autocrine role of insulin-like growth factor (IGF)-I in a human thyroid cancer cell line. *Eur J Cancer*, **28A**(11): 1904-9.

Orlandi, R., Gussow, D. H., Jones, P. T. and Winter, G. (1989) Cloning immunoglobulin variable domains for expression by the polymerase chain reaction. *Proc Natl Acad Sci U S A*, **86**(10): 3833-7.

Osipo, C., Dorman, S. and Frankfater, A. (2001) Loss of insulin-like growth factor II receptor expression promotes growth in cancer by increasing intracellular signaling from both IGF-I and insulin receptors. *Exp Cell Res*, **264**(2): 388-96.

Ottensmeyer, F. P., Beniac, D. R., Luo, R. Z. and Yip, C. C. (2000) Mechanism of transmembrane signaling: insulin binding and the insulin receptor. *Biochemistry*, **39**(40): 12103-12.

Ozato, K. and Sachs, D. H. (1981) Monoclonal antibodies to mouse MHC antigens. III. Hybridoma antibodies reacting to antigens of the H-2b haplotype reveal genetic control of isotype expression. *J Immunol*, **126**(1): 317-21.

Pandini, G., Frasca, F., Mineo, R., Sciacca, L., Vigneri, R. and Belfiore, A. (2002) Insulin/insulin-like growth factor I hybrid receptors have different biological characteristics depending on the insulin receptor isoform involved. *J Biol Chem*, **277**(42): 39684-95.

Pandini, G., Vigneri, R., Costantino, A., Frasca, F., Ippolito, A., Fujita-Yamaguchi, Y., Siddle, K., Goldfine, I. D. and Belfiore, A. (1999) Insulin and insulin-like growth factor-I (IGF-I) receptor overexpression in breast cancers leads to insulin/IGF-I hybrid

receptor overexpression: evidence for a second mechanism of IGF-I signaling. *Clin Cancer Res*, **5**(7): 1935-44.

Panka, D. J., Mudgett-Hunter, M., Parks, D. R., Peterson, L. L., Herzenberg, L. A., Haber, E. and Margolies, M. N. (1988) Variable region framework differences result in decreased or increased affinity of variant anti-digoxin antibodies. *Proc Natl Acad Sci U S A*, **85**(9): 3080-4.

Pass, H., Mew, D., Carbone, M., Matthews, W., Donington, J., Baserga, R., Walker, C., Resnicoff, M. and Steinberg, S. (1996) Inhibition of hamster mesothelioma tumorigenesis by an antisense expression plasmid to the insulin-like growth factor-1 receptor. *Cancer Res*, **56(17)**: 4044-8.

Pautsch, A., Zoephel, A., Ahorn, H., Spevak, W., Hauptmann, R. and Nar, H. (2001) Crystal structure of bisphosphorylated IGF-1 receptor kinase: insight into domain movements upon kinase activation. *Structure (Camb)*, **9**(10): 955-65.

Pavelic, K., Kolak, T., Kapitanovic, S., Radosevic, S., Spaventi, S., Kruslin, B. and Pavelic, J. (2003) Gastric cancer: the role of insulin-like growth factor 2 (IGF 2) and its receptors (IGF 1R and M6-P/IGF 2R). *J Pathol*, **201**(3): 430-8.

Pearl, M. L., Talavera, F., Gretz, H. F., 3rd, Roberts, J. A. and Menon, K. M. (1993) Mitogenic activity of growth factors in the human endometrial adenocarcinoma cell lines HEC-1-A and KLE. *Gynecol Oncol*, **49**(3): 325-32.

Pelizzola, D., Bombardieri, E., Brocchi, A., Cappelli, G., Coli, A., Federghini, M., Giganti, M., Gion, M., Madeddu, G., Maussieri, M. L. and et al. (1995) How alternative are immunoassay systems employing non-radioisotopic labels? A comparative appraisal of their main analytical characteristics. *Q J Nucl Med*, **39**(4): 251-63.

Peoples, R., Milatovich, A. and Francke, U. (1995) Hemizygosity at the insulin-like growth factor I receptor (IGF1R) locus and growth failure in the ring chromosome 15 syndrome. *Cytogenet Cell Genet*, **70**(3-4): 228-34.

Perer, E., Madan, A., Shurin, A., Zakris, E., Romeguera, K., Pang, Y. and Beech, D. (2000) Insulin-like growth factor I receptor antagonism augments response to chemoradiation therapy in colon cancer cells. *J Surg Res*, **94(1)**: 1-5.

Pettersen, E. F., Goddard, T. D., Huang, C. C., Couch, G. S., Greenblatt, D. M., Meng, E. C. and Ferrin, T. E. (2004) UCSF Chimera--a visualization system for exploratory research and analysis. *J Comput Chem*, **25**(13): 1605-12.

Peyrat, J. P., Bonneterre, J., Hecquet, B., Vennin, P., Louchez, M. M., Fournier, C., Lefebvre, J. and Demaille, A. (1993) Plasma insulin-like growth factor-1 (IGF-1) concentrations in human breast cancer. *Eur J Cancer*, **29A**(4): 492-7.

Pietrzkowski, Z., Lammers, R., Carpenter, G., Soderquist, A. M., Limardo, M., Phillips, P. D., Ullrich, A. and Baserga, R. (1992) Constitutive expression of insulin-like growth factor 1 and insulin-like growth factor 1 receptor abrogates all requirements for exogenous growth factors. *Cell Growth Differ*, **3**(4): 199-205.

Pietrzkowski, Z., Mulholland, G., Gomella, L., Jameson, B. A., Wernicke, D. and Baserga, R. (1993) Inhibition of growth of prostatic cancer cell lines by peptide analogues of insulin-like growth factor 1. *Cancer Res*, **53**(5): 1102-6.

Pollak, M. N., Polychronakos, C. and Richard, M. (1990) Insulinlike growth factor I: a potent mitogen for human osteogenic sarcoma. *J Natl Cancer Inst*, **82**(4): 301-5.

Pollak, M. N., Schernhammer, E. S. and Hankinson, S. E. (2004) Insulin-like growth factors and neoplasia. *Nat Rev Cancer*, **4**(7): 505-18.

Pommie, C., Levadoux, S., Sabatier, R., Lefranc, G. and Lefranc, M. P. (2004) IMGT standardized criteria for statistical analysis of immunoglobulin V-REGION amino acid properties. *J Mol Recognit*, **17**(1): 17-32.

Porter, R. R. (1973) Structural studies of immunoglobulins. *Science*, **180**(87): 713-6.

Potter, M., Newell, J. B., Rudikoff, S. and Haber, E. (1982) Classification of mouse VK groups based on the partial amino acid sequence to the first invariant tryptophan: impact of 14 new sequences from IgG myeloma proteins. *Mol Immunol*, **19**(12): 1619-30.

Poul, M. A., Cerutti, M., Chaabihi, H., Devauchelle, G., Kaczorek, M. and Lefranc, M. P. (1995) Design of cassette baculovirus vectors for the production of therapeutic antibodies in insect cells. *Immunotechnology*, **1**(3-4): 189-96.

Prager, D., Li, H. L., Asa, S. and Melmed, S. (1994) Dominant negative inhibition of tumorigenesis in vivo by human insulin-like growth factor I receptor mutant. *Proc Natl Acad Sci U S A*, **91**(6): 2181-5.

Promega (2005). pGEM®-T and pGEM®-T Easy Vector Systems, http://www.promega.com/tbs/tm042/tm042.pdf.

Quinn, K. A., Treston, A. M., Unsworth, E. J., Miller, M. J., Vos, M., Grimley, C., Battey, J., Mulshine, J. L. and Cuttitta, F. (1996) Insulin-like growth factor expression in human cancer cell lines. *J Biol Chem*, **271**(19): 11477-83.

Raile, K., Hoflich, A., Kessler, U., Yang, Y., Pfuender, M., Blum, W. F., Kolb, H., Schwarz, H. P. and Kiess, W. (1994) Human osteosarcoma (U-2 OS) cells express both insulin-like growth factor-I (IGF-I) receptors and insulin-like growth factor-II/mannose-6-phosphate (IGF-II/M6P) receptors and synthesize IGF-II: autocrine growth stimulation by IGF-II via the IGF-I receptor. *J Cell Physiol*, **159**(3): 531-41.

Raychaudhuri, G., McCool, D. and Painter, R. H. (1985) Human IgG1 and its Fc fragment bind with different affinities to the Fc receptors on the human U937, HL-60 and ML-1 cell lines. *Mol Immunol*, **22**(9): 1009-1019.

Reinmuth, N., Liu, W., Fan, F., Jung, Y. D., Ahmad, S. A., Stoeltzing, O., Bucana, C. D., Radinsky, R. and Ellis, L. M. (2002) Blockade of insulin-like growth factor I receptor function inhibits growth and angiogenesis of colon cancer. *Clin Cancer Res*, **8**(10): 3259-69.

Renehan, A. G., Jones, J., Potten, C. S., Shalet, S. M. and O'Dwyer, S. T. (2000) Elevated serum insulin-like growth factor (IGF)-II and IGF binding protein-2 in patients with colorectal cancer. *Br J Cancer*, **83**(10): 1344-50.

Resnicoff, M., Abraham, D., Yutanawiboonchai, W., Rotman, H. L., Kajstura, J., Rubin, R., Zoltick, P. and Baserga, R. (1995a) The insulin-like growth factor I receptor protects tumor cells from apoptosis in vivo. *Cancer Res*, **55**(11): 2463-9.

Resnicoff, M., Burgaud, J. L., Rotman, H. L., Abraham, D. and Baserga, R. (1995b) Correlation between apoptosis, tumorigenesis, and levels of insulin-like growth factor I receptors. *Cancer Res*, **55**(17): 3739-41.

Resnicoff, M., Coppola, D., Sell, C., Rubin, R., Ferrone, S. and Baserga, R. (1994) Growth inhibition of human melanoma cells in nude mice by antisense strategies to the type 1 insulin-like growth factor receptor. *Cancer Res*, **54**(18): 4848-50.

Resnik, J. L., Reichart, D. B., Huey, K., Webster, N. J. and Seely, B. L. (1998) Elevated insulin-like growth factor I receptor autophosphorylation and kinase activity in human breast cancer. *Cancer Res*, **58**(6): 1159-64.

Rey, J. M., Theillet, C., Brouillet, J. P. and Rochefort, H. (2000) Stable amino-acid sequence of the mannose-6-phosphate/insulin-like growth-factor-II receptor in ovarian carcinomas with loss of heterozygosity and in breast-cancer cell lines. *Int J Cancer*, **85**(4): 466-73.

Riechmann, L., Clark, M., Waldmann, H. and Winter, G. (1988) Reshaping human antibodies for therapy. *Nature*, **332**(6162): 323-7.

Rinderknecht, E. and Humbel, R. E. (1976) Polypeptides with nonsuppressible insulin-like and cell-growth promoting activities in human serum: isolation, chemical characterization, and some biological properties of forms I and II. *Proc Natl Acad Sci U S A*, **73**(7): 2365-9.

Rininsland, F., Johnson, T. R., Chernicky, C. L., Schulze, E., Burfeind, P. and Ilan, J. (1997) Suppression of insulin-like growth factor type I receptor by a triple-helix strategy inhibits IGF-I transcription and tumorigenic potential of rat C6 glioblastoma cells. *Proc Natl Acad Sci U S A*, **94**(11): 5854-9.

Roback, E. W., Barakat, A. J., Dev, V. G., Mbikay, M., Chretien, M. and Butler, M. G. (1991) An infant with deletion of the distal long arm of chromosome 15 (q26.1----qter) and loss of insulin-like growth factor 1 receptor gene. *Am J Med Genet*, **38**(1): 74-9.

Rohlik, Q. T., Adams, D., Kull, F. C., Jr. and Jacobs, S. (1987) An antibody to the receptor for insulin-like growth factor I inhibits the growth of MCF-7 cells in tissue culture. *Biochem Biophys Res Commun*, **149**(1): 276-81.

Roitt, I., Brostoff, J. and Male, D. (1989). *Immunology*. London, Gower Medical Publishing.

Rosen, C. J. and Pollak, M. (1999) Circulating IGF-I: New Perspectives for a New Century. *Trends Endocrinol Metab*, **10**(4): 136-141.

Rosenzweig, S. A. (2004) What's new in the IGF-binding proteins? *Growth Horm IGF Res*, **14**(5): 329-36.

Roth, B. V., Burgisser, D. M., Luthi, C. and Humbel, R. E. (1991) Mutants of human insulin-like growth factor II: expression and characterization of analogs with a substitution of TYR27 and/or a deletion of residues 62-67. *Biochem Biophys Res Commun*, **181**(2): 907-14.

Rotwein, P. (1991) Structure, evolution, expression and regulation of insulin-like growth factors I and II. *Growth Factors*, **5**(1): 3-18.

Rubin, R. and Baserga, R. (1995) Insulin-like growth factor-I receptor. Its role in cell proliferation, apoptosis, and tumorigenicity. *Lab Invest*, **73**(3): 311-31.

Rudman, S. M., Philpott, M. P., Thomas, G. A. and Kealey, T. (1997) The role of IGF-I in human skin and its appendages: morphogen as well as mitogen? *J Invest Dermatol*, **109**(6): 770-7.

Russell, S. J., Llewelyn, M. B. and Hawkins, R. E. (1992) Principles of antibody therapy. *BMJ*, **305**(6866): 1424-9.

Sachdev, D., Li, S. L., Hartell, J. S., Fujita-Yamaguchi, Y., Miller, J. S. and Yee, D. (2003) A chimeric humanized single-chain antibody against the type I insulin-like growth factor (IGF) receptor renders breast cancer cells refractory to the mitogenic effects of IGF-I. *Cancer Res*, **63**(3): 627-35.

Saint-Remy, J. M. (1997) Epitope mapping: a new method for biological evaluation and immunotoxicology. *Toxicology*, **119**(1): 77-81.

Sakano, K., Enjoh, T., Numata, F., Fujiwara, H., Marumoto, Y., Higashihashi, N., Sato, Y., Perdue, J. F. and Fujita-Yamaguchi, Y. (1991) The design, expression, and characterization of human insulin-like growth factor II (IGF-II) mutants specific for either the IGF-II/cation-independent mannose 6-phosphate receptor or IGF-I receptor. *J Biol Chem*, **266**(31): 20626-35.

Sallinen, S. L., Sallinen, P. K., Haapasalo, H. K., Helin, H. J., Helen, P. T., Schraml, P., Kallioniemi, O. P. and Kononen, J. (2000) Identification of differentially expressed genes in human gliomas by DNA microarray and tissue chip techniques. *Cancer Res*, **60**(23): 6617-22.

Sambrook, J., Fritsch, E. F. and Maniatis, T. (1989). *Molecular Cloning: A Laboratory Manual*. Cold Spring Harbor, NY, Cold Spring Harbor Lab Press.

Sato, A., Nishimura, S., Ohkubo, T., Kyogoku, Y., Koyama, S., Kobayashi, M., Yasuda, T. and Kobayashi, Y. (1992) 1H-NMR assignment and secondary structure of human insulin-like growth factor-I (IGF-I) in solution. *J Biochem (Tokyo)*, **111**(4): 529-36.

Sato, A., Nishimura, S., Ohkubo, T., Kyogoku, Y., Koyama, S., Kobayashi, M., Yasuda, T. and Kobayashi, Y. (1993) Three-dimensional structure of human insulin-like growth factor-I (IGF-I) determined by 1H-NMR and distance geometry. *Int J Pept Protein Res*, **41**(5): 433-40.

Savkur, R. S., Philips, A. V. and Cooper, T. A. (2001) Aberrant regulation of insulin receptor alternative splicing is associated with insulin resistance in myotonic dystrophy. *Nat Genet*, **29**(1): 40-7.

Savkur, R. S., Philips, A. V., Cooper, T. A., Dalton, J. C., Moseley, M. L., Ranum, L. P. and Day, J. W. (2004) Insulin receptor splicing alteration in myotonic dystrophy type 2. *Am J Hum Genet*, **74**(6): 1309-13.

Schaefer, E. M., Erickson, H. P., Federwisch, M., Wollmer, A. and Ellis, L. (1992) Structural organization of the human insulin receptor ectodomain. *J Biol Chem*, **267**(32): 23393-402.

Schaefer, E. M., Siddle, K. and Ellis, L. (1990) Deletion analysis of the human insulin receptor ectodomain reveals independently folded soluble subdomains and insulin binding by a monomeric alpha-subunit. *J Biol Chem*, **265**(22): 13248-53.

Schaffer, M. L., Deshayes, K., Nakamura, G., Sidhu, S. and Skelton, N. J. (2003) Complex with a phage display-derived peptide provides insight into the function of insulin-like growth factor I. *Biochemistry*, **42**(31): 9324-34.

Scharf, J. G., Schmidt-Sandte, W., Pahernik, S. A., Ramadori, G., Braulke, T. and Hartmann, H. (1998) Characterization of the insulin-like growth factor axis in a human hepatoma cell line (PLC). *Carcinogenesis*, **19**(12): 2121-8.

Schumacher, R., Mosthaf, L., Schlessinger, J., Brandenburg, D. and Ullrich, A. (1991) Insulin and insulin-like growth factor-1 binding specificity is determined by distinct regions of their cognate receptors. *J Biol Chem*, **266**(29): 19288-95.

Schumacher, R., Soos, M. A., Schlessinger, J., Brandenburg, D., Siddle, K. and Ullrich, A. (1993) Signaling-competent receptor chimeras allow mapping of major insulin receptor binding domain determinants. *J Biol Chem*, **268**(2): 1087-94.

Sciacca, L., Costantino, A., Pandini, G., Mineo, R., Frasca, F., Scalia, P., Sbraccia, P., Goldfine, I. D., Vigneri, R. and Belfiore, A. (1999) Insulin receptor activation by IGF-II in breast cancers: evidence for a new autocrine/paracrine mechanism. *Oncogene*, **18**(15): 2471-9.

Sciacca, L., Mineo, R., Pandini, G., Murabito, A., Vigneri, R. and Belfiore, A. (2002) In IGF-I receptor-deficient leiomyosarcoma cells autocrine IGF-II induces cell invasion and protection from apoptosis via the insulin receptor isoform A. *Oncogene*, **21**(54): 8240-50.

Scotlandi, K., Benini, S., Nanni, P., Lollini, P. L., Nicoletti, G., Landuzzi, L., Serra, M., Manara, M. C., Picci, P. and Baldini, N. (1998) Blockage of insulin-like growth factor-I receptor inhibits the growth of Ewing's sarcoma in athymic mice. *Cancer Res*, **58**(18): 4127-31.

Scott, C. D. and Firth, S. M. (2004) The role of the M6P/IGF-II receptor in cancer: tumor suppression or garbage disposal? *Horm Metab Res*, **36**(5): 261-71.

Seely, B. L., Samimi, G. and Webster, N. J. (2002) Retroviral expression of a kinase-defective IGF-I receptor suppresses growth and causes apoptosis of CHO and U87 cells in-vivo. *BMC Cancer*, **2**(1): 15.

Seino, S. and Bell, G. I. (1989) Alternative splicing of human insulin receptor messenger RNA. *Biochem Biophys Res Commun*, **159**(1): 312-6.

Sell, C., Baserga, R. and Rubin, R. (1995) Insulin-like growth factor I (IGF-I) and the IGF-I receptor prevent etoposide-induced apoptosis. *Cancer Res*, **55**(2): 303-6.

Sell, C., Dumenil, G., Deveaud, C., Miura, M., Coppola, D., DeAngelis, T., Rubin, R., Efstratiadis, A. and Baserga, R. (1994) Effect of a null mutation of the insulin-like growth factor I receptor gene on growth and transformation of mouse embryo fibroblasts. *Mol Cell Biol*, **14**(6): 3604-12.

Sell, C., Rubini, M., Rubin, R., Liu, J. P., Efstratiadis, A. and Baserga, R. (1993) Simian virus 40 large tumor antigen is unable to transform mouse embryonic fibroblasts lacking

type 1 insulin-like growth factor receptor. *Proc Natl Acad Sci U S A*, **90**(23): 11217-21.

Sesti, G., Federici, M., Lauro, D., Sbraccia, P. and Lauro, R. (2001) Molecular mechanism of insulin resistance in type 2 diabetes mellitus: role of the insulin receptor variant forms. *Diabetes Metab Res Rev*, **17**(5): 363-73.

Shapiro, D. N., Jones, B. G., Shapiro, L. H., Dias, P. and Houghton, P. J. (1994) Antisense-mediated reduction in insulin-like growth factor-I receptor expression suppresses the malignant phenotype of a human alveolar rhabdomyosarcoma. *J Clin Invest*, **94**(3): 1235-42.

Sheriff, S., Silverton, E. W., Padlan, E. A., Cohen, G. H., Smith-Gill, S. J., Finzel, B. C. and Davies, D. R. (1987) Three-dimensional structure of an antibody-antigen complex. *Proc Natl Acad Sci U S A*, **84**(22): 8075-9.

Shooter, G. K., Magee, B., Soos, M. A., Francis, G. L., Siddle, K. and Wallace, J. C. (1996) Insulin-like growth factor (IGF)-I A- and B-domain analogues with altered type 1 IGF and insulin receptor binding specificities. *J Mol Endocrinol*, **17**(3): 237-46.

Siddle, K., Urso, B., Niesler, C. A., Cope, D. L., Molina, L., Surinya, K. H. and Soos, M. A. (2001) Specificity in ligand binding and intracellular signalling by insulin and insulin-like growth factor receptors. *Biochem Soc Trans*, **29**(Pt 4): 513-25.

Siebler, T., Lopaczynski, W., Terry, C. L., Casella, S. J., Munson, P., De Leon, D. D., Phang, L., Blakemore, K. J., McEvoy, R. C., Kelley, R. I. and et al. (1995) Insulin-like growth factor I receptor expression and function in fibroblasts from two patients with deletion of the distal long arm of chromosome 15. *J Clin Endocrinol Metab*, **80**(12): 3447-57.

Singer, C. F., Hudelist, G., Lamm, W., Mueller, R., Czerwenka, K. and Kubista, E. (2004) Expression of tyrosine kinases in human malignancies as potential targets for kinase-specific inhibitors. *Endocr Relat Cancer*, **11**(4): 861-9.

Singh, R., Tavares, D. and Dagdigian, N. E. (2003). Anti-IGF-I receptor antibody (WO 03/106621 A2). U.S.A.

Soos, M., Whittaker, J., Lammers, R., Ullrich, A. and Siddle, K. (1990) Receptors for insulin and insulin-like growth factor-I can form hybrid dimers. Characterisation of hybrid receptors in transfected cells. *Biochem J*, **270(2)**: 383-90.

Soos, M. A., Field, C. E., Lammers, R., Ullrich, A., Zhang, B., Roth, R. A., Andersen, A. S., Kjeldsen, T. and Siddle, K. (1992) A panel of monoclonal antibodies for the type I insulin-like growth factor receptor. Epitope mapping, effects on ligand binding, and biological activity. *J Biol Chem*, **267**(18): 12955-63.

Soos, M. A., Field, C. E. and Siddle, K. (1993) Purified hybrid insulin/insulin-like growth factor-I receptors bind insulin-like growth factor-I, but not insulin, with high affinity. *Biochem J*, **290**(Pt 2): 419-26.

Sorensen, H., Whittaker, L., Hinrichsen, J., Groth, A. and Whittaker, J. (2004) Mapping of the insulin-like growth factor II binding site of the Type I insulin-like growth factor receptor by alanine scanning mutagenesis. *FEBS Lett*, **565**(1-3): 19-22.

Souza, R. F., Wang, S., Thakar, M., Smolinski, K. N., Yin, J., Zou, T. T., Kong, D., Abraham, J. M., Toretsky, J. A. and Meltzer, S. J. (1999) Expression of the wild-type insulin-like growth factor II receptor gene suppresses growth and causes death in colorectal carcinoma cells. *Oncogene*, **18**(28): 4063-8.

Steele-Perkins, G. and Roth, R. A. (1990) Monoclonal antibody alpha IR-3 inhibits the ability of insulin-like growth factor II to stimulate a signal from the type I receptor without inhibiting its binding. *Biochem Biophys Res Commun*, **171**(3): 1244-51.

Steller, M. A., Delgado, C. H., Bartels, C. J., Woodworth, C. D. and Zou, Z. (1996) Overexpression of the insulin-like growth factor-1 receptor and autocrine stimulation in human cervical cancer cells. *Cancer Res*, **56**(8): 1761-5.

Stenroos, K., Hurskainen, P., Blomberg, K. and Lindqvist, C. (1997) Solid phase IL-2-IL-2R alpha assay with time resolved fluorometry. *Immunol Lett*, **58**(1): 15-8.

Stenroos, K., Hurskainen, P., Eriksson, S., Hemmila, I., Blomberg, K. and Lindqvist, C. (1998) Homogeneous time-resolved IL-2-IL-2R alpha assay using fluorescence resonance energy transfer. *Cytokine*, **10**(7): 495-9.

Stetefeld, J., Jenny, M., Schulthess, T., Landwehr, R., Engel, J. and Kammerer, R. A. (2000) Crystal structure of a naturally occurring parallel right-handed coiled coil tetramer. *Nat Struct Biol*, **7**(9): 772-6.

Stoscheck, C. M. (1990) Quantitation of protein. *Methods Enzymol*, **182**: 50-68.

Strohal, R., Helmberg, A., Kroemer, G. and Kofler, R. (1989) Mouse Vk gene classification by nucleic acid sequence similarity. *Immunogenetics*, **30**(6): 475-93.

Tamura, T., Tohma, T., Ohta, T., Soejima, H., Harada, N., Abe, K. and Niikawa, N. (1993) Ring chromosome 15 involving deletion of the insulin-like growth factor 1 receptor gene in a patient with features of Silver-Russell syndrome. *Clin Dysmorphol*, **2**(2): 106-13.

Taylor, R., Soos, M. A., Wells, A., Argyraki, M. and Siddle, K. (1987) Insulin-like and insulin-inhibitory effects of monoclonal antibodies for different epitopes on the human insulin receptor. *Biochem J*, **242**(1): 123-9.

Terasawa, H., Kohda, D., Hatanaka, H., Nagata, K., Higashihashi, N., Fujiwara, H., Sakano, K. and Inagaki, F. (1994) Solution structure of human insulin-like growth factor II; recognition sites for receptors and binding proteins. *EMBO J*, **13**(23): 5590-7.

Thissen, J. P., Ketelslegers, J. M. and Underwood, L. E. (1994) Nutritional regulation of the insulin-like growth factors. *Endocr Rev*, **15**(1): 80-101.

Thompson, J. D., Higgins, D. G. and Gibson, T. J. (1994) CLUSTAL W: improving the sensitivity of progressive multiple sequence alignment through sequence weighting, position-specific gap penalties and weight matrix choice. *Nucleic Acids Res*, **22**(22): 4673-80.

Thompson, M. A., Cox, A. J., Whitehead, R. H. and Jonas, H. A. (1990) Autocrine regulation of human tumor cell proliferation by insulin-like growth factor II: an in-vitro model. *Endocrinology*, **126**(6): 3033-42.

Tong, P. Y., Tollefsen, S. E. and Kornfeld, S. (1988) The cation-independent mannose 6-phosphate receptor binds insulin-like growth factor II. *J Biol Chem*, **263**(6): 2585-8.

Torres, A. M., Forbes, B. E., Aplin, S. E., Wallace, J. C., Francis, G. L. and Norton, R. S. (1995) Solution structure of human insulin-like growth factor II. Relationship to receptor and binding protein interactions. *J Mol Biol*, **248**(2): 385-401.

Tulloch, P. A., Lawrence, L. J., McKern, N. M., Robinson, C. P., Bentley, J. D., Cosgrove, L., Ivancic, N., Lovrecz, G. O., Siddle, K. and Ward, C. W. (1999) Single-molecule imaging of human insulin receptor ectodomain and its Fab complexes. *J Struct Biol*, **125**(1): 11-8.

Turner, B. C., Haffty, B. G., Narayanan, L., Yuan, J., Havre, P. A., Gumbs, A. A., Kaplan, L., Burgaud, J. L., Carter, D., Baserga, R. and Glazer, P. M. (1997) Insulin-like growth factor-I receptor overexpression mediates cellular radioresistance and local breast cancer recurrence after lumpectomy and radiation. *Cancer Res*, **57**(15): 3079-83.

Ullrich, A., Bell, J. R., Chen, E. Y., Herrera, R., Petruzzelli, L. M., Dull, T. J., Gray, A., Coussens, L., Liao, Y. C., Tsubokawa, M. and et al. (1985) Human insulin receptor and its relationship to the tyrosine kinase family of oncogenes. *Nature*, **313**(6005): 756-61.

Ullrich, A., Gray, A., Tam, A., Yang-Feng, T., Tsubokawa, M., Collins, C., Henzel, W., Le Bon, T., Kathuria, S., Chen, E. and al., e. (1986) Insulin-like growth factor I receptor primary structure: comparison with insulin receptor suggests structural determinants that define functional specificity. *EMBO J*, **5(10)**: 2503-12.

Ullrich, A. and Schlessinger, J. (1990) Signal transduction by receptors with tyrosine kinase activity. *Cell*, **61**(2): 203-12.

Upton, Z., Francis, G. L., Chan, S. J., Steiner, D. F., Wallace, J. C. and Ballard, F. J. (1997) Evolution of insulin-like growth factor (IGF) function: production and characterization of recombinant hagfish IGF. *Gen Comp Endocrinol*, **105**(1): 79-90.

Vajdos, F. F., Ultsch, M., Schaffer, M. L., Deshayes, K. D., Liu, J., Skelton, N. J. and de Vos, A. M. (2001) Crystal structure of human insulin-like growth factor-1: detergent binding inhibits binding protein interactions. *Biochemistry*, **40**(37): 11022-9.

Valentinis, B., Morrione, A., Taylor, S. J. and Baserga, R. (1997) Insulin-like growth factor I receptor signaling in transformation by src oncogenes. *Mol Cell Biol*, **17**(7): 3744-54.

Van Regenmortel, M. H. (1989) Structural and functional approaches to the study of protein antigenicity. *Immunol Today*, **10**(8): 266-72.

Vaughan, T. J., Williams, A. J., Pritchard, K., Osbourn, J. K., Pope, A. R., Earnshaw, J. C., McCafferty, J., Hodits, R. A., Wilton, J. and Johnson, K. S. (1996) Human antibodies with sub-nanomolar affinities isolated from a large non-immunized phage display library. *Nat Biotechnol*, **14**(3): 309-14.

Vella, V., Pandini, G., Sciacca, L., Mineo, R., Vigneri, R., Pezzino, V. and Belfiore, A. (2002) A novel autocrine loop involving IGF-II and the insulin receptor isoform-A stimulates growth of thyroid cancer. *J Clin Endocrinol Metab*, **87**(1): 245-54.

Vetter, U., Schlickenrieder, J. H., Zapf, J., Hartmann, W., Heit, W., Hitzler, H., Byrne, P., Gaedicke, G., Heinze, E. and Teller, W. M. (1986) Human leukemic cells: receptor

binding and biological effects of insulin and insulin-like growth factors. *Leuk Res*, **10**(10): 1201-7.

von Horn, H., Tally, M., Hall, K., Eriksson, T., Ekstrom, T. J. and Gray, S. G. (2001) Expression levels of insulin-like growth factor binding proteins and insulin receptor isoforms in hepatoblastomas. *Cancer Lett*, **162**(2): 253-60.

Wang, H., Shen, W., Huang, H., Hu, L., Ramdas, L., Zhou, Y. H., Liao, W. S., Fuller, G. N. and Zhang, W. (2003a) Insulin-like growth factor binding protein 2 enhances glioblastoma invasion by activating invasion-enhancing genes. *Cancer Res*, **63**(15): 4315-21.

Wang, Y., Greenberg, R., Presta, L., Pachter, J. A., Hailey, J., Brams, P., Williams, D., Srinivasan, M. and Feingersh, D. (2003b). Neutralizing human anti-IGFR antibody (WO 03/100008 A2). U.S.A.

Ward, C. W., Hoyne, P. A. and Flegg, R. H. (1995) Insulin and epidermal growth factor receptors contain the cysteine repeat motif found in the tumor necrosis factor receptor. *Proteins*, **22**(2): 141-53.

Warshamana-Greene, G. S., Litz, J., Buchdunger, E., Garcia-Echeverria, C., Hofmann, F. and Krystal, G. W. (2005) The Insulin-Like Growth Factor-I Receptor Kinase Inhibitor, NVP-ADW742, Sensitizes Small Cell Lung Cancer Cell Lines to the Effects of Chemotherapy. *Clin Cancer Res*, **11**(4): 1563-71.

Weber, M. M., Fottner, C., Liu, S. B., Jung, M. C., Engelhardt, D. and Baretton, G. B. (2002) Overexpression of the insulin-like growth factor I receptor in human colon carcinomas. *Cancer*, **95**(10): 2086-95.

Webster, N. J., Resnik, J. L., Reichart, D. B., Strauss, B., Haas, M. and Seely, B. L. (1996) Repression of the insulin receptor promoter by the tumor suppressor gene product p53: a possible mechanism for receptor overexpression in breast cancer. *Cancer Res*, **56**(12): 2781-8.

Werner, H. and LeRoith, D. (1996) The role of the insulin-like growth factor system in human cancer. *Adv Cancer Res 1996;68:183-223.*

White, C. A., Johansson, M., Roberts, C. T., Ramsay, A. J. and Robertson, S. A. (2004) Effect of interleukin-10 null mutation on maternal immune response and reproductive outcome in mice. *Biol Reprod*, **70**(1): 123-31.

Whittaker, J., Groth, A. V., Mynarcik, D. C., Pluzek, L., Gadsboll, V. L. and Whittaker, L. J. (2001) Alanine scanning mutagenesis of a type 1 insulin-like growth factor receptor ligand binding site. *J Biol Chem*, **276**(47): 43980-6.

Wilfinger, W. W., Mackey, K. and Chomczynski, P. (1997) Effect of pH and ionic strength on the spectrophotometric assessment of nucleic acid purity. *Biotechniques*, **22**(3): 474-6, 478-81.

Xie, Y., Skytting, B., Nilsson, G., Brodin, B. and Larsson, O. (1999) Expression of insulin-like growth factor-1 receptor in synovial sarcoma: association with an aggressive phenotype. *Cancer Res*, **59**(15): 3588-91.

Yamaguchi, Y., Flier, J. S., Benecke, H., Ransil, B. J. and Moller, D. E. (1993) Ligand-binding properties of the two isoforms of the human insulin receptor. *Endocrinology*, **132**(3): 1132-8.

Yamaguchi, Y., Flier, J. S., Yokota, A., Benecke, H., Backer, J. M. and Moller, D. E. (1991) Functional properties of two naturally occurring isoforms of the human insulin receptor in Chinese hamster ovary cells. *Endocrinology*, **129**(4): 2058-66.

Ye, J. J., Liang, S. J., Guo, N., Li, S. L., Wu, A. M., Giannini, S., Sachdev, D., Yee, D., Brunner, N., Ikle, D. and Fujita-Yamaguchi, Y. (2003) Combined effects of tamoxifen and a chimeric humanized single chain antibody against the type I IGF receptor on breast tumor growth in vivo. *Horm Metab Res*, **35**(11-12): 836-42.

Yee, D., Lebovic, G. S., Marcus, R. R. and Rosen, N. (1989) Identification of an alternate type I insulin-like growth factor receptor beta subunit mRNA transcript. *J Biol Chem*, **264**(36): 21439-41.

Yee, D., Morales, F. R., Hamilton, T. C. and Von Hoff, D. D. (1991) Expression of insulin-like growth factor I, its binding proteins, and its receptor in ovarian cancer. *Cancer Res*, **51**(19): 5107-12.

Young, S. C., Miles, M. V. and Clemmons, D. R. (1992) Determination of the pharmacokinetic profiles of insulin-like growth factor binding proteins-1 and -2 in rats. *Endocrinology*, **131**(4): 1867-73.

Zeslawski, W., Beisel, H. G., Kamionka, M., Kalus, W., Engh, R. A., Huber, R., Lang, K. and Holak, T. A. (2001) The interaction of insulin-like growth factor-I with the N-terminal domain of IGFBP-5. *EMBO J*, **20**(14): 3638-44.

Zhang, B. and Roth, R. A. (1991) Binding properties of chimeric insulin receptors containing the cysteine-rich domain of either the insulin-like growth factor I receptor or the insulin receptor related receptor. *Biochemistry*, **30**(21): 5113-7.

Zhang, W., Gustafson, T. A., Rutter, W. J. and Johnson, J. D. (1994) Positively charged side chains in the insulin-like growth factor-1 C- and D-regions determine receptor binding specificity. *J Biol Chem*, **269**(14): 10609-13.

Zia, F., Jacobs, S., Kull, F., Jr., Cuttitta, F., Mulshine, J. L. and Moody, T. W. (1996) Monoclonal antibody alpha IR-3 inhibits non-small cell lung cancer growth in vitro and in vivo. *J Cell Biochem Suppl*, **24**: 269-75.